Characterization of oligosaccharides with capillary high performance anion exchange chromatography hyphenated to pulsed amperometric detection and ion trap mass spectrometry : application to the analysis of human lysosomal disorders

Bruggink, C.

Characterization of oligosaccharides with capillary high performance anion exchange chromatography hyphenated to pulsed amperometric detection and ion trap mass spectrometry

Application to the analysis of human lysosomal disorders

Cornelis Bruggink

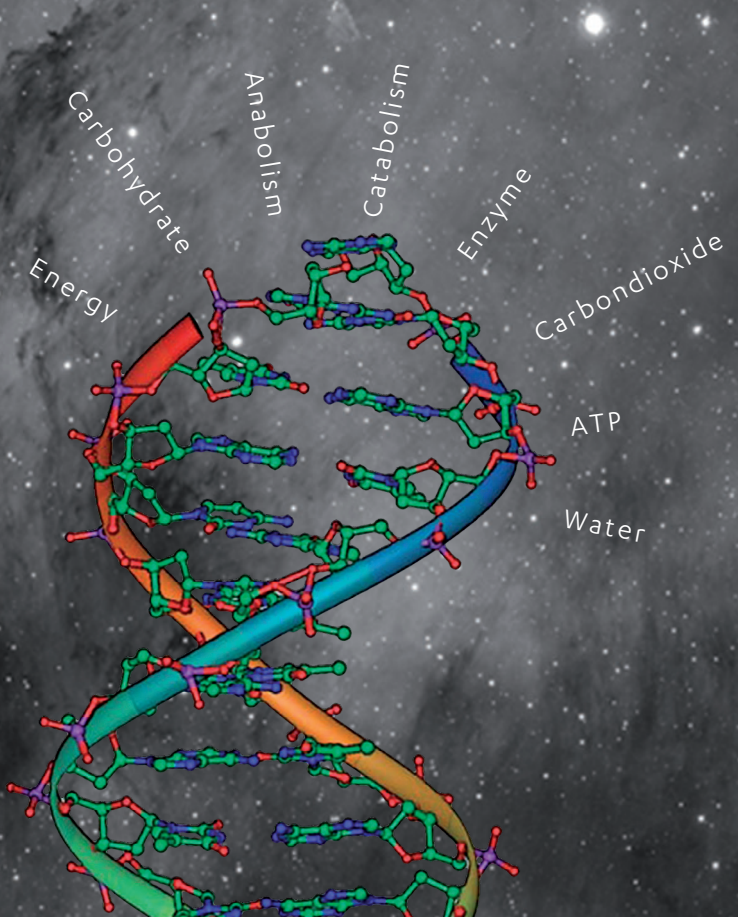

CHARACTERIZATION OF OLIGOSACCHARIDES WITH CAPILLARY HIGH PERFORMANCE ANION EXCHANGE CHROMATOGRAPHY HYPHENATED TO PULSED AMPEROMETRIC DETECTION AND ION TRAP MASS SPECTROMETRY:

Application to the analysis of human lysosomal disorders

Cornelis Bruggink

Layout & printing: Off Page, www.offpage.nl

Cover image: North America Nebula (NGC 7000) picture made by Takayuki Yoshida

Cover design and layout: Cornelis Bruggink

ISBN: 978-94-6182-156-0

The study described has been supported with prototype materials of Thermo Fisher Scientific, Sunnyvale CA.

Printing of this thesis was financially supported by: Dionex Benelux BV

CHARACTERIZATION OF OLIGOSACCHARIDES WITH CAPILLARY HIGH PERFORMANCE ANION EXCHANGE CHROMATOGRAPHY HYPHENATED TO PULSED AMPEROMETRIC DETECTION AND ION TRAP MASS SPECTROMETRY:

Application to the analysis of human lysosomal disorders

Proefschrift

ter verkrijging van
de graad van Doctor aan de Universiteit Leiden,
op gezag van Rector Magnificus prof. mr. C.J.J.M. Stolker,
volgens besluit van het College voor Promoties
ter verdedigen op woensdag 29 mei 2013
klokke 16:15 uur

door

Cornelis Bruggink
geboren te Amsterdam
In 1951

PROMOTIECOMMISSIE

Promotor:	Prof. Dr. A.M. Deelder
Copromotor:	Dr. M. Wuhrer
Overige leden:	Prof. dr. J.M.F.G. Aerts, Amsterdam Medical Center Dr. H.A. Schols, Wageningen University Prof. dr. H.P. Spaink, Leiden University Dr. Ch.M. Cobbaert Prof. dr. E. Bakker Prof. dr. H.J. Tanke

TABLE OF CONTENTS

1

GENERAL INTRODUCTION

Partially based on:
Oligosaccharide analysis by high-performance anion-exchange chromatography hyphenated to integrated pulsed amperometric detection and on-line ion-trap mass spectrometry

Cees Bruggink

Chapter 21 of Applications of ion chromatography for pharmaceutical and biological products
Editors Bhattacharyya L and Rohrer JS
John Wiley & Sons, Inc.

1.1 GLYCOBIOLOGY

Deoxyribonucleic acid (DNA) plays a central role in cell biology, because it is the biological information carrier required for the function of the cell. The flow of this information to generate other cellular molecules and metabolites is accomplished by translating parts from the DNA code into ribonucleic acid (RNA), and from RNA into the generation of proteins. Proteins and DNA alone are not the only essential classes of molecules necessary for a living cell, lipids and carbohydrates being two other classes of vast importance.

Carbohydrates can serve as energy sources, signaling molecules, or as construction components. Carbohydrates are often covalently bonded to other molecules like lipids and proteins forming glycoconjugates such as glycolipids and glycoproteins. From all proteins, more than 50% are glycosylated [1]. The glycan part of a glycoprotein is involved in many different biological processes such as protein folding, signaling, development of multicellular organisms, cell-cell communication and adhesion, cell-matrix interaction, fertilization, inflammation, and immune responses [2-9]. This list of examples is not complete but illustrates the importance of glycans. As a result of the disturbed production or degradation of glycoconjugates, a more or less severe disease can be developed [7,10].

It is essential to analyze the biochemical effects of disturbed glycoconjugate degradation in order to understand the molecular basis of the resulting human diseases. This includes the analysis of the glycan and glycoconjugates accumulated due to enzymatic defects, which is addressed in this thesis. In the following the methods applied in this thesis will be introduced (1.2.) followed by an overview on genetic, biochemical and clinical aspects of various defects in glycoconjugate degradation (1.3).

1.2 HIGH PERFORMANCE ANION-EXCHANGE CHROMATOGRAPHY WITH PULSED AMPEROMETRIC DETECTION (HPAEC-PAD)

Ion chromatography is a special form of high performance liquid chromatography for the analysis of a mixture of ionic species. For a good analysis of ions in a complex sample matrix, a separation prior to the detection is often required. This separation is needed because of interferences in the detection method due to chemical similarities of components. In these cases separation is an essential part of the analytical procedure. Another reason for applying a separation is the possibility to use nonselective detection techniques. Chromatographic techniques are particularly successful in combination of an efficient separation and instantaneous in-line detection [11,12]. Ion chromatography is routinely used for the analysis of inorganic as well as organic ions and polar components. Specifically, the analysis of carbohydrates by HPAEC-PAD is a very common and well accepted application for the characterization of free oligosaccharides which are derived from glycoproteins or glycolipids [13-15].

1.2.1 History of anion-exchange chromatography and detection of sugars

Already during decades anion-exchange chromatography has been used in different ways to separate and analyze carbohydrates. Initially Zill and colleagues made use of anionic sugar-borate complex formation and an anion-exchange resin in the borate form [16,17]. Various improvements of this method have been developed such as the use of a post column reaction prior to optical detection, gradient elution, and automation [18]. Such an automated system allowed the analysis of monosaccharides originating from glycoproteins [19]. The post column reaction with orcinol in hot concentrated sulfuric acid is very corrosive and aggressive and has been later substituted for a non-corrosive dye reaction for reducing sugars [20] or a fluorescence post column reaction [21]. These anion-exchange chromatography systems had various drawbacks such as a destructive detection method, slow elution resulting in broad peak shapes even in the case of shorter run times, and the lack of selectivity for oligosaccharides larger than dimers [22].

A big step forward in ion chromatography was the development of an agglomerated pellicular resin as stationary phase in combination with an eluent stripper column situated in front of the detector by Small *et al*. [23]. Ion chromatography was initially used for the separation of small ions and the stripper column was later named suppressor or desalter. Due to the faster exchange kinetics of this type of resin shorter run times with a better resolution were obtained in combination with chemically suppressed conductivity detection, a sensitive non-destructive detection method, without derivatization of the ions. In 1981 Hughes and Johnson reported about a sensitive electrochemical detection method for underivatized carbohydrates named pulsed amperometric detection [24].

A noble metal used as working electrode, such as platinum or gold, acts as electrochemical catalyst for oxidation reactions of carbohydrates. Consequently only a low potential is needed for detection

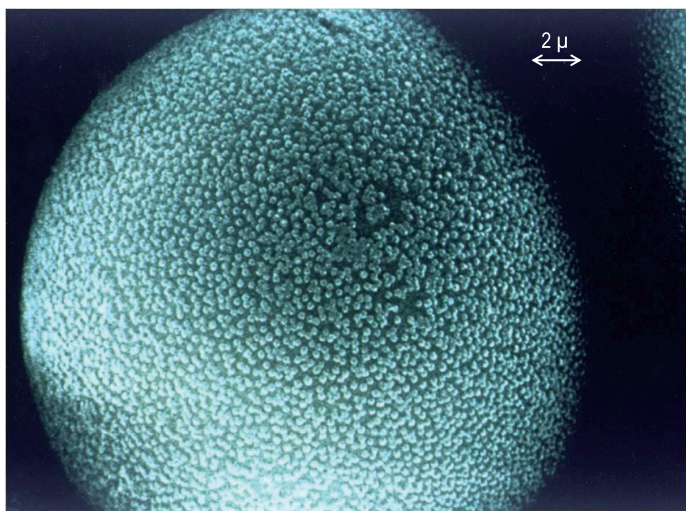

Figure 1-1. Scanning electron microscope (SEM) picture of an agglomerated pellicular resin. Reprinted with permission from [12].

and results in an optimal signal to noise ratio with a limit of detection in the pmol range. Parallel to the development of PAD carbohydrate separation was investigated employing strong anion-exchange columns packed with agglomerated pellicular resin (Figure 1-1) used with high pH eluents.

The combination of these detection and separation methods resulted in 1983 in a publication of Rocklin and Pohl describing the use of a low capacity anion-exchange resin with a high pH eluent for the separation and of carbohydrates followed by pulsed amperometric detection known as HPAEC-PAD [25].

1.2.2 Mechanism of separation

Anion-exchange chromatography can separate anionic carbohydrates that contain a sialic acid, a carboxylate, a sulfate, or a phosphate group [13,14]. Neutral carbohydrates are very weak acids and they dissociate in an eluent at a sufficiently elevated pH allowing their interaction with anion-exchange resins (Table 1-1).

From selectivity research with small anions it is known that analyte charge is the dominant retention factor, followed by the size of an ion [12]. The relevance of analyte charge is nicely illustrated in Figure 1-2 that shows the separation of phosphorylated sugars.

A monophosphorylated glucose (peak 4) elutes faster from the anion-exchanger than a diphosphorylated glucose (peak 13). In addition, at sufficient high pH neutral glycans will undergo dissociation resulting in negative charges. The influence of glycan size is illustrated in Figure 1-3 showing the separation of fructo-oligosaccharides where a higher degree of polymerization (DP) leads to longer retention times.

The separation of dihexose structural isomers in Figure 1-4 highlights the relevance of additional selectivity mechanisms other than those related to charge and size. This chromatogram shows separations of several dihexoses representing compositional isomers (i.e. peak numbers 2, 3, and 9), anomers and isomers differing in linkage positions (i.e. peak numbers 1, 4, 6, 7, and 9). Koizumi and colleagues [28] analyzed positional isomers of methyl ethers of D-glucose among other isomers with HPAEC-PAD and concluded that the reduction in retention time resulting from O-methylation follows the order of 1-OH > 4-OH ≥ 6-OH >3-OH >2-OH representing the difference in the acidity of the different alcohol groups. From this obtained data it is comprehensible that trehalose (Glc(α1-α1)Glc) elutes so early from the column (Figure 1-4) since both anomeric alcohol groups are blocked. Koizumi *et al*. also studied the retention of glucose disaccharides and compared the results with the findings obtained for O-methylated

Table 1-1. Dissociation constants of common carbohydrates in water at 25 °C [26].

Carbohydrate	**pK_a**
Fructose	12.03
Mannose	12.08
Xylose	12.15
Glucose	12.28
Galactose	12.39
Dulcitol	13.43
Sorbitol	13.60
α-Methyl glucoside	13.71

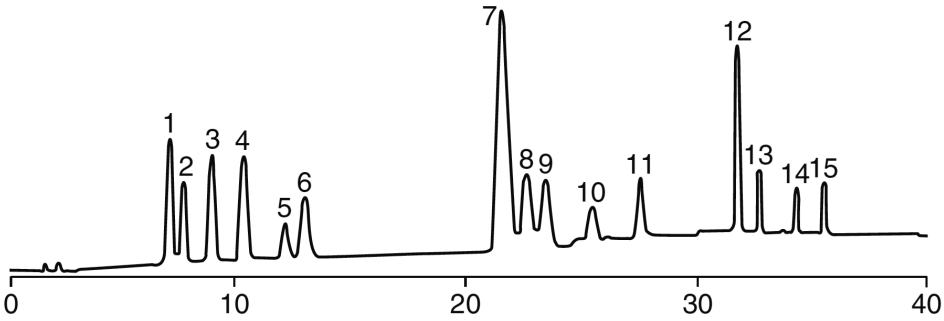

Figure 1-2. Separation of mono- and diphosphorylated monosaccharides with a CarboPac PA1 column using a sodium acetate gradient in 100 mM sodium hydroxide and PAD detection at a gold electrode. Peaks and amount (µg): (1) α-D-galactosamine-1-phosphate, 1.13; (2) α-D-glucosamine-1-phosphate, 0.45; (3) α-D-galactose-1-phosphate, 1.75; (4) α-D-glucose-1-phosphate, 1.75; (5) α-D-ribose-1-phosphate, 1.46; (6) β-D-glucose-1-phosphate, 1.75; (7) D-glucosamine-6-phosphate, 3.75; (8) D-galactose-6-phosphate, 2.04; (9) D-glucose-6-phosphate, 1.25; (10) D-fructose-1-phosphate, 0.96; (11) D-fructose-6-phosphate, 0.42; (12) α-D-glucuronic acid-1-phosphate, 3.08; (13) α-D-glucose-1,6-diphosphate, 1.06; (14) β-D-fructose-2,6-diphosphate, 0.92; (15) D-fructose-1,6-diphosphate, 0.92. Reprinted with permission from technical note 20 Thermo Fisher Scientific.

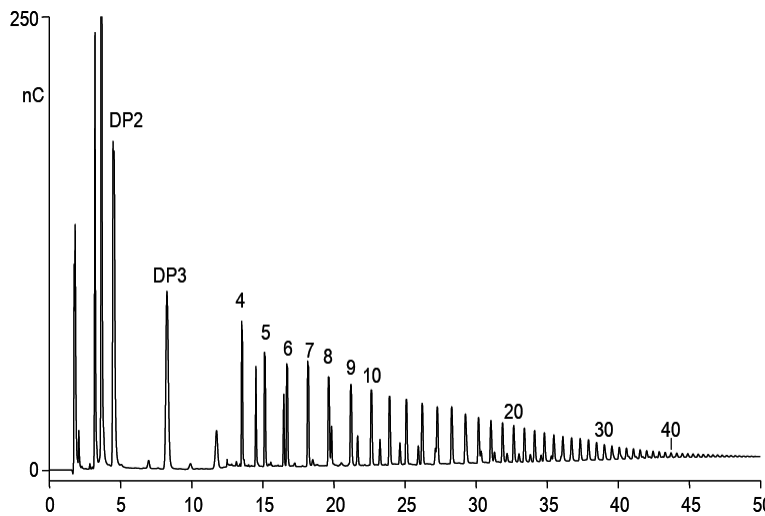

Figure 1-3. Separation of inulin with a CarboPac PA200 column using a sodium acetate gradient in 60 mM NaOH and PAD detection at a gold electrode. Reprinted with permission from [27].

glucoses showing that elution positions were somewhat effected by the configuration and hydrophobic interactions. In general, the α-isomer elutes faster from the column than the corresponding β-isomer with the exception of cellobiose and maltose (see Figure 1-4) [13,28].

A nice example of an isomeric *N*-linked oligosaccharide separation is shown in Figure 3-6, and an example of a baseline separation of two asialo-triantennary glycopeptides only differing

in the linkage of a galactose (either β1-3 or β1-4) has been published by Hardy *et al*. [29]. For a more in depth study of HPAEC oligosaccharide separations the following review articles are recommended: [13,14,29,30].

1.2.3 Detection by pulsed amperometric detection (PAD)

Underivatized carbohydrates can be sensitively detected with a gold working electrode, because aldehyde, ketone, and alcohol groups are oxidizable at 0.10 V versus a Ag/AgCl reference electrode [31]. Oxidation at this low potential is possible because gold serves as a catalyst in the oxidation reaction of the aforementioned groups [32]. To keep the gold electrode catalytically active, cleaning and activation potentials are applied after the detection potential [33]. All of these potentials are only applied for less than a second for the total sequence of potentials and their time periods being referred to as a waveform. A modern waveform provides two data points per second and is stable over a long period of time [33].

1.2.4 Mass spectrometric detection

To obtain more information from complex samples, particularly in those cases where standards are not available, mass spectrometric detection (MS) is advisable. To this end, the effluent of the column passing the amperometric detection cell can be fraction collected. These fractions need to be desalted prior to mass spectrometric analysis. Desalting can be performed off-line or more conveniently inserting a membrane device as an on-line desalter between the detector and the fraction collector [34,35]. Another approach is to analyze the fraction by HPLC-MS with the salt plug redirected to waste [36]. Direct hyphenation of MS to HPAEC using electrospray ionization (ESI) is particularly useful when the sample amount is limited, to identify glycans, and to unravel coeluting glycans in chromatograms of complex samples. The obtained signal intensity of carbohydrates is relatively low compared to that of peptides or proteins due to the low ionization efficiency of carbohydrates. Anionic carbohydrates can selectively be detected in deprotonated form with ESI-MS in the negative mode. Neutral carbohydrates easily form adducts with a proton or a metal ion so that they can be detected in the positive mode

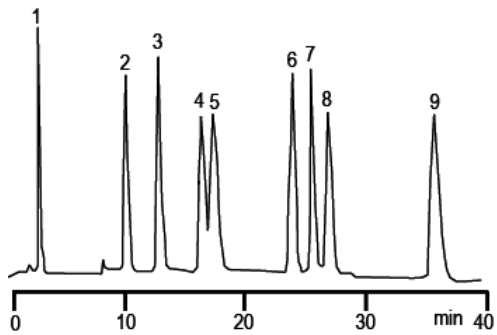

Figure 1-4. Separation of disaccharides with HPAEC-PAD. Peaks (1) Glc(α1,α1)Glc (trehalose); (2) Fru(β2,α1)Glc (sucrose); (3) Gal(β1,4)Glc (lactose); (4) Glc(α1,6)Glc (isomaltose); (5) Gal(α1,6)Glc (melibiose); (6) Glc(β1,6)Glc (gentiobiose); (7) Glc(β1,4)Glc (cellobiose); (8) Glc(α1,3)Fru (turanose); (9) Glc(α1,4)Glc (maltose). Reprinted with permission from technical note 20 version 1 Thermo Fisher Scientific.

[37,38]; see Table 1-2 for commonly used adduct ions. Mohr *et al*. [37] have studied the relative affinities of different alkali metal ions for carbohydrates, and have found that the affinity order is $Cs^+ > K^+ > Na^+ > Li^+ > H^+$. Notably, although cesium is generally most efficient at producing ions of oligosaccharides, it is inefficient in ionizing small carbohydrates [39].

Di- and trivalent metals are also capable of ionizing carbohydrates, but only singly charged quasimolecular ions are formed [40]. If the glycan contains fucose as constituent and proton adducts are formed, rearrangements can occur and the position of the fucose residue in the glycan may be changed upon tandem mass spectrometry [41-43] which may lead to structural misinterpretation. Lithium adducts are most sensitive for ionizing relatively small sugars. Carbohydrate lithium adducts easily undergo in source fragmentation [44]. While this is often viewed as a disadvantage because of signal intensity loss, it can be turned into an advantage when a single quadrupole MS detector is used to obtain more information about the eluting carbohydrate by efficient in source fragmentation [44]. Sodium adducts are more resistant to in source decay and are commonly used in MS detection. The stability of sodium adducts is such that with mild energy levels fragmentation can be induced with tandem MS allowing structural elucidation. The first piece of information to be obtained is the mass of the precursor / intact carbohydrate. From this mass and knowledge of the masses of contributing monosaccharides (e.g. hexoses have a mass increment of 162, *N*-acetylhexosamines of 203; Table 1-3) a composition can be obtained. Upon tandem MS the glycosidic cleavages provides the monosaccharide sequence, while cross-ring fragmentation can reveal linkage information, though the anomeric configuration (i.e. whether a linkage is α or β) can generally not be determined on the basis of MS spectra [45-47].

The broadly accepted nomenclature for assigning the fragmentation of carbohydrates was proposed by Domon and Costello [48] and is depicted in Figure 1-5. At the left side of the figure is the non-reducing end of the oligosaccharide, while at the right side the reducing end is situated. Abundant fragments are generated by cleavage at the glycosidic bonds. Fragments containing the non-reducing end are called B and C fragments, and Y and Z fragments contain the reducing end. A-ions are cross-ring fragments containing the non reducing part of the glycan, while X-ions are cross-ring fragments including the reducing part.

These cross-ring fragment ions are accompanied by a subscript indicating the position relative to the termini and a superscript in front indicating the cleavage positions in the ring, starting with 0 for the bond between the ring oxygen and the anomeric carbon with further counting in the clockwise direction (Figure 1-5). Linkage position information may be derived from cross-ring fragments. Table 1-4 lists mass losses observed depending on cross-ring fragmentation when tandem MS is used in the positive mode.

Table 1-2. Adduct ions and their use in the ESI (+) mode.

Adduct ion	Monoisotopic mass	Remarks
Hydrogen	1.01	Fucose rearrangement possible
Lithium	7.02	In source fragmentation easy to induce
Sodium	22.99	Commonly used
Potassium	38.96	Stable adduct
Cesium	132.91	Only for larger oligosaccharides

Table 1-3. Monoisotopic mass increments of some carbohydrates.

Carbohydrate residue	Residue Mass
Deoxyhexose	146.06
Hexose	162.05
Hexosamine	161.07
Uronic acid	176.03
N-acetylhexosamine	203.08
N-acetylneuraminic acid	291.10
N-glycolylneuraminic acid	307.09

Separation of carbohydrates with HPAEC is usually performed with sodium hydroxide in the eluent, and to elute oligosaccharides from the anion-exchange column a sodium acetate gradient is applied, while the hydroxide concentration is typically kept constant [49]. A mobile phase containing sodium hydroxide and sodium acetate is incompatible with the ESI interface of the mass spectrometer. To convert the eluent for on-line MS into a compatible fluid, a membrane based desalter is used. There are several types mentioned in the literature such as the carbohydrate membrane desalter (CMD) [34] and the anion self regenerating suppressor (ASRS) [44]. Such a membrane desalter can be considered as a cation-exchanger in the acidic form exchanging sodium ions for hydronium ions. The sodium hydroxide is converted into water while sodium acetate is converted into volatile acetic acid. The CMD and ASRS are continuously regenerated by electrolysis of water that is sometimes assisted with trifluoroacetic acid as proton donor to enhance the desalting capacity [34]. After desalting the eluent, a make-up solution is added via a T-connector to facilitate carbohydrate adduct - and spray formation, see Figure 1-6.

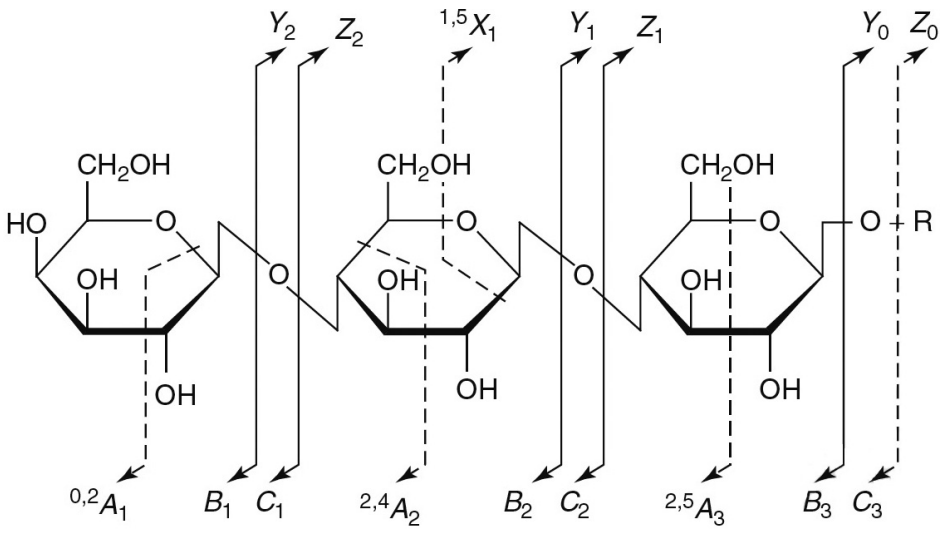

Figure 1-5. Glycan fragmentation types and their nomenclature as proposed by Domon and Costello. Reprinted with permission from [48].

Table 1-4. Mass difference relative to a C-type ion observed for sodium adducts of oligosaccharides upon A-type cross-ring cleavages of hexose (Hex) and *N*-acetylhexosamine (HexNAc) residues [45-47].

Monosaccharide		Linkage type			
Hex	**HexNAc**	**1 – 6**	**1 – 4**	**1 – 3**	**1 – 2**
-60	-101	$^{0,2}A$	$^{0,2}A$	-	-
-90	-131	$^{0,3}A$	-	-	-
-120	-161	$^{0,4}A$	$^{2,4}A$	-	$^{1,3}A$
-106	-147	$^{3,5}A$	$^{3,5}A$	-	-
-78		$^{0,2}A-H_2O$	-	-	$^{0,2}A-H_2O$

1.2.5 Application example: analytical-scale HPAEC-PAD-MS of released *N*-glycans

A mix of *N*-glycan standards representing structures such as they are typically found on therapeutic glycoproteins expressed in mammalian cell culture was analyzed by HPAEC-PAD-MS. The system was a Dionex ICS-3000 ion chromatograph consisting of a low pressure gradient pump, an isocratic pump, a chromatography detector module equipped with an electrochemical detector and cell outfitted with a gold working electrode and Ag/AgCl as reference electrode, injection valve and a dual zone temperature control, and a cooled autosampler. The MS was a Bruker HCT Ultra ion-trap equipped with an ESI interface. The separation was carried out on a CarboPac PA200 (3 x 250 mm) column from Dionex Corp. at 30 ºC and a flow rate of 360 µL/min. After the column a homemade PEEK splitter was installed which split 90 µL/min to the electrochemical cell and 270 µL/min to the desalter (ASRS-300 2 mm Dionex in the external water mode). The eluent leaving the desalter was combined with 90 µL/min 50% acetonitrile for MS detection in the positive mode detecting the glycans in the protonated form (Figure 1-6).

The resulting separation is shown in Figure 1-7. The different peaks are identified on the basis of MS and tandem MS spectra. In case of MS could only partly elucidate structure, structures were confirmed by running standard solutions of the different glycans. This application shows the successful hyphenation of on-line MS with HPAEC-PAD by adding a desalter in front of the ESI-MS/MS.

1.3 LYSOSOMAL CATABOLISM OF OLIGOSACCHARIDES

Lysosomes were described for the first time by de Duve in 1955 [50]. Unconnected lysosomes together form the endosomal-lysosomal system which is a characteristic space within a cell [50,51]. Within the lysosome an acidic environment is generated forming the digestion system of the cell. The digestion of oligomers to smaller products is mediated by hydrolases which generally have a pH optimum in the range of 3.5 to 5.0. Other proteins involved in lysosomal degradation processes are cofactors, activator proteins for glycosphingolipids, and carrier proteins that deliver catabolic products to the cytosol. The endosomal-lysosomal system has a central position in the economy of the cell [51].

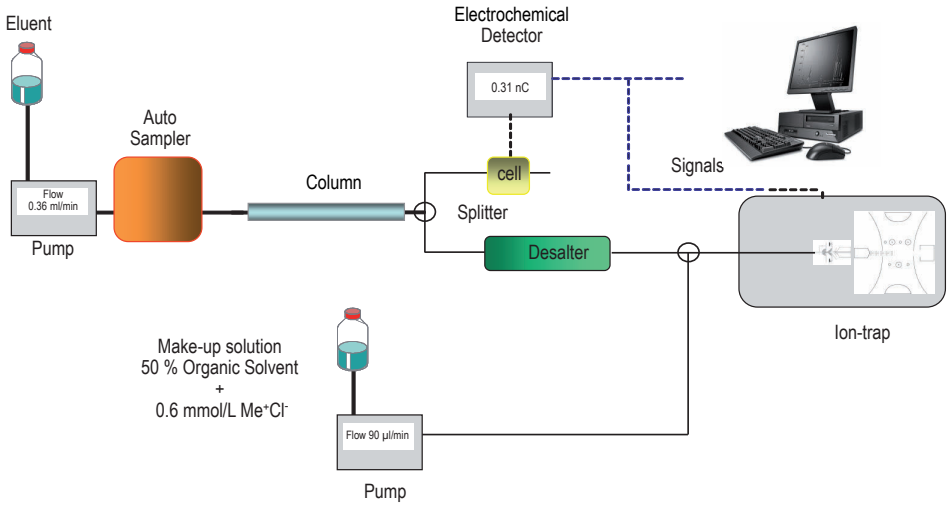

Figure 1-6. Instrumental setup for on-line HPAEC-PAD-MS. Eluent A was ultra pure water, B 200 mM NaOH, and C 400 mM NaOAc. The gradient was 0 – 5 min 50% A, 50% B, 0% C and from 5 – 65 min 0% A, 50% B, and 50% C. The PAD waveform applied to the gold working electrode was 0.00 – 0.20 s 0.10 V, 0.20 – 0.40 s 0.10 V (data collection), 0.41 – 0.42 s -2.00 V, 0.43 s 0.60 V, 0.44 – 0.50 s -0.10 V versus a Ag/AgCl reference electrode [33]. The figure is modified form [27] and reprinted with permission.

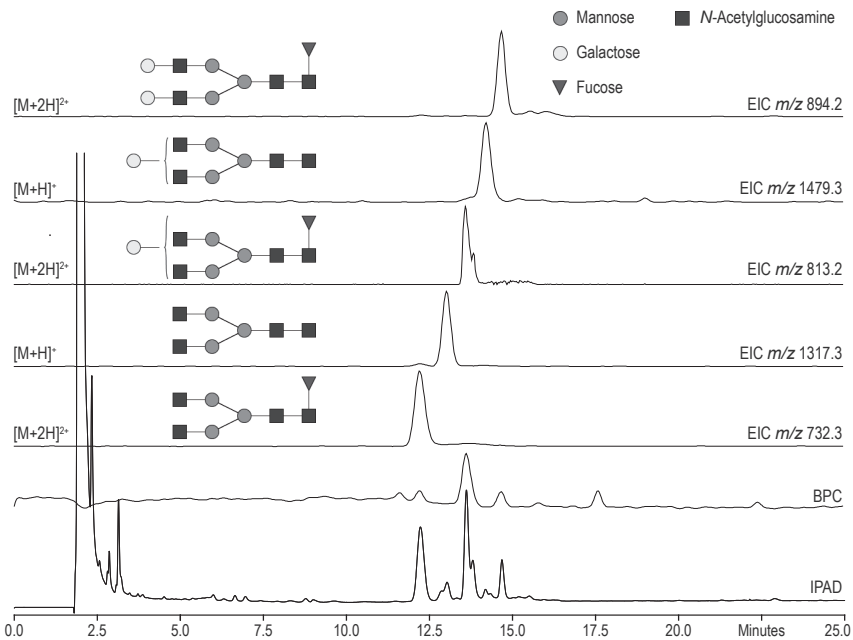

Figure 1-7. Separation of *N*-linked glycans with on-line HPAEC-PAD-MS using a CarboPac PA200 column. Reprinted with permission from [27].

1.3.1 Catabolism of Asn-linked glycoproteins in the human lysosome

There are three different types of oligosaccharides known to be linked via asparagine to human proteins: high mannose, hybrid type, and complex type N-glycans (Figure 1-8).

The acidic condition in the lysosome is required for the enzymatic activity of the lysosomal enzymes which have an acidic pH optimum and will also partially denature the protein substrates thereby making them more accessible for endo- and exohydrolases.

Complete breakdown of glycoconjugates to monomers is required to avoid lysosomal disorders that can become manifest when fragments as small as dimers are left undigested [52]. Catabolism of Asn-linked glycoproteins to monosaccharides and amino acids occurs in lysosomes. The first process happening in glycoprotein degradation is the hydrolysis of the protein backbone with endo- and exopeptidases until finally asparagine-linked glycans are left. Next, the degradation of Asn linked glycans happens in a highly ordered way (see Figure 1-9) [10]. First the removal of the core fucose (Fucα1→ 6GlcNAc) of complex type or hybrid type N-glycans and probably any peripheral fucose residues linked to the outer branches of the chain (Fuc α1 → 3GlcNAc) is performed by lysosomal α–fucosidase [10]. Aspartyl-*N*-acetyl-β-D-glucosaminidase then hydrolyses the GlcNAcβ-Asn bond followed by the removal of the reducing-end GlcNAc by endo-β-*N*-acetylglucosaminidase (chitobiase) as shown in primates and rats [52,53], leaving the oligosaccharide with only one GlcNAc at the reducing end. The

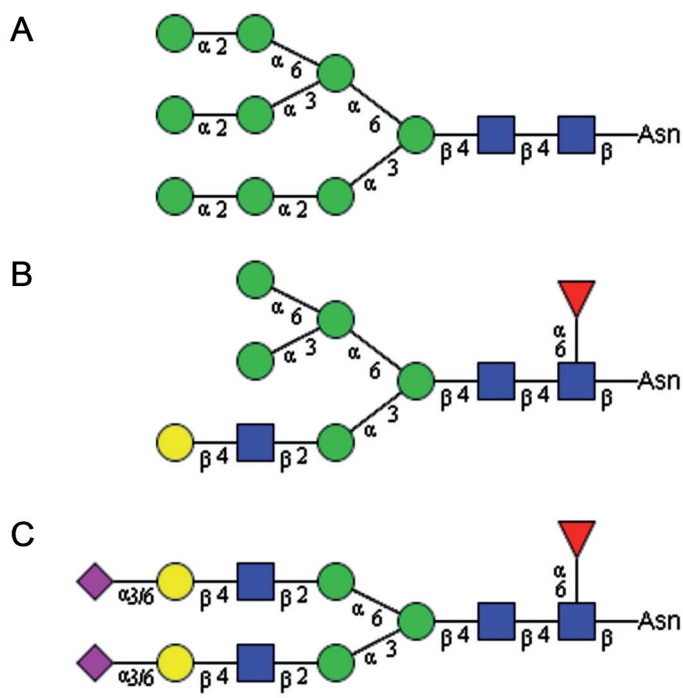

Figure 1-8. Three examples of asparagine linked oligosaccharides. High mannose type (A), hybrid type (B), complex type (C). Green circle mannose, yellow circle galactose, blue square *N*-acetylglucosamine, purple diamond *N*-acetylneuraminic acid, red triangle fucose.

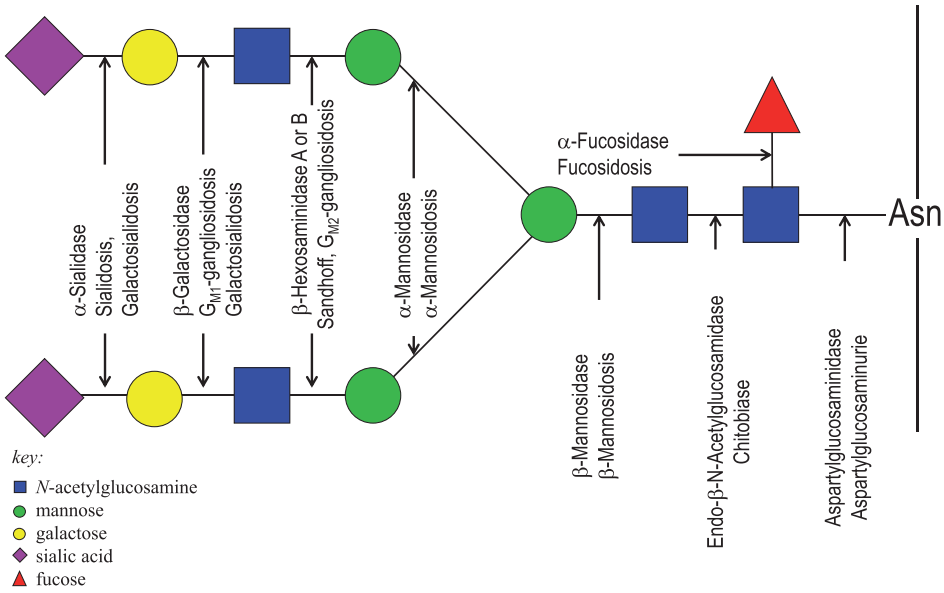

Figure 1-9. Catabolism of complex N-linked oligosaccharides by lysosomal enzymes.

oligosaccharide chain is then sequentially degraded by sialidases and / or α-galactosidases followed by β-galactosidase, β-*N*-acetylhexosaminidase, and α-mannosidase. The remaining Manβ1→4GlcNAc is split by β-mannosidase to mannose and GlcNAc. The resultant monosaccharides are removed from the lysosome by diffusion or with the help of transporter proteins. The highly ordered catabolic pathway explains in part the oligosaccharides found in the diverse Lysosomal storage disorders (LSD).

1.3.2 Catabolism of Ser/Thr-linked glycans in the human lysosome

There are several types of glycans in humans linked to serine or threonine of human glycoproteins. Glycoaminoglycans (GAGs) are attached via a xylosyl-serine linkage. Short mucin-type oligosaccharides are linked via *N*-acetylgalactosamine to serine or threonine. Other glycans are linked via mannose, *N*-acetylglucosamine and fucose to serine or threonine [10]. It is supposed that the catabolism of all these types of *O*-glycosylated proteins happens in the lysosomes. O-glycosylated peptides in urine of patients suffering from Schindler's disease have been characterized by Fourier transform ion cyclotron resonance MS [54]. Little has been published about the enzymology of the lysosomal catabolism of *O*-linked glycans with the exception of glycosaminoglycans of proteoglycans [55]. Most plausible is that the same lysosomal enzymes catalyze the hydrolysis of the same glycosidic linkages in *O*-linked glycans as in other glycoconjugates. A different type of O-linked glycosylation involves the attachment of a single *N*-acetylglucosamine to serine/threonine in nuclear and cytoskeletal proteins is transient and plays a role in intracellular signaling [56]. Its removal is catalyzed by a specific cytosolic *N*-acetylglucosaminidase [57].

1.3.3 Catabolism of glycosphingolipids in the human lysosome

Glycosphingolipids are degraded stepwise from the nonreducing end by exoglycosidases while they are still bound to the ceramide moiety. Since glycosphingolipids have sugar sequences which are in part similar to those found in N- and O-glycans, many of the glycosidases are shared. However, specialized hydrolases and activator proteins are needed for cleaving the glucose-ceramide and galactose-ceramide bonds and other linkages near the membrane.

When a glycosphingolipid contains less than four carbohydrate residues additional noncatalytic sphingolipid activator proteins (SAPs, also called saposins) are essential in human cells for the further degradation by lysosomal hydrolases [58]. In Figure 1-10 the degradation of G_{M1}-ganglioside is schematically represented. The first catabolic step is the cleavage of galactose by the combined action of β-galactosidase and saposin B resulting in leaving G_{M2}-ganglioside. The next hydrolysis step is a combined action of β-hexosaminidase A and the G_{M2} activator protein and this produces G_{M3} ganglioside. The following hydrolysis step is done in a concerted action of sialidase and saposin B and results in lactosylceramide. The concerted action of β-galactosidase and saposins B and C produces glucosylceramide. The last step in degrading the glycan moiety is the combined action of glucosylceramide-β-glucosidase and saponin C to hydrolyse glucosylceramide into glucose and ceramide. Based on this knowledge it has been concluded that free glycan moieties originating from glycosphingolipids are not expected in body fluids like urine.

1.3.4 Lysosomal storage disorder

When one or more of the lysosomal hydrolases are deficient, caused by one or more genetic defects, accumulation of undegraded substrates will happen in the lysosomes. Consequently,

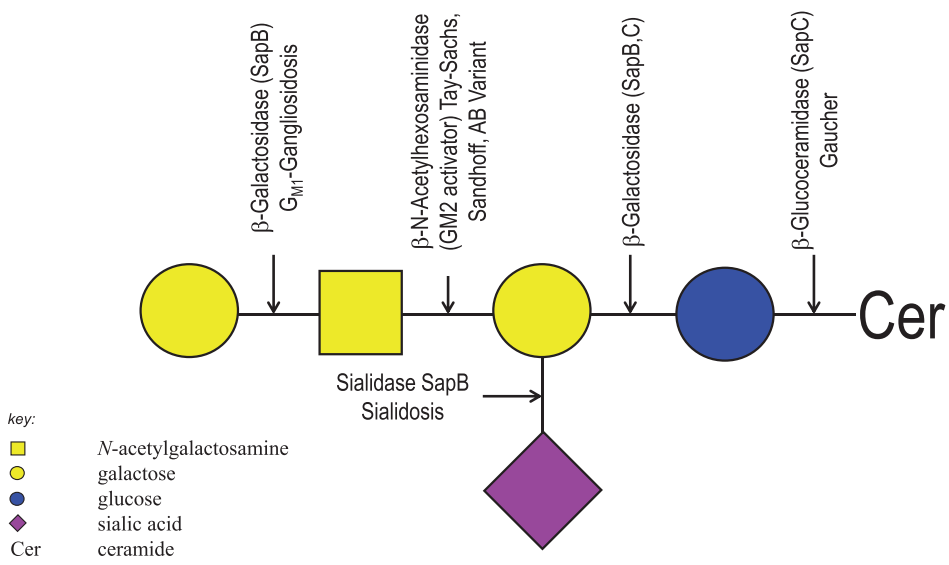

Figure 1-10. Catabolism of the glycan part of glycolipid G_{M1} ganglioside by lysosomal enzymes and cofactors.

lysosomes can swell up to 50% of the cell volume [59] and this will result into damage of many cells. The undegraded substrate will then come free into the extracellular space. Examples of possible stored products are glycosaminoglycans, oligosaccharides, glycopeptides, glycolipids, cholesterols, and sphingomyelins. There have been at least 45 of these deficiencies described forming a group of autosomal recessive inherited lysosomal storage disorders [59,60]. The majority of the lysosomal hydrolases are exoenzymes, so the accumulated and excreted substrates often share the same terminal residue, (see Table 1-5). An extensive review about the lysosome and its disorders has been written by Vellodi [50].

1.3.5 Fucosidosis

Complex type or hybrid type N-glycans may carry fucoses (Figure 1-8). Furthermore fucose can be linked α1-6 to the core *N*-acetylglucosamine that is attached to asparagine. Fucose can be α1-3 or α1-4 linked to *N*-acetylglucosamine in the branches or α1-2 to galactose residues of glycans. The required step in lysosomal degradation of these fucosylated oligosaccharides is hydrolysis of fucose by α-L-fucosidase (EC 3.2.1.51) [62]. A defect of this hydrolase is the cause of fucosidosis. The disorder was initially described by Durand *et al*. in 1968 [63], followed by the report of the defect in α-L-fucosidase by Van Hoof and Hers [64]. Fucosidosis is divided in two distinct phenotypes, but the reality is often more a continuum of severities [65]. The most severe infantile form is type I with an onset of psychomotoric retardation at the age of 3 to 18 months, coarse facies, growth retardation, dysostosis multiplex, neurologic deterioration, and remarkably increased amount of sodium chloride in the patients' sweat. In the milder phenotype, type II, the onset of psychomotoric retardation will be manifest between 1 and 2 years of age. The coarse facies, growth retardation, dysostosis multiplex, and neurologic symptoms are similar or slightly milder than those in type I. The major features that distinguish this milder phenotype from type I are the presence of angiokeratoma, longer survival, and more normal sodium chloride values in sweat.

Fucosidosis is autosomal recessively inherited and the gene symbol for α-L-fucosidase is FUCA1 that codes for the common subunit shared by the multiple forms of α-fucosidase and is situated on chromosome 1p36.11 (MIM 230000). Fucosidosis may be caused by at least 23 different mutations and 4 of these result in an amino acid substitution. For the remaining mutations it is presumed that the result will be unstable or defective mRNA, e.g. premature stop codons, frame shifts, defective splicing, and large deletions [66].

Presumed responsible mutations include the following changes: 188C → T (S63L), 758delA (frame shift), 1201G → T (G401X), 1030ins66 (in-frame insertion), IVS5 + 1G → A (splicing), 229C → T (Q77X), 1145G → A (W382X), 633C → A (Y211X), 421del C (frame shift), 794del C (frame shift), 646del A (frame shift), 340del 10 (frame shift), 549G → A (W183X), 14C → G (P5R), 1988insT (frame shift), 985A → T (N329Y), 1123G → T (E375X), 179G → A (G60D), 451delAA (frame shift), and del exons 7&8 (deletion of 2 exons), 1264C → T (Q422X). All genotypes are homozygote except 229C → T, 1145G → A, 646del A, 451delAA, and 1264C → T. This is evidence for the very high rate of consanguinity found in fucosidosis families [67].

The enzyme defect results in the accumulation and excretion of a variety of fucosylated glycoasparagines and oligosaccharides with core α1–6 linked fucose and / or antenna fucose (Figure 1-11) [68-72].

Table 1-5. Lysosomal disorders. This table is modified from [61] and reprinted with permission.

Disorder	Storage product	Protein defect
Mucopolysaccharidoses (MPS)		
MPS I (Hurler/Scheie)	Oligosaccharides of heparan sulfate, dermatan sulfate	α-Iduronidase
MPS II (Hunter syndrome)	Oligosaccharides of heparan sulfate, dermatan sulfate	Iduronate-2-sulfatase, GlcNAc-P-Transferase
MPS IIIA (Sanfilippo, Pseudo-Hurler polydystrophy A)	Heparan sulfate	Heparan *N*-sulfatase (sulfamidase) GlcNAc-P-Transferase
MPS IIIB (Sanfilippo)	Heparan sulfate	*N*-Acetyl-α-glucosaminidase
MPS IIIC (Sanfilippo, Pseudo-Hurler polydystrophy C)	Heparan sulfate	Acetyl-CoA: α-glucosamide heparan sulfate, *N*-acetyltransferase, GlcNAc-P-transferase
MPS IIID (Sanfilippo)	Heparan sulfate	*N*-Acetylglucosamine-6-sulfatase
MPS IVA (Morquio A syndrome)	Keratan sulfate, chondrotoin-6-sulfate	*N*-Acetylgalactosamine-6-sulfate sulfatase
MPS IVB (Morquio B syndrome)	Keratan sulfate	β-Galactosidase
MPS VI (Maroteaux–Lamy)	Dermantan sulfate	*N*-Acetylgalactosamine-4-sulfatase, (arylsulphatase B)
MPS VII (Sly)	Heparan sulfate, dermatan sulfate, chondroitin-4- and -6-sulfates	β-Glucuronidase
Glycoproteinoses		
Aspartylglucosaminuria	N-linked GlcNAc peptides	*N*-Aspartylglucosaminidase
Fucosidosis	Fucosyloligosaccharides, glycolipides	α-Fucosidase
α-Mannosidosis	Oligosaccharides with α-Mannose at the non-reducing end	α-Mannosidase
β-Mannosidosis	β-Mannosyl-GlcNAc	β-Mannosidase
Sialidosis (Mucolipidosis I)	Sialyloligosaccharides	Exo-α-sialylidase
Schindler disease	Peptides modified with O-linked GalNAc often carrying Gal and Neu5Ac	α-*N*-Acetylgalactosaminidase
Sphingolipidoses		
Fabry's disease	Globotrihexosylceramide (gal-gal-glc-cer), bloodgroup-B substances, digalactosylceramide	α-Galactosidase A
Farber's disease	Ceramide	Ceramidase
Gaucher's disease	Glucosylceramide	β-Glucosidase, saposin-C activator
G_{M1} gangliosidosis	G_{M1} gangliosidoside, galactosyloligosaccharides	β-Galactosidase
Tay-Sachs disease	G_{M2} gangliosidoside and related glycolipids	ß-Hexosaminidase A
Sandhoff's disease	G_{M2} gangliosidoside, G_{A2}, globoside, *N*-acetylglucosaminosyloligosaccharides	ß-Hexosaminidase A and B
Krabbe's disease	Galactosylceramide	Galactosylceramidase
Metachromatic leucodystrophy	Sulfatide, sulfated glycolipids	Arylsulfatase A, Saposin-B activator
Niemann-Pick disease, types A and B	Sphingomyeline	Sphingomyelinase
Other lipidoses		
Niemann-Pick disease type C	Cholesterol and sphingolipids	NPC1 and 2
Wolman's disease	Cholesterol esters and triglycerides	Acid lipase

Table 1-5. continued**.**

Disorder	Storage product	Protein defect
Neuronal ceroid lipofuscinosis		
Glycogen storage disease		
Glycogen storage disease type II (Pompe's disease)	Glycogen	α-Glucosidase
Multiple enzyme deficiency		
Multiple sulfatase deficiency	Glycosaminoglycans, sulfatides	Several sulfatases, Cα-formylglycine-generating enzyme
Galactosialidosis	Gangliosides, sialyloligosaccharides	Cathepsin A secondary deficient β-galactosidase and exo-α-sialidase
Mucolipidosis II/III (I-cell disease and pseudo-Hurler polydystrophy)	Oligosaccharides, mucopolysaccharides, and lipids	UDP-*N*-acetylglucosamine: lysosomal enzyme GlcNAc-P-transferase; secundary deficiency of several lysosomal enzymes
Mucolipidosis IV	Lipids and acid mucopolysaccharides	Mucolipin-1
Lysosomal transport defects		
Cystinosis	Cystine	Cystinosin
Sialic acid storage disease and Salla disease	Sialic acid	Lysosomal transport defect of free sialic acid, Sialin
Other disorders due to defects in lysosomal proteins		
Danon disease	Cytoplasmic debris and glycogen	LAMP2
Hyaluronidase deficiency	Hyaluronan	Hyaluronidase

1.3.6 α-Mannosidosis

The lysosomal storage disorder α−mannosidosis was first reported by Öckerman & Lund [73] and is caused by a deficient lysosomal α-D-mannosidase (EC 3.2.1.24). There are two types of which the most severe phenotype is the infantile type I that shows progressive rapid mental retardation, hepatosplenomegaly, severe dysostosis multiplex, and is mostly mortal between 3 and 12 years of age. The milder juvenile-adult type II form is characterized by a less progressive and milder course with survival into adulthood. The type II is accounting for 10 – 15 percent of cases. This distinction into two types is in fact a continuum of clinical findings [66,74]. α-Mannosidosis is autosomal recessively inherited and the gene coding for the precursors of α-D-mannosidase maps to the human chromosome 19p13-q12. The reported mutation for α−mannosidosis is nucleotide 212A→T which changes amino acid histidine 71 into leucine [75].

The catabolic pathway of high mannose and hybrid type N-linked glycans has been extensively reviewed by Winchester [10]. The pathways for the hydrolysis of these, both type N-glycans by human lysosomal α-D-mannosidase have been elucidated [76]. For human high mannose type glycans the α1-2 linked mannose in the middle branch of $Man_9GlcNAc$, see Figure 1-12, is rather resistant to lysosomal α-D-mannosidase. Hybrid type glycans do not contain this α1-2 linked mannose at that position. The core α1-6 linked mannose is likewise rather resistant to lysosomal α-D-mannosidase. The core tetraose $Man_3GlcNAc$ is no substrate for lysosomal α-D-mannosidase. There is evidence for the existence of a specialized lysosomal α1-6 mannosidase, still active in α−mannosidosis patients [38,77,78]. All these findings do explain the found storage products in urine from α−mannosidosis patients of which the three major mannose rich urinary metabolites are:

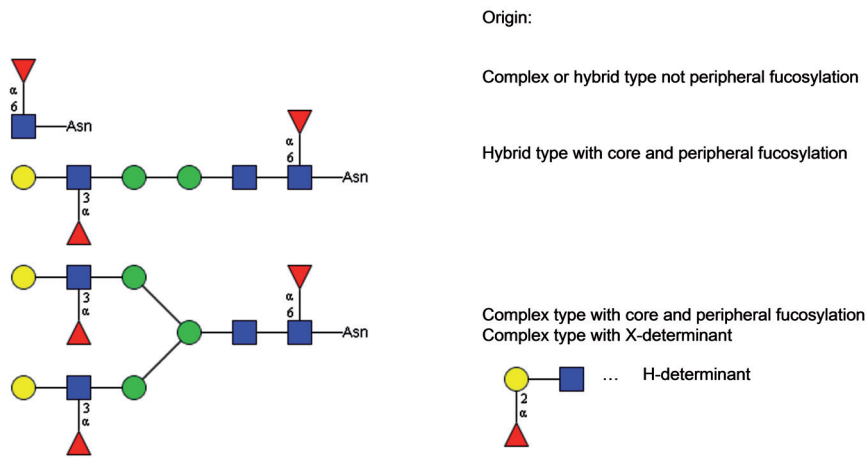

Figure 1-11. Some storage products in fucosidosis. The figure is modified from [10] and taken with permission.

Man(α1-3)Man(β1-4)GlcNAc Man(α1-2)Man(α1-3)Man(β1-4)GlcNAc Man(α1-2)Man(α1-2)Man(α1-3)Man(β1-4)GlcNAc Strecker *et al*. [79] and Yamashita *et al*. [80] have characterized additional mannose-rich oligosaccharides from urine. Until now seventeen mannose-rich oligosaccharides have been characterized from pooled urines of two mannosidosis patients [81,82], of which sixteen had been reported earlier [80,83]. All these mannose rich oligosaccharides, found in urine samples from α-mannosidosis patients, are endo-*N*-acetyl-β-glucosaminidase cleaved products. The major metabolite Man(α1-3)Man(α1-4)GlcNAc in urine is most probably derived from incompletely digested complex type glycans. The presence of a lysosomal (α1-6)mannosidase, still active in affected patients, supports this assumption [10,76].

1.3.7 Sialidosis and Galactosialidosis

Many glycan structures in glycoconjugates contain *N*-acetylneuraminic acid (Neu5Ac), one of the sialic acids, with a linkage of α2–3 or α2–6. The cause of sialidosis is a deficient acid hydrolase exo-α-sialidase (EC 3.2.1.18) [84]. Exo-α-sialidase (sialidase) cleaves both type of linkages α2–3 and α2–6 [85].

In galactosialidosis both sialidase and β-galactosidase (EC 3.2.1.23) are deficient. The deficiency of sialidase and β-galactosidase is a secondary effect of a defect of another enzyme, an associate in the large multi-enzyme complex protective protein/carboxypeptidase C (PPCA), cathepsin A.

1.3.7.1 Protective protein/carboxypeptidase C (PPCA)

The mammalian multi-enzyme complex protein/carboxypeptidase C has both protective and catalytic functions. PPCA is an association of sialidase, β-galactosidase, carboxypeptidase C (EC 3.4.16.5), and recently indications have been found that *N*-acetylgalactosamine-6-sulfate sulfatase (GALNS) (EC 3.1.6.4) also belongs to the multi-enzyme complex [86,87].

PPCA protects sialidase and β-galactosidase from fast proteolysis in the aggressive environment of the lysosome, and the interaction of sialidase with PPCA is needed for optimal activity of sialidase [87-93] (see table 1-6).

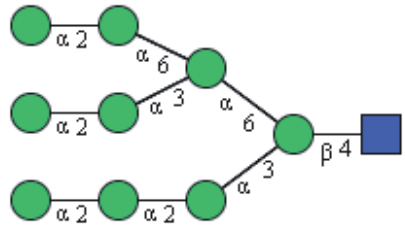

Figure 1-12. High mannose $Man_9GlcNAc$ cleavage product generated from glycoproteins by endo-*N*-acetyl-β-glucosaminidase.

1.3.7.2 Sialidosis

Due to the considerable heterogeneity of the clinical phenotypes observed a proper delineation of sialidosis is difficult. Nowadays two subtypes of sialidosis are distinguished [94,95]. The milder type I is characterized by ocular cherry-red spot and development of myoclonus at the age of 20 – 40 years. The onset of type I occurs at the age of 2 – 25 years. In more than 50% of the affected patients seizures, hyperreflexia, and ataxia are observed [96-98]. The rather severe type II sialidosis is distinguished from type I by an early onset, often at the age of 0 – 2 years. The phenotype shows ocular cherry-red spot, mental retardation, myoclonus, visceromegaly, dysotosis multiplex, hydrops/acites, and skeletal dysplasia [84,99,100]. Sialidosis is autosomal recessively inherited and the gene at location 6p21 is involved. The presumed responsible mutations are 1258G→T, amino acid change H337X; 401T→G, amino acid change L91R; 1337delC, frame shift; 7insACTC, frame shift; 779T→A, amino acid change F260Y; 1088T→C, amino acid change L303P [101,102]. As an effect of deficient sialidase in both subtypes excessive amounts of sialyloligosaccharides in urine of up to 800 x normal levels are observed [103]. Most compounds are endo-β-*N*-acetylglucosaminidase-cleaved products of complex-type sialylated *N*-glycans [104-106]. In 70% of the cases the Neu5Ac is α2–6 linked to galactose and α2–3 linked in 30% [107].

1.3.7.3 Galactosialidosis

For galactosialidosis three phenotypes are distinguished. Firstly, the severe early infantile type that shows onset between birth and 3 months of age with fetal hydrops, neonatal edema, kidney involvement, coarse facies, inguinal hernias, and telangiectasias, small dilated blood vessels near the surface of the skin. This phenotype generally leads to death before the age of 24 months. Telangiectasias has seldom been observed in the other two phenotypes.

Secondly, a mild type is observed named the late infantile type. The symptoms initiate in the first months after birth. Observations at onset are coarse facies, hepatosplenomegaly, and dysostosis multiplex, especially affecting the spine. Often cherry-red spots and / or corneal clouding are observed. The third phenotype is juvenile/adult type. This type shows a variable, broad continuous spectrum of severity of the course and of the age of onset. First symptoms become visible at 1 to 40 years of age with an average of 16 years. Often coarse facies are found, spinal changes are observed whilst dysostosis multiplex seems rare. The most observed neurologic abnormalities are myoclonus, ataxia, seizure, and progressive mental retardation. The clinical phenotype of galactosialidosis is very similar to that of sialidosis most probably due to the deficiency of sialidase which they have in common [108].

Galactosialidosis is autosomal recessively inherited and is genetically unrelated to sialidosis as the primary defect is in PPCA (Table 1-6).

The gene that transmits the disorder is localized on chromosome 20q13.1 [110]. Mainly single-base substitutions or splice-junction defects have been identified as cause.

The major clinical phenotype is caused by the deficient activity of sialidase. The resulting urinary excretion of sialyloligosaccharides has been reported to be similar to that found in sialidosis [111,112]. Comparative studies of oligosaccharides excreted by galactosialidosis and sialidosis patients have yielded conflicting results: Takahashi *et al*.[107] found excessive galactosyl-terminated oligosaccharides in galactosialidosis patients, while these compounds were not detected by van Pelt *et al*. [112,113].

1.3.8 G_{M1}-gangliosidosis

The lysosomal storage disorder G_{M1}-gangliosidosis was first described by Suzuki *et al*. [114]. G_{M1}-gangliosidosis is divided into three phenotypes. Type 1 or infantile type shows an onset mostly before 6 months of age. The development of the infant shows delay in the first 6 months and after this period severe brain damage becomes obvious. Macular cherry red spots, hepatosplenomegaly, dysmorphism, and generalized skeletal dysplasia are observed. Within two years after onset the disease is fatal. Type 2 or late infantile/juvenile type G_{M1}-gangliosidosis shows an onset between 7 months and 3 years of age and presents with a heterogeneous phenotypic appearance. The range of symptoms is the same as for type 1 but not all of them are observed in affected patients. The type 2 of the disorder is fatal within 5 years of age. The type 3 or adult/chronic form shows an onset from 3 to 10 years of age. Macular cherry red spots, dysmorphism, and hepatosplenomegaly are absent. Generalized skeletal dysplasia is observed. Type 3 is fatal after approximately 30 years of age. The 3 types of G_{M1}-gangliosidosis have the storage of ganglioside G_{M1} and oligosaccharides derived from glycoproteins in common [115,116]. G_{M1}-gangliosidosis is caused by the deficiency of β-galactosidase (EC 3.2.1.23) and is autosomal recessively inherited. The gene of human β-galactosidase is localized on chromosome 3p21.33. Heterogeneous gene mutations have been found. Five common mutations have been described: for type 1 R208C in American patients [117] and R482H in Italian patients [118]; for type 2, R201C in Japanese patients [119,120]; and for type 3, I51T in Japanese patients [119]. Galactosyl oligosaccharides are found in urine samples of patients suffering from G_{M1}-gangliosidosis [121-124]. A correlation has been established between severity of the disease and the concentration of the excreted galactosyl oligosaccharides [123,124].

Table 1-6. Relation of PPCA to LSDs [109].

Enzyme or protein	deficiency leads to	Disorder
Sialidase	⟶	Sialidosis
↑ activation		
PPCA	⟶	Galactosialidosis
↓ stabilization		
β-Galactosidase	⟶	G_{M1}-gangliosidosis

1.3.9 G_{M2}-gangliosidosis

There are three essential lysosomal polypeptides needed for the cleavage of the *N*-acetylgalactosamine at the non-reducing end for metabolic recycling of different glycan moieties such as G_{M2}-ganglioside. The G_{M2}-ganglioside requires to be complexed with the substrate-specific liftase G_{M2}-activator protein [125] to facilitate enzymatic hydrolysis of the GalNAc at the non-reducing end by β-hexosaminidase (EC 3.2.1.52). There are two isoenzymes of β-hexosaminidase: β-hexosaminidase A (Hex A) with heterodimeric structure αβ, and β-hexosaminidase B (Hex B) with homodimeric structure ββ. Hex A is the only isozyme that can hydrolyze G_{M2}-ganglioside *in vivo* [126]. The G_{M2}-ganglioside/G_{M2} activator protein complex only interacts with Hex A. Consequently there are three different variants of G_{M2}-gangliosidosis and they are caused by defects in different genes. Sandhoff *et al*. [127] proposed a classification based on the β-hexosaminidase isoenzyme that is still active in tissue of affected patients. In Tay-Sachs disease and its variants (variant B) Hex A activity is deficient and the deficiency is caused by mutations of the HEX A gene encoding for the α subunit. Sandhoff disease and its variants (variant 0) have a combined deficient activity of Hex A and Hex B and are caused by defects in the HEX B gene encoding for the β subunit common in Hex A and Hex B. In the AB variant the G_{M2}-activator protein is defect which is caused by mutations in the GM2A gene. Hydrolysis of ganglioside G_{M2} by Hex A is impaired by the absence or defective formation of the G_{M2}-activator protein/ganglioside G_{M2} complex [128].

The above-mentioned way of describing G_{M2}-gangliosidosis is impractical for describing the large spectrum of clinical variance observed. Classification by clinical designations recognizes the dominance of the encephalopathy rather than the age of onset as the primary clinical delineator [129]. The clinical phenotype of infantile acute G_{M2}-gangliosidosis is indistinguishable from Tay-Sachs disease, Sandhoff disease, and G_{M2}-activator protein deficiency (AB variant). The first signs of onset are often only recognized in retrospect but start at 3 to 5 months with mild motor weakness. Clinical observations are regression and even loss of acquired mental skills, organomegaly, ophthalmology, macular cherry red spot, macrocephaly, and death between 1 to 2 years of age.

The next phenotype is the late-onset form of G_{M2}-gangliosidosis. This phenotype is not known for variant AB. The clinical phenotype varies widely in the late onset type of Tay-Sachs and Sandhoff disease. Onset varies from late infantile period to adult age. Macular cherry red spot are less frequent observed. In some patients mental capacity can be well preserved, although often masked by dysarthria. The onset of subacute G_{M2}-gangliosidosis starts between 2 and 10 years of age by the development of ataxia and incoordination. Clinical phenotype includes regression in speech and life skills, dementia, psychomotor deterioration, increasing spasticity, and loss of vision. A vegetative state with decerebrate rigidity and involuntary extension of the upper extremities in response to external stimuli indicating brain stem damage, develops around 10 to 15 years of age, followed within a few years by death, usually due to intercurrent infections. Patients suffering chronic G_{M2}-gangliosidosis show onset from childhood to adulthood. G_{M2}-gangliosidosis is an autosomal recessively inherited disorder. HEXA maps to chromosome 15, while HEXB and GM2A maps to chromosome 5. Infantile, subacute, or chronic disease forms of G_{M2}-gangliosidosis can be distinguished in mutations of DNA. The estimated heterozygote frequencies in the general population are 0.006 for HEXA and 0.0036 for HEXB mutations. In some ethnic groups, the observed carrier frequencies are remarkably higher. The heterozygote frequency for HEXA mutations is 0.033 for the Ashkenazi

Jewish population [129,130]. For all variants of G_{M2}-gangliosidosis the major neural storage compound is ganglioside G_{M2} [130-132]. The ubiquitous storage compounds in Sandhoff disease are oligosaccharides derived from glycoproteins. Blockage of the N-glycan catabolism results in accumulation of β-endo-*N*-acetylglucosaminidase cleaved oligosaccharides carrying a single *N*-acetylglucosamine residue at the non reducing end which are found in the urine of Sandhoff disease patients [129,133-136].

1.3.10 Diagnostic methods in lysosomal storage disorders

The group of lysosomal storage disorders contains a subgroup of disorders called heteroglycanoses which are characterized by the excretion of glycans and / or glycoconjugates in urine. The only accepted method to determine these disorders unambiguously is the determination of the specific (reduced) enzyme activity. Not all clinical laboratories are equipped for these expensive and difficult assays [137]. Another way is to screen for excess urinary glycans with paper chromatography [138] or thin layer chromatography [139]. These methods are often unreliable [140,141]. Interpretation of a TLC pattern of excreted oligosaccharides is sophisticated and needs extraordinary skills [137]. HPLC appears to be an attractive alternative that could overcome some of the limitations of TLC pattern interpretation. Derivatization of glycans is necessary for UV or fluorescence detection or to obtain interaction with stationary phases commonly used in HPLC [142-144]. Derivatization of saccharides is depending on reducing ends for reductive amination reactions [145,146]. HPAEC and PAD do not depend on derivatization and are therefore more broadly applicable for characterization of saccharides [14,147,148]. Hommes *et al*. have reported on the diagnostic use of HPAEC-PAD for heteroglycanoses disorders [149].

1.4 SCOPE OF THE THESIS

High performance anion-exchange chromatography with pulsed amperometric detection is a well-accepted method for separating and characterizing carbohydrates [13,14]. Downscaling of column dimension is a viable approach in glycan analysis technology to achieve better sensitivity for the analysis of samples available in limited amount. The miniaturization of the column comes together with lower eluent flow rates, which is advantageous for mass spectroscopy. HPAEC hyphenated to an ion trap mass spectrometer is a strong analytical combination for identifying carbohydrates and for performing partial structural elucidation. This thesis reports on the development of a capillary scale HPAEC using prototype capillary columns as well as a prototype desalter which allows the hyphenation to ESI-MS. To investigate the applicability and value of capillary HPAEC in biomedical research, urine and ascitic fluid samples from patients suffering from a range of disorders that affect the lysosomal carbohydrate catabolism were investigated. In addition, amniotic fluid samples from mothers carrying a diseased child were analyzed. The selectivity of HPAEC in combination with the better sensitivity of the new platform and the informative data generated by MS detection has provided new insights into the catabolism of glycoconjugates. Thus, this thesis demonstrates the usefulness of HPAEC-PAD-MS as an analytical tool in oligosaccharide analysis, both with regard to glycan structural elucidation and to glycan profiling.

REFERENCES

1. Apweiler R, Hermjakob H, & Sharon N (1999) On the frequency of protein glycosylation, as deduced from analysis of the SWISS-PROT database. *Biochim Biophys Acta* **1473,** 4-8.
2. Slawson C, Housley MP, & Hart GW (2006) O-GlcNAc cycling: how a single sugar post-translational modification is changing the way we think about signaling networks. *J Cell Biochem* **97,** 71-83.
3. Zachara NE & Hart GW (2002) The emerging significance of O-GlcNAc in cellular regulation. *Chem Rev* **102,** 431-438.
4. Dwek RA (1996) Glycobiology: Toward Understanding the Function of Sugars. *Chem Rev* **96,** 683-720.
5. Varki A (1993) Biological roles of oligosaccharides: all of the theories are correct. *Glycobiology* **3,** 97-130.
6. Helenius A & Aebi M (2004) Roles of N-linked glycans in the endoplasmic reticulum. *Annu Rev Biochem* **73,** 1019-1049.
7. Haltiwanger RS & Lowe JB (2004) Role of glycosylation in development. *Annu Rev Biochem* **73,** 491-537.
8. Zachara NE & Hart GW (2004) O-GlcNAc a sensor of cellular state: the role of nucleocytoplasmic glycosylation in modulating cellular function in response to nutrition and stress. *Biochim Biophys Acta* **1673,** 13-28.
9. Rabinovich GA, van Kooyk Y, & Cobb BA (2012) Glycobiology of immune responses. *Ann N Y Acad Sci* **1253,** 1-15.
10. Winchester B (2005) Lysosomal metabolism of glycoproteins. *Glycobiology* **15,** 1R-15R.
11. Small,H. (1989) *Ion Chromatography*, 1989 edn. Plenium Publishing Corp., New York.
12. Weiss,J. (2004) *Handbook of Ion Chromatography*, 3 edn. VCH, Weinheim.
13. Lee YC (1990) High-performance anion-exchange chromatography for carbohydrate analysis. *Anal Biochem* **189,** 151-162.
14. Townsend RR, Hardy MR, Hindsgaul O, & Lee YC (1988) High-performance anion-exchange chromatography of oligosaccharides using pellicular resins and pulsed amperometric detection. *Anal Biochem* **174,** 459-470.
15. Hardy M.R. & Rohrer J. (2007) High-pH Anion-Exchange Chromatography (HPAEC) and Pulsed Amperometric Detection (PAD) for Carbohydrate Analysis . In *Comprehensive Glycoscience - From Chemistry to Systems Biology* (Kamerling,J.P., Boons,G.J., Lee,Y.C., Suzuki,A., Taniguchi,N., & Voragen,F., eds), pp. 303-324. Elsevier B.V..
16. Khym JX & Zill LP (1952) The Separation of Sugars by Ion Exchange. *J Am Chem Soc* **74,** 2090-2094.
17. Zill LP, Khym JX, & Cheniae GM (1953) Further Studies on the Separation of the Borate Complexes of Sugars and Related Compounds by Ion-exchange Chromatography. *J Am Chem Soc* **75,** 1339-1342.
18. Sinner M, Simatupang MH, & Dietrichs HH (1975) Automated Quantitative Analysis of Wood Carbohydrates by Borate Complex Ion Exchange Chromatography. *Wood Sci Techn* **9,** 307-322.
19. Keilich G & Ziegler D (1975) Simultaneous Assay of Neutral Sugars and Amino Sugars by an Automatic Sugar Analyzer Applications to Glycoproteins. *Hoppe Seylers Z Physiol Chem* **356,** 417-423.
20. Sinner M & Puls J (1978) Non-corrosive dye reagent for detection of reducing sugars in borate complex ion-exchange chromatography. *J Chromatogr* **156,** 197-204.
21. Honda S, Takahashi M, Kakehi K, & Ganno S (1981) Rapid, automated analysis of monosaccharides by high-performance anion-exchange chromatography of borate complexes with fluorimetric detection using 2-cyanoacetamide. *Anal Biochem* **113,** 130-138.
22. Bauer H & Voelter W (1976) Ionenaustausch-Chromatographie von Kohlenhydraten. *Chromatographia* **9,** 433-439.
23. Small H, Stevens TS, & Bauman WC (1975) Novel ion exchange chromatographic method using conductometric detection. *Anal Chem* **47,** 1801-1809.
24. Hughes S & Johnson DC (1981) Amperometric detection of simple carbohydrates at platinum electrodes in alkaline solutions by applcation of a triple-pulse potential waveform. *Anal Chim Acta* **132,** 11-22.
25. Rocklin RD & Pohl CA (1983) Determination of Carbohydrates by Anion Exchange Chromatography with Pulsed Amperometric Detection. *J liq chromatogr* **6,** 1577-1590.
26. (2011) *Lange's handbook of chemistry*, 3th edn.
27. Bruggink C. (2012) Oligosaccharide analysis by high-performance anion-exchange chromatography hyphenated to integrated pulsed amperometric detection and on-line ion-trap mass spectrometry. In *Applications of ion chromatography for pharmaceutical and biological products* (Bhattacharyya,L. & Rohrer,J.S., eds), pp. 379-391. John Wiley & Sons, Inc..

28. Koizumi K, Kubota Y, Ozaki H, Keiko S, Fukuda M, & Tanimoto T (1992) Analyses of isomeric mono-O-methyl-d-glucoses, d-glucobioses and d-glucose monophosphates by high-performance anion-exchange chromatography with pulsed amperometric detection. *J Chromatogr A* **595,** 340-345.
29. Hardy MR & Townsend RR (1988) Separation of positional isomers of oligosaccharides and glycopeptides by high-performance anion-exchange chromatography with pulsed amperometric detection. *Proc Natl Acad Sci U S A* **85,** 3289-3293.
30. Cataldi TR, Campa C, & De Benedetto GE (2000) Carbohydrate analysis by high-performance anion-exchange chromatography with pulsed amperometric detection: the potential is still growing. *Fresenius J Anal Chem* **368,** 739-758.
31. Rocklin RD, Tullsen TR, & Marucco MG (1994) Maximizing signal-to-noise ratio in direct current and pulsed amperometric detection. *J Chromatogr A* **671,** 109-114.
32. LaCourse WR & Johnson DC (1993) Optimization of Waveforms for Pulsed Amperometric Detection of Carbohydrates Based on Pulsed Voltammetry. *Anal Chem* **65,** 50-55.
33. Rocklin RD, Clarke AP, & Weitzhandler M (1998) Improved long-term reproducibility for pulsed amperometric detection of carbohydrates via a new quadruple-potential waveform. *Anal Chem* **70,** 1496-1501.
34. Thayer JR, Rohrer JS, Avdalovic N, & Gearing RP (1998) Improvements to in-line desalting of oligosaccharides separated by high-pH anion exchange chromatography with pulsed amperometric detection. *Anal Biochem* **256,** 207-216.
35. Quemener B, Desire C, Lahaye M, Debrauwer L, & Negroni L (2003) Structural characterisation by both positive- and negative-ion electrospray mass spectrometry of partially methyl-esterified oligogalacturonides purified by semi-preparative high-performance anion-exchange chromatography. *Eur J Mass Spectrom (Chichester, Eng)* **9,** 45-60.
36. Barroso B, Dijkstra R, Geerts M, Lagerwerf F, van Veelen P, & de Ru A (2002) On-line high-performance liquid chromatography/mass spectrometric characterization of native oligosaccharides from glycoproteins. *Rapid Commun Mass Spectrom* **16,** 1320-1329.
37. Mohr MD, Bornsen KO, & Widmer HM (1995) Matrix-assisted laser desorption/ionization mass spectrometry: improved matrix for oligosaccharides. *Rapid Commun Mass Spectrom* **9,** 809-814.
38. Harvey DJ (2005) Structural determination of N-linked glycans by matrix-assisted laser desorption/ionization and electrospray ionization mass spectrometry. *Proteomics* **5,** 1774-1786.
39. Penn SG, Cancilla MT, & Lebrilla CB (1996) Collision-induced dissociation of branched oligosaccharide ions with analysis and calculation of relative dissociation thresholds. *Anal Chem* **68,** 2331-2339.
40. Wong CKL & Chan T-W (1997) Cationization Processes in Matrix-assisted Laser Desorption/Ionization Mass Spectrometry: Attachment of Divalent and Trivalent Metal Ions. *Rapid Commun Mass Spectrom* **11,** 513-519.
41. Franz AH & Lebrilla CB (2002) Evidence for long-range glycosyl transfer reactions in the gas phase. *J Am Soc Mass Spectrom* **13,** 325-337.
42. Harvey DJ, Mattu TS, Wormald MR, Royle L, Dwek RA, & Rudd PM (2002) "Internal residue loss": rearrangements occurring during the fragmentation of carbohydrates derivatized at the reducing terminus. *Anal Chem* **74,** 734-740.
43. Wuhrer M, Deelder AM, & van der Burgt YE (2011) Mass spectrometric glycan rearrangements. *Mass Spectrom Rev* **30,** 664-680.
44. Bruggink C, Maurer R, Herrmann H, Cavalli S, & Hoefler F (2005) Analysis of carbohydrates by anion exchange chromatography and mass spectrometry. *J Chromatogr A* **1085,** 104-109.
45. Harvey DJ (2000) Electrospray mass spectrometry and fragmentation of N-linked carbohydrates derivatized at the reducing terminus. *J Am Soc Mass Spectrom* **11,** 900-915.
46. Spina E, Sturiale L, Romeo D, Impallomeni G, Garozzo D, Waidelich D, & Glueckmann M (2004) New fragmentation mechanisms in matrix-assisted laser desorption/ionization time-of-flight/time-of-flight tandem mass spectrometry of carbohydrates. *Rapid Commun Mass Spectrom* **18,** 392-398.
47. Weiskopf AS, Vouros P, & Harvey DJ (1998) Electrospray ionization-ion trap mass spectrometry for structural analysis of complex N-linked glycoprotein oligosaccharides. *Anal Chem* **70,** 4441-4447.
48. Domon B & Costello CE (1988) A Systematic Nomenclature for Carbohydrate Fragmentations in FAB-MS/MS Spectra of Glycoconjugates. *J Glycoconj* **5,** 397-409.
49. LaCourse,W.R. (1997) *Pusled Electrochemical Detection in High-Performance Liquid Chromatography*. John Wiley & Sons Inc., New York.
50. Vellodi A (2005) Lysosomal storage disorders. *Br J Haematol* **128,** 413-431.
51. De Duve C & Wattiaux R (1966) Functions of lysosomes. *Annu Rev Physiol* **28,** 435-492.

52. Aronson NN, Jr. & Kuranda MJ (1989) Lysosomal degradation of Asn-linked glycoproteins. *FASEB J* **3,** 2615-2622.
53. Fisher KJ & Aronson NN, Jr. (1992) Cloning and expression of the cDNA sequence encoding the lysosomal glycosidase di-N-acetylchitobiase. *J Biol Chem* **267,** 19607-19616.
54. Froesch M, Bindila L, Zamfir A, & Peter-Katalinic J (2003) Sialylation analysis of O-glycosylated sialylated peptides from urine of patients suffering from Schindler's disease by Fourier transform ion cyclotron resonance mass spectrometry and sustained off-resonance irradiation collision-induced dissociation. *Rapid Commun Mass Spectrom* **17,** 2822-2832.
55. Neufeld E.F. & Muenzer J. (2002) The Mucopolysaccharidosis. In *Lysosomal disorders* (Bunz, Gibson, & Mitchell, eds), The McGraw-Hill Companies, Inc., New York.
56. Golks A & Guerini D (2008) The O-linked N-acetylglucosamine modification in cellular signalling and the immune system. 'Protein modifications: beyond the usual suspects' review series. *EMBO Rep* **9,** 748-753.
57. Hart GW (1997) Dynamic O-linked glycosylation of nuclear and cytoskeletal proteins. *Annu Rev Biochem* **66,** 315-335.
58. Wilkening G, Linke T, Uhlhorn-Dierks G, & Sandhoff K (2000) Degradation of membrane-bound ganglioside GM1. Stimulation by bis(monoacylglycero)phosphate and the activator proteins SAP-B and GM2-AP. *J Biol Chem* **275,** 35814-35819.
59. Ramsay SL, Maire I, Bindloss C, Fuller M, Whitfield PD, Piraud M, Hopwood JJ, & Meikle PJ (2004) Determination of oligosaccharides and glycolipids in amniotic fluid by electrospray ionisation tandem mass spectrometry: in utero indicators of lysosomal storage diseases. *Mol Genet Metab* **83,** 231-238.
60. Wraith JE (2002) Lysosomal disorders. *Semin Neonatol* **7,** 75-83.
61. Futerman AH & van Meer G (2004) The cell biology of lysosomal storage disorders. *Nat Rev Mol Cell Biol* **5,** 554-565.
62. Johnson SW & Alhadeff JA (1991) Mammalian alpha-L-fucosidases. *Comp Biochem Physiol B* **99,** 479-488.
63. Durand P, Borrone C, Della Cella G, & Philippart M (1968) Fucosidosis. *Lancet* **291,** 1198.
64. Van Hoof F & Hers HG (1968) Mucopolysaccharidosis by absence of alpha-fucosidase. *Lancet* **1,** 1198.
65. Willems PJ, Gatti R, Darby JK, Romeo G, Durand P, Dumon JE, & O'Brien JS (1991) Fucosidosis revisited: a review of 77 patients. *Am J Med Genet* **38,** 111-131.
66. Thomas H.T. (2002) Disorders of Glycoprotein Degradation: a-Mannosidosis, b-Mannosidosis, Fucosidosis, and Sialidosis. In *Lysosomal disorders* (Valle, Beaudet, Vogelstein, Kinzler, Antonarakis, & Ballabio, eds).
67. Willems PJ, Seo HC, Coucke P, Tonlorenzi R, & O'Brien JS (1999) Spectrum of mutations in fucosidosis. *Eur J Hum Genet* **7,** 60-67.
68. Lundblad A, Lundsten J, Nordén NE, Sjöblad S, Svensson S, Öckerman PA, & Gehlhoff M (1978) Urinary abnormalities in fucosidosis. *Eur J Biochem* **83,** 513-521.
69. Lundblad A. (1978) Oligosaccharides from human urine. In *Methods in Enzymology* (Ginsburg,V., ed), pp. 226-235. Academic Press, New York.
70. Strecker G, Fournet B, & Montreuil J (1978) Structure of the three major fucosyl-glycoasparagines accumulating in the urine of a patient with fucosidosis. *Biochimie* **60,** 725-734.
71. Yamashita K, Kochibe N, Ohkura T, Ueda I, & Kobata A (1985) Fractionation of L-fucose-containing oligosaccharides on immobilized Aleuria aurantia lectin. *J Biol Chem* **260,** 4688-4693.
72. Michalski JC & Klein A (1999) Glycoprotein lysosomal storage disorders: alpha- and beta-mannosidosis, fucosidosis and alpha-N-acetylgalactosaminidase deficiency. *Biochim Biophys Acta* **1455,** 69-84.
73. Öckerman PA & Lund MD (1967) A generalized storage disorder resembling Hurler's syndrome. *Lancet* **290,** 239-241.
74. Desnick RJ, Sharp HL, Grabowski GA, Brunning RD, Quie PG, Sung JH, Gorlin RJ, & Ikonne JU (1976) Mannosidosis: clinical, morphologic, immunologic, and biochemical studies. *Pediatr Res* **10,** 985-996.
75. Brook JD, Shaw DJ, Meredith L, Bruns GA, & Harper PS (1984) Localisation of genetic markers and orientation of the linkage group on chromosome 19. *Hum Genet* **68,** 282-285.
76. al Daher S, De Gasperi R, Daniel P, Hall N, Warren CD, & Winchester B (1991) The substrate-specificity of human lysosomal alpha-D-mannosidase in relation to genetic alpha-mannosidosis. *Biochem J* **277 (Pt 3),** 743-751.
77. DeGasperi R, Daniel PF, & Warren CD (1992) A human lysosomal alpha-mannosidase specific for the core of complex glycans. *J Biol Chem* **267,** 9706-9712.
78. Venkatesan M, Kuntz DA, & Rose DR (2009) Human lysosomal α-mannosidases exhibit different inhibition and metal binding properties. *Protein Sci* **18,** 2242-2251.

79. Strecker G, Fournet B, Bouquelet S, Montreuil J, Dhondt JL, & Farriaux JP (1976) Chemistry of urinary mannosides excreted in mannosidosis. *Biochimie* **58,** 579-586.
80. Yamashita K, Tachibana Y, Mihara K, Okada S, Yabuuchi H, & Kobata A (1980) Urinary oligosaccharides of mannosidosis. *J Biol Chem* **255,** 5126-5133.
81. Matsuura F, Nunez HA, Grabowski GA, & Sweeley CC (1981) Structural studies of urinary oligosaccharides from patients with mannosidosis. *Arch Biochem Biophys* **207,** 337-352.
82. Jardine I, Matsuura F, & Sweeley CC (1984) Electron ionization mass spectra of reduced and permethylated urinary oligosaccharides from patients with mannosidosis. *Biomed Mass Spectrom* **11,** 562-568.
83. Norden NE, Lundblad A, Svensson S, Ockerman PA, & Autio S (1973) A mannose-containing trisaccharide isolated from urines of three patients with mannosidosis. *J Biol Chem* **248,** 6210-6215.
84. Cantz M, Gehler J, & Spranger J (1977) Mucolipidosis I: increased sialic acid content and deficiency of an alpha-N-acetylneuraminidase in cultured fibroblasts. *Biochem Biophys Res Commun* **74,** 732-738.
85. Achyuthan KE & Achyuthan AM (2001) Comparative enzymology, biochemistry and pathophysiology of human exo-alpha-sialidases (neuraminidases). *Comp Biochem Physiol B Biochem Mol Biol* **129,** 29-64.
86. Pshezhetsky AV & Potier M (1996) Association of N-acetylgalactosamine-6-sulfate sulfatase with the multienzyme lysosomal complex of beta-galactosidase, cathepsin A, and neuraminidase. Possible implication for intralysosomal catabolism of keratan sulfate. *J Biol Chem* **271,** 28359-28365.
87. Pshezhetsky AV & Ashmarina M (2001) Lysosomal multienzyme complex: biochemistry, genetics, and molecular pathophysiology. *Prog Nucleic Acid Res Mol Biol* **69,** 81-114.
88. Van Diggelen OP, Hoogeveen AT, Smith PJ, Reuser AJ, & Galjaard H (1982) Enhanced proteolytic degradation of normal beta-galactosidase in the lysosomal storage disease with combined beta-galactosidase and neuraminidase deficiency. *Biochim Biophys Acta* **703,** 69-76.
89. Suzuki Y, Sakuraba H, Hayashi K, Suzuki K, & Imahori K (1981) Beta-galactosidase-neuraminidase deficiency: restoration of beta-galactosidase activity by protease inhibitors. *J Biochem* **90,** 271-273.
90. D'Azzo A, Hoogeveen A, Reuser AJ, Robinson D, & Galjaard H (1982) Molecular defect in combined beta-galactosidase and neuraminidase deficiency in man. *Proc Natl Acad Sci U S A* **79,** 4535-4539.
91. Verheijen FW, Palmeri S, Hoogeveen AT, & Galjaard H (1985) Human placental neuraminidase. Activation, stabilization and association with beta-galactosidase and its protective protein. *Eur J Biochem* **149,** 315-321.
92. Vinogradova MV, Michaud L, Mezentsev AV, Lukong KE, El Alfy M, Morales CR, Potier M, & Pshezhetsky AV (1998) Molecular mechanism of lysosomal sialidase deficiency in galactosialidosis involves its rapid degradation. *Biochem J* **330 (Pt 2),** 641-650.
93. van der Spoel A, Bonten E, & D'Azzo A (1998) Transport of human lysosomal neuraminidase to mature lysosomes requires protective protein/cathepsin A. *EMBO J* **17,** 1588-1597.
94. Durand P, Gatti R, Cavalieri S, Borrone C, Tondeur M, Michalski JC, & Strecker G (1977) Sialidosis (mucolipidosis I). *Helv Paediatr Acta* **32,** 391-400.
95. Lowden JA & O'Brien JS (1979) Sialidosis: a review of human neuraminidase deficiency. *Am J Hum Genet* **31,** 1-18.
96. O'Brien JS (1977) Neuraminidase deficiency in the cherry red spot-myoclonus syndrome. *Biochem Biophys Res Commun* **79,** 1136-1141.
97. Thomas GH, Tipton RE, Ch'ien LT, Reynolds LW, & Miller CS (1978) Sialidase (alpha-n-acetyl neuraminidase) deficiency: the enzyme defect in an adult with macular cherry-red spots and myoclonus without dementia. *Clin Genet* **13,** 369-379.
98. Rapin I, Goldfischer S, Katzman R, Engel J, Jr., & O'Brien JS (1978) The cherry-red spot--myoclonus syndrome. *Ann Neurol* **3,** 234-242.
99. Spranger JW & Wiedemann HR (1970) The genetic mucolipidoses. Diagnosis and differential diagnosis. *Humangenetik* **9,** 113-139.
100. Kelly TE & Graetz G (1977) Isolated acid neuraminidase deficiency: a distinct lysosomal storage disease. *Am J Med Genet* **1,** 31-46.
101. Bonten E, van der Spoel A, Fornerod M, Grosveld G, & D'Azzo A (1996) Characterization of human lysosomal neuraminidase defines the molecular basis of the metabolic storage disorder sialidosis. *Genes Dev* **10,** 3156-3169.
102. Pshezhetsky AV, Richard C, Michaud L, Igdoura S, Wang S, Elsliger MA, Qu J, Leclerc D, Gravel R, Dallaire L, & Potier M (1997) Cloning, expression and chromosomal mapping of human lysosomal sialidase and characterization of mutations in sialidosis. *Nat Genet* **15,** 316-320.
103. Aylsworth AS, Thomas GH, Hood JL, Malouf N, & Libert J (1980) A severe infantile sialidosis: clinical, biochemical, and microscopic features. *J Pediatr* **96,** 662-668.

104. Strecker G, Peers MC, Michalski JC, Hondi-Assah T, Fournet B, Spik G, Montreuil J, Farriaux JP, Maroteaux P, & Durand P (1977) Structure of nine sialyl-oligosaccharides accumulated in urine of eleven patients with three different types of sialidosis. Mucolipidosis II and two new types of mucolipidosis. *Eur J Biochem* **75,** 391-403.
105. Dorland L, Haverkamp J, Vliegenthart JF, Strecker G, Michalski JC, Fournet B, Spik G, & Montreuil J (1978) 360-MHz 1H nuclear-magnetic-resonance spectroscopy of sialyl-oligosaccharides from patients with sialidosis (mucolipidosis I and II). *Eur J Biochem* **87,** 323-329.
106. Strecker G & Michalski JC (1978) Biochemical basis of six different types of sialidosis. *FEBS Lett* **85,** 20-24.
107. Takahashi Y, Nakamura Y, Yamaguchi S, & Orii T (1991) Urinary oligosaccharide excretion and severity of galactosialidosis and sialidosis. *Clin Chim Acta* **203,** 199-210.
108. D'Azzo A., Andria G., Strisciuglio P., & Galjaard H. (2002) Galactosialidosis. In *Lysosomal disorders* (Valle, Beaudet, Vogelstein, Kinzler, Antonarakis, & Bellabio, eds), pp. 3811-3828. The McGraw-Hill Companies, Inc., New York.
109. van Pelt J, Isolation and structural analysis of sialyloligosaccharides from sialidosis and galactosialidosis fibroblasts, placenta and urine. 1-136. 1988. Rijksuniversiteit Utrecht. Ref Type: Thesis/Dissertation.
110. Wiegant J, Galjart NJ, Raap AK, & D'Azzo A (1991) The Gene Encoding Human Protective Protein (PPGB) is on Chromosome 20. *Genomics* **10,** 345-349.
111. Cantz M & Ulrich-Bott B (1990) Disorders of glycoprotein degradation. *J Inherit Metab Dis* **13,** 523-537.
112. van Pelt J, Kamerling JP, Bakker HD, & Vliegenthart JF (1991) A comparative study of sialyloligosaccharides isolated from sialidosis and galactosialidosis urine. *J Inherit Metab Dis* **14,** 730-740.
113. van Pelt J, Hard K, Kamerling JP, Vliegenthart JF, Reuser AJ, & Galjaard H (1989) Isolation and structural characterization of twenty-one sialyloligosaccharides from galactosialidosis urine. An intact N,N'-diacetylchitobiose unit at the reducing end of a diantennary structure. *Biol Chem Hoppe Seyler* **370,** 191-203.
114. Suzuki K & Chen CC (1967) Brain ceramide hexosides in Tay-Sachs disease and generalized gangliosidosis (GM1-gangliosidosis). *J Lipid Res* **8,** 105-113.
115. Suzuki Y., Nanba E., Matsuda J., Higaki K., & Oshima A. (2002) β-Galactosidase Deficiency (β-Galactosidosis): GM1 Gangliosidosis and Morquio B Disease. In *Lysosomal disorders* (Vall, Beaudet, Bunz, Vogelstein, Kinzler, Antonarakis, Ballabio, Gibson, & Mitchell, eds).
116. Takahashi Y & Orii T (1989) Severity of GM1 gangliosidosis and urinary oligosaccharide excretion. *Clin Chim Acta* **179,** 153-162.
117. Boustany RM, Qian WH, & Suzuki K (1993) Mutations in acid beta-galactosidase cause GM1-gangliosidosis in American patients. *Am J Hum Genet* **53,** 881-888.
118. Mosna G, Fattore S, Tubiello G, Brocca S, Trubia M, Gianazza E, Gatti R, Danesino C, Minelli A, & Piantada M (1992) A homozygous missense arginine to histidine substitution at position 482 of the beta-galactosidase in an Italian infantile GM1-gangliosidosis patient. *Hum Genet* **90,** 247-250.
119. Yoshida K, Oshima A, Shimmoto M, Fukuhara Y, Sakuraba H, Yanagisawa N, & Suzuki Y (1991) Human beta-galactosidase gene mutations in GM1-gangliosidosis: a common mutation among Japanese adult/chronic cases. *Am J Hum Genet* **49,** 435-442.
120. Nishimoto J, Nanba E, Inui K, Okada S, & Suzuki K (1991) GM1-gangliosidosis (genetic beta-galactosidase deficiency): identification of four mutations in different clinical phenotypes among Japanese patients. *Am J Hum Genet* **49,** 566-574.
121. Lundblad A, Sjöblad S, & Svensson S (2011) Characterization of a Penta- and Octasaccharide from urine of a paitient with juvenile GM1-gangliosidosis. *Arch Biochem Biophys* **188,** 130-136.
122. Ohkura T, Yamashita K, & Kobata A (1981) Urinary oligosaccharides of GM1-gangliosidosis. Structures of oligosaccharides excreted in the urine of type 1 but not in the urine of type 2 patients. *J Biol Chem* **256,** 8485-8490.
123. Yamashita K, Ohkura T, Okada S, Yabuuchi H, & Kobata A (1981) Urinary oligosaccharides of GM1-gangliosidosis. Different excretion patterns of oligosaccharides in the urine of type 1 and type 2 subgroups. *J Biol Chem* **256,** 4789-4798.
124. Warner TG, Robertson AD, Mock AK, Johnson WG, & O'Brien JS (1983) Prenatal diagnosis of GM1 gangliosidosis by detection of galactosyl-oligosaccharides in amniotic fluid with high-performance liquid chromatography. *Am J Hum Genet* **35,** 1034-1041.
125. Kolter T & Sandhoff K (2005) Principles of lysosomal membrane digestion: stimulation of sphingolipid degradation by sphingolipid activator proteins and anionic lysosomal lipids. *Annu Rev Cell Dev Biol* **21,** 81-103.
126. Hou Y, Tse R, & Mahuran DJ (1996) Direct determination of the substrate specificity of the alpha-active site in heterodimeric beta-hexosaminidase A. *Biochemistry (Mosc)* **35,** 3963-3969.

127. Sandhoff K, Andreae U, & Jatzewitz H (1968) Deficient hexosaminidase activity in an exceptional case of Tay-Sachs disease with additional storage of kidney globoside in visceral organs. *Pathol Eur* **3,** 278-285.
128. Sandhoff K, Harzer K, Wässle W, & Jatzewitz H (1971) Enzyme alterations and lipid storage in three variants of Tay-Sachs disease. *J Neurochem* **18,** 2469-2489.
129. Gravel R.A., Kaback M.M., Proia R.L., Sandhoff K., & Suzuki K. (2002) The GM2. In *Lysosomal disorders* (Valle, Beaudet, Vogelstein, Kinzler, Antonarakis, & Bellabio, eds), McGraw-Hill, New York.
130. Mahuran DJ (1999) Biochemical consequences of mutations causing the GM2 gangliosidoses. *Biochim Biophys Acta* **1455,** 105-138.
131. Rubin M, Karpati G, Wolfe LS, Carpenter S, Klavins MH, & Mahuran DJ (1988) Adult onset motor neuronopathy in the juvenile type of hexosaminidase A and B deficiency. *J Neurol Sci* **87,** 103-119.
132. Hoffman LM, Amsterdam D, Brooks SE, & Schneck L (1977) Glycosphingolipids in fetal Tay-Sachs disease brain and lung cultures. *J Neurochem* **29,** 551-559.
133. Bolhuis PA, Oonk JG, Kamp PE, Ris AJ, Michalski JC, Overdijk B, & Reuser AJ (1987) Ganglioside storage, hexosaminidase lability, and urinary oligosaccharides in adult Sandhoff's disease. *Neurology* **37,** 75-81.
134. Kolter T & Sandhoff K (2006) Sphingolipid metabolism diseases. *Biochim Biophys Acta* **1758,** 2057-2079.
135. Strecker G, Herlant-Peers MC, Fournet B, & Montreul J (1977) Structure of seven oligosaccharides excreted in the urine of a patient with Sandhoff's disease (GM2 gangliosidosis-variant O). *Eur J Biochem* **81,** 165-171.
136. Warner TG, De Kremer RD, Applegarth D, & Mock AK (1986) Diagnosis and characterization of GM 2 gangliosidosis type II (Sandhoff disease) by analysis of the accumulating N-acetyl-glucosaminyl oligosaccharides with high performance liquid chromatography. *Clin Chim Acta* **154,** 151-164.
137. Sewell AC, Gehler J, & Spranger J (1979) Comprehensive urinary screening for inborn errors of complex carbohydrate metabolism. *Klin Wochenschr* **57,** 581-585.
138. Strecker G (1977) Fractionation and characterization of acidic oligosaccharides and glycopeptides from normal and pathological urines. *J Chromatogr* **143,** 553-569.
139. Humbel R & Collart M (1975) Oligosaccharides in urine of patients with glycoprotein storage diseases. I. Rapid detection by thin-layer chromatography. *Clin Chim Acta* **60,** 143-145.
140. Okada S, Kato T, Miura S, Yabuuchi H, Nishigaki M, Kobata A, Chivo H, & Furuyama JL (1978) Hypersialyloligosaccharidu ria in mucolipidoses: a method for diagnosis. *Clin Chim Acta* **86,** 159-167.
141. Sewell AC (1979) An improved thin-layer chromatographic method for urinary oligosaccharide screening. *Clin Chim Acta* **92,** 411-414.
142. An Y, Young SP, Hillman SL, Van Hove JL, Chen YT, & Millington DS (2000) Liquid chromatographic assay for a glucose tetrasaccharide, a putative biomarker for the diagnosis of Pompe disease. *Anal Biochem* **287,** 136-143.
143. Neville DC, Dwek RA, & Butters TD (2009) Development of a single column method for the separation of lipid- and protein-derived oligosaccharides. *J Proteome Res* **8,** 681-687.
144. Wuhrer M, Deelder AM, & Hokke CH (2005) Protein glycosylation analysis by liquid chromatography-mass spectrometry. *J Chromatogr B Biomed Sci App* **825,** 124-133.
145. Anumula KR (2006) Advances in fluorescence derivatization methods for high-performance liquid chromatographic analysis of glycoprotein carbohydrates. *Anal Biochem* **350,** 1-23.
146. Ruhaak LR, Zauner G, Huhn C, Bruggink C, Deelder AM, & Wuhrer M (2010) Glycan labeling strategies and their use in identification and quantification. *Anal Bioanal Chem* **397,** 3457-3481.
147. Townsend RR, Hardy MR, & Lee YC (1989) Separation of oligosaccharides using high-performance anion-exchange chromatography with pulsed amperometric detection. *Methods Enzymol* **179,** 65-76.
148. Wang WT, Erlansson K, Lundgren T, & Zopf D (1990) High-performance liquid chromatography of sialic acid-containing oligosaccharides and acidic monosaccharides. *Anal Biochem* **190,** 182-187.
149. Hommes FA & Varghese M (1991) High-performance liquid chromatography of urinary oligosaccharides in the diagnosis of glycoprotein degradation disorders. *Clin Chim Acta* **203,** 211-224.

2

ANALYSIS OF CARBOHYDRATES BY ANION-EXCHANGE CHROMATOGRAPHY AND MASS SPECTROMETRY

2.1 ABSTRACT

A versatile liquid chromatographic platform has been developed for analyzing underivatized carbohydrates using high-performance anion-exchange chromatography (HPAEC) followed by an inert PEEK splitter that splits the effluent to the integrated pulsed amperometric detector (IPAD) and to an on-line single quadrupole mass spectrometer (MS). Common eluents for HPAEC such as sodium hydroxide and sodium acetate are beneficial for the amperometric detection but not compatible with electrospray ionization (ESI). Therefore a membrane-desalting device was installed after the splitter and prior to the ESI interface converting sodium hydroxide into water and sodium acetate into acetic acid. To enhance the sensitivity for the MS detection, 0.5 mmol/l lithium chloride was added after the membrane desalter to form lithium adducts of the carbohydrates. To compare sensitivity of IPAD and MS detection glucose, fructose, and sucrose were used as analytes. A calibration with external standards from 2.5 to 1000 pmole was performed showing a linear range over three orders of magnitude. Minimum detection limits (MDL) with IPAD were determined at 5 pmole levels for glucose to be 0.12 pmole, fructose 0.22 pmole and sucrose 0.11 pmole. With MS detection in the selected ion mode (SIM) the lithium adducts of the carbohydrates were detected obtaining MDL's for glucose of 1.49 pmole, fructose 1.19 pmole, and sucrose 0.36 pmole showing that under these conditions IPAD is 3–10 times more sensitive for those carbohydrates. The applicability of the method was demonstrated analyzing carbohydrates in real world samples such as chicory inulin where polyfructans up to a molecular mass of 7000 g/mol were detected as quadruple charged lithium adducts. Furthermore mono-, di-, tri, and oligosaccharides were detected in chicory coffee, honey and beer samples.

Cees Bruggink [a], Rolf Maurer [b], Heiko Herrmann [c], Silvano Cavalli [d], Frank Hoefler [e]

[a] Dionex B.V., Lange Bunder 5, 4854 MB Bavel, The Netherlands
[b] Dionex (Switzerland) AG, Solothurnerstrasse 259, CH-4600 Olten, Switzerland
[c] Dionex GmbH, Am Wörtzgarten 10, D-65510 Idstein, Germany
[d] Dionex S.r.l., Via Tulipani 1, 20090 Pieve Emanuele, Italy
[e] Dionex (Europe) Management AG, Solothurnerstrasse 259, CH-4600 Olten, Switzerland

Journal of Chromatography A (2005) 1085; 104–109.

2.2 INTRODUCTION

Liquid chromatographic methods play an important role in determining carbohydrates. Normal-phase and porous graphitized carbon allow the separation of underivatized carbohydrates. Underivatized carbohydrates lacks a chromophore and in combination with an isocratic separation refractive index detection can be performed while evaporating light scattering can be used following isocratic and gradient separations [1,2]. A well-established technique for determining underivatized carbohydrates is anion-exchange chromatography (HPAEC) using alkali hydroxide and alkali acetate based eluents [3,4]. The high efficient separation of sugar alcohols, mono-, di- and oligosaccharides up to a degree of polymerization (DP) of 60 is possible [4]. Today, selective and sensitive detection integrated pulsed amperometric detection (IPAD) is used, which is directly compatible with the high ionic strength of these eluents [5].

For verification of the identity of individual sugars the retention times of the peaks are compared with those obtained from reference solutions. Fractions are collected of unknown peaks and identified offline by MS, NMR or other techniques [6].

For further development of carbohydrate analysis online MS detection is required for faster and more reliable identification and peak conformation according to their mass to charge ratio. Interfacing anion-exchange chromatography with mass spectrometric detection is a technological challenge. Typical alkali acetate and hydroxide eluents are not compatible with atmospheric pressure ionization (API) due to their non-volatility and high conductance, therefore, a desalting device is installed between the column and the MS. The desalter converts the alkali hydroxide and acetate into water and acetic acid continuously exchanging the alkali cations by hydronium ions using a selective cation-exchange membrane and a regenerant [4,7].

To enhance sensitivity of the neutral carbohydrates, 0.5 mmol/l LiCl is added after the desalter and prior to the MS using a T-piece and an auxiliary pump. Lithium chloride is forming charged complexes with carbohydrates. The sugars can be detected as Li-adducts $[M + Li]^+$ at $[M + 7]^+$ in the positive mode or as chloride adducts in negative mode $[M + Cl]^-$, while the positive charged complexes are detected with higher sensitivity.

In source collision induced fragmentation (CID) of carbohydrates after ESI can be achieved in single quadrupole MS accelerating the ions into the focusing RF lens region with a high enough voltage applied to the exit cone. The formed fragment ions are from glycosidic cleavage and can confirm that an unknown eluting peak is a carbohydrate or not.

In the analytical system, the MS detector and the amperometric detection cell are placed in parallel after the analytical column with the aid of a flow splitter.

When normal bore columns are used, the amperometric detection cell and the MS detector are usually installed in series. When narrow bore columns are used, there will be a higher degree of loss of separation when they are installed in series then when they are installed in parallel. The main cause of this loss in chromatographic efficiency is the void volume of the reference electrode cavity in the amperometric cell.

The system is evaluated in isocratic separation mode for mono- and disaccharides. Here the MS detection is compared to the IPAD detection for response and minimum detection limit. Then employability for gradient separation is shown with a native inulin sample.

The applicability of food and beverage samples for the analyses of neutral carbohydrates will be shown. Oligosaccharides are analyzed in a native inulin sample, chicory coffee, lager beer and honey.

2.3 EXPERIMENTAL

2.3.1 Chemicals

Sodium hydroxide (50%, w/w) and sodium acetate were obtained from J.T. Baker (Deventer, The Netherlands). Fresh demineralized water was obtained from an Elga Purelab Ultra Analytic system from Rossmark Waterbehandeling B.V. (Ede, The Netherlands). Chicory inulin was a sample from Warcoing Research (Belgium, Warcoing).

2.3.2 Instrumentation

The schematic drawing of the complete chromatographic system is depicted in Fig. 2-1. The BioLC system from Dionex (Sunnyvale, CA, USA) consisted of a GP50 low-pressure quaternary gradient pump, an ED50A electrochemical detector, an AS50 autosampler with sample cooling, thermal compartment for thermal stabilizing of the column and amperometric cell and a 25 µl injection loop. The single quadrupole MS used, was manufactured by Thermo Electron for Dionex.

To pump the 0.5 mmol/l LiCl solution at a flow rate of 0.05 ml/min, an AXP-MS auxiliary pump from Dionex was used. To control the complete system and to realize data acquisition and analysis the Chromeleon® chromatography management system from Dionex was used.

2.3.2.1 Analytical column

The separation was performed on a CarboPac PA200 (3 mm×250 mm) with a CarboPac PA200 guard (3 mm×50 mm) column from Dionex. The stationary phase is a 5.5 µm diameter

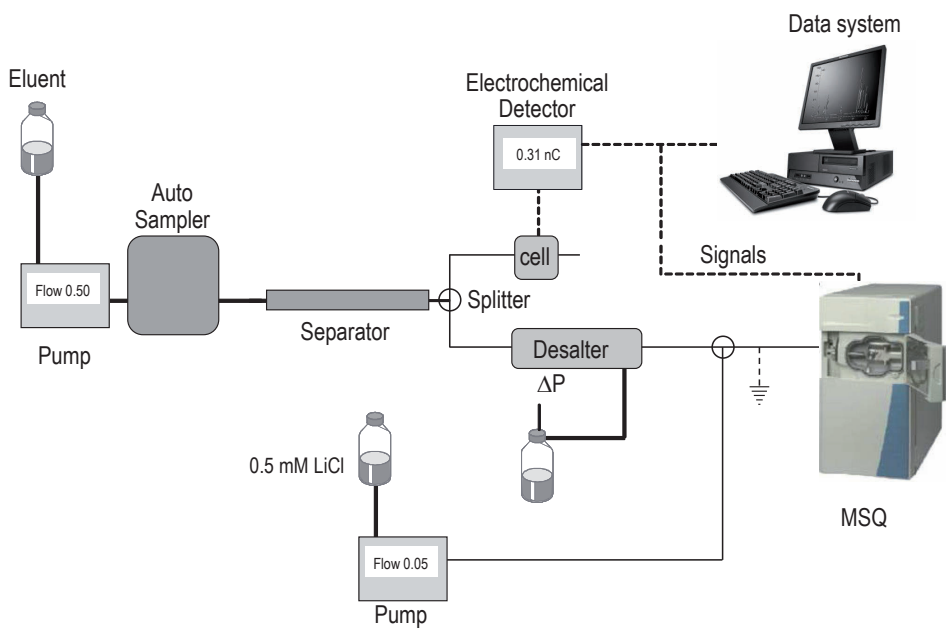

Figure 2-1. Schematics of the chromatographic system.

ethylvinylbenzene/divinylbenzene substrate (55% cross-linking), agglomerated with 34 nm MicroBead™ 6% cross-linked quaternary amine functionalized latex.

2.3.2.2 Flow splitter for detection

To split the effluent after the analytical column a flow splitter was built entirely from PEEK material (Scivex Upchurch Scientific Division, USA). The splitter consisted of a Micro-TEE (P-775) and two PEEK tubings (300 mm×0.075 mm I.D.). One of the PEEK tubings was connected between the MicroTEE and the electrochemical detection cell and the other tubing was connected to the MicroTEE and desalter for the MS detection. PEEK material was used because of inertness. To avoid changing of the split ratio, due to varying backpressure from the ESI probe during optimizing the probe temperature, the total backpressure of the splitter was set to 1.4MPa. The internal volume (1.5 µl) of the splitter resulted in no extra band broadening. The split ratio of the flow splitter is 1:1.

2.3.2.3 Desalter

A cation-exchange membrane in the acid-form was used, as an in-line desalter, to convert the eluate into an ESI compatible solution. The membrane was continuously regenerated with acid generated by electrolysis of water. It efficiently exchanges Na^+ ions originated from the eluent for H_3O^+ ions [7-9]. Neutral and anionic compounds will pass the desalter to the mass spectrometer. As desalter, an ASRS Ultra II 2mm (volume <15 µl) from Dionex was used. The water was fed from an air-pressurized bottle into the regenerant chamber at a flow rate of 5 ml/min. For the isocratic separation conditions a regenerant current of 45 mA was applied and for the gradient conditions 286 mA.

2.3.3 Detection

The ED50A detector delivered to the electrochemical cell the following potential waveform: E_1 = 0.1V (t_d = 0.00–0.20 s, t_1 = 0.20–0.40 s), E_2 =–2.0V (t_2 = 0.41–0.42 s) E_3 = 0.6V (t_3 = 0.43 s), E_4 =–0.1V (t_4 = 0.44–0.50 s) versus a Ag/AgCl reference electrode to a gold work electrode [10]. The standard 25 µm gasket was installed. The inlet stainless steel tube of the cell was removed to reduce internal volume. The PEEK tubing, coming from the flow splitter, was directly connected to the cell.

Neutral carbohydrates were detected in the positive ion mode in the MS after formation of quasi-molecular ions with the added lithium ions. For efficient ionization of the eluted carbohydrates a make-up solution (0.5 mM LiCl) was pumped into the eluent flow at a flow rate of 50 µl/min. This flow was delivered via a MicroTEE (P-775 Scivex). The mixture was directed to the electrospray ionization (ESI) interface of the MSQ quadrupole mass spectrometer. The ESI-MS was operated at the following conditions: probe temperature 525 °C, nitrogen pressure 0.5 MPa, cone voltage 75 volts. When a higher degree of fragmentation was required the cone voltage was set to 100 volts.

2.3.4 Chromatographic conditions

Isocratic separation was done with a flow rate of 0.50 ml/min at 30 °C and 60 mM NaOH as eluent. A ternary gradient elution with the same flow rate and temperature was used with the following eluents: eluent A, water; eluent B, 600 mM NaOH; eluent C, 500 mM NaOAc.

The gradient was as follows: 80% A+ 20% B (0–5 min) isocratic to convert the column into the hydroxide form; 90% A+ 10% B (5–20 min) isocratic equilibration of the column and after 15 min the sample was injected; 25.5% A+ 10% B+ 64.5% C (20–48 min) linear acetate gradient; 25.5% A+ 10% B+ 64.5% C (48–50 min) isocratic.

2.3.5 Samples

A chicory coffee, a lager beer and a honey were bought off-the-shelf. From the chicory coffee 2.5 g were dissolved in 100 ml demineralized water and filtered through a 0.2 µm membrane filter before injection. The lager beer sample was degassed by placing it for 5 min into an ultrasonic bath and five times diluted with demineralized water prior to injection. From the honey sample 100 mg were diluted to 100 ml with demineralized water and filtered through a 0.2 µm membrane filter before injection.

2.4 RESULTS AND DISCUSSION

2.4.1 Evaluation of the detection performance

To evaluate the sensitivity and selectivity of the system an isocratic separation was used for the separation of glucose, fructose and sucrose, see Fig. 2-2. The three carbohydrates are well separated and from 500 pmol injection a mass spectrum with good signal to noise ratio was obtained, see Fig. 2-3. At a cone voltage of 75V the quasi-molecular ion at *m/z* 349 is clearly the base peak of sucrose. Also fragment ions from glycosidic cleavages were observed, numbering system proposed by Domon and Costello [11] is used and shown in the same figure. The mass loss of 162 (Y fragment at *m/z* 187) is a clear indication for a hexose. The fragment ion at *m/z* 205 is a water adduct of the Y fragment. Such water adducts are easily formed in the ESI of the MSQ mass spectrometer. B fragment ion at *m/z* 169 is a glycosidic cleavage on the other side of the oxygen atom.

To study the signal response of both detectors a calibration using external standards was performed and the limit of detection was determined, both for IPAD and MS. The calibration range was over 3 orders of magnitude (2.5–1000 pmole) with seven different levels of each carbohydrate. The calibration curve fit of the different signals is reported in Table 2-1.

By repeated injections of 5 pmole of each carbohydrate the minimum detection limit was determined, see Table 2-1 and Fig. 2-4. Selected ion monitoring (SIM) was used to study sensitivity and minimum detection limit of the MS, because the signal to noise ratio in this mode is better than in scan mode with a quadrupole MS. The limit of detection for glucose and fructose is approximately 10 times and for sucrose three times better in pulsed amperometric detection compared to mass spectrometric detection.

2.4.2 Gradient performance of the system

To explore the gradient performance of the chromatographic system a gradient separation was developed for native inulin and is shown in Fig. 2-5. Inulin is mainly a mixture of two linear fructan oligosaccharides (FOS), one with a terminal sucrose (GFn) the other with a fructopyranose (Fm) unit, up to a high degree of polymerization (DP) [12]. Both homologous series have their own retention behavior. Despite good separation, coelution of the FOS is also observed.

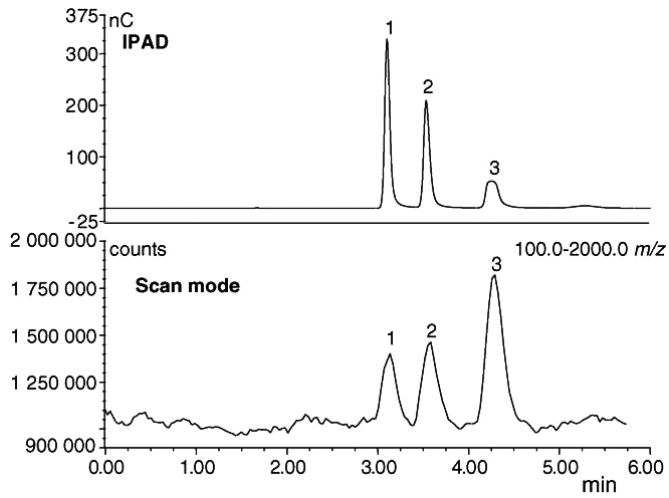

Figure 2-2. Isocratic separation of 500 pmole each of glucose (1), fructose (2) and sucrose (3). The IPAD chromatogram is obtained from the amperometric detector. The lower chromatogram is obtained from the MS in scanning mode for 100–2000*m/z*.

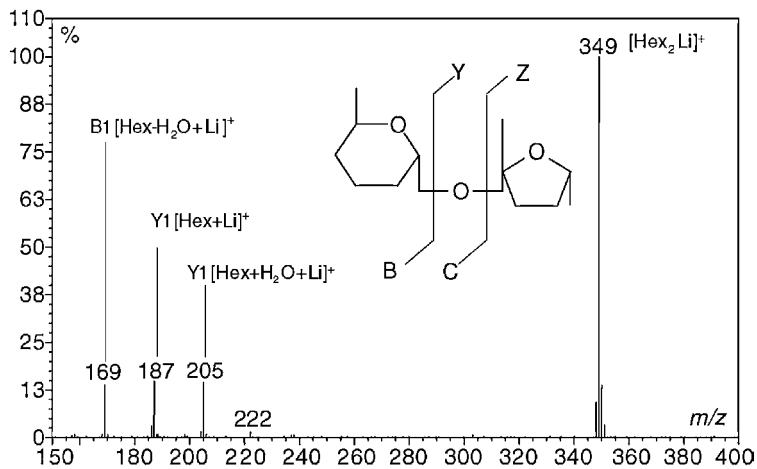

Figure 2-3. Mass spectrum of sucrose.

An example is the peak at 18.24 min. Extracting ion chromatograms from the MS data at appropriate mass to charge ratios, unveiled both series. In Table 2-2 retention times of the fructo-oligosaccharides are reported. Retention times printed in italic are indicating coeluting compounds.

As an example of coeluting peaks the mass spectrum in Fig. 2-6 shows two mass peaks, one at *m/z* 1159 (GF_6) and the other one at *m/z* 835 (F_5). MS data helps to unveil coeluting compounds, because they are not isobaric. Multiple charged adducts were observed for fructan

Table 2-1. Calibration curves and minimum detection limits.

	Curve	Slope	Corr. Coeff.	SIM MDL (pmole)	IPAD MDL (pmole)
Glucose SIM 187	−0.13946	291.988	0.99992	1.49	0.12
Fructose SIM 187	−0.05785	131.603	0.99997	1.19	0.22
Sucrose SIM 349	−0.02718	62.920	0.99998	0.36	0.11

MDL = t_s x σ, n = 7 based on peak area of 5 pmole. t_s is Students *t*

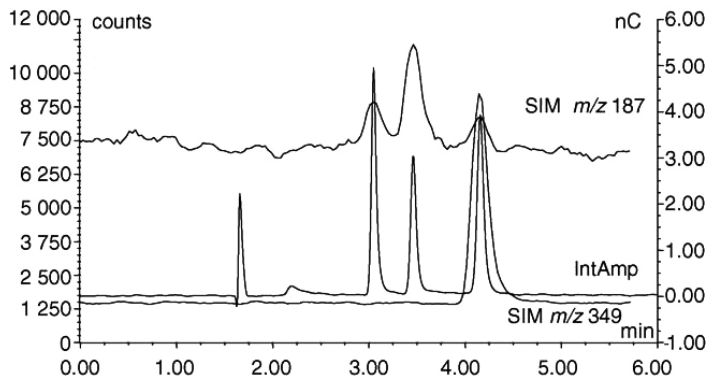

Figure 2-4. 5 pmole of glucose, fructose and sucrose. IPAD and SIM channels of *m/z* 187 and 349.

oligosaccharides with higher molecular mass. From Table 2-2 it can be observed that DP1 to 7 are singly charged adducts, from DP6 to 25 doubly charged adducts with an overlap for DP6 and DP7. Triply charged adducts were observed from DP13 and higher, not shown. Quadruple charged adducts were observed from DP26 and higher, not shown. As an example for multiply charged adducts the mass spectrum of GF_6 is shown in Fig. 2-6. Singly charged GF_6 is observed at *m/z* 1159 and the double charged lithium adduct of GF_6 at *m/z* 583. We observed under these conditions for every 1000 Da increase in molecular mass the charge is raised by one extra unit.

2.4.3 Determination of oligohexoses in food and beverage samples

The same gradient conditions as for inulin were used for separating all food and beverage samples. In Figs. 2-7 and 2-8 the resulting chromatograms of chicory coffee and lager beer are shown. The chromatograms obtained in IPAD are very complex showing a high number of unresolved peaks. This is caused by the fact that integrated pulsed amperometric detection is not only selective for carbohydrates, but also for amines like amino acids, peptides, proteins and Maillard reaction products such as Amadori and Heyn's products is expected in these samples. The MS can be of help to identify oligohexoses by extracting mass selective chromatograms. Moreover, the cationic desalter membrane is very acidic and will protonate amines and as a result remove them prior to MS detection.

Extracted ion chromatograms of the chicory coffee sample for mass to charge ratios of neutral oligohexoses show mainly DP1 to DP11. Up to DP8 are shown in Fig. 2-7. The extracted

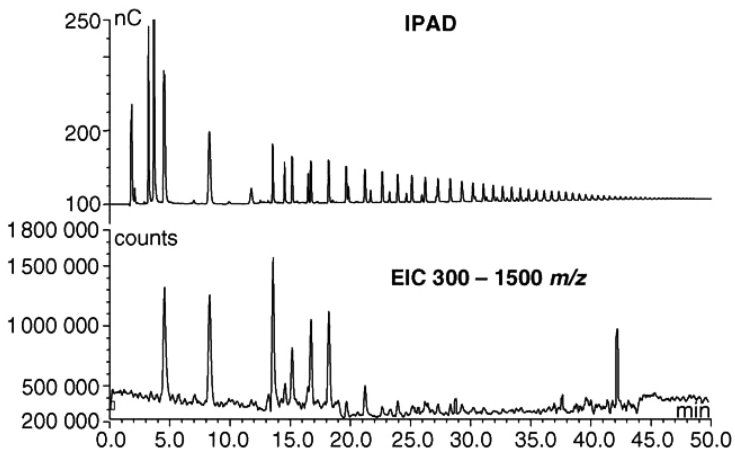

Figure 2-5. Gradient separation of 7.5 µg inulin. The IPAD chromatogram is obtained from the amperometric detector. The lower chromatogram is extracted from the MS data range of *m/z* 300–1500.

Table 2-2. Retention times and mass to charge ratios of fructan oligosaccharides.

GFn (min)	Fm (min)		Charge		
		DP	z = +1	z = +2	z = +3
8.33	14.55	3	511		
13.56	16.52	4	673		
15.21	*18.24*	5	835		
16.76	19.89	6	997	502	
18.24	Not found	7	1159	583	
19.69	23.24	8		664	
21.20	24.65	9		745	
22.63	25.96	10		826	
23.91	27.18	11		907	
25.11	*28.34*	12		988	
26.24	29.22	13		1069	715
27.30		14		1151	769
28.31		15		1232	823

mass selective chromatograms from DP1 to DP8 unveil the retention time ranges of the individual oligosaccharides for example mass to charge ratio at *m/z* 187 elute from 3 to 5 min, while the pentasaccharides at *m/z* 835 elute between 14 and 18 min. Fig. 2-8 presents extracted mass chromatograms of DP1 to DP10 of the lager beer sample. Oligohexoses up to DP14 were observed in this sample. In contrast of the chicory coffee sample, the beer sample contains lower concentrations of mono- and disaccharides and relative high concentrations at *m/z* 511 (DP3) and at *m/z* 673 (DP4) in comparison to mono- and disaccharides.

The honey sample contains mainly mono- and dihexoses as shown in Fig. 2-9. The chromatogram is relatively simple compared to chicory coffee and beer. Major components

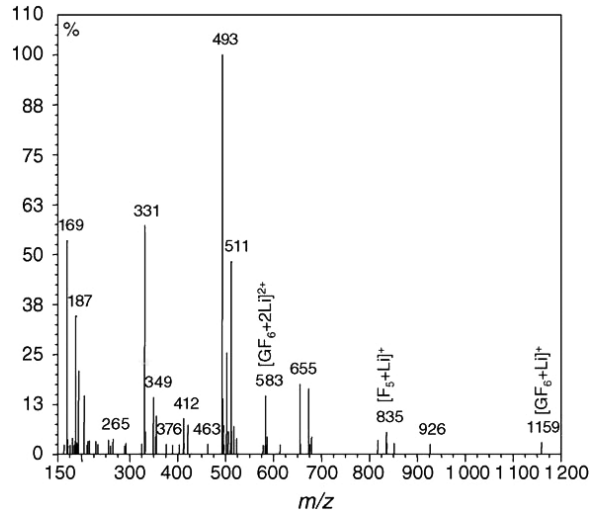

Figure 2-6. Mass spectrum of the peak at retention time 18.24 min.

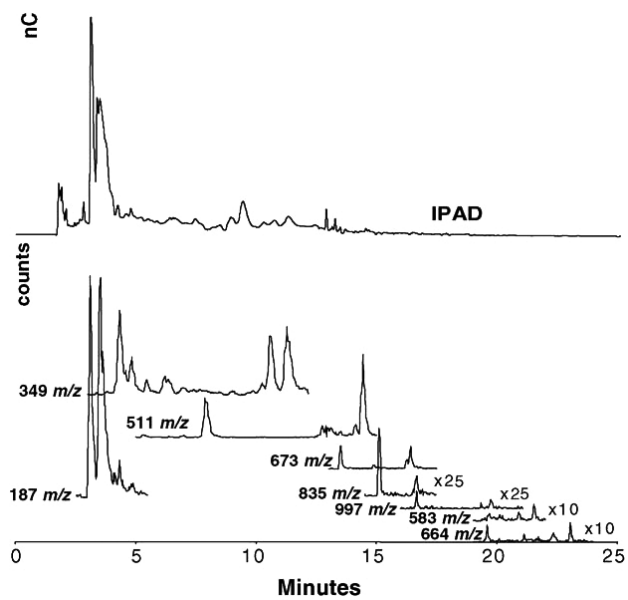

Figure 2-7. Chicory coffee 25 mg/ml, 25 µl injected. The upper chromatogram is obtained from the amperometric detector. The lower signals are mass extracted chromatograms of oligohexoses up to DP8.

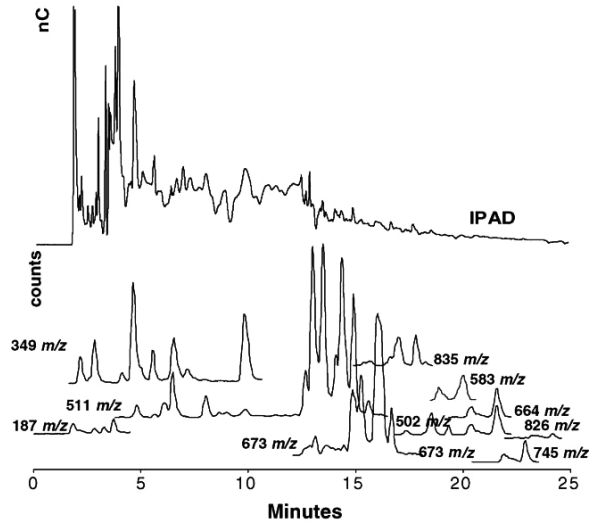

Figure 2-8. Lager beer degassed 5x diluted, 25 µl injected. The upper chromatogram is obtained from the amperometric detector. The lower signals are mass extracted chromatograms of oligohexoses up to DP10.

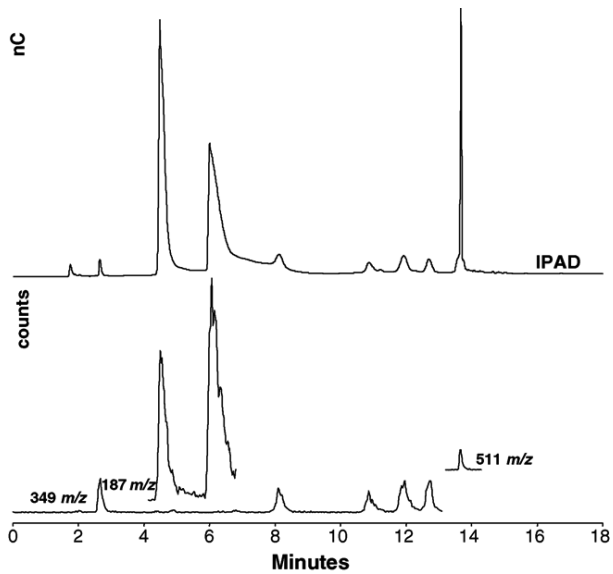

Figure 2-9. Honey 1 mg/ml, 5 µl injected. The upper chromatogram is obtained from the amperometric detector. The lower signals are mass extracted chromatograms of oligohexoses up to DP3.

are the monosaccharides and low abundant are the di- and trisaccharides. These examples show the broad applicability of the chromatographic platform determining carbohydrates in complex samples with minimal sample preparation.

2.5 CONCLUSIONS

A versatile narrow bore column liquid chromatography platform has been developed for the analysis of underivatized carbohydrates. Applicability is shown with complex food and beverage samples. It demonstrates the successful combination of integrated pulsed amperometric and an on-line single quadrupole mass spectrometric detection, following gradient anion-exchange separation. Although there can be significant sensitivity differences between the MS and IPAD detection, mass selective detection is beneficial for confirmation of sugars in food and beverage samples. In source formed fragment ions can confirm that unknown components are carbohydrates. Only cleavages of glycosidic linkages were observed. The resulting mass loss of a monosaccharide unit is a very strong indication for detecting carbohydrates. Coelutions of compounds can be determined with MS detection. The different isobaric polyfructan chains in inulin with terminal fructose or sucrose are identified according to their mass to charge ratio and retention times. Multiple charged Li adduct formation is observed as high as four for molecule masses above 4200 g/mol (DP 26), enabling use of a single quadrupole mass spectrometer with an upper mass range of 2000 m/z to detect the higher molecular weight compounds.

REFERENCES

1. Honda S (1984) High-performance liquid chromatography of mono- and oligosaccharides. *Anal Biochem* **140,** 1-47.
2. Anumula KR (2000) High-sensitivity and high-resolution methods for glycoprotein analysis. *Anal Biochem* **283,** 17-26.
3. Lee YC (1990) High-performance anion-exchange chromatography for carbohydrate analysis. *Anal Biochem* **189,** 151-162.
4. Cataldi TR, Campa C, & De Benedetto GE (2000) Carbohydrate analysis by high-performance anion-exchange chromatography with pulsed amperometric detection: the potential is still growing. *Fresenius J Anal Chem* **368,** 739-758.
5. Rocklin RD, Tullsen TR, & Marucco MG (1994) Maximizing signal-to-noise ratio in direct current and pulsed amperometric detection. *J Chromatogr A* **671,** 109-114.
6. Lee KB, Loganathan D, Merchant ZM, & Linhardt RJ (1990) Carbohydrate analysis of glycoproteins. A review. *Appl Biochem Biotechnol* **23,** 53-80.
7. Thayer JR, Rohrer JS, Avdalovic N, & Gearing RP (1998) Improvements to in-line desalting of oligosaccharides separated by high-pH anion exchange chromatography with pulsed amperometric detection. *Anal Biochem* **256,** 207-216.
8. van der Hoeven RAM, Tjaden UR, van der Greef J, van Casteren WHM, Schols HA, Voragen AGJ, & Bruggink C (1998) Recent progress in high-performance anion-exchange chromatography/ionspray mass spectrometry for molecular mass determination and characterization of carbohydrates using static and scanning array detection. *J Mass Spectrom* **33,** 377-386.
9. Torto N, Hofte A, Tjaden UR, Gorton L, Marko-Varga G, Bruggink C, & van der Greef J (1998) Microdialysis-introduction high-performance anion-exchange chromatography/ionspray mass spectrometry for monitoring of online-desalted carbohydrate hydrolysates. *J Mass Spectrom* **33,** 334-341.
10. Rocklin RD, Clarke AP, & Weitzhandler M (1998) Improved long-term reproducibility for pulsed amperometric detection of carbohydrates via a new quadruple-potential waveform. *Anal Chem* **70,** 1496-1501.

11. Domon B & Costello CE (1988) A Systematic Nomenclature for Carbohydrate Fragmentations in FAB-MS/MS Spectra of Glycoconjugates. *J Glycoconj* **5,** 397-409.

12. De Leenheer F (1996) Production and use of inulin: Industrial reality with a promising future. In *Carbohydrates as Organic Raw Materials III* (van Bekkum H, Roper H, & Voragen F, eds), pp. 67-92. CRF, The Hague.

3

OLIGOSACCHARIDE ANALYSIS BY CAPILLARY-SCALE HIGH-pH ANION-EXCHANGE CHROMATOGRAPHY WITH ON-LINE ION-TRAP MASS SPECTROMETRY

3.1 ABSTRACT

A capillary-scale high-pH anion-exchange chromatography (HPAEC) system for the analysis of carbohydrates was developed, in combination with two parallel on-line detection methods of sub-picomolar sensitivity: (1) pulsed amperometric detection (PAD); (2) capillary-scale desalting followed by electrospray ion-trap (IT) mass spectrometry (MS). The capillary chromatographic system combined the superb selectivity of HPAEC that allows routine separation of isomeric oligosaccharides with the information on monosaccharide sequence and linkage positions obtained by MS/MS fragmentation using the IT-MS. The applicability of the system in biomedical research was demonstrated by its use for the analysis of a urine sample of a G_{M1}-gangliosidosis patient. Isomeric glycans in the sample could be resolved by HPAEC and assigned on the basis of the monosaccharide linkage information revealed by on-line IT-MS/MS.

Cees Bruggink [a,c], Manfred Wuhrer [a], Carolien A.M. Koeleman [a], Victor Barreto [b], Yan Liu [b], Chris Pohl [b], Arnd Ingendoh [d], Cornelis H. Hokke [a], André M. Deelder [a]

[a] Biomolecular Mass Spectrometry Unit, Department of Parasitology, Center for Infectious Diseases, Leiden University Medical Center, P.O. Box 9600, 2300 RC Leiden, The Netherlands
[b] Dionex Corporation, 1228 Titan Way, Sunnyvale, CA 94088-3603, USA
[c] Dionex BV, Lange Bunder 5, 4854 MB Bavel, The Netherlands
[d] Bruker Daltonik GmbH, Fahrenheitstr. 4, 28359 Bremen, Germany

Journal of Chromatography B (2005) 829; 136–143.

3.2 INTRODUCTION

Within the panel of analytical techniques available for the characterization of oligosaccharides, chromatographic methods play a central role [1,2]. While reverse-phase HPLC of oligosaccharides requires derivatization [2,3], other stationary phases such as normal-phase and porous graphitized carbon allow the separation of both derivatized and native oligosaccharides [2-4]. Photometric detection of native carbohydrates is insensitive because they lack a natural chromophore or fluorophore, and therefore derivatization at the reducing end is usually required to allow detection in the sub-picomol range by fluorescence detection [5]. An alternative, sensitive and widely used chromatographic system for the separation and analysis of underivatized carbohydrates is high-pH anion-exchange chromatography with pulsed amperometric detection (HPAEC-PAD) [6,7]. This chromatographic system is based on the fact that carbohydrates are weak acids [8], which form anions in an eluent of high pH. In addition, the presence of aldehydes, ketones and multiple hydroxyl groups in carbohydrates makes them relatively attractive electrochemical analytes and pulsed amperometry therefore allows the detection of oligosaccharides at low picomol levels [9] when using a 4 mm I.D. analytical column.

Both on-line-coupling to mass spectrometry and downscaling of the column dimensions to the capillary- or nano-scale are important for the development of glycan analysis technology that is compatible with current standards in biomedical research. These requirements have already been met for the graphitized carbon stationary phase [3,4,10], normal phase (NPLC) [11,12] and reversed phase liquid chromatography (RPLC) [3,13]. In the case of HPAEC-PAD, however, oligosaccharide separation with on-line desalting and on-line mass spectrometry has so far only been demonstrated at the narrow bore (2 mm column I.D.) [14-16] and at the analytical scale (4 mm column I.D.) [17].

This study describes the implementation of a prototype capillary bore (0.381 mm I.D.) column for HPAEC with on-line pulsed amperometric detection and on-line electrospray ion-trap mass spectrometry (IT-MS). MS coupling was made possible with an experimental on-line capillary-scale desalter. The system exhibits sub-picomol sensitivity, both in amperometric and in mass spectrometric detection, and was found to be particularly useful for the characterization of complex biological samples due to its high chromatographic resolution combined with the MS/MS capabilities of the ion-trap mass spectrometer.

3.3 EXPERIMENTAL

3.3.1 Chemicals

Analytical reagent grade sodium hydroxide (50%, w/w), sodium acetate, sulphuric acid and sodium chloride were obtained from J.T. Baker (Deventer, The Netherlands). Acetonitril was from Biosolve (Valkenswaard, The Netherlands). All solutions were prepared with water from a Milli-Q synthesis system from Millipore BV (Amsterdam, The Netherlands). The asialo diantennary glycan was a gift from Dr. D.H. van den Eijnden (Free University, Amsterdam). Chicory inulin was obtained from Warcoing Research (Warcoing, Belgium).

3.3.2 Chromatographic system

A schematic drawing of the complete instrumental set-up is shown in Fig. 3-1. The BioLC system from Dionex (Sunnyvale, CA, USA) consisted of a microbore GP40 gradient pump, a Famos micro autosampler with a full PEEK-injector and a 0.41 µl loop, and an ED40 electrochemical detector, all controlled by Chromeleon software (Dionex).

Coupled to the system was an Esquire 3000 ion-trap mass spectrometer from Bruker Daltonik (Bremen, Germany), equipped with an electrospray ionization source. A microbore AGP-1 from Dionex was used as an auxiliary pump (see Section 3.3.3.2).

3.3.2.1 Flow splitter for providing the eluent

To accomplish a flow rate of 10 µl/min, a homemade flow splitter (split ratio 56:1) constructed entirely from PEEK was inserted between the gradient pump and the autosampler. The eluent flow was split up via a TEE (P-715; Scivex Upchurch Scientific, Oak Harbor, WA, USA). The analytical column was connected to the TEE by 1256 cm×0.075 mm I.D. tubing. To the other exit of the TEE 1316 cm×0.125 mm I.D. and in addition 894 cm×0.750 mm I.D. tubing was connected.

To determine flow rates at various places in the capillary system a 25 µl syringe without plunger was coupled to the appropriate exit and the filling time was measured with a stopwatch.

3.3.2.2 Analytical column

A prototype capillary column (250 mm×0.381 mm I.D.) packed with CarboPac PA200 resin was manufactured by Dionex. The stationary phase is a 5.5 µm diameter ethylvinylbenzene/divinylbenzene substrate (55% cross-linking), agglomerated with 34 nm MicroBead™ 6% cross-linked quaternary amine functionalized latex.

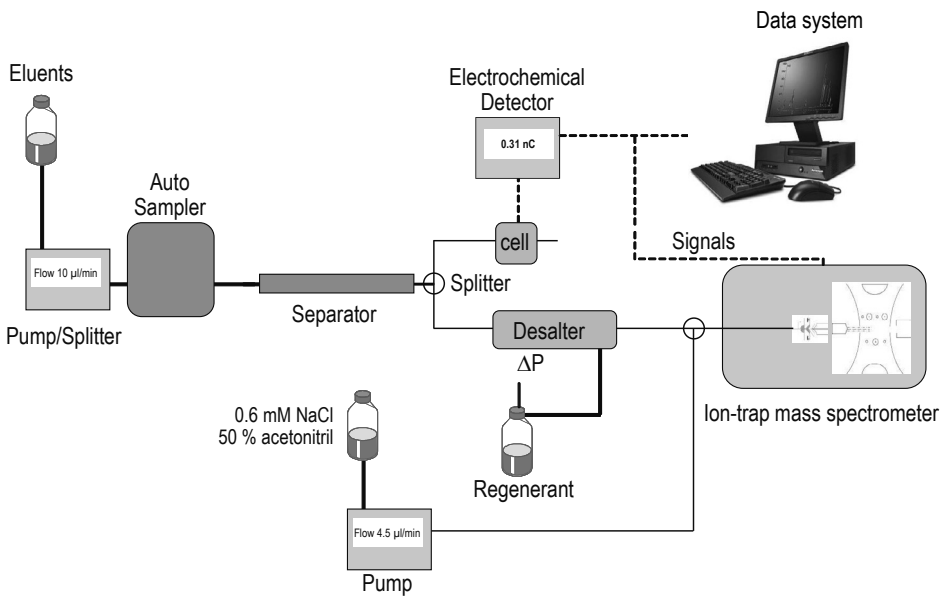

Figure 3-1. Schematic representation of the experimental set-up of capillary HPAEC with electrochemical as well as on-line-mass spectrometric detection.

3.3.2.3 Flow splitter for detection

To avoid unacceptable loss of resolution, the detectors were coupled to the outlet of the analytical column in parallel. The desalter was connected to a PEEK TEE (P-715 from Scivex Upchurch Scientific Division) and put in-line with the mass spectrometer with a total of 150 cm×0.075 mm I.D. PEEK tubing. The electrochemical cell and 350 cm×0.075 mm I.D. PEEK tubing were connected to the other outlet of the TEE. This resulted in a split ratio of 11 to 5 for MS to PAD. The total backpressure was 210 kPa, which was found to be sufficient to minimize system flow fluctuations.

3.3.2.4 Desalter

To convert the eluent into an electrospray ionization (ESI)-compatible solution, a capillary in-line desalter was prepared. The desalter consisted of a Nafion cation-exchange capillary (15 cm×0.102 mm I.D.×0.254 mm O.D.) housed in a PEEK column (250 cm×4 mm I.D.) with inlet and outlet liquid connecting ports. Provisions were made so that there were separate fluid connections to the cation exchange capillary tubing in the PEEK column. The cation exchange capillary was maintained predominantly in the hydronium form by flowing dilute sulfuric acid through the PEEK column so that the capillary was fully immersed in the solution of sulfuric acid. Using the capillary desalter, neutral and anionic compounds pass to the mass spectrometer, and the eluent is converted into water and acetic acid.

3.3.3 Detection

3.3.3.1 Electrochemical detection

The ED40 detector delivered to the electrochemical cell the following waveform: E_1 = 0.1V (t_d = 0.00–0.20 s, t_1 = 0.20–0.40 s), E_2 =–2.0V (t_2 = 0.41–0.42 s), E_3 = 0.6V (t_3 = 0.43 s), E_4 =–0.1V (t_4 = 0.44–0.50 s) versus an Ag/AgCl reference electrode [18]. A gold work electrode and a 25 µm gasket were installed. The inlet stainless steel tube of the cell was removed to minimize void volume. The electrochemical cell was placed in the low-pressure splitter outlet as described in Section 3.3.2.3.

3.3.3.2 Mass spectrometry

For efficient ionization of the eluted carbohydrates and in order to get a stable electrospray, a make-up solution (0.6 mM NaCl in 50% acetonitrile) was pumped into the eluent flow via a MicroTEE (P-775 Scivex). To obtain a flow rate of 4.6 µl/min for the make-up solution, the auxiliary pump was equipped with a homemade low-pressure PEEK splitter with a split ratio of 1:46.5. The mixture was directed to the electrospray ionization (ESI) interface of an Esquire 3000 ion-trap mass spectrometer from Bruker Daltonik. Neutral carbohydrates were detected with MS in the positive ion mode as sodium adducts. Analyses were routinely performed in the automatic MS/MS mode. The mass spectrometer was operated at the following conditions: dry temperature 325 °C, nebulizer 103 kPa, dry gas 7 l/min, capillary –3500V and target mass m/z 850.

3.3.4 Separation conditions

The GP40 pumped with a flow rate of 10 µl/min and was provided with the following eluents: eluent A, water; eluent B, 500mM NaOH; eluent C, 500mM sodium acetate. All separations were performed at room temperature. The asialo diantennary *N*-glycan was chromatographed under isocratic conditions (70% A+ 30% B). The ternary gradient for fructan oligosaccharides was as follows: The column was first washed with 76% A+ 24% B (–20 to –14 min; isocratic) in

order to convert the column into the hydroxide form, followed by an equilibration with 88% A+ 12% B (–14 to 0 min; isocratic). Elution was achieved with a linear acetate gradient to 25.5% A+ 12% B+ 62.5% C (0–55 min). For analysis of urinary oligosaccharides from patients with G_{M1}-gangliosidosis the gradient was as follows: 76% A+ 24% B (–20 to –14 min; isocratic); 88% A+ 12% B (–14 to 0 min; isocratic); linear hydroxide gradient to 60% A+ 40% B (0–9.1 min); 60% A+ 40% B (9.1–12.5 min; isocratic); linear gradient to 85.2% A+ 12% B+ 2.8% C (12.5–21.6 min); linear acetate gradient to 60.5%A+ 12% B+ 27.5% C (21.6–104 min). The samples were injected at 0 min.

3.3.5 Preparation of urine samples

Oligosaccharides of urine samples were isolated with graphitized carbon solid phase extraction, according the method described by Packer et al. [19]. Two hundred µl of urine was diluted with 1800 µl water and loaded on a Carbograph SPE cartridge (300 mg; Alltech Associates Inc., Deerfield, IL, USA). The cartridge was washed with water (6 ml) and the neutral oligosaccharides were subsequently eluted with 3ml 25% acetonitrile. The eluate was concentrated under a stream of nitrogen at room temperature until the volume was decreased to 50%. The remaining solution was lyophilized and reconstituted in 200 µl water.

3.4 RESULTS

3.4.1 Characterisation of the desalter

In order to determine the desalting capacity of the prototype on-line capillary desalter, various concentrations of NaOH were pumped through at a flowrate of 10 µl/min over a time range of at least 60 min, with a regenerant flow of 825 µl/min. The regenerant concentration was kept constant at 12.5 mM sulphuric acid. Higher concentrations of regenerant were avoided in order to prevent the breakthrough of the sulphate ions according to the Donnan-exclusion [20,21]. The conductivity of the effluent was continuously monitored and every 10 min the pH was checked with universal pH-paper. It was determined that the desalting capacity of the capillary desalter is 225 mM NaOH for the tested eluent flow rate of 10 µl/min. The resulting effluent conductivity was 54 µS/cm, the pH was 7 and was stable for at least 60 min. To determine to which extent the desalter contributed to peak broadening, the system was tested with a 0.41 µl injection of an inulin solution of 300 µg/ml. Inulin contains two linear homologous series of fructan oligosaccharides (FOS) [22,23]. The most abundant series terminates in sucrose, the other in fructopyranosyl. FOS from inulin were separated with a sodium acetate gradient in sodium hydroxide with the electrochemical cell directly installed after the capillary column (Fig. 3-2A).

Alternatively, the desalter in the sodium form was installed between the column and the electrochemical cell (Fig. 3-2B). For the registered peak pair 1, which eluted in the isocratic part of the separation, resolution was 0.94 and 0.70 without and with the desalter, respectively. For peak pair 2, which eluted in the gradient part of the separation, the resulting resolutions were 8.38 versus 5.47. The retention time shift caused by the desalter was 8 s and corresponded to an internal volume of 1.35 µl.

3.4.2 Gradient performance and detection of fructan oligosaccharides

To test the gradient performance of the instrumental set-up, a solution of 1 mg/ml inulin was chromatographed. The estimated gradient delay time to the electrochemical detector was 11.2

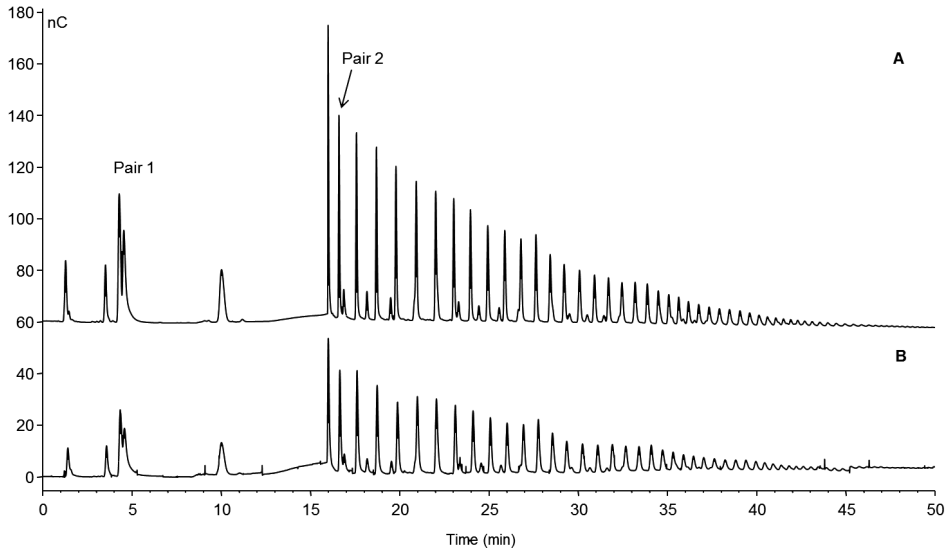

Figure 3-2. Capillary HPAEC-PAD separation of fructan oligosaccharides. The chromatographic behaviour of fructan oligosaccharides from 123 ng native chicory inulin was compared with and without on-line-desalting. (A) The electrochemical cell was directly connected to the column. (B) The capillary desalter was positioned between the column and the electrochemical cell.

min. Extracted ion chromatograms (EIC) of FOS up to DP13 (degree of polymerization) are shown in Fig. 3-3. At higher masses doubly charged sodium adducts were observed. By use of extracted ion chromatograms co-eluting variants could be discriminated such as two species eluting at approximately 20 min, namely DP5 (*m/z* 851.3) and DP7 (*m/z* 1175.7). In each EIC corresponding to a certain DP, two fully separated peaks were present, representing sodium adducts of the two isobaric variants, which demonstrated the separation potential of the HPAEC system. From the extracted ion chromatograms it turned out that the homologous series terminating in fructopyranose exhibited more retention than the series terminating in glucopyranose.

As analyses were performed in the automatic MS/MS mode, fragmentation spectra were obtained for most of the FOS. Fig. 3-4B and C shows MS/MS spectra of the two isobaric DP5 variants, which exhibited similar fragmentation patterns, yet varied in the relative intensities of the fragment ions. The MS/MS spectra show mainly cleavages of glycosidic linkages and ions representing a loss of 90 Da (*m/z* 437.2 and 275.2). This loss of 90 Da can arise from ring fragmentation as indicated in Fig. 3-4B.

3.4.3 Signal response of the detectors

Signal response of the system has been investigated for both detectors under isocratic conditions with the asialo *N*-linked diantennary glycan. Five concentrations in the range of 0.16–100 pmol were tested in three fold. The IPAD signal was linear up to 20 pmol, while the MS signal was linear over the whole range investigated (regression coefficient >0.999 for IPAD and MS). A sub-picomolar detection limit was achieved, as demonstrated in Fig. 3-5. From the total amount of 160 fmol diantannary oligosaccharide injected on column, about 50 fmol was directed to the electrochemical detector and 110 fmol to the mass spectrometer.

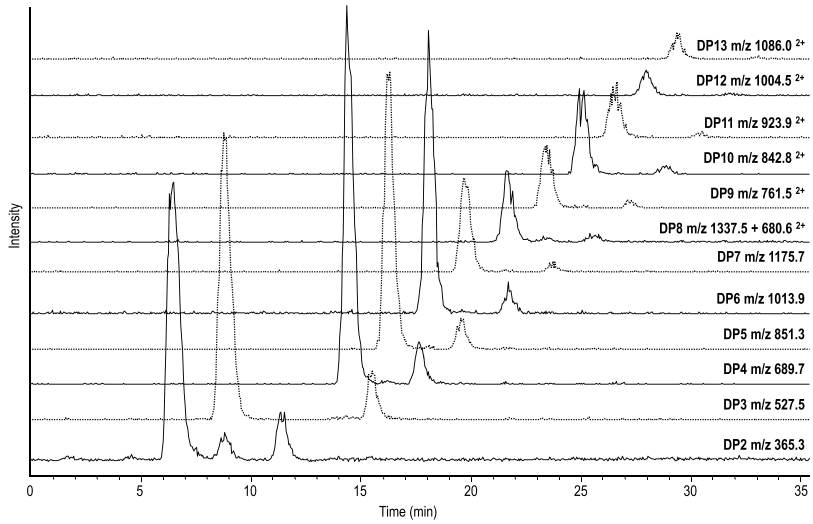

Figure 3-3. Capillary HPAEC-on-line-MS analysis of fructan oligosaccharides. Fructan oligosaccharides from 410 ng native chicory inulin were analyzed by capillary HPAEC with on-line-desalting and electrospray-MS detection. Extracted ion chromatograms are given for fructan oligosaccharides of various degrees of polymerization (DP) which were detected as sodium adducts.

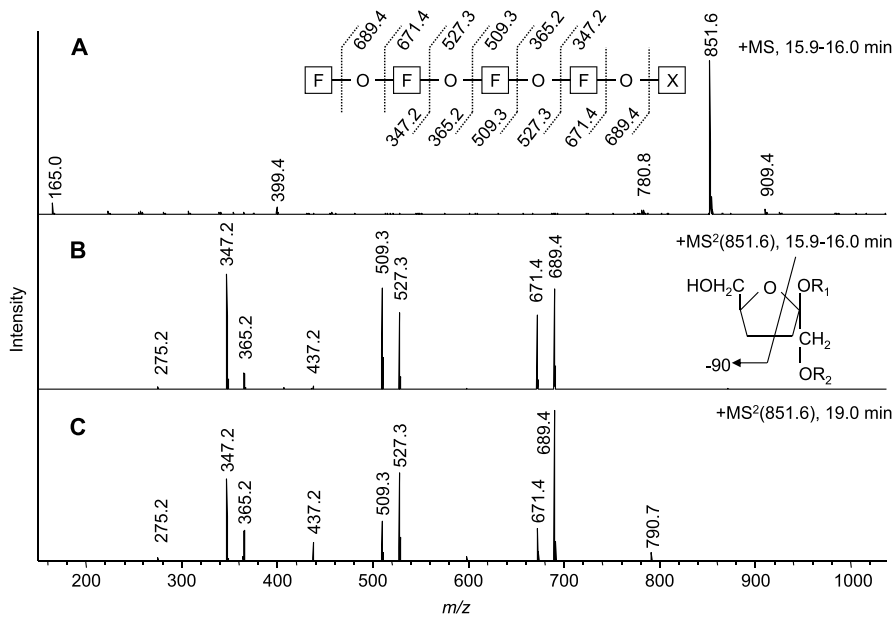

Figure 3-4. Mass spectra of the two isobaric sodium adducts of DP5 fructans. Part (A) shows the MS spectrum of $[GF_4 + Na]^+$; parts (B) and (C) are the MS^2 spectra with *m/z* 851.6 as precursor ion, where (B) represents GF_4 and (C) F_5. In the fragmentation scheme, F stands for fructofuranosyl and X is glucopyranosyl or fructopyranosyl, R_1 and R_2 stand for the rest part of the oligosaccharide chain and R_2 can also be a H.

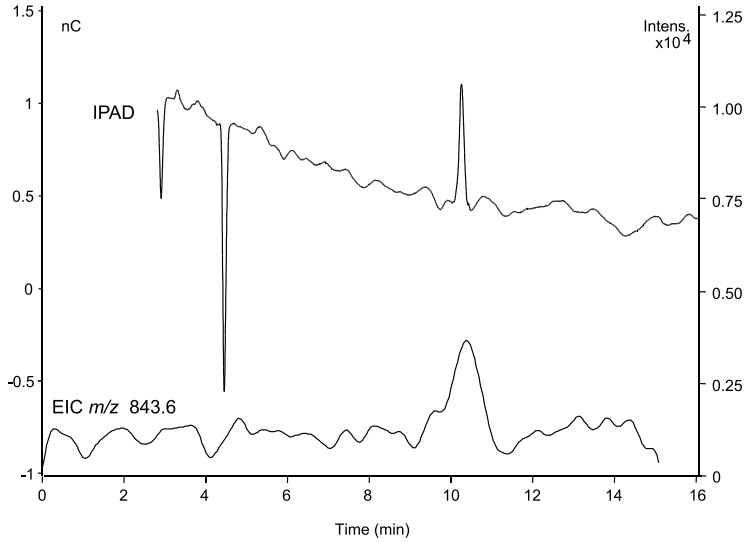

Figure 3-5. Analysis of an 160 fmol aliquot of an asialo diantennary glycan by combined capillary HPAEC-PAD/online-MS detection. The chromatogram obtained from the electrochemical detector (IPAD) is corrected for the 2.68 min retention difference with the online-MS detection (EIC) of the double-sodiated species.

3.4.4 Urine sample of a G_{M1}-gangliosidosis patient

As a relevant example of a clinical application, a urine sample of a G_{M1}-gangliosidosis patient was analyzed with the system. The resulting chromatogram is given in Fig. 3-6. Oligosaccharides from urine were extracted using a carbon cartridge, and the equivalent of 400 nl urine was injected on the column. The electrochemical detector gave a complex peak pattern (not shown). On-line mass spectrometric detection revealed the presence of a dihexose (most likely lactose) as well as complex oligosaccharides of composition $H_{3-7}N_{1-5}$ (H: hexose; N: *N*-acetylhexosamine), which were detected in monosodiated form (H_3N_2 and H_3N) or disodiated form (H_5N_3, H_6N_4 and H_7N_5; Fig. 3-6). In accordance with literature data [24,25], we interpreted H_3N_2, H_5N_3, H_6N_4 and H_7N_5 as monoantennary, diantennary, triantennary and tetraantennary endo-β-*N*-acetylglucosaminidase cleaved products of complex type *N*-glycan structures, respectively.

This assignment was corroborated by the obtained MS/MS data. Oligosaccharides of composition H_3N were interpreted as glycolipid degradation products and exhibited a reducing end hexose–hexose moiety, which is in accordance with the lactosyl core structure of mammalian-type-glycolipids. Of the complex LC–MS/MS data set covering all these species, the data for H_3N_2 species will be presented in detail, as capillary HPAEC in conjunction with on-line desalting/mass spectrometry succeeded to completely resolve two isobaric structures of this composition (Fig. 3-6). Both structures A (elution at 8.9 min; Fig. 3-6) and B (elution at 12.9 min) were detected in sodiated form with a monoisotopic mass of 933.5 Da. The obtained MS/MS data of the two isomeric species were acquired in the automatic mode and are assigned according to the nomenclature of Domon and Costello [26] (Fig. 3-7A and B). Based on linkage-specific fragmentation, these data allowed the assignment of the two isomers to published structures of

urine oligosaccharides in G_{M1}-gangliosidosis [24,25]: Both oligosaccharides seemed to contain a *N*-acetylhexosamine at the reducing end, which displayed specific ring fragmentations (^{0,2}A at *m/z* 832 and ^{2,4}A at *m/z* 772). These fragments, together with the lack of a ^{0,3}A ring cleavage (no signal at *m/z* 802), are characteristic for a 4-substituted *N*-acetylhexosamine, according to the ring fragmentation rules established for sodiated oligosaccharides [27-29]. The observed series of B-ions results in a monosaccharide sequence of H–N–H–H–N for both isomers (Fig. 3-7A and B). For compound A, the observed ring fragmentations (^{0,2}A at *m/z* 670, ^{0,3}A at *m/z* 640 and ^{0,4}A at *m/z* 610) of the hexose next to the reducing-end *N*-acetylhexosamine are typical for a substituent in the 6 position (Fig. 3-7A) [27-29]. Based on this information, compound A was concluded to be the G_{M1}-gangliosidosis urinary oligosaccharide Gal(β1–4)GlcNAc((β1–2)Man(α1-6)Man(β1–4)GlcNAc (Fig. 3-7A), which has been characterized before [24,25].

A lack of these ring fragments is typical for a substituent in the 3 position [27-29]. We conclude, therefore, compound B to be the isomer Gal(β1–4)GlcNAc((β1–2)Man(α1–3)Man(β1–4)GlcNAc (Fig. 3-7B), which has likewise been found previously in G_{M1}- gangliosidosis urine [24,25].

3.5 DISCUSSION

We here describe a capillary-scale HPAEC system for the separation of oligosaccharides with both electrochemical and on-line mass spectrometric detection. With respect to electrochemical

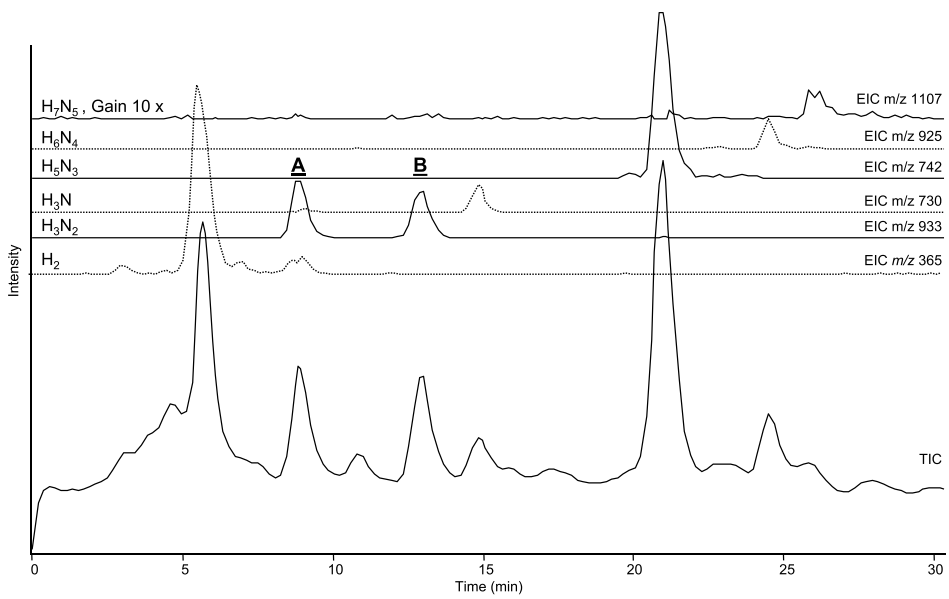

Figure 3-6. HPAEC-on-line-MS of oligosaccharides from the urine sample of a G_{M1}-gangliosidosis patient. TIC is the total ion chromatogram. The extracted ion chromatograms (EIC) represent the major pseudomolecular ions registered. Several of the EIC show the separation of isobaric structures. Fragment-ion analysis of the well-separated H_3N_2 species A and B is shown in Fig. 3-7. H, Hexose; N, *N*-acetylhexosamine.

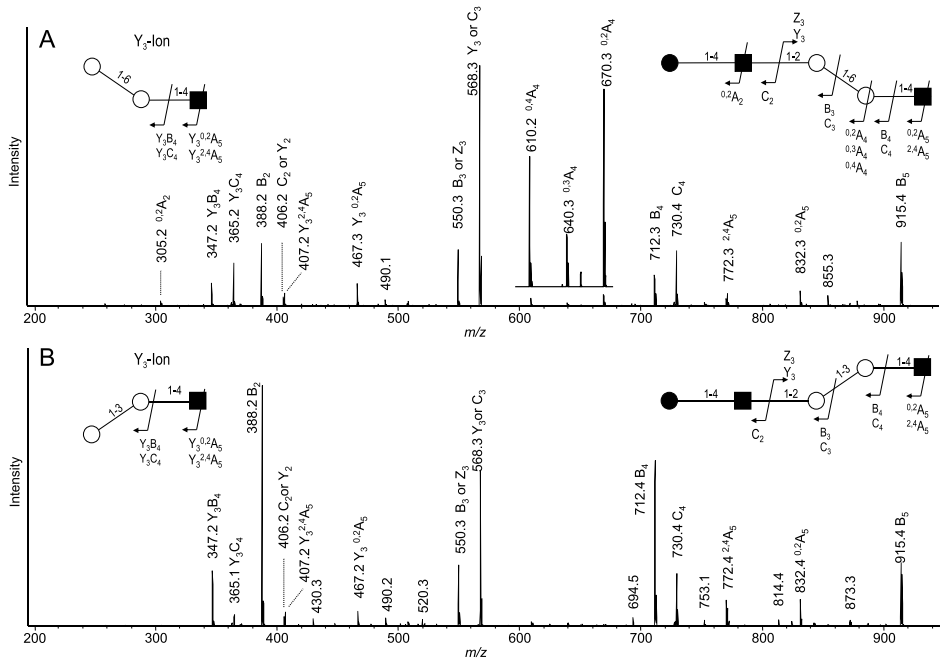

Figure 3-7. Fragment ion analysis of H_3N_2 species. H_3N_2 species A and B, as indicated in Fig. 3-6, were subjected to MS^2 analysis in their sodiated form (*m/z* 933.5; A and B, respectively). The observed fragment ions are schematically interpreted according to the nomenclature of Domon and Costello [26]. Empty circle, mannose; filled circle, galactose; filled square, *N*-acetylglucosamine.

detection, the system displayed the usual excellent performance of HPAEC for the separation of oligosaccharides [6,7]. The downscaling from a narrow bore to a capillary-scale system involved reduction of the dead volume of a standard electrochemical cell by the surprisingly straightforward exchange of the metal inlet tube for a PEEK tube with a internal diameter of 75 µm. Regarding mass spectrometric detection, an on-line desalting step was incorporated in the system in order to allow electrospray ionization-MS at high sensitivity. The degree of peak broadening generated by the desalter was found to be insignificant, and the superb chromatographic performance of HPAEC resulted in the resolution of isomeric structures. The MS detector is particularly useful for the analysis of complex mixtures as for example the fructan oligosaccharides, where it allows the differentiation between co-eluting carbohydrates.

While the desalter was found to work efficiently with concentrations of sodium ions up to 225 mM for longer periods, the system tolerated significantly higher concentrations of sodium ions for short periods when run in the gradient mode. During the separation of fructan oligo- and polysaccharides of inulin the eluent concentration raised up to 372.5 mM sodium, while detection by IT-MS remained excellent, indicating that desalting was still sufficient.

In a previous study, HPAEC was performed at the microbore scale (column of 2 mm I.D.), allowing a lower detection limit of 17 pmol for maltoheptaose (DP7 of (α1–4)-glucose oligomer) [30]. When corrected for the different column diameters, this would result in a theoretical

sensitivity of 615 fmol at a 380 µm I.D. capillary system (17 pmol × (380 µm/2000 µm)^2). The capillary-scale system used in this study (380 µm I.D.) actually exhibited even higher sensitivity, as demonstrated with the mass spectrometric detection of 110 fmol of a diantennary glycan (3.3). When compared to the 2 mm I.D. system [30], mass spectrometric sensitivity increased by a factor of 100. For amperometric detection, the detection limit was found to be around 50 fmol, which means a sensitivity gain by a factor of 50 compared to the results with a 4mm I.D. column published by Rocklin et al. [9,18].

As the Esquire 3000 IT-MS used in the current study was formerly used for nano-scale (75 µm I.D.) normal phase-LC/MS of oligosaccharides, sensitivities of the systems can directly be compared: nano-scale normal phase-LC–MS with a nanoelectrospray source exhibited sensitivities of approximately 1 fmol for both native [11] and derivatized oligosaccharides [12]. When correcting for the differences in column I.D., this would yield a theoretical sensitivity of 25 fmol at the 380 µm I.D. scale.

HPAEC with pulsed amperometric detection has been used for diagnostic purposes of glycoprotein degradation disorders [31]. From the chromatograms generated by HPAEC it was not possible however to identify each observed component, such in strong contrast to the system presented here which includes on-line MS detection to provided mass and fragmentation data. We have evaluated our system using G_{M1}-gangliosidosis urinary oligosaccharides. The total ion chromatogram of Fig. 3-6 shows the most abundant oligosaccharides and their masses. Two separated isomeric oligosaccharides could be assigned based on mass and fragmentation patterns to urinary oligosaccharide structures, which are described in the literature on G_{M1}-gangliosidosis [24,25]. Moreover, polymeric carbohydrates with the α1–6 linkage type are known to elute faster from an anion-exchange resin than isomers with a α1–3 linkage [7], which is in line with the obtained results.

Based on the presented data, we would like to conclude that the system, which combines the high separation power of HPAEC at a thus far unattained capillary-scale with the oligosaccharide sequence and linkage information provided by on-line ion-trap MS/MS, is a powerful new tool for (clinical) glycomics studies.

REFERENCES

1. Honda S (1984) High-performance liquid chromatography of mono- and oligosaccharides. *Anal Biochem* **140,** 1-47.
2. Anumula KR (2000) High-sensitivity and high-resolution methods for glycoprotein analysis. *Anal Biochem* **283,** 17-26.
3. Wuhrer M, Deelder AM, & Hokke CH (2005) Protein glycosylation analysis by liquid chromatography-mass spectrometry. *J Chromatogr B Biomed Sci App* **825,** 124-133.
4. Barroso B, Dijkstra R, Geerts M, Lagerwerf F, van Veelen P, & de Ru A (2002) On-line high-performance liquid chromatography/mass spectrometric characterization of native oligosaccharides from glycoproteins. *Rapid Commun Mass Spectrom* **16,** 1320-1329.
5. Royle L, Mattu TS, Hart E, Langridge JI, Merry AH, Murphy N, Harvey DJ, Dwek RA, & Rudd PM (2002) An analytical and structural database provides a strategy for sequencing O-glycans from microgram quantities of glycoproteins. *Anal Biochem* **304,** 70-90.
6. Cataldi TR, Campa C, & De Benedetto GE (2000) Carbohydrate analysis by high-performance anion-exchange chromatography with pulsed amperometric detection: the potential is still growing. *Fresenius J Anal Chem* **368,** 739-758.

7. Lee YC (1990) High-performance anion-exchange chromatography for carbohydrate analysis. *Anal Biochem* **189,** 151-162.
8. Rendleman JA (1973) Ionization of Carbohydrates in the Presence of Metal Hydroxides and Oxides. In *Carbohydrates in Solution* pp. 51. Washington DC.
9. Rocklin RD, Tullsen TR, & Marucco MG (1994) Maximizing signal-to-noise ratio in direct current and pulsed amperometric detection. *J Chromatogr A* **671,** 109-114.
10. Kawasaki N, Itoh S, Ohta M, & Hayakawa T (2003) Microanalysis of N-linked oligosaccharides in a glycoprotein by capillary liquid chromatography/mass spectrometry and liquid chromatography/tandem mass spectrometry. *Anal Biochem* **316,** 15-22.
11. Wuhrer M, Koeleman CA, Deelder AM, & Hokke CH (2004) Normal-phase nanoscale liquid chromatography-mass spectrometry of underivatized oligosaccharides at low-femtomole sensitivity. *Anal Chem* **76,** 833-838.
12. Wuhrer M, Koelman CA, Hokke CH, & Deelder AM (2004) Nano-scale liquid chromatography-mass spectrometry of 2-aminobenzamide-labeled oligosaccharides at low femtomole sensitivity. *Int J Mass Spectrom* **232,** 51-57.
13. Gennaro LA, Harvey DJ, & Vouros P (2003) Reversed-phase ion-pairing liquid chromatography/ion trap mass spectrometry for the analysis of negatively charged, derivatized glycans. *Rapid Commun Mass Spectrom* **17,** 1528-1534.
14. Torto N, Hofte A, Tjaden UR, Gorton L, Marko-Varga G, Bruggink C, & van der Greef J (1998) Microdialysis-introduction high-performance anion-exchange chromatography/ionspray mass spectrometry for monitoring of online-desalted carbohydrate hydrolysates. *J Mass Spectrom* **33,** 334-341.
15. van der Hoeven RAM, Tjaden UR, van der Greef J, van Casteren WHM, Schols HA, Voragen AGJ, & Bruggink C (1998) Recent progress in high-performance anion-exchange chromatography/ionspray mass spectrometry for molecular mass determination and characterization of carbohydrates using static and scanning array detection. *J Mass Spectrom* **33,** 377-386.
16. Rumbold K, Okatch H, Torto N, Siika-Aho M, Gubitz G, Robra KH, & Prior B (2002) Monitoring on-line desalted lignocellulosic hydrolysates by microdialysis sampling micro-high performance anion exchange chromatography with integrated pulsed electrochemical detection/mass spectrometry. *Biotechnol Bioeng* **78,** 822-828.
17. Richardson S, Cohen A, & Gorton L (2001) High-performance anion-exchange chromatography-electrospray mass spectrometry for investigation of the substituent distribution in hydroxypropylated potato amylopectin starch. *J Chromatogr A* **917,** 111-121.
18. Rocklin RD, Clarke AP, & Weitzhandler M (1998) Improved long-term reproducibility for pulsed amperometric detection of carbohydrates via a new quadruple-potential waveform. *Anal Chem* **70,** 1496-1501.
19. Packer NH, Lawson MA, Jardine DR, & Redmond JW (1998) A general approach to desalting oligosaccharides released from glycoproteins. *Glycoconj J* **15,** 737-747.
20. Small,H. (1989) *Ion Chromatography*, 1989 edn., pp. 65, Plenium Publishing Corp., New York.
21. Weiss,J. (1995) *Ion Chromatography*, 2 edn., pp.74, VCH, Weinheim.
22. De Leenheer L (1994) Production and use of inulin: Industrial reality with a promising future. In *Carbohydrates as Organic Raw Materials III* (van Bekkum H, Roper H, & Voragen F, eds), pp. 67-92. CRF, The Hague.
23. Niness KR (1999) Inulin and oligofructose: what are they? *J Nutr* **129,** 1402S-1406S.
24. Yamashita K, Ohkura T, Okada S, Yabuuchi H, & Kobata A (1981) Urinary oligosaccharides of GM1-gangliosidosis. Different excretion patterns of oligosaccharides in the urine of type 1 and type 2 subgroups. *J Biol Chem* **256,** 4789-4798.
25. Klein A, Lebreton A, Lemoine J, Perini JM, Roussel P, & Michalski JC (1998) Identification of urinary oligosaccharides by matrix-assisted laser desorption ionization time-of-flight mass spectrometry. *Clin Chem* **44,** 2422-2428.
26. Domon B & Costello CE (1988) A Systematic Nomenclature for Carbohydrate Fragmentations in FAB-MS/MS Spectra of Glycoconjugates. *J Glycoconj* **5,** 397-409.
27. Spina E, Sturiale L, Romeo D, Impallomeni G, Garozzo D, Waidelich D, & Glueckmann M (2004) New fragmentation mechanisms in matrix-assisted laser desorption/ionization time-of-flight/time-of-flight tandem mass spectrometry of carbohydrates. *Rapid Commun Mass Spectrom* **18,** 392-398.
28. Harvey DJ (2000) Electrospray mass spectrometry and fragmentation of N-linked carbohydrates derivatized at the reducing terminus. *J Am Soc Mass Spectrom* **11,** 900-915.
29. Weiskopf AS, Vouros P, & Harvey DJ (1998) Electrospray ionization-ion trap mass spectrometry for structural analysis of complex N-linked glycoprotein oligosaccharides. *Anal Chem* **70,** 4441-4447.

30. van der Hoeven RAM, Hofte AJP, Tjaden UR, van der Greef J, Torto N, Gorton L, Marko-Varga G, & Bruggink C (1998) Sensitivity improvement in the analysis of oligosaccharides by online high-performance anion-exchange chromatography/ionspray mass spectrometry. *Rapid Commun Mass Spectrom* **12,** 69-74.

31. Hommes FA & Varghese M (1991) High-performance liquid chromatography of urinary oligosaccharides in the diagnosis of glycoprotein degradation disorders. *Clin Chim Acta* **203,** 211-224.

4

GLYCAN PROFILING OF URINE, AMNIOTIC FLUID AND ASCITIC FLUID FROM GALACTOSIALIDOSIS PATIENTS REVEALS NOVEL OLIGOSACCHARIDES WITH REDUCING END HEXOSE AND ALDOHEXONIC ACID RESIDUES

4.1 ABSTRACT

Urine, amniotic fluid and ascitic fluid samples of galactosialidosis patients were analyzed and structurally characterized for free oligosaccharides using capillary high-performance anion-exchange chromatography with pulsed amperometric detection and online mass spectrometry. In addition to the expected endo-β-*N*-acetylglucosaminidase-cleaved products of complex-type sialylated *N*-glycans, *O*-sulfated oligosaccharide moieties were detected. Moreover, novel carbohydrate moieties with reducing-end hexose residues were detected. On the basis of structural features such as a hexose–*N*-acetylhexosamine–hexose–hexose consensus sequence and di-sialic acid units, these oligosaccharides are thought to represent, at least in part, glycan moieties of glycosphingolipids. In addition, C_1-oxidized, aldohexonic acid containing versions of most of these oligosaccharides were observed. These observations suggest an alternative catabolism of glycosphingolipids in galactosialidosis patients: oligosaccharide moieties from glycosphingolipids would be released by a hitherto unknown ceramide glycanase activity. The results show the potential and versatility of the analytical approach for structural characterization of oligosaccharides in various body fluids.

Cees Bruggink[1,2], Ben J. H. M. Poorthuis[3], Monique Piraud[4], Roseline Froissart[4], André M. Deelder[1] and Manfred Wuhrer[1]

[1] Biomolecular Mass Spectrometry Unit, Department of Parasitology, Leiden University Medical Center, Leiden, The Netherlands
[2] Dionex Benelux BV, Amsterdam, The Netherlands
[3] Department of Medical Biochemistry, Academic Medical Center, Amsterdam, The Netherlands
[4] Laboratoire des Maladies Héréditaires du Métabolisme et Dépistage Néonatal, Centre de Biologie Est, Hospices Civils de Lyon, Bron, France

The FEBS Journal (2010) 277; 2970–2986

4.2 INTRODUCTION

Galactosialidosis is an autosomal recessive lysosomal storage disease, caused by deficiency of both α-neuraminidase (EC 3.2.1.18) and β-galactosidase (EC 3.2.1.23) activities [1], resulting from a defect in the protective protein cathepsin A (EC 3.4.16.5). This lysosomal protein protects α-neuraminidase and β-galactosidase from proteolytic degradation [2] by formation of a complex involving cathepsin A, β-galactosidase, α-neuraminidase and *N*-acetylgalactosamine-6-sulfate sulfatase (EC 3.1.6.4) [3,4].

Galactosialidosis is characterized by excessive excretion of sialyloligosaccharides in the urine, an increase in the amount of bound sialic acid in various tissues, and severe clinical symptoms [5,6]. Three clinical subtypes can be distinguished, depending on the age of onset and severity of the symptoms: the early infantile type with fetal hydrops, ascites, visceromegaly, skeletal dysplasia and early death, usually by 8–12 months of age; the late infantile type with cardiac involvement, hepatosplenomegaly, growth retardation and mild mental retardation; and the juvenile/adult type with progressive neurological deterioration without visceromegaly. Coarse faces, cherry red spots in the macula and vertebral changes are usually present [7,8]. Biochemical diagnosis is made by demonstration of increased excretion of oligosaccharides by thin layer chromatography [9] and by demonstrating a combined deficiency of α-neuraminidase and β-galactosidase in patient cells.

Several activity studies on the structural analysis of sialyloligosaccharides from urine of galactosialidosis patients [10,11] have been published. van Pelt *et al*. [12] described 21 sialylated oligosaccharides. Twenty of these were endo-β-*N*-acetylglucosaminidase-cleaved products of complex-type sialylated *N*-glycans, and one was a di-sialylated diantennary structure with an intact *N,N'*-diacetylchitobiose unit at the reducing end.

Here we report the analysis of oligosaccharides from galactosialidosis patients using a previously described capillary high-performance anion-exchange chromatography (HPAEC) method with combined integrated pulsed amperometric (PAD) and ion-trap mass spectrometric detection and analysis [13]. In addition to urine samples, ascitic fluid and amniotic fluid obtained from mothers pregnant with a galactosialidosis fetus were analyzed. Amniotic fluid is of importance for prenatal diagnosis of many lysosomal storage disorders such as galactosialidosis [14].

In addition to the expected endo-β-*N*-acetylglucosaminidase-cleaved products of complex-type sialylated *N*-glycans, oligosaccharide structures that had not been previously found were detected in the samples from galactosialidosis patients. These newly found oligosaccharide structures included *O*-sulfated oligosaccharide moieties, carbohydrate moieties of glycosphingolipids, and C_1-oxidized (aldohexonic acid) carbohydrate moieties of glycosphingolipids. On the basis of the presence of carbohydrate moieties of glycosphingolipids, we speculate about the potential involvement of a ceramide glycanase in the catabolism of glycosphingolipids in humans.

4.3 RESULTS

Glycans from seven urine samples from six galactosialidosis patients, five amniotic fluid samples from five mothers carrying a fetus suffering from galactosialidosis, and two ascitic fluid samples were analyzed by HPAEC-PAD-MS (Table 4-1). In addition, four urine samples from healthy

Table 4-1. Information about the samples and patients. ND, not detected.

Sample Code	Details	Creatinine (mmol/L)
U1	Urine patient AB, 12 days old, Lyon France	1,0
U2	Urine patient AV, 6 days old, Lyon France	2,3
U3, U4	Urine patient MO, Lyon France	n.d.
U5	Urine patient BO, 127 days old, Lyon France	1,2
U6	Urine patient B07/0175, Amsterdam Netherlands	1,6
U7	Urine patient B07/0845.1, Leiden Netherlands 8 weaks old	0,5
Amfl1	Amniotic fluid patient AB, 30 weeks fetus, Lyon France	n.d.
Amfl2	Amniotic fluid patient AS, 29 weeks fetus, Lyon France	n.d.
Amfl3	Amniotic fluid patient W, 23 weeks of amenorrhoea, Lyon France	n.d.
Amfl4	Amniotic fluid patient LA, 22 weeks fetus, Lyon France	n.d.
Amfl5	Amniotic fluid patient GG, protein 3.5 g/L, Nijmegen Netherlands	0,08
Asf1	Ascite fluid patient AB, Lyon France	n.d.
Asf2	Ascite fluid patient AS, Lyon France	n.d.

individuals were investigated. Figure 4-1 shows a typical HPAEC-PAD chromatogram from a urine sample of a galactosialidosis patient.

4.3.1 *N*-glycan-derived structures

The typical endo-β-*N*-acetylglucosaminidase cleavage products of complex-type *N*-sialyloligosaccharides were found in all urine samples, amniotic fluid samples and ascitic fluid samples (see Fig. 4-2, n1–n6) [12]. A varying number of isomers were detected for the various *N*-glycan compositions, and these were analyzed by MS/MS, as summarized in Table 4-2. *N*-glycan-derived structure n1 had the composition HNS (H, hexose; N, *N*-acetylhexosamine; S, *N*-acetylneuraminic acid), and two isomers of n1 were detected. Tandem mass spectrometry indicated the structure Neu5Ac(α2–3/6)Gal(β1–4)GlcNAc. On the basis of chromatographic retention [15] in combination with the tandem mass spectrometric data [16], we speculate that *N*-acetylneuraminic acid (Neu5Ac) is (α2–6)-linked in the first n1 isomer and (α2–3)-linked in the second isomer. Specifically, the relatively low signal intensity of the fragment ion at *m/z* 655.2 from the second eluting isomer [16] suggests an α2–3-linked Neu5Ac.

Moreover, larger complex sialyloligosaccharides were found with the composition $H_{3-6}N_{2-4}S_{1-3}$. In accordance with literature data [12], we interpreted the three isomers H_3N_2S as sialyl-mono antennary endo-β-*N*-acetylglucosaminidase cleavage products of complex-type *N*-glycan structures (Fig. 4-2, n2). Similarly, the two isomers H_5N_3S were assigned to sialylated diantennary structures (Fig. 4-2, n3), the two isomers $H_5N_3S_2$ as di-sialylated diantennary structures (Fig. 4-2, n4), the two isomers $H_6N_4S_2$ as di-sialylated triantennary structures (Fig. 4-2, n5), and the three isomers $H_6N_4S_3$ as tri-sialylated triantennary structures (Fig. 4-2, n6). These assignments were corroborated by the MS/MS data (Table 4-2).

In addition to the expected endo-β-*N*-acetylglucosaminidase-cleaved products of complex-type sialylated *N*-glycans, some *O*-sulfated versions were also found in low amounts (see Table 4-3 and Fig. 4-2, s1–s4). The detected carbohydrate HSO_3NS eluted in the time window for

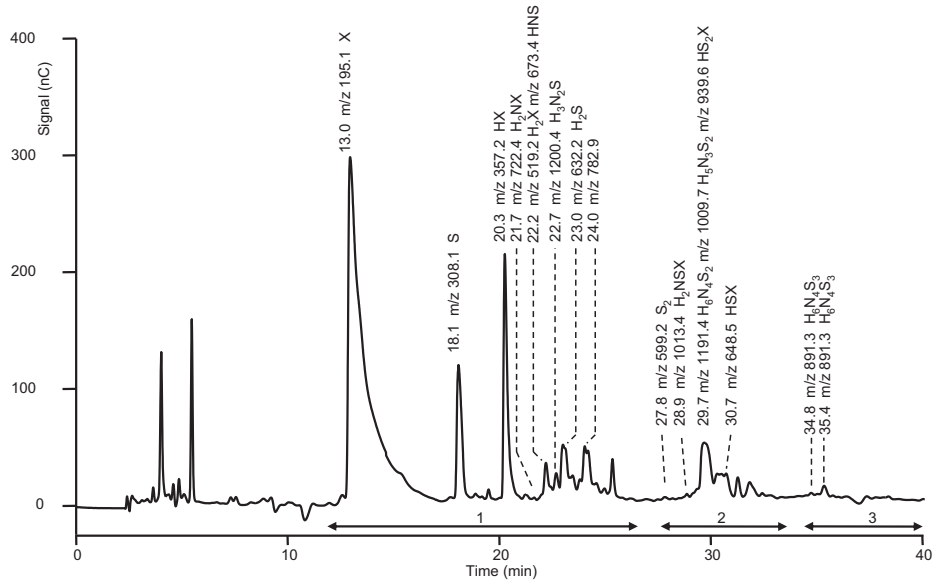

Figure 4-1. Capillary HPAEC-PAD chromatogram of oligosaccharides from a urine sample of a galactosialidosis patient. H, hexose; N, *N*-acetylhexosamine; S, *N*-acetylneuraminic acid; X, aldohexonic acid. The numbers above the horizontal arrows represents the number of acidic groups.

double negatively charged carbohydrates (Fig. 4-1). The MS/MS fragment ions Y_1 (*m/z* 219.9) and Y_2 (*m/z* 462.0) indicated the sequence Neu5Ac–$HexSO_3$–HexNAc (Fig. 4-3). The $^{0,2}A_3$ ring fragment ion at *m/z* 652.1 is typical of a 1–4 glycosidic link [16,17] between $HexSO_3$ and HexNAc.

The lack of significant fragment ions between the fragment ions Y_1 and Y_2 is indicative of a 2–3 linkage between Neu5Ac and $HexSO_3$. These data are consistent with a Neu5Ac(α2–3)Gal-6-SO_3(β1–4) GlcNAc *N*-glycan antenna structure or *O*-glycan structural motif [18]. Moreover, the presence of complex *O*-sulfated sialylated oligosaccharides with the composition $H_{3-5}SO_3N_{2-3}S_{1-2}$ (see Table 4-2), was indicated by MS. Based on observed retention times, mass spectrometric data (Table 4-2) and literature data, these glycans were assigned to sulfated variants of the above-mentioned endo-β-*N*-acetylglucosaminidase cleavage products of complex-type sialylated *N*-glycan structures: the two isomers of composition $H_3SO_3N_2S$ were assigned to *O*-sulfated sialylated monoantennary glycans (Fig. 4-2, s2), the four isomers $H_5SO_3N_3S$ as *O*-sulfated monosialylated diantennary glycans (Fig. 4-2, s3), and the two isomers $H_5SO_3N_3S_2$ as *O*-sulfated, disialylated diantennary glycans (Fig. 4-2, s4).

4.3.2 Glycans with reducing-end hexoses

In addition to the *N*-glycan-derived signals, the LC-MS/MS data provided evidence for the presence of a group of oligosaccharides of composition $H_{0-3}N_{0-1}S_{0-2}$ (g1–g11, Table 4-2). Tandem mass spectrometry indicated a sequence Hex–HexNAc–Hex–Hex or truncated versions thereof for most of these oligosaccharides, decorated with up to two Neu5Ac. Di-sialyl motifs (Neu5Ac linked to Neu5Ac) were also observed. Structural characterization of these oligosaccharides is described below.

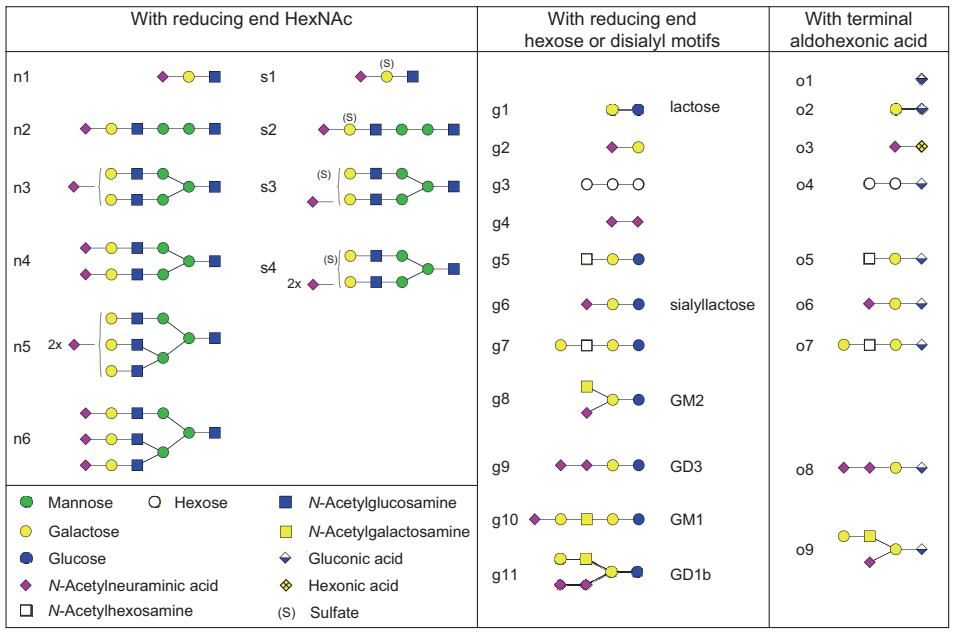

Figure 4-2. Schematic overview of the proposed structures of free oligosaccharides in body liquids from galactosialidosis patients. The codes n1–n6, s1–s4, g1–g11 and o1–o9 refer to Tables 4-2 and 4-3.

Two isomers of the glycan H_2 were detected. The retention time of the late-eluting H_2 isomer was identical to that of maltose (Glc(α1–4)Glc; Table 4-2). The retention time of the early-eluting H_2 isomer was identical to that of lactose, and Fig. 4-4A shows the MS/MS spectrum obtained. Fragment ion C_1 (*m/z* 178.9) indicates the composition H_2 and the ring fragment ion (*m/z* 220.8) corresponds to a loss of 120, which is interpreted as a $^{2,4}A_2$ ring fragment typical of a 1–4 linkage between the hexoses [16,17].

Four isomers were found with the composition H_2S (Table 4-2). The MS/MS spectrum of the first eluting isomer with retention time of 10.5 min is shown in Fig. 4-4B. The fragment ions B_1, C_2, Y_1 and Y_2 indicate the sequence Neu5Ac–Hex–Hex. The ring fragments $^{0,2}A_3$ and $^{0,2}A_3$-18 in combination with lack of the $^{0,3}A_3$ ring fragment ion are typical of a 1–4 linkage between the hexoses [16,17]. The lack of relevant ring fragment ions between fragment ions B_1 and C_2 is indicative of a 2–3 linkage between Neu5Ac and Hex. These combined data are consistent with sialyllactose (Neu5Ac(α2–3)Gal(β1–4)Glc) (g6, Table 4-2). The MS/MS fragmentation spectra of the remaining three isomers with the composition H_2S are indicative of the sequence Neu5Ac–Hex–Hex, for which the structure has been partly elucidated (Table 4-2).

An oligosaccharide species with composition H_2S_2 was detected at 29.1 min (g9, Table 4-2). The fragment ion B_2 (*m/z* 581.2) consists of two *N*-acetylneuraminic acids, indicating a sialic acid–sialic acid motif. Fragment ion Y_3 (*m/z* 632.2) is in accordance with two Hex decorated with Neu5Ac (Fig. 4-4C). These details indicate the sequence Neu5Ac–Neu5Ac–Hex–Hex.

Two isomers were detected with the composition H_3N (*m/z* 706.2) (g7, Table 4-2). The MS/MS spectrum of the isomer eluting at 12.7 min is shown in Fig. 4-4D. The fragment ions B_2 (*m/z*

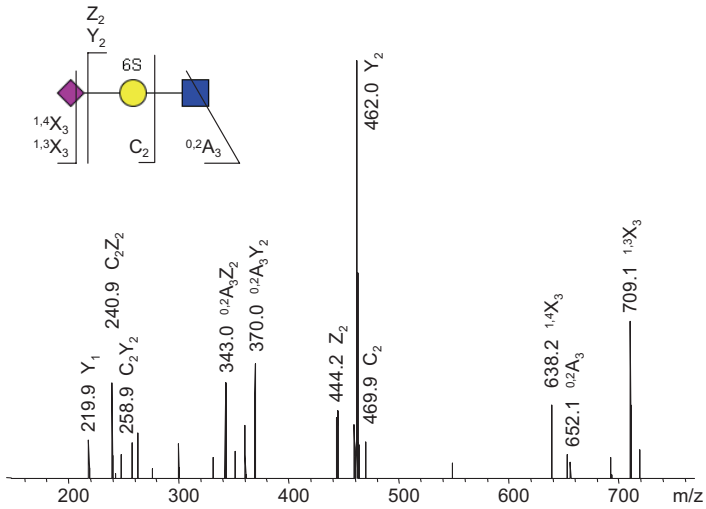

Figure 4-3. Negative-ion fragmentation spectrum of the proposed 6'-sulfated sialyl lactosamine.

363.5) and C_2 (*m/z* 381.9) corresponded to Hex linked to HexNAc. The fragments C_3 (*m/z* 543.9) and C_2 (*m/z* 381.9) indicated two Hex at the reducing end. Based on the ring fragment ions $^{0,2}A_4$ and $^{0,2}A_4$-18 and the lack of $^{0,3}A_4$, a 1–4 linkage was deduced for the two hexoses at the reducing terminus [16,17], in accordance with a lactose core structure. From the combined data, we postulate that this oligosaccharide has the glycan structure Hex–HexNAc–Gal(β1–4)Glc.

Two isomers with the composition H_3NS were detected at *m/z* 997.3 (g10, Table 4-2). The MS/MS spectrum of the isomer eluting at 22.0 min is shown in Fig. 4-4E. The fragment ions B_1, C_1, B_2, C_2, B_3, C_3, and C_4 are indicative of the sequence Neu5Ac–Hex–HexNAc–Hex–Hex. The proposed linear sequence was supported by the abundant signals B_3 and C_3. The lack of ring fragments between C_2 and C_1 is indicative of a 2–3 linkage between Neu5Ac and the adjacent hexose. No relevant ring fragments were observed between C_2 and C_3, which is consistent with a 1–3 linkage between Hex and HexNAc. The ring fragment ions $^{0,2}A_4$ and $^{2,4}A_4$, and the lack of $^{0,3}A_4$, are indicative of a 1–4 linkage between HexNAc and the adjacent hexose. The ring fragment ions $^{0,2}A_5$, $^{0,2}A_5$-18 and $^{2,4}A_5$, and the lack of $^{0,3}A_5$, are indicative of a 1–4 link between the reducing end Hex and the adjacent Hex [16,17]. Based on these data, we propose the structure Neu5Ac(α2–3)Hex(β1–3)HexNAc(β1–4)Gal(β1–4)Glcβ.

An oligosaccharide of composition $H_3N_1S_2$ was detected (g11, Table 4-2). MS/MS analyses revealed an intense signal at *m/z* 563.6 ($B_{2\alpha}$-H_2O), which indicates a di-sialic acid motif. This oligosaccharide was interpreted to be an extended version of g9, and the structure Hex–HexNAc–(Neu5Ac–Neu5Ac)–Hex–Hex is proposed. Moreover, a Neu5Ac–Neu5Ac disaccharide was detected (g4, Table 4-2), as well as oligosaccharides of composition H_2F_1 (where F stands for deoxyhexose) and $H_2N_1F_1$ (Table 4-2).

4.3.3 Glycans with aldohexonic acid

In addition, evidence was obtained from the LC–MS/MS data for the presence of C_1-oxidized glycans (Fig. 4-2, o1–o9). The innermost residue of these oligosaccharides was found to be

Table 4-2. Structural data for detected oligosaccharides moieties.

Glycan composition	Species	Ret. time (min)	Signal m/z	MS/MS fragment ions	Proposed Structures	
HNS	n1	22,3	673.6 [M-H]$^-$	655.2 -H_2O; 572.2 $^{0,2}A_3$; 544.2 $^{0,2}A_3$-H_2O; 512.1 $^{2,4}A_3$; 470.1 C_2; 452.1 B_2; 410.1 $^{0,2}A_2$;392.2 $^{0,2}A_2$-H_2O; 380.2 $^{0,3}A_2$; 350.1 $^{0,4}A_2$; 332.1 $^{0,4}A_2$-H_2O; 308.0 C_1; 290.0 B_1	Fig. 2 n1	Neu5Ac(α2–6)Gal(β1–4)GlcNAc
		26,9	673.6 [M-H]$^-$	655.2 -H_2O; 572.2 $^{0,2}A_3$; 544.2 $^{0,2}A_3$-H_2O; 512.0 $^{2,4}A_3$; 470.1 C_2; 452.2 B_2; 410.2 $^{0,2}A_2$;392.2 $^{0,2}A_2$-H_2O; 380.0 $^{0,3}A_2$; 308.0 C_1; 290.0 B_1	Fig. 2 n1	Neu5Ac(α2–3)Gal(β1–4)GlcNAc
H_3N_2S	n2	22,3	1200.4 [M-H]$^-$	1182.6 -H_2O; 1122.5; 1099.4 $^{0,2}A_6$; 1081.3 $^{0,2}A_6$-H_2O; 998.2; 979.3 B_5; 943.3; 937.3 $^{0,2}A_5$; 835.4 C_4; 818.5; 747.9 $^{2,4}A_5Y_5$; 728.8 Z_4; 686.6 $^{2,4}X_4$; 655.0 B_3; 536.2	Fig. 2 n2	Neu5Ac(α2–3/6)Gal(β1–4) GlcNAc(β1–2)Man(α1–6)Man(β1–4) GlcNAc
		22,5	1200.4 [M-H]$^-$; 1298.5 [M+H_2SO_4-H]$^-$	1182.6 -H_2O; 1122.5; 1099.5 $^{0,2}A_6$; 1081.5 $^{0,2}A_6$-H_2O; 1039.5 $^{2,4}A_6$; 997.5 C_5; 979.6 B_5; 835.4 C_4; 817.4 B_4; 748.4 $^{2,4}A_5Y_5$; 673.4 C_3; 655.4 B_3; 572.3 $^{0,2}A_3$; 526.1 $^{3,5}A_3$; 470.2 C_2; 452.2 B_2; 424.2 $^{1,5}A_2$; 410.1 $^{0,2}A_3$	Fig. 2 n2	Neu5Ac(α2–6)Gal(β1–4)GlcNAc(β1–2)Man(α1–3)Man(β1–4)GlcNAc
		23,3	1200.4 [M-H]$^-$; 1298.5 [M+H_2SO_4-H]$^-$	1182.4 -H_2O; 1165.1; 1122.5; 1099.4 $^{0,2}A_6$; 1081.3 $^{0,2}A_6$-H_2O; 1063.4; 1039.3 $^{2,4}A_6$; 1021.4; 997.3 C_5; 979.2 B_5; 961.2; 910.4; 835.2 C_4; 819.2 $^{0,3}X_5$; 817.2 B_4; 784.4; 779.4; 791.1; 775.4 $^{0,2}A_4$; 773.4; 748.2 $^{2,4}A_5Y_5$; 744.3; 696.3; 674.0; 672.4; 655.3 B_3; 619.1; 592.3; 586.1; 568.0; 554.2 $^{0,2}A_3$-H_2O; 536.1; 526.1 $^{3,5}A_3$; 424.1 $^{1,5}A_2$; 381.1	Fig. 2 n2	Neu5Ac(α2–3)Gal(β1–4)GlcNAc(β1–2) Man(α1–3)Man(β1–4)GlcNAc
H_5N_3S	n3	23,7	1727.8 [M-H]$^-$	1709.8 -H_2O; 1668.8 $^{2,4}X_5$; 1626.7 $^{0,2}A_6$; 1608.7 $^{0,2}A_6$-H_2O; 1566.7 $^{2,4}A_6$; 1524.7 C_5; 1506.8 B_5; 1316.6 $^{0,2}X_{5\beta}Y_{5\alpha}$; 1275.5 $^{2,4}A_6Y_{5\alpha}$; 1113.6 $^{2,4}A_6Y_{4\alpha}$; 1053.7 $Z_{3\alpha}$; 979.3 $C_{5\alpha}Z_{2\beta}$; 961.3 $B_{5\alpha}Z_{2\beta}$; 835.3 $C_{4\alpha}$; 817.4 $B_{4\alpha}$	Fig. 2 n3	Neu5Ac(α2–3/6)Gal(β1–4) GlcNAc(β1–2)Man(α1–6)(Gal(β1–4) GlcNAc(β1–2)Man(α1–3))Man(β1–4) GlcNAc
		27,6	1727.8 [M-H]$^-$		Fig. 2 n3	
$H_5N_3S_2$	n4	27,3	1009.0 [M-2H]$^{2-}$	1709.6 $Z_{5\alpha\beta}$; 1626.6 $^{0,2}A_6Y_{5\alpha}$; 1548.7 $^{2,4}A_6Z_{5\alpha}$; $C_5Y_{5\alpha}$; 1050.5; 1000.3 -H_2O; 958.9 $^{0,2}A_6$; 907.8 $^{0,3}A_{5\beta}$; 835.6 C_4; 817.7 B_4; 655.6 B_3; 290.2 B_1	Fig. 2 n4	Neu5Ac(α2–6)Gal(β1–4)GlcNAc(β1–2)Man(α1–6)(Neu5Ac(α2–6) Gal(β1–4)GlcNAc(β1–2)Man(α1–3)) Man(β1–4)GlcNAc
		28	1009.0 [M-2H]$^{2-}$	1797.6 B_5; 1727.6 Y_5; 1709.6 Z_5; 1626.6 $^{0,2}A_6Y_5$; 1608.5 $^{0,2}A_6Z_5$; 1566.4 $^{2,4}A_6Y_5$; 1524.5 C_5Y_5; 1000.4 -H_2O; 958.8 $^{0,2}A_6$; 907.4 $^{0,3}A_{5\beta}$; 835.3 C_4; 817.3 B_4; 673.2 C_3; 655.3 B_3; 452.1 B_2; 424.1 $^{1,5}A_2$; 410.1 $^{0,2}A_2$; 350.0 $^{0,4}A_2$; 307.9 C_1; 290.0 B_1	Fig. 2 n4	Neu5Ac(α2–3/6)Gal(β1–4) GlcNAc(β1–2)Man(α1–6) (Neu5Ac(α2–3/6)Gal(β1–4) GlcNAc(β1–2)Man(α1–3))Man(β1–4) GlcNAc

$H_6N_4S_2$	n5	27,4	1191.4 $[M-2H]^{2-}$		Fig. 2 n5	
		31,4	1191.4 $[M-2H]^{2-}$		Fig. 2 n5	
$H_6N_4S_3$	n6	31,3	891.3 $[M-2H]^{3-}$; 1337.4 $[M-2H]^{2-}$	2075.8; 2074.9 Z_6Y_6 or Y_6Z_6; 2016.0; 1995.1; 1992.9; 1974.6; 1973.8; 1931.8; 1890.6; 1889.8; 1871.8; 1608.4; 1474.4; 1473.6 $B_{4\alpha}$; 1328.7 $-H_2O$; 1279.1 $^{1,4}X_{6\alpha,\beta,\gamma}$; 1203,4; 1202.3; 1201.3; 1200.5 $C_{4\alpha}Y_{5\alpha}$; 1192.1; 1191.4 Y_5; 1184.7; 1183.9; 1182.4 Z_5; 1152.8; 1142.7; 1141.0; 1133.6; 1132.8; 1111.5; 1111.1; 1092.6; 1090.0 $C_5Y_{5\alpha}$; 1081.4; 1039.7; 1009.3; 1000.3; 981.0; 979.2 $B_5Y_{2\alpha}$; 963.3; 962.2 $B_5Z_{2\alpha}$; 944.4; 907.2 $C_5Y_{3\alpha}$; 885.5 $-H_2O$; 879.0; 860.0; 857.3 $^{0,2}A_6$; 852.0 $^{2,5}X_6$; 851.1 $^{0,4}X_6$; 838.1; 837.4 $^{2,4}A_6$; 835.5 C_4; 823.3 C_5; 817.2 B_4; 798.3; 775.2 $^{0,2}A_4$; 750.0; 745.3 $C_{4\alpha}$; 737.2; 736.1; 673.3 C_3; 655.2 B_3; 536.1; 470.1 C_2; 424.1 $^{1,5}A_2$; 306.2; 290.0 B_1;	Fig. 2 n6	Neu5Ac(α2–3)Gal(β1–4)GlcNAc(β1–2)Man(α1–6)(Neu5Ac(α2–3)Gal(β1–4)GlcNAc(β1–2)(Neu5Ac(α2–6)Gal(β1–4)GlcNAc(β1–4))Man(α1–3))Man(β1–4)GlcNAc
		32,4	891.3 $[M-2H]^{3-}$		Fig. 2 n6	
		34,6	891.3 $[M-2H]^{3-}$		Fig. 2 n6	
HSO_3NS	s1	32	753.2 $[M-H]^-$; 851.1 $[M+H_2SO_4-H]^-$	709.1 $^{1,3}X_3$; 652.1 $^{0,2}A_3$; 638.2 $^{1,4}X_3$; 469.9 C_2; 462.0 Y_2; 444.2 Z_2; 370.0; 361.1 $^{0,2}A_3Y_2$; 352.0; 343.0 $^{0,2}A_3Z_2$; 331.9 $B_2^{0,4}X_3$-SO_3; 301.0 $^{2,4}A_3Y_2$; 276.8 $B_2^{3,5}X_3$-SO_3; 263.8 $^{0,2}A_3Z_2$-SO_3; 258.9 C_2Y_2; 248.9 $C_2^{0,2}X_3$-SO_3; 240.9 C_2Z_2; 219.9 Y_1	Fig. 2 s1	NeuAc(α2-3)Gal(6S)(β1-4)GlcNAc
$H_3SO_3N_2S$	s2	36,5	639.7 $[M-2H]^{2-}$	990.2; 989.2 Y_5; 987.0 $^{0,3}A_5$; 971.1 $^{3,5}A_5$; 951.2 $^{1,5}A_5$-SO_3; 915.3 C_4; 890.2; 888.2 $^{0,2}A_6Y_5$; 886.1 $C_5^{0,3}X_6$; 871.5 $C_4^{1,3}X_6$; 870.1 $^{0,2}A_6Z_5$; 829.5; 828.2 $^{2,4}A_6Y_5$; 786.1 C_5Y_5; 768.0 C_5Z_5; 726.2 $C_5^{1,3}X_5$; 693.9 $C_4^{0,2}X_6$; 655.1 B_3-SO_3; 647.8 $^{2,4}A_5Z_5$; 630.6 $-H_2O$; 629.5 $C_3^{1,3}X_6$-SO_3; 624.1 C_4Y_5; 622.2 $^{0,3}A_3$; 620.3 $B_2^{1,4}X_6$; 611.3 $B_3^{1,3}X_6$-SO_3; 600.5 $^{3,5}A_6Y_4$; 594.1; 589.1 $^{0,2}A_6$; 588.1 B_4Z_5; 580.1; 571.9 $C_5^{1,5}X_5$; 559.0 $^{2,4}A_6$; 541.1 $^{2,5}A_6$-SO_3; 538.6; 58.1 C_5; 537.0 $^{2,5}X_6$; 529.1 B_5; 519.1 $^{2,4}X_6$-SO_3; 516.1 $C_5^{1,3}X_6$; 484.0 $C_5^{2,4}X_4$; 478.5 $^{0,4}A_3$; 470.0 C_2; 457.0 C_4; 449.0 $C_2^{2,4}X_6$; 448.1 B_4; 444.0 C_3Z_5; 427.5 $C_5^{0,2}X_6$; 418.8 $B_5^{0,2}X_6$; 398.0 $^{1,5}A_3Z_5$; 397.6 $B_4^{2,4}X_6$; 397.0 $^{3,5}A_6Y_3$; 380.0 $^{1,4}A_2$; 375.9 C_3; 357.1 $B_2^{3,5}X_6$; 302.1 $^{3,5}A_3$; 292.7 $^{2,4}A_6Y_5$; 290.0 B_1; 215.3 $B_2^{2,4}X_6$; 210.8 $B_4^{2,5}X_4$	Fig. 2 s2	Neu5Ac(α2–3)Gal(6S)(β1–4)GlcNAc(β1–2)Man(α1–6)Man(β1–4)GlcNAc
		38,9	639.7 $[M-2H]^{2-}$		Fig. 2 s2	Neu5Ac(α2–3/6)Gal(6S)(β1–4)GlcNAc(β1–2)Man(α1–3)Man(β1–4)GlcNAc

Table 4-2. continued.

Glycan composition	Species	Ret. time (min)	Signal m/z	MS/MS fragment ions	Proposed Structures	
$H_5SO_3N_3S$	s3	34,6	903.3 $[M\text{-}2H]^{2-}$	1446.3 $^{0,2}A_5Z_{4\beta}$; 886.4; 859.2; 826 $^{3,5}X_{5\beta}$; 774.1 $^{2,5}A_6Z_{2\alpha}$; 757.6 E_3-ion; 638.1 $B_5Z_{5\alpha}$; 613.2 $^{2,5}A_6Z_{3\beta}$; 612.2 $B_{4\alpha}$ $^{2,5}X_{6\alpha}$; 595.0; 594.2 $^{3,5}A_6Z_{4\alpha}$; 483.1 $Y_{3\alpha}$ $^{2,5}X_{5\beta}$; 308.1 C_1; 290.3 B_1	Fig. 2 s3	Gal(6S)(β1–4)GlcNAc(β1–2) Man(α1–6)(Neu5Ac(α2–3)Gal(β1–4) GlcNAc(β1–2)Man(α1–3))Man(β1–4) GlcNAc
		39,3	903.3 $[M\text{-}2H]^{2-}$		Fig. 2 s3	
		41,4	903.3 $[M\text{-}2H]^{2-}$		Fig. 2 s3	
		45,4	903.3 $[M\text{-}2H]^{2-}$		Fig. 2 s3	
$H_5SO_3N_3S_2$	s4	39,6	1048.8 $[M\text{-}2H]^{2-}$		Fig. 2 s4	Neu5Ac(α2–3/6)Gal(6S)(β1–4) GlcNAc(β1–2)Man(α1–6) (Neu5Ac(α2–3/6)Gal(β1–4) GlcNAc(β1–2)Man(α1–3))Man(β1–4) GlcNAc
H_2	g1	7,6	341.2 $[M\text{-}H]^-$	323.0 $-H_2O$; 220.8 $^{2,4}A_2$; 178.9 C_1	Fig. 2 g1; Fig. 4A	Gal(β1–4)Glc
		8,2	341.2 $[M\text{-}H]^-$; 439.1 $[M+H_2SO_4\text{-}H]^-$	281.0 $^{0,2}A_2$; 235.0 $^{3,5}A_2$; 220.8 $^{2,4}A_2$; 178.9 C_1; 160.9 B_1		Glc(α1–4)Glc
HS	g2	24,4	470.2 $[M\text{-}H]^-$	410.0 $^{0,2}A_2$; 379.9 $^{0,3}A_2$; 370.0; 308.0 C_1; 290.0 B_1; 271.8; 220.0; 194.8; 169.9		NeuAc(α2–6)Gal
		25,1	470.2 $[M\text{-}H]^-$; 568.2 $[M+H_2SO_4\text{-}H]^-$	357.8; 307.8 C_1; 290.0 B_1; 272.9; 269.7; 219.8; 201.7; 173.8; 169.9	Fig. 2 g2	NeuAc(α2–3)Gal
H_3	g3	7,6	503.2 $[M\text{-}H]^-$; 601.2 $[M+H_2SO_4\text{-}H]^-$	369.2 $^{1,5}X_3$; 341.1 C_2; 323.1 B_2; 281.0 $^{0,2}A_2$; 262.8 $^{0,2}A_2\text{-}H_2O$; 234.8 $^{3,5}A_2$; 221.0 $^{2,4}A_2$; 202.9 $^{2,4}A_2\text{-}H_2O$; 178.9 C_1; 160.9 B_1		Hex(1–4)Hex(1–3)Hex
		9,1	503.2 $[M\text{-}H]^-$; 601.2 $[M+H_2SO_4\text{-}H]^-$	341.1 C_2; 323.1 B_1; 250.9 $^{0,3}A_2$; 220.9 $^{0,4}A_2$; 178.9 C_1; 160.9 B_1		Hex(1–6)Hex(1–3)Hex
		20,4	503.2 $[M\text{-}H]^-$; 601.2 $[M+H_2SO_4\text{-}H]^-$	443.4 $^{0,2}A_3$; 424.7 $^{0,2}A_3\text{-}H_2O$; 383.1 $^{2,4}A_3$; 341.1 C_2;322.8 B_2; 295.4 $^{1,5}A_2$; 280.9 $^{0,2}A_2$; 237.0 $^{2,5}X_2$; 234.7 $^{3,5}A_2$; 220.8 $^{2,4}A_2$; 178.9 C_1; 160.8 B_1	Fig. 2 g3	Gal(α1–4)Gal(β1–4)Glc
S_2	g4	27,7	599.2 $[M\text{-}H]^-$; 697.2 $[M+H_2SO_4\text{-}H]^-$	581.1 $-H_2O$; 511.1 $^{0,2}A_2$; 495.0 $^{2,5}A_2$; 410.0 $^{0,4}A_2$; 380.0 $^{1,5}X_2$; 308.0 C_1; 290.0 B_1		Neu5Ac(α2–8)Neu5Ac
		25,5	599.2 $[M\text{-}H]^-$			

H_2N	g5	9,6	544.2 $[M-H]^-$; 642.2 $[M+H_2SO_4-H]^-$	526.1; 383.0; 290.0; 271.9; 169.9	Fig. 2 g5	GlcNAc(β1–4)Gal(β(–4)Glc
H_2S	g6	10,5	632.2 $[M-H]^-$; 730.2 $[M+H_2SO_4-H]^-$	614.0 -H_2O; 588.1 $^{1,3}X_3$; 572.1 $^{0,2}A_3$; 554.0 $^{0,2}A_3$-H_2O; 535.9; 470.0 C_2; 411.0 $^{0,2}X_3$; 408.0; 385.9; 341.1 Y_2; 290.0 B_1; 178.9 Y_1	Fig. 2 g6; Fig. 4B	Neu5Ac(α2–3)Gal(β1–4)Glc
		13,3	632.2 $[M-H]^-$; 730.2 $[M+H_2SO_4-H]^-$	614.0 -H_2O; 598.6; 588.1 $^{1,3}X_3$; 534.3; 532.3; 472.1; 470.9; 469.9 C_2; 456.2; 411.0 $^{0,2}X_3$; 341.1 Y_2; 307.9 C_1; 290.0 B_1; 178.9 Y_1		Neu5Ac(α2–3)Hex(1–3)Hex or Neu5Ac(α2–3)Gal(1–3)Gal
		14,6	632.2 $[M-H]^-$; 730.2 $[M+H_2SO_4-H]^-$	614.0 -H_2O; 599.1; 588.1 $^{1,3}X_3$; 535.0; 534.2; 524.1; 472.2; 470.1 C_2; 411.1 $^{0,2}X_3$; 434.0; 416.1; 411.0; 408.0 B_2 $^{1,3}X_3$; 404.0; 386.0; 341.0 Y_2; 337.0 B_2 $^{1,4}X_3$; 305.9 $^{0,4}A_2$-CO_2; 292.0; 290.0 B_1; 178.8 Y_1		Neu5Ac(α2–6)Hex(1–3)Hex or Neu5Ac(α2–6)Gal(β1–3)Glc
		20,9	632.2 $[M-H]^-$; 730.2 $[M+H_2SO_4-H]^-$	614.0 -H_2O; 572.1 $^{0,2}A_3$; 571.2; 554.1 $^{0,2}A_3$-H_2O; 536.0; 512.1 $^{2,4}A_3$; 494.0 $^{2,4}A_3$-H_2O; 472.0; 470.1 C_2; 468.1; 452.0 B_2; 441.0 $^{0,3}X_3$; 411.0 $^{0,2}X_3$; 410.0 $^{0,2}A_2$; 408.1; 392.1 $^{0,2}A_2$-H_2O; 380.0 $^{0,3}A_2$; 350.0 $^{0,4}A_2$; 334.0; 332.0; 316.0; 308.0 C_1; 306.0 $^{0,4}A_2$-CO_2; 290.0 B_1		Neu5Ac(α2–6)Hex(1-4)Glc or Neu5Ac(α2–6)Gal(β1–4)Glc
H_3N	g7	9,5	706.2 $[M-H]^-$; 804.3 $[M+H_2SO_4-H]^-$	688.0 -H_2O or D-ion; 646.2 $^{0,2}A_4$; 628.1 $^{0,2}A_4$-H_2O; 585.6 $^{0,4}A_4$; 544.1 C_3; 424.2 $^{1,3}A_3$; 382.0 C_2; 280.9 $^{0,2}A_2$; 263.0 $^{0,2}A_4Z_2$		Gal(β1–4)GlcNAc(β1–2)Man(α1–6) Man
		12,7	706.2 $[M-H]^-$; 804.3 $[M+H_2SO_4-H]^-$; 902.3 $[M+2H_2SO_4-H]^-$	646.3 $^{0,2}A_4$; 628.1 $^{0,2}A_4$-H_2O; 543.9 C_3;381.9 C_2;363.5 B_2;202.1 C_2Z_3	Fig. 2 g7; Fig. 4D	Gal(β1–3)GalNAc(β1–4)Gal(β1–4)Glc
H_2NS	g8	22,8	835.3 $[M-H]^-$	817.3 -H_2O; 715.2 $^{2,4}A_3$; 673.0 C_3; 655.3 B_3; 572.0 $^{0,2}A_3Y_{2\beta}$; 494.2 $^{2,4}A_3Z_{2\beta}$; 290.1 $B_{1\alpha}$	Fig. 2 g8	GalNAc(β1–4)[Neu5Ac(α2–3)] Gal(β1–4)Glc
H_2S_2	g9	29,1	923.3 $[M-H]^-$	632.2 Y_3; 581.1 B_2; 538.1 B_3 $^{2,5}X_4$; 379.9 C_2 $^{1,5}X_4$; 290.0 B_1; 178.9 Y_1	Fig. 2 g9; Fig. 4C	Neu5Ac(α2–8)Neu5Ac(α2–3) Gal(β1–4)Glc
H_3NS	g10	22	997.3 $[M-H]^-$; 1095.3 $[M+H_2SO_4-H]^-$	979.2 –H_2O; 937.2 $^{0,2}A_5$; 920.1; 919.2 $^{0,2}A_5$-H_2O; 877.0 $^{2,4}A_5$; 835.1 C_4; 818.4; 776.5 $^{0,2}A_4$; 717.1; 715.1 $^{2,4}A_4$; 673.2 C_3; 655.3 B_3; 595.1; 586.1; 572.0 $^{1,5}X_4$; 555.4; 554.3 B_3 $^{2,4}X_5$; 526.2 Z_3; 511.9 $^{2,4}A_3$; 470.1 C_2; 452.2 B_2; 379.8; 383.0; 351.0 B_2 $^{2,4}X_3$; 332.0 B_2 $^{0,4}X_5$; 308.0 C_1; 290.0 B_1	Fig. 2 g10; Fig.4E	Neu5Ac(α2–3)Gal(β1–3)GalNAc(β1–4) Gal(β1–4)Glc
		24	997.3 $[M-H]^-$; 1095.3 $[M+H_2SO_4-H]^-$			
H_3NS_2	g11	29,5	643.7 $[M-2H]^{2-}$	999.4; 998.2; 997.4 $Y_{3\alpha}$; 563.6 $B_{2\alpha}$-H_2O; 562.6 C_3; 471.1; 290.0 $B_{1\alpha}$; 271.9 $B_{1\alpha}$-H_2O	Fig. 2 g11	Gal(β1–3)GalNAc(β1–4)[Neu5Ac(α2–8)Neu5Ac(α2–3)]Gal(β1–4)Glc
X	o1	13,3	195.1 $[M-H]^-$		Fig. 2 o1	GluconA
HX	o2	19,2	357.2 $[M-H]^-$; 455.1 $[M+H_2SO_4-H]^-$	339.1 -H_2O; 321.0; 297.1 $^{2,4}X_2$; 277.2; 258.7; 237.0 $^{0,2}X_2$; 220.9 $^{2,4}A_2$; 195.0 Y_1; 178.9 C_1; 176.9 Z_1; 160.9 B_1; 158.9 Z_1-H_2O	Fig. 2 o2; Fig. 5A	Gal(β1–4)GluconA
SX	o3	26,4	486.1 $[M-H]^-$		Fig. 2 o3	

Table 4-2. continued.

Glycan composition	Species	Ret. time (min)	Signal m/z	MS/MS fragment ions	Proposed Structures	
H_2X	o4	22,6	519.2 $[M-H]^-$; 617.1 $[M+H_2SO_4-H]^-$	382.7 $^{2,4}A_3$; 356.9 Y_2; 297.5 $^{2,4}X_2$ or $^{0,2}A_3Y_2$; 221.0 $^{2,4}A_2$; 177.1 Z_1; 161.0 B_1	Fig. 2 o4	Gal(α1–4)Gal(β1–4)GluconA
HNX	o5	24,3	560.2 $[M-H]^-$; 658.2 $[M+H_2SO_4-H]^-$	406.8; 399.0; 398.1; 396.0; 394.8; 323.0; 235.8; 179.0; 160.9	Fig. 2 o5	
		38,2	560.2 $[M-H]^-$	543.0; 540.9; 516.0; 480.0; 463.0; 462.2; 445.1; 349.2; 348.1; 345.0; 284.8	Fig. 2 o5	
HSX	o6	26	648.5 $[M-H]^-$	630.2 $-H_2O$; 604.3 $-CO_2$; 586.6 $-H_2CO_3$; 544,2 $-C_3H_4O_4$; 510.2; 491.2; 428.0; 357.1 Y_2; 339.0 Z_2; 310.7 $^{1,5}A_3Y_2$; 307.9 C_1	Fig. 2 o6; Fig. 5B	Neu5Ac(α2–3)Gal(β1–4)GluconA
H_2NX	o7	21,4	722.4 $[M-H]^-$; 820.3 $[M+H_2SO_4-H]^-$	704.2 $-H_2O$; 628.2; 602.3 $^{0,2}X_4$; 586.2 $[M-CH_2OH(CHOH)_2CO_2H-H]^-$; 560.2 Y_3; 543.9 C_3; 421.8; 406.1 Z_3-$(CH_2OH(CHOH)_2CO_2H)$; 402.7; 357.0 Y_2; 298.2; 267.9; 262.7; 234.0; 220.9 C_2Y_3	Fig. 2 o7; Fig. 5D	Gal(β1–3)GalNAc(β1–4)Gal(β1–4) GluconA
HS_2X	o8	29,4	939.6 $[M-H]^-$	895.4 $-CO_2$; 841.5; 648.3 Y_3; 604.2 Y_3-CO_2; 581.3 B_2; 370.0; 357.1 Y_2; 290.0 B_1	Fig. 2 o8; Fig. 5C	Neu5Ac(α2–8)Neu5Ac(α2–3) Gal(β1–4)GluconA
H_2NSX	o9	27,4	1013.4 $[M-H]^-$; 1111.4 $[M+H_2SO_4-H]^-$	995.5 $-H_2O$; 969.7 $-CO_2$; 951.7 $-H_2CO_3$; 909.5 $-C_3H_4O_4$; 817.5 B_3; 722.3 $Y_{2\beta}$; 704.1 $Z_{2\beta}$; 537,2; 406.2 $Z_{3\alpha}Z_{2\beta}$-$(CH_2OH(CHOH)_2CO_2H$; 380.1; 364.1 $B_{2\alpha}$; 357.1 $Y_2Y_{2\beta}$	Fig. 2 o9; Fig. 5E	Gal(β1–3)GalNAc(β1–4)[Neu5Ac(α2–3)]Gal(β1–4)GluconA
		30,8	1013.4 $[M-H]^-$			
H_2F		8,5	487.2 $[M-H]^-$; 585.3 $[M+H_2SO_4-H]^-$	426.9 $^{0,2}A_3$; 409.0 $^{0,2}A_3-H_2O$; 325.1 C_2; 306.9 B_2; 295.0 $^{1,5}A_3Y_2$; 246.0 $^{2,5}A_3Z_2$; 204.9 $^{1,3}A_2$; 178.9 Y_1; 162.9 C_1; 160.9 Z_1		Fuc(α1–2)Gal(β1–4)Glc
H_2NF		7	690.2 $[M-H]^-$; 788.3 $[M+H_2SO_4-H]^-$	592.1; 528.0 $C_{2\alpha}$; 526.7; 363.9 $C_{2\alpha}Z_{2\beta}$; 348.1 $C_{2\alpha}Z_{2\alpha}$; 347.7; 244.0 $^{2,4}A_{2\alpha}$/ $Z_{2\alpha}Y_{2\beta}$; 212.0		Hex(1–3)(Fuc4/3)HexNAc(1–4)Hex

an aldohexonic acid (X) with a carboxyl group at C_1. This monosaccharide differs by +16 Da from hexose and by +2 Da from hexuronic acid (oxidation of the alcohol group at C_6). The aldohexonic acid-containing oligosaccharides (o1–o9) showed close structural similarities to the above-mentioned glycans with reducing-end hexose oligosaccharides (g1–g11). The structural interpretation obtained for these glycans is presented below.

A component at *m/z* 357.2 was detected and interpreted as HX on the basis of the MS/MS spectrum (Fig. 4-5A). Fragment ion B_1 (*m/z* 160.9) and C_1 (*m/z* 178.9) indicate terminal hexose, and Z_1 (*m/z* 176.9) and Y_1 (*m/z* 195.0) result from aldohexonic acid. The fragment ion with mass *m/z* 158.9 is interpreted as a mass loss of 18 Da from the Z_1 ion. For the fragment ion with mass *m/z* 220.9, carbon chain cleavages at C_2–C_3 and C_4–C_5 of the aldohexonic acid were assumed. A linkage of hexose to the C_4 of aldohexonic acid is postulated. The proposed structure for HX is Gal(β1–4)GluconA (gluconic acid), which may be interpreted as the C_1-oxidized form of lactose.

A glycan with the composition HSX (*m/z* 648.5) was detected at retention time 26.0 min (Table 4-2). The MS/MS spectrum is shown in Fig. 4-5B. The fragment ions C_1 (*m/z* 307.9), Y_2 (*m/z* 357.1), Z_2 (*m/z* 339.0) and $[M–CH_2OCH_2OCOO–H]^-$ (*m/z* 544.2) are indicative of the sequence Neu5Ac–Hex–HexonA (aldohexonic acid). Fragment ions at *m/z* 604.3 $[M–CO_2–H]^-$ and (*m/z* 586.3) $[M–CO_2–H_2O–H]^-$ are indicative of a carboxylic acid. For the fragment ion with *m/z* 544.2, cleavage between C_3 and C_4 in the aldohexonic acid is proposed, indicating that the aldohexonic acid is linked via C_4 to the adjacent hexose. Therefore, the structure Neu5Ac(α2–3) Gal(β1–4)GluconA is proposed, which represents the C_1-oxidized version of sialyllactose.

A glycan with the composition HS_2X (*m/z* 939.6) was observed at retention time 29.4 min (o8, Table 4-2). The MS/MS spectrum (Fig. 4-5C) shows the fragment ions B_1 (*m/z* 290.0), B_2 (*m/z* 581.3), Y_2 (*m/z* 357.1) and Y_3 (*m/z* 648.3), which is consistent with the sequence Neu5Ac–Neu5Ac–Hex–HexonA. The fragment ions Y_3-CO_2 (*m/z* 604.2) and $[M–CO_2–H]^-$ (*m/z* 895.4) are indicative of a carboxylic acid group.

A glycan with the composition H_2NX (*m/z* 722.4) was observed at retention time 21.4 min (o7, Table 4-2). The MS/MS spectrum (Fig. 4-5D) shows the fragment ions C_3 (*m/z* 543.9), Y_2 (*m/z* 357.0) and Y_3 (*m/z* 560.2), which is consistent with the sequence Hex–HexNAc–Hex–HexonA. For the fragment ions with masses *m/z* 586.2 and *m/z* 406.1, carbon chain cleavages at C_2–C_3 and C_4–C_5 of the aldohexonic acid are assumed. The fragment ion with mass m/z 406.1 originated from fragment ion Z_3. From these details, the structure Hex–HexNAc–Gal(β1–4)–HexonA (Fig. 4-2, o7) is proposed, which is interpreted as the C_1-oxidized version of oligosaccharide g7 (see above).

A glycan with the composition H_2NSX (*m/z* 1013.4) was detected at retention time 27.4 min (o9, Table 4-2).The fragment ions $[M–CO_2–H]^-$ (*m/z* 969.7) and $[M–CO_2–H_2O–H]^-$ (*m/z* 951.7) are indicative of a carboxylic acid group (Fig. 4-5E). For fragment ion $[M–CH_2OCH_2OCOO–H]^-$ (*m/z* 909.5), a cleavage between C_3 and C_4 of the aldohexonic acid is proposed. Moreover, the MS/MS spectrum shows the fragment ions $B_{2\alpha}$ (*m/z* 364.1), $Y_2Y_{2\beta}$ (*m/z* 357.1), $Z_{2\beta}$ (*m/z* 704.1), $Y_{2\beta}$ (*m/z* 722.3) and B_3 (*m/z* 817.5), which are consistent with the sequence Hex–HexNAc–[Neu5Ac]–Hex–HexonA.

Other C_1-oxidized oligosaccharide moieties were an aldohexonic acid carrying a sialic acid residue (o3), oligosaccharide o4, which represents a C_1-oxidized version of g3, and o5, which is interpreted as C_1-oxidized version of g5 (for details, see Table 4-2).

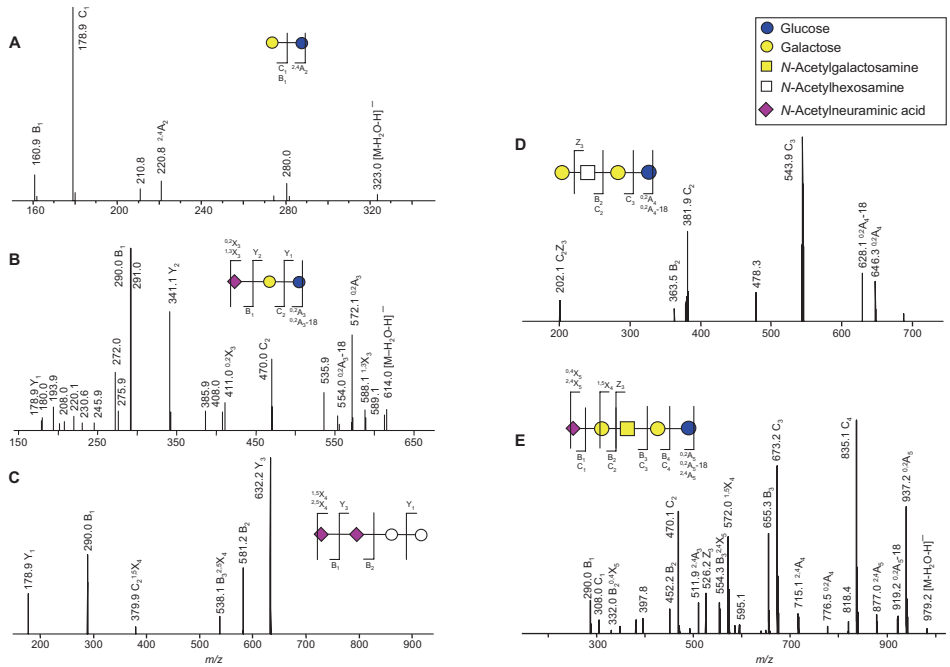

Figure 4-4. Negative-ion fragmentation mass spectra of oligosaccharides with reducing-end hexose residues with the proposed structures: (A) lactose, precursor ion *m/z* 341.2, g1; (B) sialyllactose, precursor ion *m/z* 632.2, g6; (C) lactose carrying a disialyl motif, precursor ion *m/z* 923.3, g9; (D) H_3N tetrasaccharide, precursor ion *m/z* 706.2, g7; (E) H_3NS pentasaccharide, precursor ion *m/z* 997.3, g10.

4.3.4 Glycan profiling of body fluids

LC-MS data were obtained for four urine samples from control individuals as well as seven urine samples, five amniotic fluid samples and two ascitic fluid samples from galactosialidosis patients. In the four urine samples of healthy controls, lactose (*m/z* 341.2), sialylhexose (*m/z* 470.2) and sialyllactose (*m/z* 632.2) were detected (data not shown). For the body fluid samples of galactosialidosis patients, the relative abundances of the mass spectrometric signals are given in Table 4-3. The two major classes of detected oligosaccharides are the endo-β-*N*-acetylglucosaminidase-cleaved products of complex-type sialylated *N*-glycans derivatives (n1–n6) and oligosaccharides with reducing-end hexose residues or disialyl motifs (g1–g11), with mean relative abundances of 37.1% and 44.8%, respectively. Sulfated glycans (s1–s4), which are presumably derived from complex-type *N*-glycans, accounted for a mean of 1.6% of all detected glycans. The relative abundance of aldohexonic acid-based oligosaccharides (o1–o9) differed considerably between urine samples on the one hand (mean 29.7%) and amniotic fluid and ascitic fluid samples on the other (mean 3.1%).

In all samples, the same set of complex-type *N*-glycan-derived structures was found, with the exception of H_5N_3S (n3) and $H_6N_4S_2$ (n5) in ascitic fluid samples Asf1 and Asf2, respectively (Table 4-3). In all samples, complex-type *N*-glycan derivatives with very high relative abundance were sialyl-*N*-acetyllactosamine (HNS; n1), disialylated diantennary structures

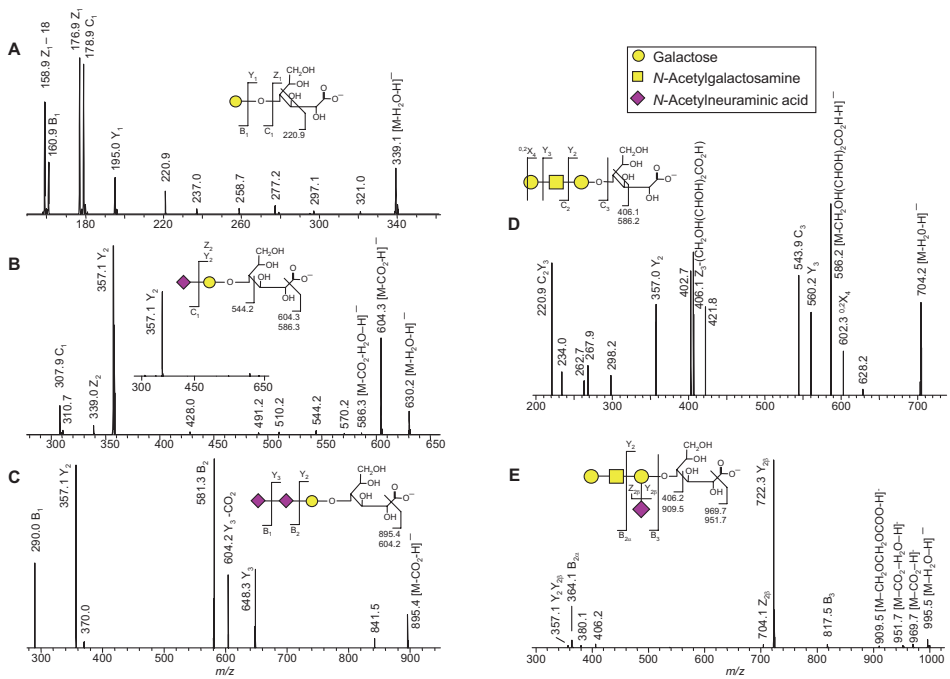

Figure 4-5. Negative-ion fragmentation mass spectra of C_1-oxidized oligosaccharides with the proposed structures: (A) C_1-oxidized lactose, precursor ion *m/z* 357.2, o2; (B) C_1-oxidized sialyllactose, precursor ion *m/z* 648.5, o6; (C) C_1-oxidized lactose carrying a disialyl motif, precursor ion *m/z* 939.6, o8; (D) C_1-oxidized version of H_3N tetrasaccharide, precursor ion *m/z* 722.4; o7; (E) C_1-oxidized version of the H_3NS pentasaccharide, precursor ion *m/z* 1013.4; o9.

($H_5N_3S_2$; n4) and sialylated monoantennary structures (H_3N_2S; n2). In amniotic fluid and ascitic fluid, tri-sialylated triantennary *N*-glycans ($H_6N_4S_3$; n6) were clearly next in order of relative abundance (Table 4-3).

Sulfated *N*-glycan derived structures were detected in all samples (Table 4-3). In three urine samples, the entire set of four sulfated *N*-glycans could be detected (Table 4-3, U2, U4 and U6). In one urine sample (U2), three isomers were detected for $H_5SO_3N_3S_2$ (data not shown).

Free oligosaccharides with reducing-end hexoses were detected in all samples. In two samples (Table 4-3, U1 and Amf5), the entire set of 11 oligosaccharides (g1–g11) was detected. The most abundant species of this glycan group in urine samples was sialyllactose (relative mean abundance 16.4% for g6, H_2S; Table 4-3), while the proposed sialylgalactose was the most abundant species in the amniotic and ascitic fluid samples (mean 20.4% for g2, HS; Table 4-3). Sialyllactose was observed with similar relative abundances in urine, amniotic and ascitic fluid samples (g6, Table 4-3). In urine sample U7, the relative amount of lactose was high (39.9%), and was one or two orders of magnitude lower for the other analyzed samples (g1, Table 4-3). The disialyl glycan (g4) was detected in all samples and had a mean relative abundance of 4.8%. Other glycans containing a disialyl motif (g9 and g11) were detected at low relative intensities (< 0.5%). Only in three of the 14 samples analyzed were neither of these species detected.

Table 4-3. Oligosaccharides observed in various body fluids of galactosialidosis patients. Mean retention time, mass to charge ratio and relative area are given for glycans detected in urine (U), amniotic fluid (Amf) or ascitic fluid (Asf). H, hexose; N, *N*-acetylhexosamine; S, *N*-acetylneuraminic acid; X, aldohexonic acid; SO_3, sulphate; +, trace amount; –, not detected.

				Sample:		U1	U2	U3	U4
	Fig. 2	**Composition**	***m/z***	**charge**	**Ret. Time**	**%**	**%**	**%**	**%**
With reducing-end	n1	HNS	673,4	$[M^-H]^-$	22.3	4,1	14,5	18,3	15,9
	n2	H_3N_2S	1200,4	$[M^-H]^-$	23.0	2,8	10,6	3,4	7,5
	n3	H_5N_3S	1727,8	$[M^-H]^-$	23.9	0,3	0,6	0,2	0,6
	n4	$H_5N_3S_2$	1009,0	$[M^-2H]^{2-}$	27.3	5,9	17,6	3,6	9,6
	n5	$H_6N_4S_2$	1191,4	$[M^-2H]^{2-}$	27.4	0,5	1,3	0,5	1,1
	n6	$H_6N_4S_3$	891,3	$[M^-3H]^{3-}$	31.3	0,4	1,2	0,5	1,2
						14,1	45,7	26,5	36,0
Sulfated glycans	s1	H(S)NS	753,2	$[M^-H]^-$	32.0	0,3	0,6	1,4	2,3
	s2	$H_3(S)N_2S$	639,7	$[M^-2H]^{2-}$	36.5	0,3	1,3	-	0,5
	s3	$H_5(S)N_3S$	903,3	$[M^-2H]^{2-}$	34.6	-	0,3	-	0,2
	s4	$H_5(S)N_3S_2$	1048,8	$[M^-2H]^{2-}$	39.6	+	0,2	0,1	0,2
						0,6	2,4	1,5	3,2
With reducing-end hexose or disyalyl motif	l1	H_2	341,2	$[M^-H]^-$	7.6	1,2	1,9	5,3	3,6
	l2	HS	470,2	$[M^-H]^-$	24.4	3,4	4,4	9,4	8,6
	l3	H_3	503,2	$[M^-H]^-$	9.1	0,2	3,4	3,5	3,2
	l4	S_2	599,2	$[M^-H]^-$	27.7	3,3	4,2	4,9	8,2
	l5	H_2N	544,2	$[M^-H]^-$	9.6	0,9	1,8	3,4	4,3
	l6	H_2S	632,2	$[M^-H]^-$	22.7	8,1	10,8	29,9	22,2
	l7	H_3N	706,2	$[M^-H]^-$	12.7	1,8	0,8	2,4	0,8
	l8	H_2NS	835,3	$[M^-H]^-$	22.8	1,5	4,1	2,0	4,2
	l9	H_2S_2	923,3	$[M^-H]^-$	29.1	+	0,1	-	-
	l10	H_3NS	997,3	$[M^-H]^-$	22.0	0,7	0,4	0,2	0,5
	l11	H_3NS_2	643,7	$[M^-2H]^{2-}$	29.5	0,4	-	0,1	0,1
						21,6	31,8	61,0	55,7
With terminal aldohexonic acid	o1	X	195,1	$[M^-H]^-$	13.3	62,3	1,6	1,0	2,0
	o2	HX	357,2	$[M^-H]^-$	19.2	0,8	17,3	3,0	2,2
	o3	SX	486,1	$[M^-H]^-$	26.4	0,2	0,1	-	0,2
	o4	H_2X	519,2	$[M^-H]^-$	22.6	0,3	0,9	-	-
	o5	HNX	560,2	$[M^-H]^-$	24.3	0,2	0,1	6,1	0,3
	o6	HSX	648,5	$[M^-H]^-$	26.0	-	-	0,8	0,5
	o7	H_2NX	722,4	$[M^-H]^-$	21.4	-	-	-	-
	o8	HS_2X	939,6	$[M^-H]^-$	29.4	-	+	0,1	-
	o9	H_2NSX	1013,4	$[M^-H]^-$	27.4	-	-	-	-
						63,7	20,1	11,1	5,2

U5 %	U6 %	U7 %	Avg U %	Amf1 %	Amf2 %	Amf3 %	Amf4 %	Amf5 %	Asf1 %	Asf2 %	Avg A %	Avg OA %
15,1	9,6	15,0	13,2	22,5	19,9	22,7	25,4	20,5	19,2	19,1	21,3	17,3
0,9	4,0	0,5	4,2	6,0	7,3	5,0	4,7	4,7	3,7	5,8	5,3	4,8
0,2	0,4	0,1	0,3	+	0,5	0,2	0,8	0,3	-	0,1	0,4	0,4
2,2	5,5	1,2	6,5	18,7	22,3	16,5	17,5	22,0	9,1	14,3	17,2	11,9
0,4	0,4	0,1	0,6	1,2	1,4	0,9	1,4	1,5	0,4	-	1,1	0,8
0,3	0,2	0,2	0,6	5,2	4,8	3,5	3,4	4,9	1,3	2,6	3,7	2,1
19,2	20,0	17,0	25,5	53,6	56,2	48,9	53,2	53,9	33,8	41,8	48,8	37,1
2,3	0,6	0,3	1,1	-	-	-	0,4	0,7	0,7	3,0	1,2	1,1
+	0,3	-	0,6	0,8	1,3	0,9	0,9	1,0	-	-	1,0	0,8
+	0,2	-	0,2	0,3	-	0,4	-	-	0,4	-	0,4	0,3
-	+	-	0,1	-	-	-	-	0,6	-	-	0,6	0,3
2,4	1,1	0,3	1,6	1,1	1,3	1,4	1,3	2,2	1,1	3,0	1,6	1,6
4,2	1,2	39,9	8,2	0,9	0,4	-	0,7	1,5	2,3	2,3	1,3	5,0
6,0	2,6	5,1	5,6	19,1	14,4	21,9	14,7	13,4	36,1	23,1	20,4	13,0
3,1	-	2,9	2,7	-	-	-	-	0,6	-	-	0,6	2,4
7,2	4,3	0,9	4,7	3,0	5,0	5,6	7,3	6,8	2,4	4,6	5,0	4,8
3,3	0,9	1,6	2,3	1,2	0,8	0,9	1,3	1,1	0,9	1,1	1,1	1,7
17,2	6,5	20,2	16,4	12,3	14,3	14,7	16,4	14,2	17,8	17,8	15,4	15,9
0,4	0,5	0,3	1,0	0,2	-	-	0,4	0,1	-	-	0,2	0,8
0,9	1,9	0,6	2,2	4,1	3,5	4,0	2,1	3,4	1,0	3,5	3,1	2,6
0,1	+	+	0,1	-	0,3	-	0,2	0,4	-	0,3	0,3	0,2
0,1	0,2	+	0,3	0,3	-	-	0,3	0,3	-	-	0,3	0,3
-	-	-	0,2	-	-	-	-	0,2	-	-	0,2	0,2
42,3	18,1	71,6	43,1	41,1	38,6	47,1	43,6	41,9	60,6	52,8	46,5	44,8
3,1	18,6	8,9	13,9	0,9	-	-	-	1,1	2,2	+	1,4	10,2
27,9	37,0	1,5	12,8	1,3	1,0	-	1,3	0,2	0,9	1,8	1,1	7,4
0,2	0,1	-	0,2	0,4	0,5	-	-	0,4	-	-	0,4	0,3
1,5	0,5	-	0,8	1,5	1,6	2,3	-	-	1,5	-	1,7	1,3
0,9	0,2	0,5	1,2	0,1	0,7	0,4	0,6	0,3	-	0,6	0,4	0,8
2,7	3,8	-	1,9	-	-	-	-	-	-	-		1,9
-	0,2	-	0,2	-	-	-	-	-	-	-		0,2
-	0,2	0,1	0,1	-	-	-	-	-	-	-		0,1
-	0,3	+	0,3	-	-	-	-	-	-	-		0,3
36,1	60,8	11,1	29,7	4,2	3,9	2,7	1,9	2,0	4,6	2,4	3,1	16,4

In the amniotic and ascitic fluid samples, aldohexonic acid-containing oligosaccharides o1–o5 were detected. In the urine samples, high levels of aldohexonic acid-containing glycans were often observed, with the exception of U4 (Table 4-3). In U1, U6 and U7, gluconic acid (o1) has high abundance, and high levels of C_1-oxidized lactose (o2) were observed in urine samples U2, U5 and U6.

4.4 DISCUSSION

Using a prototype capillary HPAEC-PAD-MS system, we observed *N*-glycan-derived oligosaccharide structures (Fig. 4-2, n1–6) in urine, amniotic fluid and ascitic fluid samples from various galactosialidosis patients as described previously [12]. The new set-up also allowed detection of new oligosaccharides in the samples from galactosialidosis patients: (a) *O*-sulfated oligosaccharide moieties, (b) carbohydrate moieties with reducing-end hexoses, and (c) oligosaccharides with C_1-oxidized hexose. The detection of relatively low amounts of *O*-sulfated oligosaccharide moieties and C_1-oxidized carbohydrate moieties, especially in the amniotic and ascitic fluid samples, is made possible by the sensitivity gain achieved by coupling of a capillary HPAEC-PAD to the MS system compared to use of a normal-bore HPAEC-PAD [13,19]. Importantly, the analytical setup allows analysis of glycans with reducing ends, reduced termini and C_1 oxidation, which makes it more broadly applicable than methods that depend on reducing ends for reductive amination reactions [20]. An important aspect of HPAEC is its ability to separate structural isomers, as documented previously [13,15]. Hence, HPAEC-PAD-MS represents a valuable addition to the repertoire of LC-MS methods for oligosaccharide analysis.

Almost all carbohydrate structures described here are terminated with galactose and / or sialic acid residues, which can be explained by the defect of cathepsin A in galactosialidosis patients, resulting in insufficient protection of β-galactosidase and α-neuraminidase against excessive intra-lysosomal degradation [2]. Cathepsin A is one of four enzymes in a lysosomal multi-enzyme complex comprising *N*-acetylgalactosamine-6-sulfate sulfatase, β-galactosidase, cathepsin A and α-neuraminidase [3,4].

The enzyme *N*-acetylgalactosamine-6-sulfatase or galactose-6-sulfatase has been shown to be specific for 6-sulfated galactose and *N*-acetylgalactosamine [21,22]. The structures s1–s4 (Fig. 4-2) are interpreted as being derived from complex-type *N*-linked carbohydrates. 6'-sulfated sialyllactosamine (s1) has also been found on *O*-linked glycan moieties [18], which may therefore represent an alternative source of this glycan.

Tandem mass spectrometry provided evidence that at least some of the oligosaccharide chains with hexose at the reducing end have a Gal(β1–4)Glc (lactose) core structure. This group of glycans (g1–g11) shares structural features with milk oligosaccharides, plasma oligosaccharides and previously described urinary oligosaccharides from healthy individuals [23-25]. The structures g1 and g6 in Fig. 4-2 can be interpreted as lactose (g1) and sialyllactose (g6), which are known to be present in various body fluids [24,26-28]. Moreover, the tetrasaccharide g7 may be interpreted as lacto-*N*-tetraose, and g10 may represent a sialylated version thereof. As these structures are in part identical with milk sugars, they may be of limited diagnostic value. Several glycosyltransferases have been identified in urine and amniotic fluid [29-32], but no-one, to the best of our knowledge, has demonstrated that glycosyltransferases are active in these fluids.

Notably, the detected structures g4 (S_2), g8 (H_2NS), g9 (H_2S_2), g10 (H_3NS) and g11 (H_3NS_2) all exhibited structural motifs that are typically found on glycosphingolipids. g4 is interpreted as a predominantly glycosphingolipid-derived disialyl motif, and the oligosaccharides g8, g9, g10 and g11 are postulated to represent, at least in part, reducing-end glycan moieties of the gangliosides GM2, GD3, GM1 and GD1b, respectively (Fig. 4-2, g8–g11). In addition, the structures g5 and g7 may also be interpreted as partly glycosphingolipids derived (ganglio-, lacto- or lactoneo- series).

To our knowledge, such intact oligosaccharide moieties have hitherto not been described as glycosphingolipids degradation products. According to the literature, catabolism of glycosphingolipids starts from the non-reducing end while the glycan is still bound to the ceramide, and is performed by a variety of exoglycosidases, which are often also involved in the degradation of *N*-glycans and *O*-glycans [33,34]. This process leads to the release of monosaccharides and results in glucosylceramide and galactosylceramide, which may be degraded further by glycosidic bond cleavage. Additional proteins such as saposins (sphingolipid activator proteins) are required for the catabolism of glycosphingolipids [35]. A blockage of glycosphingolipid degradation, as occurs in Fabry's disease as a result of a lack of α-galactosidase activity, leads to accumulation of the glycosphingolipid substrate, which in Fabry's disease is globotriaosylceramide [34]. Consequently, in galactosialidosis, only intact glycosphingolipids would be expected to be secreted, not the glycan moieties as described here. Our finding of free oligosaccharide moieties presumably derived from glycosphingolipids implies the existence of an endoglycosylceramidase involved in an alternative glycosphingolipid catabolic pathway. While such an enzyme has not been described for vertebrates, endoglycoceramidases (EC 3.2.1.123) have been found and characterized for invertebrates [36-39]. The enzymatic activity of the postulated endoglycoceramidase may depend on saposins [35], and may represent a side activity of glucosylceramidase (EC 3.2.1.45) facilitated by specific saposins. With regard to the disaccharide of two sialic acid residues (Fig. 4-2, g4), it is unclear which enzyme would catalyze the release of this disaccharide unit from gangliosides.

The last group of newly found oligosaccharides is characterized by C_1-oxidized hexose residues (o1–o9). This group of glycans appears to be strongly related to the above-described glycans with reducing-end hexoses (g1–g11), suggesting C_1 oxidation of these oligosaccharide moieties. The glycans o8 and o9 may be interpreted as C_1-oxidized versions of ganglioside-derived glycan moieties (Fig. 4-2). The C_1-oxidized oligosaccharides were found in urine samples at relatively high amounts (mean 30%; Table 4-3). C_1-oxidized carbohydrate moieties were also found in amniotic fluid samples, albeit at lower relative amounts (mean 3%; Table 4-3). The cause of C_1 oxidation of the reducing end is unknown. We can exclude the possibility that these species were observed due to oxidation of reducing sugars during the chromatographic process and the subsequent MS detection, as we observed chromatographic separation of the reducing glycans from the C_1-oxidized species, clearly indicating that these species were already present in the samples prior to HPAECPAD-MS analysis. With regard to the origin of the C_1-oxidized glycans, it is possible to speculate about a non-enzymatic oxidation reaction that may have occurred before the urine and amniotic samples were collected, or during sample storage. Alternatively, an enzymatic oxidation may be postulated. The possibility that an enzyme of microbial origin is responsible, as described for *Escherichia coli* [40-44], appears not to be likely, as the oxidation products were not only observed in urine samples, but also in amniotic fluid, which is considered

to be sterile. Alternatively, it could be speculated that a human enzymatic activity might be present in the liver or kidney, for example, that causes C_1 oxidation of glycosphingolipid glycan moieties. This enzyme may act in conjunction with the postulated endoglycoceramidase.

Together with our previous study on G_{M1} gangliosidosis [13], this study shows the potential value of capillary HPAEC-PAD-MS for analyzing oligosaccharides from clinical samples. This prototype analytical system features femtomolar sensitivity for both pulsed amperometric detection and mass spectrometric detection [13]. Moreover, it allows the analysis of oligosaccharides in both positive-ion mode [13] and negative-ion mode, as shown here. Based on the excellent MS/MS features of the ion trap mass spectrometer, informative fragment spectra of sodium adducts [13] and deprotonated species (this study) can be obtained with minute amounts of material, thus allowing insights into defects of glycoconjugate degradation and lysosomal storage diseases.

4.5 EXPERIMENTAL PROCEDURES

4.5.1 Materials

Analytical reagent-grade sodium hydroxide (50% w/w), sodium acetate, sulfuric acid and sodium chloride were obtained from J.T. Baker (Deventer, The Netherlands). Acetonitrile was obtained from Biosolve (Valkenswaard, The Netherlands). All solutions were prepared using water from a Milli-Q synthesis system from Millipore BV (Amsterdam, The Netherlands). Details of the urine, amniotic fluid and ascitic fluid samples are given in Table 4-1.

4.5.2 Capillary HPAEC

The capillary chromatographic system consists of a modified BioLC system from Dionex (Sunnyvale, CA), comprising a microbore GP40 gradient pump, a Famos micro autosampler with a full polyaryletherketone (PAEK) injector equipped with a 1 µL loop, and an ED40 electrochemical detector. BioLC control, data acquisition from the ED40 detector and signal integration are supported by chromeleon software (Dionex). This modified system has been described in detail previously [13]. A prototype capillary column 250 mm long with internal diameter 0.4 mm, packed with CarboPac PA200 resin, was manufactured by Dionex. The GP40 flow rate was 0.53 mL•min^{-1}, and the eluent flow was split using a custom-made polyether ether ketone (PEEK) splitter to 10 µL·min^{-1}. The pump was provided with the following eluents: eluent A, water; eluent B, 500 mM NaOH; eluent C, 500 mM NaOAc. All separations were performed at room temperature. The following ternary gradient was used for the separation: 76% A + 24% B (–20 to –14 min), isocratic sodium hydroxide wash; 88% A + 12% B (–14 to 0 min), isocratic equilibration of the column; 42.6% A + 12% B + 45.4% C (0–40 min), linear sodium acetate gradient was used for the separation. The ED40 detector applies the following waveform to the electrochemical cell: E_1 = 0.1 V (t_d = 0.00–0.20 s, t_1 = 0.20–0.40 s), E_2 = –2.0 V (t_2 = 0.41–0.42 s), E_3 = 0.6 V (t_3 = 0.43 s), E_4 = –0.1 V (t_4 = 0.44–0.50 s) versus an Ag/AgCl reference electrode [45]. A gold work electrode and a 25 µm gasket were installed.

4.5.3 Mass spectrometry

Coupled to the chromatographic system was an Esquire 3000 ion-trap mass spectrometer from Bruker Daltonics (Bremen, Germany), equipped with an electrospray ionization source.

To convert the HPAEC eluate into an ESI-compatible solution, an in-line prototype desalter (Dionex) was used, continuously regenerated with diluted sulfuric acid [13]. A modified microbore AGP-1 from Dionex was used as an auxiliary pump: to obtain efficient ionization of the eluted carbohydrates, 50% acetonitrile was pumped into the eluent flow via a MicroTEE (P-775, Upchurch Scientific, Oak Harbor, WA, USA) at a flow rate of 4.6 µl·min^{-1}. The mixture was directed to the electrospray ionization interface of the Esquire 3000. The carbohydrates were detected using the MS in the negative-ion mode. The MS was operated under the following conditions: dry temperature 325 °C, nebulizer 103 kPa, dry gas 7 L·min^{-1}, target mass *m/z* 850, scan speed 13 000 *m/z* per s in MS and MS/MS mode. For tandem MS, automatic selection of three precursors was applied.

4.5.4 Sample preparation

Oligosaccharides of the samples were isolated by graphitized carbon solid-phase extraction, as described previously [46]. A 200 µL sample was diluted with 1800 µL demineralized water and loaded on a Carbograph SPE (210142) from Alltech Associates Inc. (Deerfield, IL, USA). The cartridge was washed with 6 mL of demineralized water. The oligosaccharides were eluted from the column using 3 mL of 25% acetonitrile containing 0.05% trifluoroacetic acid. The eluate was evaporated under a nitrogen stream at room temperature until the volume had decreased by 50%. The remaining solution was lyophilized and reconstituted with 200 µL demineralized water.

4.6 ACKNOWLEDGEMENTS

We would like to thank Professor Ron Wevers (Radboud University Nijmegen Medical Center, The Netherlands) and Dr Pim Onkenhout (Leiden University Medical Center, The Netherlands) for kindly providing samples, Dr Cornelis H. Hokke for fruitful discussions, Rob Bruggink for providing essential input for producing the capillary desalter, and Chris Pohl, Yan Liu, Victor Barretto and Franck van Veen from Dionex for essential support of this research.

REFERENCES

1. Wenger DA, Tarby TJ, & Wharton C (1978) Macular cherry-red spots and myoclonus with dementia: coexistent neuraminidase and beta-galactosidase deficiencies. *Biochem Biophys Res Commun* **82,** 589-595.
2. D'Azzo A, Hoogeveen A, Reuser AJ, Robinson D, & Galjaard H (1982) Molecular defect in combined beta-galactosidase and neuraminidase deficiency in man. *Proc Natl Acad Sci U S A* **79,** 4535-4539.
3. Pshezhetsky AV & Potier M (1996) Association of N-acetylgalactosamine-6-sulfate sulfatase with the multienzyme lysosomal complex of beta-galactosidase, cathepsin A, and neuraminidase. Possible implication for intralysosomal catabolism of keratan sulfate. *J Biol Chem* **271,** 28359-28365.
4. Pshezhetsky AV & Ashmarina M (2001) Lysosomal multienzyme complex: biochemistry, genetics, and molecular pathophysiology. *Prog Nucleic Acid Res Mol Biol* **69,** 81-114.
5. Lowden JA & O'Brien JS (1979) Sialidosis: a review of human neuraminidase deficiency. *Am J Hum Genet* **31,** 1-18.
6. Takahashi Y, Nakamura Y, Yamaguchi S, & Orii T (1991) Urinary oligosaccharide excretion and severity of galactosialidosis and sialidosis. *Clin Chim Acta* **203,** 199-210.
7. Groener J, Maaswinkel-Mooy P, Smit V, van der Hoeven M, Bakker J, Campos Y, & D'Azzo A (2003) New mutations in two Dutch patients with early infantile galactosialidosis. *Mol Genet Metab* **78,** 222-228.

8. Okamura-Oho Y, Zhang S, & Callahan JW (1994) The biochemistry and clinical features of galactosialidosis. *Biochim Biophys Acta* **1225,** 244-254.
9. Sewell AC (1981) Simple laboratory determination of excess oligosaccharidurie. *Clin Chem* **27,** 243-245.
10. van Pelt J, Kamerling JP, Vliegenthart JF, Hoogeveen AT, & Galjaard H (1988) A comparative study of the accumulated sialic acid-containing oligosaccharides from cultured human galactosialidosis and sialidosis fibroblasts. *Clin Chim Acta* **174,** 325-335.
11. van Pelt J, Kamerling JP, Vliegenthart JF, Verheijen FW, & Galjaard H (1988) Isolation and structural characterization of sialic acid-containing storage material from mucolipidosis I (sialidosis) fibroblasts. *Biochim Biophys Acta* **965,** 36-45.
12. van Pelt J, Hard K, Kamerling JP, Vliegenthart JF, Reuser AJ, & Galjaard H (1989) Isolation and structural characterization of twenty-one sialyloligosaccharides from galactosialidosis urine. An intact N,N'-diacetylchitobiose unit at the reducing end of a diantennary structure. *Biol Chem Hoppe Seyler* **370,** 191-203.
13. Bruggink C, Wuhrer M, Koeleman CA, Barreto V, Liu Y, Pohl C, Ingendoh A, Hokke CH, & Deelder AM (2005) Oligosaccharide analysis by capillary-scale high-pH anion-exchange chromatography with on-line ion-trap mass spectrometry. *J Chromatogr B Analyt Technol Biomed Life Sci* **829,** 136-143.
14. Ramsay SL, Maire I, Bindloss C, Fuller M, Whitfield PD, Piraud M, Hopwood JJ, & Meikle PJ (2004) Determination of oligosaccharides and glycolipids in amniotic fluid by electrospray ionisation tandem mass spectrometry: in utero indicators of lysosomal storage diseases. *Mol Genet Metab* **83,** 231-238.
15. Townsend RR, Hardy MR, Hindsgaul O, & Lee YC (1988) High-performance anion-exchange chromatography of oligosaccharides using pellicular resins and pulsed amperometric detection. *Anal Biochem* **174,** 459-470.
16. Harvey DJ (2005) Fragmentation of negative ions from carbohydrates: part 3. Fragmentation of hybrid and complex N-linked glycans. *J Am Soc Mass Spectrom* **16,** 647-659.
17. Pfenninger A, Karas M, Finke B, & Stahl B (2002) Structural analysis of underivatized neutral human milk oligosaccharides in the negative ion mode by nano-electrospray MS^n (part 1: methodology). *J Am Soc Mass Spectrom* **13,** 1331-1340.
18. Hemmerich S, Leffler H, & Rosen SD (1995) Structure of the O-glycans in GlyCAM-1, an endothelial-derived ligand for L-selectin. *J Biol Chem* **270,** 12035-12047.
19. van der Hoeven RAM, Hofte AJP, Tjaden UR, van der Greef J, Torto N, Gorton L, Marko-Varga G, & Bruggink C (1998) Sensitivity improvement in the analysis of oligosaccharides by online high-performance anion-exchange chromatography/ionspray mass spectrometry. *Rapid Commun Mass Spectrom* **12,** 69-74.
20. Anumula KR (2006) Advances in fluorescence derivatization methods for high-performance liquid chromatographic analysis of glycoprotein carbohydrates. *Anal Biochem* **350,** 1-23.
21. Glossl J, Truppe W, & Kresse H (1979) Purification and properties of N-acetylgalactosamine 6-sulphate sulphatase from human placenta. *Biochem J* **181,** 37-46.
22. Glossl J & Kresse H (1982) Impaired degradation of keratan sulphate by Morquio A fibroblasts. *Biochem J* **203,** 335-338.
23. Koseki M & Tsurumi K (1977) A convenient method for the isolation of 3'-sialyllactose from normal human urine. *J Biochem* **82,** 1785-1788.
24. Arthur PG, Kent JC, & Hartmann PE (1989) Microanalysis of the metabolic intermediates of lactose synthesis in human milk and plasma using bioluminescent methods. *Anal Biochem* **176,** 449-456.
25. Ninonuevo MR, Park Y, Yin H, Zhang J, Ward RE, Clowers BH, German JB, Freeman SL, Killeen K, Grimm R, & Lebrilla CB (2006) A strategy for annotating the human milk glycome. *J Agric Food Chem* **54,** 7471-7480.
26. Ramsay SL, Meikle PJ, Hopwood JJ, & Clements PR (2005) Profiling oligosaccharidurias by electrospray tandem mass spectrometry: quantifying reducing oligosaccharides. *Anal Biochem* **345,** 30-46.
27. An Y, Young SP, Hillman SL, Van Hove JL, Chen YT, & Millington DS (2000) Liquid chromatographic assay for a glucose tetrasaccharide, a putative biomarker for the diagnosis of Pompe disease. *Anal Biochem* **287,** 136-143.
28. Maury CP & Wegelius O (1981) Urinary sialyloligosaccharide excretion as an indicator of disease activity in rheumatoid arthritis. *Rheumatol Int* **1,** 7-10.
29. Chester MA (1974) The occurrence of a beta-galactosyltransferase in normal human urine. *FEBS Lett* **46,** 59-62.
30. Serafini-Cessi F, Malagolini N, & Dall'Olio F (1988) Characterization and partial purification of beta-N-acetylgalactosaminyltransferase from urine of Sd(a+) individuals. *Arch Biochem Biophys* **266,** 573-582.
31. Nelson JD, Jato-Rodriguez JJ, & Mookerjea S (1973) Occurrence of soluble glycosyltransferases in human amniotic fluid. *Biochem Biophys Res Commun* **55,** 530-537.

32. Nelson JD, Jato-Rodriguez JJ, & Mookerjea S (1974) The occurrence and properties of soluble UDP-galactose:glycoprotein galactosyltransferase in human amniotic fluid. *Can J Biochem* **52,** 42-50.
33. Sandhoff K & Kolter T (2003) Biosynthesis and degradation of mammalian glycosphingolipids. *Philos Trans R Soc Lond B Biol Sci* **358,** 847-861.
34. Kolter T & Sandhoff K (2006) Sphingolipid metabolism diseases. *Biochim Biophys Acta* **1758,** 2057-2079.
35. Kolter T & Sandhoff K (2005) Principles of lysosomal membrane digestion: stimulation of sphingolipid degradation by sphingolipid activator proteins and anionic lysosomal lipids. *Annu Rev Cell Dev Biol* **21,** 81-103.
36. Ito M & Yamagata T (1986) A novel glycosphingolipid-degrading enzyme cleaves the linkage between the oligosaccharide and ceramide of neutral and acidic glycosphingolipids. *J Biol Chem* **261,** 14278-14282.
37. Ito M & Yamagata T (1989) Purification and characterization of glycosphingolipid-specific endoglycosidases (endoglycoceramidases) from a mutant strain of Rhodococcus sp. Evidence for three molecular species of endoglycoceramidase with different specificities. *J Biol Chem* **264,** 9510-9519.
38. Li YT & Li SC (1989) Ceramide glycanase from leech, Hirudo medicinalis, and earthworm, Lumbricus terrestris. *Methods Enzymol* **179,** 479-487.
39. Horibata Y, Sakaguchi K, Okino N, Iida H, Inagaki M, Fujisawa T, Hama Y, & Ito M (2004) Unique catabolic pathway of glycosphingolipids in a hydrozoan, Hydra magnipapillata, involving endoglycoceramidase. *J Biol Chem* **279,** 33379-33389.
40. Hugh R & Leifson E (1953) The taxonomic significance of fermentative versus oxidative metabolism of carbohydrates by various gram negative bacteria. *J Bacteriol* **66,** 24-26.
41. Taylor WH & Juni E (1961) Pathways for biosynthesis of a bacterial capsular polysaccharide. I. Carbohydrate metabolism and terminal oxidation mechanisms of a capsuleproducing coccus. *J Bacteriol* **81,** 694-703.
42. Hommes RW, Postma PW, Tempest DW, Neijssel OM, Dokter P, & Dione JA (1984) Evidence of a quinoprotein glucose dehydrogenase apoenzyme in several strains of *Escherichia coli*. *FEMS Microbiol Lett* **24,** 329-333.
43. Liu ST, Lee LY, Tai CY, Hung CH, Chang YS, Wolfram JH, Rogers R, & Goldstein AH (1992) Cloning of an *Erwinia herbicola* gene necessary for gluconic acid production and enhanced mineral phosphate solubilization in *Escherichia coli* HB101: nucleotide sequence and probable involvement in biosynthesis of the coenzyme pyrroloquinoline quinone. *J Bacteriol* **174,** 5814-5819.
44. Yan Z, Caldwell GW, & McDonell PA (1999) Identification of a gluconic acid derivative attached to the N-terminus of histidine-tagged proteins expressed in bacteria. *Biochem Biophys Res Commun* **262,** 793-800.
45. Rocklin RD, Clarke AP, & Weitzhandler M (1998) Improved long-term reproducibility for pulsed amperometric detection of carbohydrates via a new quadruple-potential waveform. *Anal Chem* **70,** 1496-1501.
46. Packer NH, Lawson MA, Jardine DR, & Redmond JW (1998) A general approach to desalting oligosaccharides released from glycoproteins. *Glycoconj J* **15,** 737-747.

5

ANALYSIS OF URINARY OLIGOSACCHARIDES IN LYSOSOMAL STORAGE DISORDERS BY CAPILLARY HIGH-PERFORMANCE ANION-EXCHANGE CHROMATOGRAPHY-MASS SPECTROMETRY

5.1 ABSTRACT

Many lysosomal storage diseases are characterized by an increased urinary excretion of glycoconjugates and oligosaccharides that are characteristic for the underlying enzymatic defect. Here, we have used capillary high-performance anion-exchange chromatography (HPAEC) hyphenated to mass spectrometry to analyze free oligosaccharides from urine samples of patients suffering from the lysosomal storage disorders fucosidosis, α-mannosidosis, G_{M1}-gangliosidosis, G_{M2}-gangliosidosis, and sialidosis. Glycan fingerprints were registered, and the patterns of accumulated oligosaccharides were found to reflect the specific blockages of the catabolic pathway. Our analytical approach allowed structural analysis of the excreted oligosaccharides and revealed several previously unpublished oligosaccharides. In conclusion, using online coupling of HPAEC with mass spectrometric detection, our study provides characteristic urinary oligosaccharide fingerprints with diagnostic potential for lysosomal storage disorders.

Cees Bruggink[1,2], Ben J. H. M. Poorthuis[3], André M. Deelder[1], Manfred Wuhrer[1]

[1] Biomolecular Mass Spectrometry Unit, Department of Parasitology, Leiden University Medical Center, Leiden, The Netherlands.
[2] Thermo Fisher Scientific, Amsterdam, The Netherlands.
[3] Department of Medical Biochemistry, Academic Medical Center, Amsterdam, The Netherlands.

Analytical and Bioanalytical Chemistry (2012) 403; 1671–1683.

5.2 INTRODUCTION

Fucosidosis, α-mannosidosis, G_{M1}-gangliosidosis, G_{M2}-gangliosidosis, and sialidosis are autosomal recessive lysosomal storage diseases (LSD). These LSDs are the result of defects of one or more enzymes or cofactors involved in the catabolism of glycoconjugates that takes place in the lysosome. Fucosidosis is caused by a deficient lysosomal α-L-fucosidase (EC 3.2.1.51) and results in secretion of fucosyl-oligosaccharides [1,2]. Deficient lysosomal α-D-mannosidase (EC 3.2.1.24) causes α-mannosidosis and excessive urinary excretion of oligomannosidic glycans [3-5]. Sialidosis is caused by deficient acid exo-α-sialidase (EC 3.2.1.18) [6]. The urinary excretion of sialyloligosaccharides is similar to that found in galactosialidosis [1,7]. G_{M1}-gangliosidosis is a neurosomatic disease due to the deficient activity of β-galactosidase (EC 3.2.1.23) [8,9]. In addition to the storage of G_{M1}-gangliosides, glycoconjugates with β-galactose at the non-reducing end are increased in patients' urine.

G_{M2}-gangliosidosis is a group of three disorders (1) Tay-Sachs disease, (2) Sandhoff disease, and (3) AB variant. For all variants of G_{M2}-gangliosidosis, the major neural storage compound is ganglioside G_{M2} [10-12]. Only in Sandhoff disease oligosaccharides derived from glycoproteins accumulate due to the deficiency of β-hexosaminidase A in addition to the (functional) deficiency of β-hexosaminidase B [13]. Blockage of the *N*-glycan catabolism results in accumulation of oligosaccharides carrying a single *N*-acetylglucosamine residue at the non-reducing end in tissues and urine of Sandhoff disease patients [14-16]. The current study includes the analysis of urine samples of patients suffering from Sandhoff disease.

Biochemical screening of these LSDs is usually performed using thin-layer chromatography (TLC) [17-19], since TLC is relatively easy to perform and does not require expensive equipment. However, interpretation of a TLC pattern of excreted oligosaccharides requires much experience in pattern recognition. On the other hand, liquid chromatography combined with UV [20] or fluorescence [21] detection is easier to reproduce and to interpret [22,23].

Hyphenation of liquid chromatography with mass spectrometry allows the detailed characterization of oligosaccharides [24]. We have previously described a capillary high-performance anion-exchange chromatograph (HPAEC) setup with combined integrated pulsed amperometric detection (IPAD) and ion-trap mass spectrometric detection which was used to characterize oligosaccharides from urine of G_{M1}-gangliosidosis [25] and galactosialidosis [26] patients. This combination of chromatography IPAD and mass spectrometric detection allows detailed glycan analysis and characterization, when compared with TLC, HPLC, or HPAEC-IPAD without mass spectrometry (MS). Using this analytical setup we report on the analysis of oligosaccharides in urine samples of fucosidosis, α-mannosidosis, G_{M1}-gangliosidosis, G_{M2}-gangliosidosis, and sialidosis patients. The results provided in glycan fingerprints that are found to be characteristic for the individual diseases and reflect the specific enzymatic defects.

5.3 MATERIALS AND METHODS

5.3.1 Materials

Analytical-reagent-grade sodium hydroxide (50% *w/w*), sodium acetate, sulfuric acid, and sodium chloride were obtained from J.T. Baker (Deventer, The Netherlands). Acetonitrile was

from Biosolve (Valkenswaard, The Netherlands). All solutions were prepared using water from a Milli-Q synthesis system from Millipore BV (Amsterdam, The Netherlands). Details on urine samples are given in Table 5-1.

5.3.2 Sample preparation

Oligosaccharides of the samples were isolated with graphitized carbon solid-phase extraction, as described previously [27]. A 200-µL sample was diluted with 1800 µL water and loaded on a Carbograph SPE (210142) from Alltech Associates Inc. (Deerfield, IL). The cartridge was washed with 6 mL of demineralized water. The oligosaccharides were eluted from the column with 3 mL of 25% acetonitrile containing 0.05% trifluoroacetic acid. The eluate was evaporated under a nitrogen stream at room temperature until the volume was decreased by 50%. The remaining solution was lyophilized and reconstituted with 200 µL water.

5.3.3 Capillary HPAEC

The capillary chromatographic system consists of a modified Dionex BioLC system from Thermo Fisher Scientific (Sunnyvale, CA, USA) comprising a microbore GP40 gradient pump, a Famos micro-autosampler with a full PEEK (polyether ether ketone) injector equipped with a 1 µL loop and an ED40 electrochemical detector. BioLC control, data acquisition from the ED40 detector, and signal integration was supported by Dionex Chromeleon software (Themo Fisher Scientific). This modified system has been described in detail before [25]. A prototype capillary column (250 x 0.4 mm I.D.) packed with CarboPac PA200 resin was manufactured by Thermo Fisher Scientific. The GP40 eluent flow was split by a homemade PEEK splitter to 10 $\mu L \cdot min^{-1}$. The pump was provided with the following eluents: eluent A, water; eluent B, 500 mM sodium hydroxide; eluent C, 500 mM sodium acetate. All separations were performed at room temperature. The following ternary gradient was used for separating oligosaccharides of fucosidosis, G_{M2}-gangliosidosis, and sialidosis: 76% A + 24% B (-20 to -14 min) isocratic sodium hydroxide column wash; 88% A + 12% B (-14 to 0 min) isocratic equilibration of the column; a linear sodium acetate gradient (0–55 min) to 25.5% A + 12% B + 62.5% C was used for the separation. For separating oligosaccharides of α-mannosidosis and G_{M1}-gangliosidosis, the following ternary gradient was used: 76% A + 24% B (-20 to -14 min) isocratic sodium hydroxide column wash; 88% A + 12% B (-14 to 0 min) isocratic equilibration of the column; linear sodium hydroxide gradient (0 to 9.1 min) to 60% A + 40% B; 60% A + 40% B (9.1 to 12.5 min) isocratic;

Table 5-1. Information about the urine samples. The age at the time point of sample gathering is given.

Sample code	Disorder	Sex	Age (years)	Creatinine (mmol/L)
U1	Fucosidosis	M	18	2.22
U2	G_{M1}-gangliosidosis	F	0.42	1.04
U3	G_{M2}-gangliosidosis	M	0.75	5.37
U4	G_{M2}-gangliosidosis	M	0.58	1.04
U5	α-Mannosidosis	M	22	18.86
U6	α-Mannosidosis	F	7	8.46
U7	α-Mannosidosis	M	20	14.52
U8	Sialidosis	F	Unknown	Not determined

linear gradient (12.5 to 21.6 min) to 85.2% A + 12% B + 2.8% C; linear sodium acetate gradient (21.6 to 104 min) to 60.5% A + 12% B + 27.5% C. Samples were injected at time 0.0 min.

The ED40 detector applies the following waveform to the electrochemical cell: E_1 = 0.1 V (t_d = 0.00–0.20 s, t_1 = 0.20–0.40 s), E_2 = –2.0 V (t_2 = 0.41–0.42 s), E_3 = 0.6 V (t_3 = 0.43 s), E_4 = –0.1 V (t_4 = 0.44–0.50 s) versus an Ag/AgCl reference electrode [28]. A 1 mm gold work electrode and a 25 µm gasket were installed.

5.3.4 Mass spectrometry

Coupled to the chromatographic system was an Esquire 3000 ion trap mass spectrometer from Bruker Daltonics (Bremen, Germany), equipped with an electrospray ionization source. To convert the HPAEC eluate into an ESI compatible solution, an in-line prototype desalter (Thermo Fisher Scientific) was used which was continuously regenerated with 12.5 mM sulfuric acid with a flow rate of 0.8 ml/min [25]. A modified microbore AGP-1 (Thermo Fisher Scientific) was used as an auxiliary pump: to obtain efficient ionization of the eluted carbohydrates in the positive mode, 0.6 mM NaCl in 50% acetonitrile was pumped into the eluent flow via a MicroTEE (P-775 Upchurch Scientific, Oak Harbor, WA, USA) at a flow rate of 4.6 µL·min^{-1}. The mixture was directed to the electrospray ionization interface of the Esquire 3000 used in the positive mode. The MS was operated at the following conditions: dry temperature 325 °C, nebulizer 103 kPa, dry gas 7 l·min^{-1}, capillary voltage -3,500V, target mass *m/z* 850, scan speed 13,000 *m/z* / s in MS, scan range 150 – 2,000 *m/z*, ICC target 50,000 or maximum accumulation time 50 ms, and MS/MS mode. For tandem MS automatic selection of three precursors was applied with absolute threshold 10000 or 5% relative, smart fragmentation amplification 30%–100% and 1.40 V, fragmentation time 40 ms.

5.3.5 System suitability check

To check the correct functioning of the complete instrumental setup, every sequence started with analyzing a 50 nmol·ml^{-1} lactose solution with 60 mM NaOH as eluent. The resulting MS chromatogram should pass the following criteria: The retention time 7.5 min ± 15%; in the total ion current chromatogram, the baseline level intensity should be ≤4.5 e6, the noise intensity ≤7.5 e5; for the extracted ion chromatogram (*m/z* 365 ± 0.5), the peak height intensity ≥4.5 e6 with a peak width at half height of ≤55 s.

5.3.6 Data analysis

MS as well as MS/MS spectra were manually interpreted using DataAnalysis (version 3.3, Bruker Daltonics). The extracted ion chromatograms (EIC) were used in order to determine the peak area of oligosaccharides present in the MS spectra. Signals of all detected charge states and isomers corresponding to the same compound were added up. Peak areas were normalized to the sum of all glycan peak areas of one sample.

5.4 RESULTS

Free oligosaccharides from eight urine samples of patients suffering from various LSDs including fucosidosis, α-mannosidosis, G_{M1}-gangliosidosis, G_{M2}-gangliosidosis, and sialidosis

(Table 5-1) were analyzed by HPAEC-IPAD-MS to investigate disease-related, excreted degradation products. A total of 54 glycans were analyzed in these urine samples as sodium adducts using positive ion mode mass spectrometry. The set of 54 glycans was established by manual assignment of glycan species from all HPAEC-MS(/MS) data. This set includes glycans described previously in literature for the LSDs included in this study [2,9,15,16,25,29-40] as well as the glycans found previously for galactosialidosis samples [26].

5.4.1 Urinary glycans in fucosidosis

Eight fucosylated oligosaccharides were detected in the urine sample of a fucosidosis patient, and the EIC of four of these fucosyl oligosaccharides are shown in Fig. 5-1. The neutral, fucosylated oligosaccharides were observed in an early retention time window (7 to 15 min), while the acidic species HNSF resulted in signals between 22 and 25 min. In order to enable relative quantification of the oligosaccharides, the signals were normalized to the overall intensity of detected MS signals. Glycan species were characterized by tandem mass spectrometry as exemplified for the fucosyl disaccharide Fuc-HexNAc which had a relative abundance of 10.6% (Table 5-2; Fig. 5-2). The MS/MS fragmentation spectrum (Fig. 5-2) showed Z_1 and B_1 fragments as well as a prominent signal arising from the loss of water (*m/z* 372.1). Cross-ring cleavages at *m/z* 229.0 ($^{0,4}A_2$), 259.0 ($^{0,3}A_2$), and 289.0 ($^{0,2}A_2$) suggest a 1-6 linkage for the fucose residue [41-43]. From the total set of 54 glycan compositions observed in this study, 17 were found to be present in the fucosidosis sample (see Supplementary materials Table S5-1) resulting in a glycan fingerprint as shown in Fig. 5-3a. Of the eight fucosylated oligosaccharides detected, three have already been previously shown to be related to fucosidosis [2,29,30,37,44].

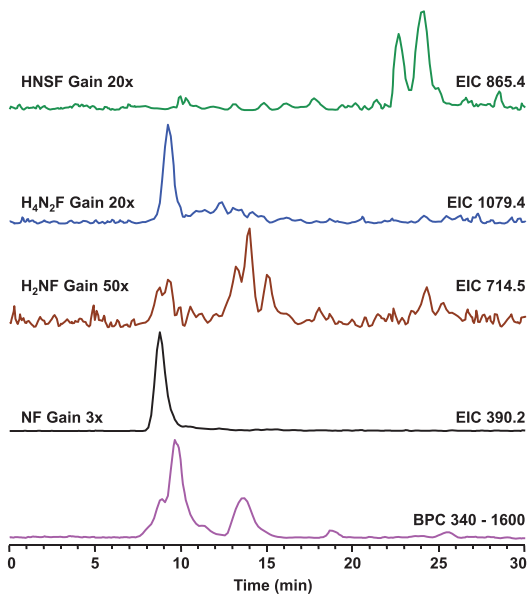

Figure 5-1. Separation of oligosaccharides in urine of a fucosidosis patient. H = hexose, N = *N*-acetylhexosamine, F = fucose, S = *N*-acetylneuraminic acid, BPC = base peak chromatogram.

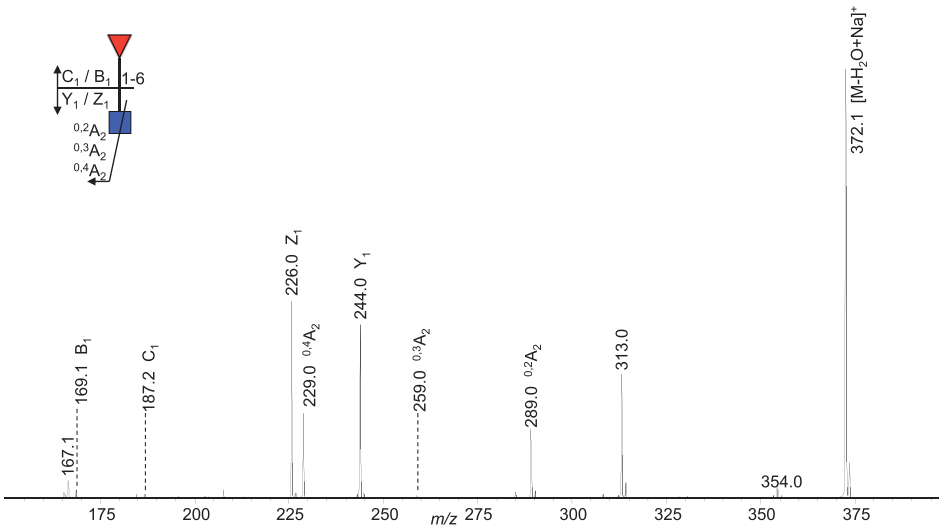

Figure 5-2. Positive-ion fragmentation mass spectrum of the monosodiated disaccharide $HexNAc_1Fuc_1$ (precursor ion at *m/z* 390.2) from urine of a fucosidosis patient. Red triangle = fucose, blue square = *N*-acetylglucosamine.

5.4.2 Urinary glycans in α-mannosidosis

Three urine samples of three different α-mannosidosis patients from two different families were analyzed. In all three samples, 17 endo-β-*N*-acetylglucosaminidase cleavage products of mannose-rich oligosaccharides of composition $Hex_{2-9}HexNAc_1$ were detected [33,45] (Table 5-2, Supplementary materials Table S5-2). The proposed structures are derived from literature [32,33,45] as well as from the obtained tandem MS data. An example of a fragment ion spectrum of the major $Hex_3HexNAc_1$ isomer is shown in Fig. 5-4. The $^{0,2}A_3$ and $^{2,4}A_3$ ions are typical for a 4-substituted HexNAc at the reducing end [41-43]. The cross-ring fragment $^{0,3}A_2$ (*m/z* 275.2) is indicative for a 6-substituted hexose [41-43]. The $B_2Y_{2\alpha}$ ion (D-ion, *m/z* 347.3) reveals the composition of the 6-antenna [42]. Histograms giving the relative abundances of the observed glycans are shown in Figs. 5-3b,c,d. The three urine samples resulted in very similar profiles including a prominent signal corresponding to $Hex_2HexNAc_1$. The whole set of oligomannosidic structures was detected ($Hex_{2-9}HexNAc_1$) showing decreasing signals with increasing size.

5.4.3 Urinary glycans in G_{M1}-gangliosidosis

Extracted ion chromatograms of the disease-related glycans found in the urine of a G_{M1}-gangliosidosis patient are represented in Fig. 5-5. Twenty glycan compositions were detected, and six of those structures with the composition $Hex_{3-7}HexNAc_{2-5}$ are presumably disease-related (Table 5-2, Supplementary materials Table S5-3). The compositions as well as the tandem mass spectrometric data (see Supplementary materials Table S5-3) suggest these glycans to be endo-β-*N*-acetylglucosaminidase cleavage products of complex type *N*-glycans. Composition $Hex_3HexNAc_2$ was interpreted as monoantennary and $Hex_5HexNAc_3$ as diantennary structure.

Table 5-2. Oligosaccharide species detected in urine samples U1–U8 and their relative area. Comp., composition; Fuc., fucosidosis; GM1-gang., G_{M1}-gangliosidosis; Sial., sialidosis.

			Relative area							
			Fuc.	G_{M1}-gang.	G_{M2}-gangliosidosis		α-Mannosidosis			Sial.
Comp.	Registered m/z	Charge state	U1	U2	U3	U4	U5	U6	U7	U8
HF	349.2	$[M+Na]^+$	2.6%	0.6%	0.7%	16.0%	1.9%	1.6%	2.1%	1.7%
H_2F	511.3	$[M+Na]^+$	0.3%	4.4%	0.5%	0.7%	0.2%	0.0%	0.3%	2.8%
NF	390.2	$[M+Na]^+$	10.6%	0.0%	0.2%	0.0%	0.1%	0.0%	0.0%	0.3%
HNF	552.5	$[M+Na]^+$	14.1%	0.6%	0.5%	0.2%	0.6%	0.2%	1.2%	1.2%
H_2NF	714.5	$[M+Na]^+$	0.3%	0.9%	0.6%	0.8%	0.9%	0.3%	1.0%	1.1%
H_2NF_2	860.5	$[M+Na]^+$	2.3%	0.0%	0.2%	0.1%	0.7%	3.2%	0.7%	0.0%
H_3N_2F	1079.4	$[M+Na]^+$	1.3%	0.0%	0.0%	0.0%	0.0%	0.0%	0.0%	0.0%
HNSF	865.4	$[M-H+2Na]^+$	2.3%	0.0%	0.3%	0.0%	0.0%	0.0%	0.0%	0.0%
H_2N_2	771.5	$[M+Na]^+$	1.6%	0.0%	7.6%	7.6%	0.2%	0.1%	0.1%	0.3%
H_3N_2	933.5; 478.3	$[M+Na]^+$; $[M+2Na]^{2+}$	0.0%	16.2%	0.6%	0.4%	0.1%	0.2%	0.1%	6.5%
H_4N_2	1095.5	$[M+Na]^+$	0.7%	0.7%	0.0%	0.0%	0.1%	0.0%	0.0%	0.0%
H_4N_3	1298.5; 660.9	$[M+Na]^+$; $[M+2Na]^{2+}$	0.0%	0.5%	0.0%	0.0%	0.0%	0.0%	0.0%	0.0%
H_3N_3	1136.5; 580.0	$[M+Na]^+$; $[M+2Na]^{2+}$	0.0%	0.0%	8.0%	8.2%	0.0%	0.0%	0.0%	0.0%
H_3N_4	1339.4; 681.2	$[M+Na]^+$; $[M+2Na]^{2+}$	0.0%	0.0%	14.8%	15.5%	0.0%	0.0%	0.0%	0.0%
H_2N_3	974.6	$[M+Na]^+$	0.0%	0.0%	1.3%	1.2%	0.0%	0.0%	0.0%	0.0%
H_5N_3	1460.6; 742.1	$[M+Na]^+$; $[M+2Na]^{2+}$	0.0%	27.1%	0.0%	0.0%	0.0%	0.0%	0.2%	0.3%
H_6N_4	924.5	$[M+Na]^+$	0.0%	3.0%	0.0%	0.0%	0.0%	0.0%	0.0%	0.0%
H_7N_5	1107.0	$[M+2Na]^{2+}$	0.0%	0.3%	0.0%	0.0%	0.0%	0.0%	0.0%	0.0%
HN	406.2	$[M+Na]^+$	1.4%	1.9%	3.6%	2.5%	0.0%	0.0%	0.0%	5.4%
H_2N	568.4	$[M+Na]^+$	0.5%	0.3%	0.9%	1.8%	53.7%	50.1%	54.7%	1.1%
H_3N	730.4	$[M+Na]^+$	0.0%	0.5%	0.4%	0.5%	14.1%	13.9%	15.2%	1.3%
H_4N	892.5	$[M+Na]^+$	0.0%	0.0%	0.3%	0.3%	11.9%	13.5%	12.6%	1.4%
H_5N	1054.5	$[M+Na]^+$	0.0%	0.0%	0.2%	0.0%	3.2%	4.0%	3.2%	0.0%
H_6N	1216.5	$[M+Na]^+$	0.0%	0.0%	0.0%	0.0%	1.3%	1.5%	1.2%	0.0%
H_7N	1378.5; 700.9	$[M+Na]^+$; $[M+2Na]^{2+}$	0.0%	0.0%	0.0%	0.0%	0.6%	0.7%	0.5%	0.0%

H_8N	1540.4; 782.0	$[M+Na]^+$; $[M+2Na]^{2+}$	0.0%	0.0%	0.0%	0.0%	0.5%	0.5%	0.4%	0.0%
H_9N	1702.8; 863.0	$[M+Na]^+$; $[M+2Na]^{2+}$	0.0%	0.0%	0.0%	0.0%	0.2%	0.2%	0.3%	0.0%
HS	516.3	$[M-H+2Na]^+$	0.8%	0.0%	0.2%	0.4%	0.1%	0.1%	0.0%	1.0%
H_2S	678.5; 656.5	$[M-H+2Na]^+$; $[M+Na]^+$	2.7%	1.5%	2.3%	2.3%	0.7%	0.5%	0.6%	2.2%
NS			0.0%	0.0%	0.0%	0.0%	0.0%	0.0%	0.0%	0.0%
HNS	719.5; 697.6	$[M-H+2Na]^+$; $[M+Na]^+$	2.9%	0.7%	1.6%	1.6%	0.4%	0.6%	0.5%	2.7%
N_2S	760.3; 738.4	$[M-H+2Na]^+$; $[M+Na]^+$	0.0%	0.0%	0.1%	0.2%	0.0%	0.0%	0.0%	0.0%
H_3N_2S	1246.8; 635.1	$[M-H+2Na]^+$; $[M-H+3Na]^{2+}$	0.0%	0.0%	0.0%	0.0%	0.0%	0.0%	0.0%	18.7%
H_5N_3S	898.3; 887.6	$[M-H+3Na]^{2+}$; $[M+2Na]^{2+}$	0.0%	0.2%	0.0%	0.0%	0.0%	0.0%	0.0%	3.2%
$H_5N_3S_2$	1055.1; 1044.1	$[M-2H+4Na]^{2+}$; $[M-H+3Na]^{2+}$	0.0%	0.0%	0.0%	0.0%	0.0%	0.0%	0.0%	8.7%
$H_6N_4S_2$	1237.4	$[M-2H+4Na]^{2+}$	0.0%	0.0%	0.0%	0.0%	0.0%	0.0%	0.0%	0.0%
$H_6N_4S_3$			0.0%	0.0%	0.0%	0.0%	0.0%	0.0%	0.0%	0.0%
$H_7N_5S_2$			0.0%	0.0%	0.0%	0.0%	0.0%	0.0%	0.0%	0.0%
$H_7N_5S_3$			0.0%	0.0%	0.0%	0.0%	0.0%	0.0%	0.0%	0.0%
$H_3(SO_3)N_2S$	1348.2; 674.5	$[M-2H+3Na]^+$; $[M-H+3Na]^{2+}$	0.0%	0.0%	0.0%	0.0%	0.0%	0.0%	0.0%	2.4%
$H_5(SO_3)N_3S$	1854.3; 949.4	$[M-H+2Na]^+$; $[M-2H+4Na]^{2+}$	0.0%	0.0%	0.0%	0.0%	0.0%	0.0%	0.0%	0.9%
$H_5(SO_3)N_3S_2$	2166.6; 1083.8	$[M-2H+3Na]^+$; $[M-H+3Na]^{2+}$	0.0%	0.0%	0.0%	0.0%	0.0%	0.0%	0.0%	1.0%
$H_6(SO_3)N_4S_3$			0.0%	0.0%	0.0%	0.0%	0.0%	0.0%	0.0%	0.0%
H_2NS			0.0%	0.0%	0.0%	0.0%	0.0%	0.0%	0.0%	0.0%
S_2			0.0%	0.0%	0.0%	0.0%	0.0%	0.0%	0.0%	0.0%
HX			0.0%	0.0%	0.0%	0.0%	0.0%	0.0%	0.0%	0.0%
H_2X			0.0%	0.0%	0.0%	0.0%	0.0%	0.0%	0.0%	0.0%
HNX	606.5; 584.3	$[M-H+2Na]^+$; $[M+Na]^+$	0.0%	0.5%	0.0%	0.0%	0.0%	0.0%	0.0%	0.0%
HNSX			0.0%	0.0%	0.0%	0.0%	0.0%	0.0%	0.0%	0.0%
SX			0.0%	0.0%	0.0%	0.0%	0.0%	0.0%	0.0%	0.0%
N_2NeuGc			0.0%	0.0%	0.0%	0.0%	0.0%	0.0%	0.0%	0.0%
H_2	365.2	$[M+Na]^+$	48.7%	35.8%	46.7%	32.4%	7.1%	4.9%	3.2%	26.6%
H_3	527.3	$[M+Na]^+$	5.2%	3.8%	6.2%	5.6%	0.9%	2.9%	1.1%	6.5%
H_4	689.5	$[M+Na]^+$	1.6%	0.5%	2.2%	0.7%	0.4%	1.0%	0.8%	2.8%

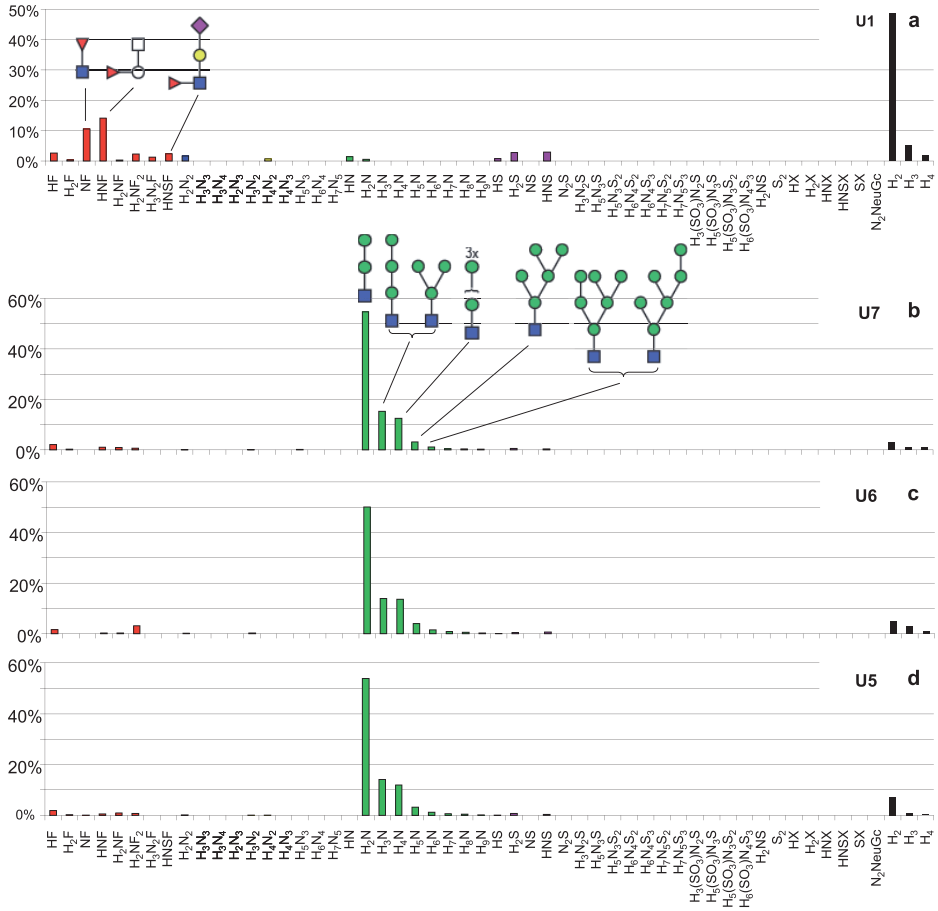

Figure 5-3. Histograms showing the relative abundance of the detected glycans in the urine sample (Table 5-1) of lysosomal storage disorders fucosidosis (a), α-mannosidosis (b, c, and d). H or white circle = hexose, N or white square = *N*-acetylhexosamine, F or red triangle = fucose, S or purple diamond = *N*-acetylneuraminic acid, NeuGc = *N*-glycolylneuraminic acid, X = hexonic acid, SO_3 = sulfate, yellow circle = galactose, green circle = mannose, blue square = *N*-acetylglucosamine.

Species carrying additional $Hex_1HexNAc_1$ units were found to be attached resulting in $Hex_6HexNAc_4$ and $Hex_7HexNAc_5$ species carrying more antennae as well as LacNAc repeats [9,34,35]. In addition, a relatively low amount of a trisaccharide with the composition $Hex_1HexNAc_1HexonA_1$ was detected (Table 5-2). A histogram showing the relative abundance of the observed glycans is given in Fig. 5-3e with high signals corresponding to $Hex_3HexNAc_2$ and $Hex_5HexNAc_3$. The tandem MS spectrum of the disodiated diantennary *N*-glycan with the composition $Hex_5HexNAc_3$ (*m/z* 742.1) is shown in Fig. 5-6. The cross-ring fragments $^{0,2}A_5$ and $^{2,4}A_5$ are typical for a 4-substituted reducing end HexNAc [41-43]. The fragment ion $B_4Y_{2\alpha}$ (D-ion, *m/z* 712.3) reveals the composition of the 6-antenna [42]. The characterization of the two well-separated isomers with the composition $Hex_3HexNAc_2$ has been reported earlier [25].

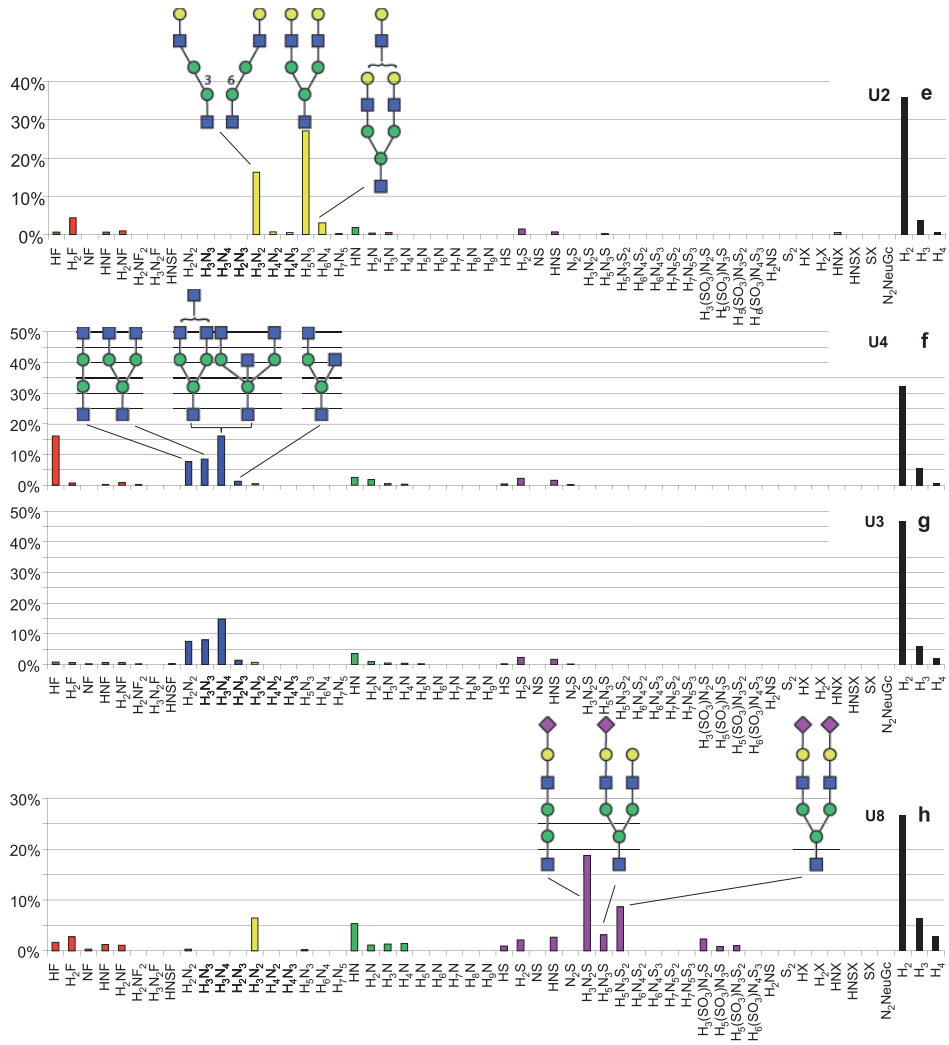

Figure 5-3 Continued. G_{M1}-gangliosidosis (e), G_{M2}-gangliosidosis (f and g), and sialidosis (h). H or white circle = hexose, N or white square = *N*-acetylhexosamine, F or red triangle = fucose, S or purple diamond = *N*-acetylneuraminic acid, NeuGc = *N*-glycolylneuraminic acid, X = hexonic acid, SO_3 =.sulfate, yellow circle = galactose, green circle = mannose, blue square = *N*-acetylglucosamine.

5.4.4 Urinary glycans in G_{M2}-gangliosidosis

The analysis of the urine samples of two G_{M2}-gangliosidosis patients revealed 11 G_{M2}-gangliosidosis-related glycan isomers (Table 5-2, Supplementary materials Table S5-4) with the composition $Hex_{2-3}HexNAc_{2-4}$. The proposed structures reported in Supplementary materials Table S5-4 are based on our MS/MS results and on the known urinary oligosaccharides related to β-hexosaminidase deficiency in G_{M2}-gangliosidos [15,16]. $Hex_2HexNAc_2$ corresponds to a

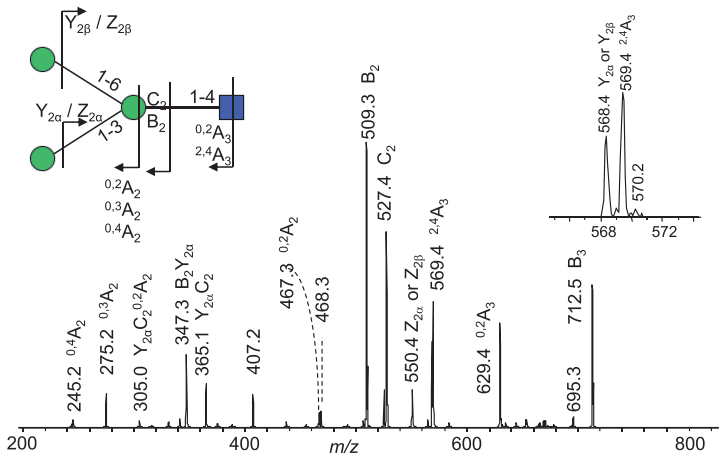

Figure 5-4. Positive-ion fragmentation mass spectrum of the monosodiated tetrasaccharide $Man_3GlcNAc_1$ (precursor ion at *m/z* 730.6) from urine of an α-mannosidosis patient. Green circle = mannose, blue square = *N*-acetylglucosamine.

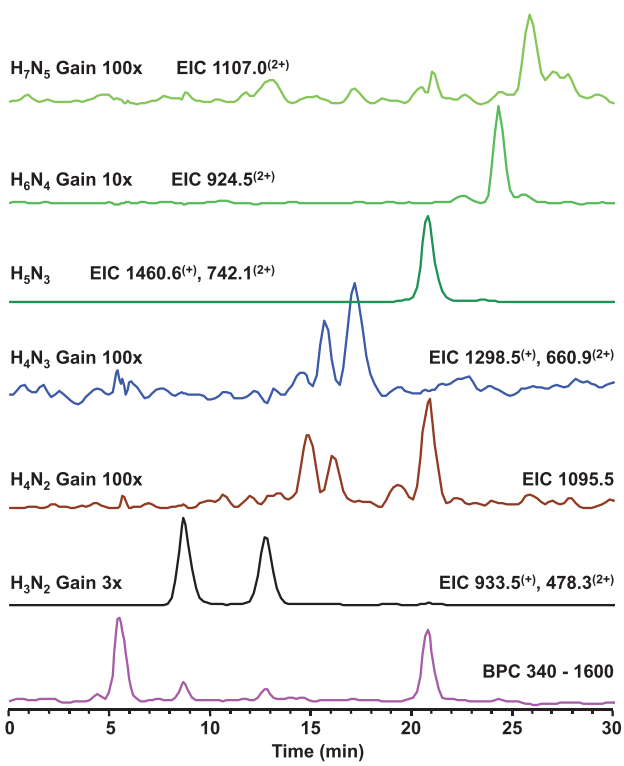

Figure 5-5. Separation of oligosaccharides in urine of a G_{M1}-gangliosidosis patient. H = hexose, N = *N*-acetylhexosamine, BPC = base peak chromatogram.

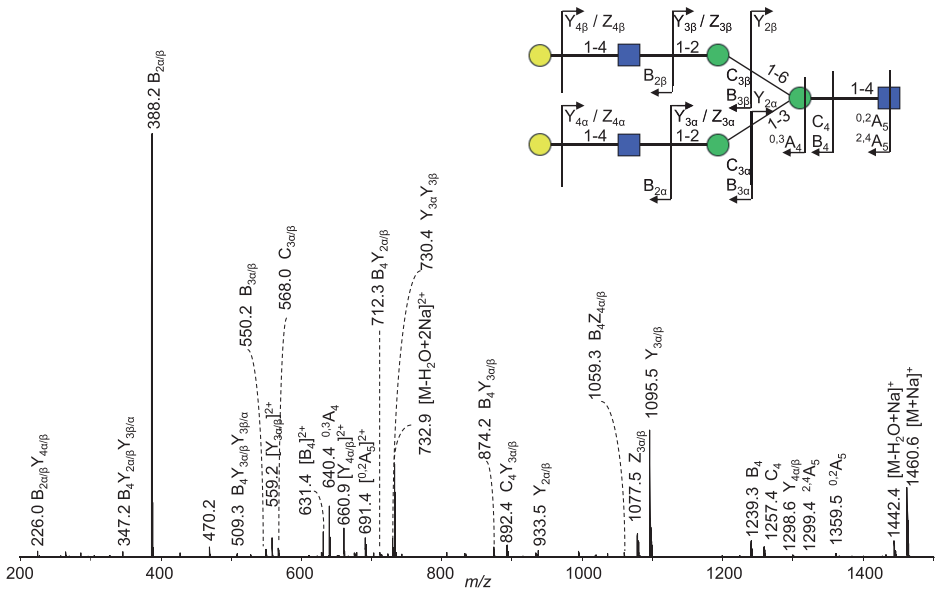

Figure 5-6. Positive-ion fragmentation mass spectrum of the disodiated diantennary oligosaccharide $Hex_5HexNAc_3$ (precursor ion at *m/z* 742.1) from urine of a G_{M1}-gangliosidosis patient. Yellow circle = galactose, green circle = mannose, blue square = *N*-acetylglucosamine.

monoantennary, $Hex_2HexNAc_3$ to a bisected monoantennary, $Hex_3HexNAc_3$ to a diantennary, and $Hex_3HexNAc_4$ to a triantennary or bisected diantennary structure [16]

Fig. 5-7 shows an excellent example of the isomeric separation of the two reported monoantennary glycans ($Hex_2HexNAc_2$; *m/z* 771.5). The EIC corresponding to $Hex_2HexNAc_2$ (*m/z* 771.5) shows the separation of these isobaric structures (retention times 10.3 and 11.9 min; Fig. 5-7), and the MS/MS spectra are shown in Fig. 5-8. The observed series of B-ions are in accordance with a monosaccharide sequence of HexNAc-Hex-Hex-HexNAc for both isomers. Both oligosaccharides contain *N*-acetylhexosamine at the reducing end, which shows the cross-ring fragments $^{0,2}A_4$ (*m/z* 670) and $^{2,4}A_4$ (*m/z* 610) indicative for a 4-substituted *N*-acetylhexosamine [41-43]. The observed cross-ring fragments $^{0,2}A_3$ (*m/z* 508), $^{0,3}A_3$ (*m/z* 478), and $^{0,4}A_3$ (*m/z* 448) observed for the adjacent hexose are typical for a 6-substitution. Based on the observed MS/MS data and literature data [15], glycan A was identified as the G_{M2}-gangliosidosis urinary tetrasaccharide GlcNAc(β1-2) Man(α1-6)Man(β1-4)GlcNAc. A lack of A_3 cross-ring fragments, which is typical for a 3-substituted sugar, indicates that glycan B is the isomer GlcNAc(β1-2)Man(α1-3)Man(β1-4)GlcNAc. Hence, the linkage-specific fragmentation allowed the assignment of the observed glycans to two urinary glycans related to G_{M2}-gangliosidosis [15]. Moreover, the isomeric separation is emphasized by the different elution times of the three isomers corresponding to $Hex_3HexNAc_3$ registered in monosodidated (*m/z* 1136.5) as well as disodiated (*m/z* 580.0) form. Figs. 5-3f and 5-3g show the relative abundance of the detected glycans for the two urine samples. In both samples, a high relative abundance of $Hex_2HexNAc_2$ (both samples 7.6%), $Hex_2HexNAc_3$ (1.3% and 1.2%), $Hex_3HexNAc_3$ (8.0% and 8.2%), and $Hex_3HexNAc_4$ (14.8% and 15.5%) was observed.

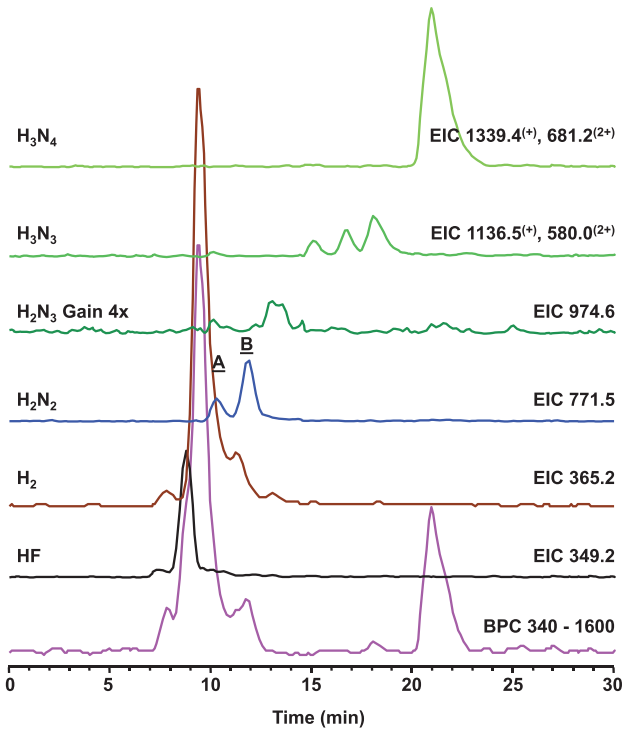

Figure 5-7. Separation of oligosaccharides in urine of a G_{M2}-gangliosisis patient. Fragment ion spectra of the species A and B is shown in Fig. 5-8. F = fucose, H = hexose, N = *N*-acetylhexosamine, BPC = base peak chromatogram.

5.4.5 Urinary glycans in sialidosis

Analysis of the urine of a sialidosis patient revealed eight disease-related sialylated oligosaccharides (Table 5-2, Supplementary materials Table S5-5). Structures with a high relative abundance such as $Hex_3HexNAc_2$ (6.5%), HexHexNAc (5.4%), $Hex_3HexNAc_2Neu5Ac$ (18.7%), and $Hex_5HexNAc_3Neu5Ac_2$ (8.7%) were detected (Fig. 5-3h). The presence of sulfated sialyloligosaccharides $H_{3\text{-}5}SO_3N_{2\text{-}3}S_{1\text{-}2}$ is noteworthy [26].

5.5 DISCUSSION

Using a prototype capillary HPAEC-IPAD-MS system for analyzing a set of 54 glycans in eight urine samples from patients with lysosomal storage disorders such as fucosidosis, α-mannosidosis, G_{M1}-gangliosidosis, G_{M2}-gangliosidosis, and sialidosis (Table 5-1), we were able to find disease-related glycan structures. In addition, we identified glycan structures that are most probably diet- (human milk) or blood-group-related and are not related to the investigated disorders [37,46-51] (see Table 5-2 and Supplementary materials tables S5-1–S5-5). All urine samples, except for those of the mannosidosis patients, were found to contain a high relative amount

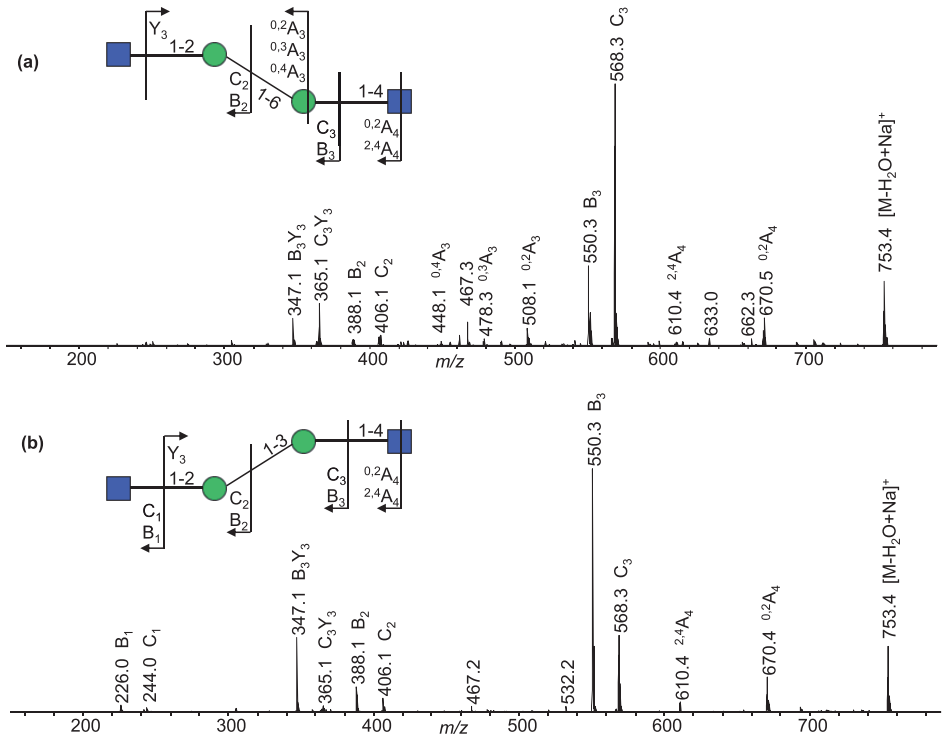

Figure 5-8. Positive-ion fragmentation mass spectra of two isomeric monosodiated tetrasaccharides $Hex_2HexNAc_2$ (precursor ion at *m/z* 771.5) from urine of a G_{M2}-gangliosisis patient. The separation of A and B is shown in Fig. 5-7. Green circle = mannose, blue square = *N*-acetylglucosamine.

of dihexose which is most likely a dietary product [37,46,47]. The presence of dietary products in urine is not surprising. We reported in a previous research about free oligosaccharides such as lactose, sialylhexose, and sialyllactose that we detected as major abundant carbohydrates in control urine samples of four healthy individuals [26].

Detection was performed using an ion trap mass spectrometer which was operated in automatic tandem MS mode resulting in informative fragment ion spectra for many glycans. Linkage-specific fragment ions [41-43] together with the known structural selectivity of high-performance anion-exchange chromatography [52-54] and literature knowledge on urinary oligosaccharides of LSDs [30,55] made it possible to assign structures to most of the observed chromatographic signals.

Literature on fucosidosis reports that fucosylglycoasparagines are the most abundant glycoconjugates found in the urine of these patients [2,56]. These glycoconjugates are not expected to show up in our analysis, as they will presumably adsorb to or pass through the membrane of the online desalter. This phenomenon is due to the high negative charge density of the fiber wall which is expected to result in strong interactions with cations such as glycopeptides entering the desalter [25]. Instead, we detected free fucosylsaccharides in the urine samples. The most abundant one is the disaccharide Fuc(α1-6)GlcNAc (Table 5-2, Supplementary materials Table S5-1, Figs. 5-2 and 5-3A) which is characteristic for this disorder [2,56,57]. Moreover, a

trisaccharide with composition $Hex_1HexNAc_1Fuc_1$ was found for fucosidosis (Fig. 5-3a). This trisaccharide is possibly the previously reported GalNAc(α1-3)[Fucα1-2)]Gal [56]. In addition, Tsay *et al*. [58] and Nishigaki *et al*. [59] reported the presence of a fucosylated decasaccharide, however, this structure has neither been detected by us nor by Strecker *et al*. [56].

Moreover, 17 endo-β-*N*-acetylglucosaminidase cleavage products including chromatographically separated isomers were detected in all three urine samples of patients suffering from α-mannosidosis (see Supplementary materials Table S5-2). These findings are in agreement with previous results reported by Matsuura *et al*. [33]. The authors identified in their study a similar number of endo-β-*N*-acetylglucosaminidase cleavage products [33]. However, while we observed three $Hex_4HexNAc_1$ isomers, three $Hex_5HexNAc_1$ isomers, and one $Hex_7HexNAc_1$ isomer, these authors found two, two, and three isomers, respectively (see Supplementary materials Table S5-2).

One of the three isomers of $Hex_3HexNAc_3$ found in the urine samples from patients suffering from G_{M2} gangliosidosis is in accordance with the diantennary structure with the core trimannose previously described by Strecker *et al*. [15,60] while the other two isomers are probably monoantennary structures decorated with a GlcNAc(β1-3)Gal(β1-4)GlcNAc(β1-2) antenna. In the current study, we reported eight glycan structures that are related to sialidosis (see Supplementary materials Table S5-5). Of these eight glycans, five have been previously identified in sialidosis [39,40,50,61]. We interpreted the structure of the glycan with the composition $Hex_1HexNAc_1Neu5Ac_1$ as Neu5Ac(α2-3/6)Gal(β1-4)GlcNAc and being related to sialidosis [50], although, based on our data, we cannot exclude that Neu5Ac(α2-3/6)Gal(β1-4) GlcNAc might be sialyllactosamine from milk [37,62,63]. All sialidosis-relevant carbohydrate structures described here are terminated with sialic acid residues, in accordance with the primary defect in exo-α-sialidase. In addition, three *O*-sulfated oligosaccharides with terminal sialic acid residues were detected in the urine sample (Table 5-2) showing structures previously detected by us in galactosialidosis [26]. This may imply that the *O*-sulfated carbohydrates reported here are indeed related to the exo-α-sialidase deficiency found in both galactosialidosis and sialidosis. MS detection in the positive ion mode is known to be less sensitive for negatively charged glycans such as sialyl- and *O*-sulfated-oligosaccharides. Therefore, this sample has also been analyzed in the negative ion mode and indeed more sialylated-, *O*-sulfated-glycans, and glycans having reducing end aldohexonic acid residue were observed due to the improved sensitivity for the detection of negatively charged molecules (data not shown).

All together, this publication shows the value of capillary HPAEC-IPAD-MS for analyzing oligosaccharides in clinical urine samples without the need for derivatization. This prototype analytical system features femtomol sensitivity for both pulsed amperometric detection and mass spectrometric detection [25] allowing the relatively low abundant *O*-sulfated-glycan moieties to be detected. In contrast to other liquid chromatography methods relying on reducing end labeling for detection and/or separation [64,65] HPAEC-IPAD as well as HPAEC-MS do not depend on glycan labeling. Consequently, we were able to detect an oxidized oligosaccharide with an innermost aldohexonic acid residue in the G_{M1}-ganglioside urine sample. Moreover, the setup used in this study enables the separation of isomeric glycans. Based on the efficient fragment ion analysis using an ion trap instrument, informative fragment spectra of sodium adducts can be obtained with minute amounts of material, allowing insights into defects of glycoconjugates degradation, and investigation of metabolic and catabolic pathways.

Although the used instrumentation is a prototype, similar analyses can be performed using commercially available narrow bore ion chromatographs [66], with presumably less sensitivity due to the bigger dimensions and higher flow rates. The desalter in such a system is based on a flat semi-permeable cation exchange membrane and regenerated by electrolysis of water [67,68].

LC-MS in general and the here described method in particular are analytically powerful. In the current research paper, we demonstrated that the HPAEC-MS technology in combination with MS/MS information on structural isomers is suitable for determining characteristic glycan fingerprints in lysosomal storage diseases which may have diagnostic potential.

5.6 ACKNOWLEDGMENT

We would like to thank Dr. André Klein, Laboratoire de Biochimie et de Biologie Moléculaire, UAM de Glycopathologies, Centre de Biologie et Pathologie, Lille, France, for kindly providing a urine sample; Dr. Crina Balog for her support with data analysis; Rob Bruggink for providing essential input for producing the capillary desalter; Chris Pohl, Yan Liu, Victor Barretto, and Franck van Veen from Thermo Fisher Scientific for essential support of this research.

SUPPLEMENTARY MATERIAL

Table S5-1. Oligosaccharide species detected in the fucosidosis sample U1. Comp., composition; Ret., retention; Rel. area., relative area.

	Comp.	Registered m/z	Charge state	Ret. time (min)
Disease related glycans	NF	390.2	$[M+Na]^+$	8.8
	H_2NF	714.5	$[M+Na]^+$	9.1
	H_3N_2F	1079.4	$[M+Na]^+$	9.2
	HNSF	865.4	$[M-H+2Na]^+$	22.7
				24.0
	H_2NF_2	860.5	$[M+Na]^+$	8.9
	HF	349.2	$[M+Na]^+$	8.9
	H_2F	511.3	$[M+Na]^+$	9.4
	HNF	552.5	$[M+Na]^+$	8.9
Other glycans	H_2	365.2	$[M+Na]^+$	9.7
	H_3	527.3	$[M+Na]^+$	11.0
				12.7
				23.6
	H_4	689.5	$[M+Na]^+$	23.9
				25.3
	HN	406.2	$[M+Na]^+$	9.4
	H_2N	568.4	$[M+Na]^+$	9.8
	H_2N_2	771.5	$[M+Na]^+$	14.3
	HNS	719.5/ 697.2	$[M+Na]^+$ $[M-H+2Na]^+$	25.2
	HS	516.1	$[M-H+2Na]^+$	25.6
	H_2S	678.5	$[M-H+2Na]^+$	25.7

	Rel. area	
Fragment ions	**U1**	**Proposed structure**
244.0 N; 226.0 N-18; 187.2 F; 169.1 F-18	10.6%	Fuc(α1-6)GlcNAc [2,29,30,37,44]
	0.3%	
	1.3%	
719.5 HNS; 552.4 HNF; 534.3 HNF-18; 516.2 HS; 498.0 HS-18; 405.9 HN; 388.1 HN-18; 336.0 S-18; 318.1 S-2x18	0.8%	NeuAc(α2-3/6)Gal(β1-4)[Fuc(α1-3)] GlcNAc
552.2 HNF; 534.1 HNF-18; 516.0 HS; 498.2 HS-18; 354.2 S; 336.0 S-18	1.6%	
714.4 H_2NF; 696.1 H_2NF-18; 657.3 H_2F_2; 568.3 H_2N; 552.4 HNF; 550.4 H_2N-18; 534.3 HNF-18; 532.5 H_2N-2x18; 405.9 HN; 388.1 HN-18; 370.3 HN-2x18; 349.1 HF; 244.0 N	2.3%	GalNAc(α1-3)[Fuc(α1-2)]Gal(β1-4) [Fuc(α1-3)]Glc [37]
	2.6%	Fuc(α1-2)Gal [37]
	0.3%	Fuc[Gal(β1-4)Glc [37,46,47]
406.1 HN; 388.1 HN-18; 372.1 NF-18; 244.0 N; 226.0 N-18; 208.0 N-2x18; 203.0 H; 187.1 F; 185.0 H-18; 169.0 F-18	14.2%	GalNAc(α1-3)[Fuc(α1-2)]Gal [37]
203.0 H; 185.0 H-18	49.1%	
365.1 H_2; 347.1 H_2-18; 203.1 H; 185.0 H-18	2.4%	
365.1 H_2; 347.1 H_2-18; 203.1 H; 185.0 H-18	1.5%	
365.1 H_2; 347.1 H_2-18; 203.0 H; 185.0 H-18	1.4%	
527.3 H_3; 509.2 H_3-18; 365.3 H_2; 346.9 H_2-18	0.5%	
527.3 H_3; 509.2 H_3-18; 365.1 H_2; 347.0 H_2-18	1.2%	
	1.4%	
	0.5%	
	1.6%	
516.2 HS; 498.1 HS-18; 406.1 HN; 354.0 S; 336.0 S-18; 226.0 N	3.0%	NeuAc(α2-3/6)Gal(β1-4)GlcNAc [50]
	0.8%	Neu5Ac-Hex
498.2 HS-18; 354.0 S; 365.1 H_2; 336.0 S-18	2.7%	NeuAc(α2-3/6)Gal(β1-4)Glc [50]

Table S5-2. Oligosaccharide species detected in the α-mannosidosis samples U5, U6, and U7. Comp., composition; Ret., retention.

	Comp.	Registered m/z	Charge state	Ret. time (min)	Fragment ions
Disease related glycans	H_2N	568.4	$[M+Na]^+$	5.8	406.2 HN; 388.1 HN-18; 365.2 H_2; 347.2 H_2-18; 244.1 N; 226.0 N-18; 203.1 H
	H_3N	730.4	$[M+Na]^+$	8.1	568.3 H_2N; 550.3 H_2N-18; 527.3 H_3; 509.2 H_3-18; 388.2 HN-18; 365.1 H_2; 347.2 H_2-18; 329.0 H_2-2x18; 244.1 N; 226.0 N-18
				8.9	527.2 H_3; 509.2 H_3-18; 406.2 HN; 388.1 HN-18; 365.3 H_2; 347.2 H_2-18; 329.2 H_2-2x18; 244.2 N; 226.2 N-18
	H_4N	892.5	$[M+Na]^+$	10.6	730.2 H_3N; 712.3 H_3N-18; 689.4 H_4; 671.3 H_4-18; 527.1 H_3; 509.3 H_3-18; 406.3 HN; 347.1 H_2-18
				12.8	730.2 H_3N; 712.3 H_3-18; 689.3 H_4; 671.3 H_4-18; 568.4 H_2N; 550.3 H_2N-18; 527.2 H_3; 509.3 H_3-18; 491.3 H_3-2x18; 406.2 HN; 388.3 HN-18; 365.3 H_2; 347.2 H_2-18; 329.2 H_2-2x18; 244.2 N
				15.4	730.2 H_3N; 712.3 H_3N-18; 689.3 H_4; 671.3 H_4-18; 568.2 H_2N; 527.3 H_3; 509.2 H_3-18; 491.1 H_3N-2x18; 406.0 HN; 388.1 HN-18; 365.1 H_2; 347.2 H_2-18
	H_5N	1054.5	$[M+Na]^+$	15.9	874.5 H_4N-18; 851.3 H_5; 833.4 H_5-18; 712.8 H_3N-18; 689.3 H_4; 671.3 H_4-18; 568.3 H_2N; 550.2 H_2N-18; 527.1 H_3; 509.3 H_3-18; 491.2 H_3-2x18
				16.7	851.4 H_5; 833.4 H_5-18; 712.3 H_3N-18; 689.4 H_4; 671.3 H_4-18; 653.4 H_4-2x18; 568.3 H_2N; 527.1 H_3; 509.3 H_3-18; 365.1 H_2; 347.1 H_2-18
				18.6	892.3 H_4N; 851.3 H_5; 833.1 H_5-18; 730.3 H_3N; 689.3 H_4; 671.4 H_4-18; 568.4 H_2N; 550.0 H_2N-18; 509.2 H_3-18; 491.1 H_3-2x18; 365.1 H_2; 346.9 H_2-18
	H_6N	1216.5	$[M+Na]^+$	19.2	1054.3 H_5N; 1036.4 H_5N-18; 1013.4 H_6; 995.4 H_6-18; 892.4 H_4N; 874.4 H_4N-18; 851.3 H_5; 833.3 H_5-18; 730.3 H_3N; 671.4 H_4-18; 653.3 H_4-2x18; 568.3 H_2N; 527.3 H_3; 509.3 H_3-18; 491.2 H_3-2x18
				19.9	1054.5 H_5N; 1036.4 H_5N-18; 1013.3 H_6; 995.4 H_6-18; 892.3 H_4N; 851.3 H_5; 833.4 H_5-18; 730.2 H_3N; 689.3 H_4; 671.4 H_4-18; 527.5 H_3; 509.1 H_3-18; 347.1 H_2-18
				21.4	
	H_7N	700.9 1378.5	$[M+2Na]^{2+}$ $[M+Na]^+$	21.7	1198.3 H_6N-18; 1175.4 H_7; 1157.3 H_7-18; 1054.5 H_5N; 1036.4 H_5N-18; 1013.2 H_6; 995.4 H_6-18; 892.3 H_4N; 874.3 H_4N-18; 851.2 H_5; 833.1 H_5-18; 712.4 H_3N; 689.4 H_4; 671.4 H_4-18; 509.1 H_3-18; 491.3 H_3-2x18
	H_8N	782.0 1540.4	$[M+2Na]^{2+}$ $[M+Na]^+$	15.8	
				23.9	671.1 H_4-18; 346.9 H_2-18
				25.5	
	H_9N	863.0 1702.8	$[M+2Na]^{2+}$ $[M+Na]^+$	25.8	

Relative area			
U5	**U6**	**U7**	**Proposed structure**
52.9%	49.6%	53.7%	Man(α1-2)Man(α1-3)Man(β1-4)GlcNAc [31-33,45]
1.2%	1.4%	1.0%	Man(α1-6)[Man(α1-3)]Man(β1-4)GlcNAc [33,45]
12.7%	12.3%	13.9%	Man(α1-2)Man(α1-3)Man(β1-4)GlcNAc [31-33,45]
0.4%	0.4%	0.3%	
10.7%	12.5%	11.1%	Man(α1-2)Man(α1-2)Man(α1-3)Man(β1-4)GlcNAc [32,33,45]
0.6%	0.5%	0.9%	Man(α1-3)Man(α1-6)[Man(α1-3)]Man(β1-4)GlcNAc [32]
0.7%	0.6%	0.7%	Man(α1-3)Man(α1-6)[Man(α1-2)Manα1-3)]Man(β1-4)GlcNAc [32,33,45]
2.4%	3.4%	2.4%	Man(α1-6)[Man(α1-3)]Man(α1-6)[Man(α1-3)]Man(β1-4)GlcNAc [32,33,45]
0.2%	0.1%	0.3%	
0.5%	0.6%	0.4%	Man(α1-2)Man(α1-6)[Man(α1-3)]Man(α1-6)[Man(α1-3)]Man(β1-4) GlcNAc [32,33,45]
0.7%	0.9%	0.8%	Man(α1-6)[Man(α1-3)]Man(α1-6)[Man(α1-2)Man(α1-3)]Man(β1-4) GlcNAc [32,33,45]
0.1%	0.1%	0.2%	Man(α1-2)Man(1-6)[Man(α1-3)]Man(α1-6)[Manα1-3)]Man(β1-4) GlcNAc [32,33,45]
0.6%	0.7%	0.5%	Man(α1-2){Man(α1-6)[Man(α1-3)]Man(α1-6)[Man(α1-2)Man(α1-3)] Man(β1-4)GlcNAc [32,33,45]
0.1%	0.1%		
0.3%	0.4%	0.4%	2xMan(α1-2){Man(α1-6)[Man(α1-3)]Man(α1-6)[Man(α1-2)Man(α1-3)] Man(β1-4)GlcNAc [32,33,45]
0.1%	0.1%		
0.2%	0.2%	0.3%	Man(α1-2)Man(α1-6)[Man(α1-2)Man(α1-3)]Man(α1-6)[Man(α1-2) Man(α1-2)Man(α1-3)]Man(β1-4)GlcNAc [32,33,45]

Table S5-2. continued

	Comp.	Registered m/z	Charge state	Ret. time (min)	Fragment ions
Other glycans	H_2	365.2	$[M+Na]^+$	5.3	
	H_3	527.3	$[M+Na]^+$	6.8	
				7.8	365.2 H_2; 347.2 H_2-18; 203.0 H
				9.3	
				9.6	365.2 H_2; 347.2 H_2-18; 203.0 H; 185.0 H-18
				15.7	
				16.8	
				17.5	365.2 H_2; 347.3 H_2-18; 203.0 H; 185.1 H-18
				18.7	
				20.7	
	H_4	689.4	$[M+Na]^+$	8.4	527.2 H_3; 509.3 H_3-18; 365.2 H_2; 347.2 H_2-18
				25.7	527.3 H_3; 509.2 H_3-18; 365.2 H_2; 347.2 H_2-18
	HN	406.3	$[M+Na]^+$	4.3	
	H_2N_2	771.1	$[M+Na]^+$	10.2	
	H_3N_2	933.5	$[M+Na]^+$	8	
	H_4N_2	1095.5	$[M+Na]^+$	8	
				18.6	
	H_5N_3	741.9	$[M+2Na]^{2+}$	21.4	
	H_2NF_2	860.5	$[M+Na]^+$	4.1	714.3 H_2NF; 696.3 H_2NF-18; 657.4 H_2F_2; 568.3 H_2N; 552.2 HNF; 550.2 H_2N-18; 534.3 HNF-18; 511.3 H_2F; 406.3 HN; 388.2 HN-18; 349.2 HF; 331.1 HF-18; 244.1 N
	HF	349.2	$[M+Na]^+$	3.9	
	H_2F	511.2	$[M+Na]^+$	9.8	
	NF	390.2	$[M+Na]^+$	3.1	
	HNF	552.4	$[M+Na]^+$	3.8	406.2 HN; 388.1 HN-18; 349.3 HF; 243.8 N; 226.2 N-18; 203.1 H
	HS	516.2	$[M-H+2Na]^+$	23.8	
	H_2NF	714.4	$[M+Na]^+$	4.6	
	HNS	697.4 719.4	$[M+Na]^+$ $[M-H+2Na]^+$	22.5	
	H_2S	656.5 678.3	$[M+Na]^+$ $[M-H+2Na]^+$	25.0	516,7 HS; 498,0/476,2 HS-18; 365.3 H_2; 347.0 H_2-18; 354,3/332.3 S; 336,2/314.1 S-18

Relative area			
U5	**U6**	**U7**	**Proposed structure**
7.0%	4.8%	3.2%	
0.2%	0.1%	0.2%	
0.3%	0.8%	0.5%	
	0.2%		
0.2%	0.5%	0.2%	
0.1%	0.2%		
0.0%	0.2%		
0.1%	0.5%	0.2%	
	0.3%		
	0.2%		
	0.4%	0.2%	
0.4%	0.6%	0.6%	
1.4%	1.0%	1.6%	
0.2%	0.1%	0.1%	
0.1%	0.2%		
		0.2%	
0.7%	3.1%	0.7%	GalNAc(α1-3)[Fuc(α1-2)]Gal(β1-4)[Fuc(α1-3)]Glc [37]
1.9%	1.6%	2.1%	
0.2%		0.3%	
0.1%			
0.6%	0.2%	1.2%	GalNAc(α1-3)[Fuc(α1-2)]Gal [37]
0.1%	0.1%		
0.9%	0.2%	0.9%	
0.4%	0.6%	0.5%	
0.7%	0.5%	0.6%	Neu5Ac(α2-3)Gal(β1-4)Glc [50]

Table S5-3. Oligosaccharide species detected in the G_{M1}-gangliosidosis sample U2. X, hexonic acid; GluconA, gluconic acid; Comp., composition; Ret., retention; Rel. area., relative area.

	Comp.	Registered m/z	Charge state	Ret. time (min)
Disease related glycans	H_3N_2	933.5 478.3	$[M+Na]^+$ $[M+2Na]^{2+}$	8.8
		933.5 478.3	$[M+Na]^+$ $[M+2Na]^{2+}$	12.8
	H_4N_2	1095.5	$[M+Na]^+$	15.0
		1095.5	$[M+Na]^+$	16.1
		1095.5	$[M+Na]^+$	21.0
	H_4N_3	1298.5 660.9	$[M+Na]^+$ $[M+2Na]^{2+}$	15.8
		1298.5 660.9	$[M+Na]^+$ $[M+2Na]^{2+}$	17.3
	H_5N_3	1460.6/ 742.1	$[M+Na]^+$ $[M+2Na]^{2+}$	20.9
	H_6N_4	924.5	$[M+2Na]^{2+}$	22.7
		924.5	$[M+2Na]^+$	24.4
		924.5	$[M+2Na]^+$	25.7
	H_7N_5	1107.0	$[M+2Na]^{2+}$	25.9

Fragment ions	Rel. area U2	Proposed structure
730.4 H_3N; 712.3 H_3N-18; 568.3 H_2N; 550.3 H_2N-18; 406.2 HN; 388.2 HN-18; 365.2 H_2; 347.2 H_2-18	8.5%	Gal(β1-4)GlcNAc(β1-2)Man(α1-6) Man(β1-4)GlcNAc [9,25,34-36,44]
730.4 H_3N; 712.4 H_3N-18; 568.3 H_2N; 550.3 H_2N-18; 406.2 HN; 388.2 HN-18; 365.1 H_2; 347.2 H_2-18	7.2%	Gal(β1-4)GlcNAc(β1-2)Man(α1-3) Man(β1-4)GlcNAc [9,25,34-36,44]
933.3 H_3N_2; 915.1 H_4N_2-18; 892.2 H_4N; 874.3 H_4N-18; 753.4 H_2N_2-18; 730.3 H_3N; 712.1 H_3N-18; 568.2 H_2N; 550.3 H_2N-18; 532.2 H_2N-2x18; 527.3 H_3; 509.0 H_3-18; 406.4 HN; 388.2 HN-18; 365.1 H_2	0.2%	Gal(β1-4)GlcNAc(β1-2)Man(α1-6) [Man(α1-3)]Man(β1-4)GlcNAc [9]
933.3 H_3N_2; 892.2 H_4N; 874.4 H_4N-18; 730.3 H_3N; 568.2 H_2N; 550.3 H_2N-18; 509.2 H_3-18; 388.1 HN-18	0.1%	Man(α1-6)[Gal(β1-4)GlcNAc(β1-2) Man(α1-3)]Man(β1-4)GlcNAc Yamashita, 1981 49 /id}[44]
	0.3%	
	0.2%	
1077.7/550.3 H_4N_2-18; 933.3 H_3N2; 550.3 H_2N-18 or H_4N_2-9; 388.1 HN-18 or H_2N_2-9	0.4%	Gal(β1-4)GlcNAc(β1-2)[Gal(β1-4) GlcNAc(β1-4)]Man(α1-3)Man(β1-4) GlcNAc [35]
1298.6 H_4N_3; 1280.5 H_4N_3-18; 1257.6 H_5N_2; 1239.6 H_5N_2-18; 1095.6 H_4N_2; 1077.6 H_4N_2-18; 1059.6 H_4N_2-2x18; 933.5 H_3N_2; 915.4 H_3N_2-18; 892.5 H_4N; 874.6 H_4N-18;771.4 H_2N_2; 730.5 H_3N; 712.4 H_3N-18; 694.3 H_3N-2x18; 568.4 H_2N; 550.3 H_2N-18; 532.4 H_2N-2x18; 527.3 H_3; 514.1 H_2N-3x18; 509.3 H_3-18; 405.9 HN; 388.2 HN-18; 370.2 HN-2x18; 365.3 H_2; 347.2 H_2-18; 329.2 H_2-2x18; 244.0 N; 226.0 N-18; 208.1 N-2x18	26.2%	Gal(β1-4)GlcNAc(β1-2)Man(α1-6) [Gal(β1-4)GlcNAc(β1-2)Man(α1-3)] Man(β1-4)GlcNAc [9,34-36,44]
1442.7 H_5N_3-18; 1257.4 H_5N_2; 1239.5 H_5N_2-18; 892.3 H_4N; 651.7 H_4N_3-9; 570.8 H_3N_3-9; 388.2 HN-18	0.2%	
1622.4 H_6N_3; 1501.4 H_4N_4; 1460.5 H_5N_3; 1442.5 H_5N_3-18; 1424.4 H_5N_3-2x18; 1303.6 H_3N_4-2x18; 1298.6 H_4N_3; 1280.6 H_4N_3-18; 1257.6 H_5N_2; 1239.5 H_5N_2-18; 1118.5 H_3N_3-18; 1095.4 H_4N_2; 1077.6 H_4N_2-18; 1059.3 H_4N_2-2x18; 915.4 H_3N_2-18; 892.2 H_4N; 874.4 H_4N-18; 843.4 H_5N_4; 838.2 H_4N-3x18; 822.9 H_6N_3; 813.7 H_6N_3-9; 762.4 H_4N_4; 753.2 H_2N_2-18, H_4N_4-9; 741.9 H_5N_2; 735.2 H_2N_2-2x18; 732.9 H_5N_3-9; 730.2 H_3N; 712.3 H_3N-18; 660.8 H_4N_3; 640.3 H_5N_2; 570.3 H_3N_3; 568.3 H_2N; 559.3 H_4N_2; 552.6 H_3N_3-3x9;550.2 H_2N-18; 406.2 HN; 388.2 HN-18; 347.2 H_2; 329.2 H_2-18	2.5%	Gal(β1-4)GlcNAc(β1-2)Man(α1-6) [Gal(β1-4)GlcNAc(β1-2)][Gal(β1-4) GlcNAc(β1-4)]Man(α1-3)]Man(β1-4) GlcNAc [9,34-36]
1604.5 H_6N_3-18; 1442.4 H_5N_3-18; 1257.4 H_5N_2; 1239.2 H_5N_2-18; 1095.4 H_4N_2; 1077.5 H_4N_2-18; 892.5 H_4N 874.4 H_4N-18; 822.8 H_6N_3; 753.3 H_2N_2-18; 730.3 H_3N; 550.2 H_4N_2; 388.2 HN-18	0.2%	Gal(β1-4)GlcNAc(β1-3)Gal(β1-4) GlcNAc(β1-2)Man(α1-6)[Gal(β1-4) GlcNAc(β1-2)Man(α1-3)]Man(β1-4) GlcNAc [9,34-36]
1825.7 H_6N_3; 1807.6 H_6N_3-18; 1663.6/843.4 H_5N_4; 1627.5 H_5N_4-2x18; 1622.6/822.7 H_6N_3; 1501.9 H_4N_4; 1460.6/741.7 H_5N_3; 1442.5 H_5N_3-18; 1298.5 H_4N_3; 1257.7 H_5N_2; 1239.5/631.4 H_5N_2-18; 1095.5 H_4N_2; 1077.4 H_4N_2-18; 1059.3 H_4N_2-2x18; 1016.9 H_6N_5-9; 1005.3 H_7N_4; 933.4/478.1 H_3N_2; 924.3 H_6N_4; 915.4 H_6N_4-9; 813.8 H_6N_3-9; 804.8 H_6N_3-2x9; 771.1 H_2N_2; 753.3 H_2N_2-18; 550.4 H_2N-18; 388.2 HN-18	0.2%	Gal(β1-4)GlcNAc(β1-6)][Gal(β1-4) GlcNAc(β1-2)]Man(α1-6)[[Gal(β1-4) GlcNAc(β1-4)][Gal(β1-4)GlcNAc(β1-2)]Man(α1-3)]Man(β1-4)GlcNAc [9,34,36]

Table S5-3. continued

	Comp.	Registered m/z	Charge state	Ret. time (min)
Other glycans	H_2	365.1	$[M+Na]^+$	3.0
				4.6
				5.6
				7.1
				9.0
	HN	406.3	$[M+Na]^+$	5.3
	H_3	527.3	$[M+Na]^+$	3.8
				6.5
				7.5
				14.0
				15.4
				16.5
				19.2
	H_4	689.4	$[M+Na]^+$	22.1
	HF	349.2	$[M+Na]^+$	2.9
				4.6
	H_2F	511.3	$[M+Na]^+$	4.6
	H_2N	568.3	$[M+Na]^+$	6.2
	H_3N	730.4	$[M+Na]^+$	9.0
				14.8
	H_2NF	714.4	$[M+Na]^+$	3.8
	HNF	552.3	$[M+Na]^+$	3.8
	H_2S	656.4 678.4	$[M+Na]^+$ $[M-H+2Na]^+$	25.3
	HNS	697.4 719.4	$[M+Na]^+$ $[M-H+2Na]^+$	23.5
			$[M+Na]^+$ $[M-H+2Na]^+$	25.0
	H_3N_3S	887.8	$[M+2Na]^{2+}$	20.7
	HNX	584.3/ 606.5	$[M+Na]^+$ $[M-H+2Na]^+$	20.6

Fragment ions	Rel. area U2	Proposed structure
203.0 H	1.4%	
203.0 H	0.1%	
203.0 H; 185.0 H-18	30.4%	
203.1 H; 185.1 H-18	0.5%	
203.1 H; 185.0 H-18	2.3%	
226.1 N; 203.0 H; 185.0 H-18	1.8%	
365.1 H_2, 3471,1 H_2-18; 202.9 H	0.2%	
365.2 H_2; 347.1 H_2-18; 203.0 H; 185.0 H-18	1.1%	
365.1 H_2; 347.2 H_2-18; 203.1 H	0.2%	
365.2 H_2; 347.2 H_2-18; 185.0 H-18	0.3%	
365.1 H_2; 347.2 H_2-18; 203.0 H; 184.8 H-18	1.3%	
365.2 H_2; 347.1 H_2-18; 202.9 H; 185.0 H-18	0.3%	
365.2 H_2; 347.0 H_2-18; 203.0 H	0.2%	
527.1 H_3; 509.2 H_3-18; 347.2 H_2-18; 203.0 H	0.1%	
527.2 H_3; 509.2 H_3-18; 365.3 H_2; 347.2 H_2-18; 203.1 H	0.4%	
	0.2%	
	0.4%	
365.2 H_2, 347.2 H_2-18; 203.1 H; 185.1 H-18	4.2%	Fuc{Gal(β1-4)Glc [37,46,47,56]
	0.3%	
550.2 H_2N; 406.2 HN; 388.2 HN-18	0.5%	
568.2 H_2N; 550.3 H_2N-18; 406.2 HN; 388.2 HN-18; 203.1 H	3.2%	
568.3 H_2N; 550.4 H_2N-18; 406.2 HN; 388.2 HN-18; 226.1 N; 203.0 H	0.9%	
406.2 HN; 388.2 HN-18; 203.1 H	0.6%	GalNAc(α1-3)[Fuc(α1-2)]Gal [37]
476.1 HS-18; 365.3 H_2; 347.2 H_2-18; 314.3 S-18; 202.9 H	1.4%	NeuAc(α2-3)Gal(β1-4)Glc [37,50]
516.2 HS; 336.1 S-18	0.2%	NeuAc(α2-6)Gal(β1-4)GlcNAc [37,50]
539.1 NS-18; 406.5 HN; 226.0 N	0.4%	
	0.2%	
	0.4%	

Table S5-4. Oligosaccharide species detected in the G_{M2}-gangliosidosis samples U3 and U4. Comp., composition; Ret., retention.

	Comp.	Registered m/z	Charge state	Ret. time (min)
Disease related glycans	H_2N_2	771.5	$[M+Na]^+$	10.3
		771.5	$[M+Na]^+$	11.9
	H_3N_3	1136.5	$[M+Na]^+$	15.1
		580.0	$[M+2Na]^{2+}$	
		1136.5	$[M+Na]^+$	16.8
		580.0	$[M+2Na]^{2+}$	
		1136.5	$[M+Na]^+$	18.1
		580.0	$[M+2Na]^{2+}$	
	H_3N_4	681.2	$[M+2Na]^{2+}$	10.0
		1339.4	$[M+Na]^+$	12.9
		681.2	$[M+2Na]^{2+}$	
		681.2	$[M+2Na]^{2+}$	14.0
		681.2	$[M+2Na]^{2+}$	17.5
		1339.4	$[M+Na]^+$	20.0
		681.2	$[M+2Na]^{2+}$	
	H_2N_3	974.6	$[M+Na]^+$	1.1

	Relative Area		
Fragment ions	**U3**	**U4**	**Proposed structure**
568.3 H_2N; 550.3 H_2N-18; 406.1 HN; 388.1 HN-18; 365.1 H_2; 347.1 H_2-18		1.6%	GlcNAc(β1-2)Man(α1-3)Man(β1-4) GlcNAc [15,16,44]
568.3 H_2N; 550.3 H_2N-18; 406.1 HN; 388.1 HN-18; 365.1 H_2; 347.1 H_2N-18; 244.0 N; 226.0 N-18	7.6%	6.0%	GlcNAc(β1-2)Man(α1-6)Man(β1-4) GlcNAc [15]
933.4 H_3N_2; 915.3 H_3N_2-18; 771.5 H_2N_2; 730.4 H_3N; 712.3 H_3N-18; 568.2 H_2N; 550.2 H_2N-18	0.6%	1.1%	GlcNAc(β1-2)Man(α1-6)[GlcNAc(β1-2) Man(α1-3)]Man(β1-4)GlcNAc [15,16,44]
933.4 H_3N_2; 915.3 H_3N_2-18; 730.5 H_3N; 712.4 H_3N-18; 550.3 H_2N-18	3.6%	1.3%	
933.5 H_3N_2; 915.3 H_3N_2-18; 730.5 H_3N; 712.3 H_3N-18; 568.3 H_2N; 550.2 H_2N-18; 347.1 H_2-18	3.8%	5.8%	
	0.4%		
1136.4 H_3N_3; 1118.5 H_3N_3-18; 974.6 H_2N_3; 933.3 H_3N_2; 915.4 H_3N_2-18; 730.6 H_3N; 712.3 H_3N-18; 568.4 H_2N; 550.4 H_2N-18; 532.3 H_2N-2x18; 406.1 HN; 387.9 HN-18	5.5%		GlcNAc(β1-2)Man(α1-6)[GlcNAc(β1-2) [GlcNAc(β1-4)]Man(α1-3)]Man(β1-4) GlcNAc [44,44,60]
1136.4/579.8 H_3N_2; 1118.5/570.9 H_3N_3-18; 974.3 H_2N_3; 933.4/478.2 H_3N_2; 915.3 H_3N_2-18; 897.4 H_3N_2-2x18; 771.3 H_2N_2; 753.4 H_2N_2-18; 712.2 H_3N-18; 591.4 HN_2-18; 568.4 H_2N; 388.2 HN-18; 244.0 N; 226.0 N-18	7.1%	15.5%	GlcNAc(β1-2)[GlcNAc(β1-4)]Man(α1-6) [GlcNAc(β1-2)Man(α1-3)]Man(β1-4) GlcNAc [15]
1136.4/579.8 H_3N_2; 1118.4/570.8 H_3N_3-18; 974.3 H_2N_3; 933.3/478.2 H_3N_2; 915.3/469.2 H_3N_2-18; 771.5 H_2N_2; 730.4 H_3N; 591.3 HN_2-18; 489.7 H_2N_2-9; 388.1 HN-18; 364.8 H_2; 347.1 H_2-18; 226.0 N-18	1.7%		
1136.4 H_3N_3; 1118.5 H_3N_3-18; 974.3 H_2N_3; 933.4 H_3N_2; 915.3 H_3N_2-18; 897.4 H_3N_2-2x18; 771.3 H_2N_2; 753.4 H_2N_2-18; 712.2 H_3N-18; 591.4 HN_2-18; 568.4 H_2N; 388.2 HN-18; 244.0 N; 226.0 N-18	0.1%		
771.4 H_2N_2; 753.4 H_2N_2-18; 609.4 HN_2; 568.3 H_2N; 550.3 H_2N-18; 365.0 H_2; 347.1 H_2-18	1.3%	1.2%	GlcNAc(β1-2)Man(α1-3)[GlcNAc(β1-4)] Man(β1-4)GlcNAc [16,44]

Table S5-4. continued

	Comp.	Registered m/z	Charge state	Ret. time (min)
Other glycans	H_2	365.2	$[M+Na]^+$	7.8
				9.4
				11.3
	HN	406.2	$[M+Na]^+$	8.8
	H_3	527.3	$[M+Na]^+$	7.8
				11.1
				12.1
				14.2
				16.2
				18.7
				23.1
	H_4	689.5	$[M+Na]^+$	22.7
				23.2
	HF	349.2	$[M+Na]^+$	8.8
	H_2F	511.3	$[M+Na]^+$	9.8
	NF	390.2	$[M+Na]^+$	8.3
	H_2N	568.4	$[M+Na]^+$	9.7
				11.9
	H_3N	730.4	$[M+Na]^+$	9.3
	H_4N	892.4	$[M+Na]^+$	9.8
	H_5N	1054.5	$[M+Na]^+$	11.0
	H_2NF	714.5	$[M+Na]^+$	9.4
	H_2NF_2	860.4	$[M+Na]^+$	7.6
	HNF	552.5	$[M+Na]^+$	8.8
	H_2S	656.5 678.5	$[M+Na]^+$ $[M-H+2Na]^+$	23.8
	N_2S	738.4 760.3	$[M+Na]^+$ $[M-H+2Na]^+$	25.1
	HNS	719.4	$[M-H+2Na]^+$	23.5
	HNSF	865.4	$[M-H+2Na]^+$	22.3
		865.4	$[M-H+2Na]^+$	24.3
	HS	516.4	$[M-H+2Na]^+$	23.8
	HX	381.2 403.2	$[M+Na]^+$ $[M-H+2Na]^+$	20.4

	Relative Area		
Fragment ions	**U3**	**U4**	**Proposed structure**
203.0 H		0.3%	
203.0 H; 185.0 H-18	47.0%	30.3%	
203.0 H; 185.0 H-18		0.8%	
244.0 N; 226.0 N-18; 203.0 H; 185.2 H-18	3.6%	2.5%	
		0.2%	
365.1 H_2; 347.0 H_2-18; 185.2 H-18	1.6%	0.8%	
365.0 H_2; 347.0 H_2-18; 203.1 H; 184.9 H-18	0.7%	1.3%	
	0.8%	0.5%	
365.1 H_2; 347.0 H_2-18; 203.0 H; 185.1 H-18	0.4%	1.4%	
365.1 H_2; 203.0 H; 185.0 H-18	0.7%	0.7%	
365.1 H_2; 347.0 H_2-18; 202.9 H; 185.0 H-18	2.0%	0.7%	
527.2 H_3; 509.2 H_3-18; 365.0 H_2; 347.0 H_2-18; 203.0 H	0.7%	0.3%	
527.2 H_3; 509.3 H_3-18; 365.0 H_2; 347.0 H_2-18	1.5%	0.4%	
203.0 H; 185.1 H-18; 169.1 F-18	0.7%	15.5%	
365.1 H_2; 347.1 H_2-18; 330.8 HF-18	0.6%	0.7%	
	0.2%		
347.1 H_2-18	0.9%	1.7%	
	0.1%		
	0.4%	0.5%	
	0.3%	0.3%	
	0.2%		
568.4 H_2N; 552.4 HNF; 550.3 H_2N-18; 534.3 HNF-18; 406.2 HN; 389.9 NF; 388.1 HN-18; 372.1 NF-18; 365.1 H_2; 244.1 N; 203.0 H	0.6%	0.8%	
	0.2%	0.1%	
406.1 HN; 388.1 HN-18; 226.0 N-18; 207.8 N-2x18; 203.0 H; 185.1 H-18	0.5%	0.2%	
498.2 HS-18; 364.8 H_2; 336.0 S-18	2.3%	2.2%	
	0.1%	0.1%	
516.2 HS; 498.3 HS-18; 406.0 HN; 388.1 HN-18; 353.9 S; 336.0 S-18	1.6%	1.5%	NeuAc(α2-6)Gal(β1-4)GlcNAc [37,50]
	0.2%		
	0.1%		
353.7 S; 335.9 S-18	0.2%	0.4%	
240.9 X; 203.0 H		3.6%	Gal(β1-4)GluconA [26]

Table S5-5. Oligosaccharide species detected in the sialidosis samples. Comp., composition; Ret., retention; Rel. area., relative area.

	Comp.	Registered m/z	Charge state	Ret. time (min)
Disease related glycans	HNS	697.6 719.5	$[M+Na]^+$ $[M-H+2Na]^+$	21.3
	H_3N_2S	1224.5 1246.8 624.1 635.1	$[M+Na]^+$ $[M-H+2Na]^+$ $[M+2Na]^{2+}$ $[M-H+3Na]^{2+}$	21.8
	H_5N_3S	887.6 898.3	$[M+2Na]^{2+}$ $[M-H+3Na]^{2+}$	23.7
	$H_5N_3S_2$	1033.1 1044.1 1055.1	$[M+2Na]^{2+}$ $[M-H+3Na]^{2+}$ $[M-2H+4Na]^{2+}$	29.1
	$H_6N_4S_2$	1237.4	$[M-2H+4Na]^{2+}$	28.8
	$H_3SO_3N_2S$	1304.3 1348.2 664.0 674.5 685.8	$[M+Na]^+$ $[M-2H+3Na]^+$ $[M+2Na]^{2+}$ $[M-H+3Na]^{2+}$ $[M-2H+4Na]^{2+}$	21.8
	$H_5SO_3N_3S$	1854.3 1876.3 927.2 938.3 949.4	$[M-H+2Na]^+$ $[M-2H+3Na]^+$ $[M+2Na]^{2+}$ $[M-H+3Na]^{2+}$ $M-2H+4Na]^{2+}$	22.0
	$H_5SO_3N_3S_2$	2166.6 1083.8	$[M-2H+3Na]^+$ $[M-H+3Na]^{2+}$	33.8

	Rel. area	
Fragment ions	**U8**	**Proposed structure**
516.2 HS; 498.2 HS-18; 406.1 HN; 388.1 HN-18; 354.0 S; 336.1 S-18; 318.0 S-2x18; 226.0 N-18	2.7%	NeuAc(α2-6)Gal(β1-4)GlcNAc [37,50]
1043.4/533.3 H_3NS; 1025.4/524.3 H_3NS-18; 933.4/477.9 H_3N_2; 915.4 H_3N_2-18; 881.5/452.3 H_2NS; 863.3/443.0 H_2NS-18; 771.4 H_2N_2; 753.5 H_2N_2-18; 730.4 H_3N; 712.5 H_3N-18; 719.4 HNS; 701.4 HNS-18; 568.4 H_2N; 550.2 H_2N-18; 516.3 HS; 498.3 HS-18; 406.1 HN; 388.1 HN-18; 365.0 H_2; 347.3 H_2-18; 354.0 S; 336.0 S-18; 243.9 N; 226.0 N-18; 208.0 N-2x18; 203.1 H; 185.0 H-18	18.7%	Neu5Ac(α2-3)Gal(β1-4) GlcNAc(β1-2)Man(α1-3)Man(β1-4) GlcNAc [38-40]
1460.5 H_5N_3; 1442.6 H_5N_3-18; 1408.6 H_4N_2S; 1390.3 H_4N_2S-18; 1257.6 H_3N_2; 1095.5 H_4N_2; 1077.6 H_4N_2-18; 1025.2 H_3NS-18; 915.4 H_3N_2-18; 892.2 H_4N; 881.3 H_2NS; 797.4 H_4N_3S-9; 796.9 H_5N_2S; 771.5 H_2N_2; 694.5 H_3N-2x18; 640.5 H_5N_2; 605.0 H_4NS-9; 568.2 H_2N; 541.0 H_4N_2-2x9; 388.2 HN-18; 336.1/314.0 S-18	3.2%	Neu5Ac(α2-3/6)Gal(β1-4) GlcNAc(β1-2)Man(α1-6)[Gal(β1-4) GlcNAc(β1-2)Man(α1-3)]Man(β1-4) GlcNAc [38,39]
1773.4/898.5 H_5N_3S; 1733.1/1755.3/889.4 H_5N_3S-18; 1571.4/797.5 H_4N_3S-18; 1570.5 H_5N_2S; 1460.2/741.9 H_5N_3; 1408.4 H_4N_2S; 1368.8 H_4N_2S-18; 1095.5 H_4N_2; 953.4 $H_5N_2S_2$; 915.5 H_3N_2-18; 892.1 H_4N; 701.2 HNS-18; 694.4 H_3N-2x18; 605.3 H_4NS-9; 596.1 H_4NS-2x9; 313.9 S	8.7%	Neu5Ac(α2-3/6)Gal(β1-4) GlcNAc(β1-2)Man(α1-6) [Neu5Ac(α2-3/6)Gal(β1-4) GlcNAc(β1-2)Man(α1-3)]Man(β1-4) GlcNAc [38-40]
	0.0%	
933.5 $H_3(SO_3)N_2$; 701.4 $H(SO_3)NS$-18; 645.6/634.9 H_3N_2S; 634.5 $H_2(SO_3)N$; 516.3 $H(SO_3)S$; 196.0 HN	2.4%	Neu5Ac(α2-3)Gal(6SO3)(β1-4) GlcNAc(β1-2)Man(α1-3/6) Man(β1-4)GlcNAc [26]
	0.9%	Neu5Ac, SO3(6){Gal(β1-4) GlcNAc(β1-2)Man(α1-6)[Gal(β1-4) GlcNAc(β1-2)Man(α1-3)]Man(β1-4) GlcNAc [26]
	1.0%	2xNeu5Ac, SO3(6){Gal(β1-4) GlcNAc(β1-2)Man(α1-6)[Gal(β1-4) GlcNAc(β1-2)Man(α1-3)]Man(β1-4) GlcNAc [26]

Table S5-5. continued

	Comp.	Registered m/z	Charge state	Ret. time (min)
	H_2	365.2	$[M+Na]^+$	6.2
				7.4
				8.7
				10.2
				13.5
	HS	516.3	$[M-H+2Na]^+$	21.7
	H_3	527.3	$[M+Na]^+$	8.9
				13.5
				18.2
				20.8
				22.5
				28.1
	H_4	689.5	$[M+Na]^+$	19.4
				21.2
	HN	406.2	$[M+Na]^+$	7.4
	H_2N	568.5	$[M+Na]^+$	7.5
	H_3N	730.6	$[M+Na]^+$	8.5
				12.1
Other glycans	H_4N	892.6	$[M+Na]^+$	10.3
	H_2N_2	771.3	$[M+Na]^+$	9.9
	H_3N_2	933.5 478.4	$[M+Na]^+$ $[M+2Na]^{2+}$	11.1
		933.5 478.4	$[M+Na]^+$ $[M+2Na]^{2+}$	13.4
	H_5N_3	742.0	$[M+2Na]^{2+}$	18.4
	H_2S	656.5 678.5	$[M+Na]^+$ $[M-H+2Na]^+$	12.8
				21.8
	HF	349.2	$[M+Na]^+$	5.9
	H_2F	511.4	$[M+Na]^+$	7.0
	NF	390.2	$[M+Na]^+$	6.5
	HNF	552.5	$[M+Na]^+$	6.7
				7.0
	H_2NF	714.5	$[M+Na]^+$	6.7

	Rel. area	
Fragment ions	**U8**	**Proposed structure**
203.0 H	1.5%	
203.0 H;185.1 H-18	18.9%	
202.9 H;185.1 H-18	3.5%	
203.0 H;185.0 H-18	2.4%	
203.0 H;185.1 H-18	0.3%	
	1.0%	
365.2 H_2; 347.1 H_2-18; 203.1 H; 185.0 H-18	3.2%	
365.1 H_2; 347.0 H_2-18; 203.1 H; 185.1 H-18	0.3%	
365.1 H_2; 347.0 H_2-18; 203.1 H; 185.1 H-18	0.6%	
	0.6%	
365.1 H_2; 347.1 H_2-18; 203.1 H; 185.0 H-18	0.9%	
	0.7%	
	0.0%	
527.3 H_3; 509.3 H_3-18; 365.0 H_2; 347.0 H_2-18; 203.0 H	2.8%	
244.0 N; 226.0 N-18; 203.0 H; 185.1 H-18	5.4%	
365 H_2; 347.0 H_2-18; 244.2 N	1.1%	
568.4 H_2N; 550.2 H_2N-18; 527.4 H_3; 509.3 H_3-18; 406.0 HN; 388.2 HN-18; 364.9 H_2; 347.0 H_2-18	1.3%	
568.3 H_2N; 550.3 H_2N-18; 509.3 H_3-18; 406.1 HN; 388.1 HN-18; 365.1 H_2; 347.2 H_2-18; 244.1 N; 226.0 N-18; 203.0 H		
730.4 H_3N; 689.4 H_4; 671.2 H_4-18; 568.3 H_2N; 550.3 H_2N-18; 509.4 H_3-18; 406.0 HN; 347.1 H_2-18	1.4%	
388.1 HN-18	0.3%	
771.5 H_2N_2; 753.5 H_2N_2-18; 730.5 H_3N; 712.4 H_3N-18; 609.4 HN_2; 568.4 H_2N; 550.3 H_2N-18; 527.3 H_3; 509.2 H_3-18; 406.2 HN; 388.2 HN-18; 365.1 H_2; 347.2 H_2-18	2.1%	
771.4 H_2N_2; 753.5 H_2N_2-18; 730.4 H_3N; 712.4 H_3N-18; 568.4 H_2N; 550.4 H_2N-18; 509.4.3 H_3-18; 406.1 HN; 388.2 HN-18; 365.1 H_2; 347.1 H_2-18	4.4%	
1298.5 H_4N_3; 1280.3/651.6 H_4N_3-18; 1257.4/640.2 H_5N_2; 1239.4 H_5N_2-18;1095.4 H_4N_2; 1077.4/550.2 H_4N_2-18; 933.4 H_3N_2; 694.4 H_2N-2x18; 568.4 H_2N; 550.2 H_2N-18; 509.0 H_3-18; 451.0 H_3N_2-3x9; 388.1 HN-18; 329.0 H_2-2x18; 226.0 N-18	0.3%	
	0.4%	
516.3 HS; 498.2 HS-18; 480.1 HS-2x18; 365.0 H_2; 354.1/332.1 S; 336.0/313.9 S-18; 317.9/296.0 S-2x18	1.7%	
	1.7%	
365.1 H_2; 349.1 HF; 347.1 H_2-18; 331.1 HF-18; 203.0 H; 185.0 H-18	2.8%	Fuc{Gal(β1-4)Glc [37,46,47]
	0.3%	
406.1 HN;388.2 HN-18; 349.1 HF; 243.9 N; 226.1 N-18; 203.0 H	0.0%	GalNAc(α1-3)[Fuc(α1-2)]Gal [37]
406.1 HN; 390.2 NF; 388.2 HN-18; 372.0 NF-18; 226.0 N-18; 203.0 H	1.2%	
568.3 H_2N; 552.1 HNF; 550.4 H_2N-18; 534.3 HNF-18; 406.1 HN; 388.2 HN-18; 372.1 NF-18; 226.1 N-18; 208.0 N-2x18; 203.0 H	1.1%	

REFERENCES

1. Cantz M & Ulrich-Bott B (1990) Disorders of glycoprotein degradation. *J Inherit Metab Dis* **13,** 523-537.
2. Lundblad A, Lundsten J, Nordén NE, Sjöblad S, Svensson S, Öckerman PA, & Gehlhoff M (1978) Urinary abnormalities in fucosidosis. *Eur J Biochem* **83,** 513-521.
3. Ockerman PA (1969) Diseases of glycoprotein storage. *Lancet* **1,** 734.
4. Ockerman PA, Autio S, & Norden NE (1973) Diagnosis of mannosidosis. *Lancet* **1,** 207-208.
5. Winchester B (2005) Lysosomal metabolism of glycoproteins. *Glycobiology* **15,** 1R-15R.
6. Cantz M, Gehler J, & Spranger J (1977) Mucolipidosis I: increased sialic acid content and deficiency of an alpha-*N*-acetylneuraminidase in cultured fibroblasts. *Biochem Biophys Res Commun* **74,** 732-738.
7. van Pelt J, Kamerling JP, Bakker HD, & Vliegenthart JF (1991) A comparative study of sialyloligosaccharides isolated from sialidosis and galactosialidosis urine. *J Inherit Metab Dis* **14,** 730-740.
8. Landing BH, Silverman FN, Chadwick DL, Lahey ME, Jacoby MD, & Raig JM (1964) Familial neurovisceral lipidosis. An analysis of eight cases of a syndrome previously reported as "Hurler-variant," "Pseudo-Hurler," and "Tay-Sachs disease with visceral involvement". *Am J Dis Child* **108,** 503-522.
9. Takahashi Y & Orii T (1989) Severity of GM1 gangliosidosis and urinary oligosaccharide excretion. *Clin Chim Acta* **179,** 153-162.
10. Rubin M, Karpati G, Wolfe LS, Carpenter S, Klavins MH, & Mahuran DJ (1988) Adult onset motor neuronopathy in the juvenile type of hexosaminidase A and B deficiency. *J Neurol Sci* **87,** 103-119.
11. Hoffman LM, Amsterdam D, Brooks SE, & Schneck L (1977) Glycosphingolipids in fetal Tay-Sachs disease brain and lung cultures. *J Neurochem* **29,** 551-559.
12. Mahuran DJ (1999) Biochemical consequences of mutations causing the GM2 gangliosidoses. *Biochim Biophys Acta* **1455,** 105-138.
13. Hou Y, Tse R, & Mahuran DJ (1996) Direct determination of the substrate specificity of the alpha-active site in heterodimeric beta-hexosaminidase A. *Biochemistry (Mosc)* **35,** 3963-3969.
14. Kolter T & Sandhoff K (2006) Sphingolipid metabolism diseases. *Biochim Biophys Acta* **1758,** 2057-2079.
15. Strecker G, Herlant-Peers MC, Fournet B, & Montreul J (1977) Structure of seven oligosaccharides excreted in the urine of a patient with Sandhoff's disease (GM2 gangliosidosis-variant O). *Eur J Biochem* **81,** 165-171.
16. Warner TG, De Kremer RD, Applegarth D, & Mock AK (1986) Diagnosis and characterization of GM 2 gangliosidosis type II (Sandhoff disease) by analysis of the accumulating *N*-acetyl-glucosaminyl oligosaccharides with high performance liquid chromatography. *Clin Chim Acta* **154,** 151-164.
17. Sewell AC (1979) An improved thin-layer chromatographic method for urinary oligosaccharide screening. *Clin Chim Acta* **92,** 411-414.
18. Kin NM (1987) Comparison of the urinary glycoconjugates excreted by patients with type I and type II fucosidosis. *Clin Chem* **33,** 44-47.
19. Schindler D, Kanzaki T, & Desnick RJ (1990) A method for the rapid detection of urinary glycopeptides in alpha-*N*-acetylgalactosaminidase deficiency and other lysosomal storage diseases. *Clin Chim Acta* **190,** 81-91.
20. An Y, Young SP, Hillman SL, Van Hove JL, Chen YT, & Millington DS (2000) Liquid chromatographic assay for a glucose tetrasaccharide, a putative biomarker for the diagnosis of Pompe disease. *Anal Biochem* **287,** 136-143.
21. Neville DC, Dwek RA, & Butters TD (2009) Development of a single column method for the separation of lipid- and protein-derived oligosaccharides. *J Proteome Res* **8,** 681-687.
22. Warner TG, Turner MW, Toone JR, & Applegarth D (1986) Prenatal diagnosis of infantile GM 2 gangliosidosis type II (Sandhoff disease) by detection of *N*-acetylglucosaminyl-oligosaccharides in amniotic fluid with high-performance liquid chromatography. *Prenat Diagn* **6,** 393-400.
23. Peelen GO, de Jong JG, & Wevers RA (1994) HPLC analysis of oligosaccharides in urine from oligosaccharidosis patients. *Clin Chem* **40,** 914-921.
24. Wuhrer M, Koeleman CA, Deelder AM, & Hokke CH (2004) Normal-phase nanoscale liquid chromatography-mass spectrometry of underivatized oligosaccharides at low-femtomole sensitivity. *Anal Chem* **76,** 833-838.
25. Bruggink C, Wuhrer M, Koeleman CA, Barreto V, Liu Y, Pohl C, Ingendoh A, Hokke CH, & Deelder AM (2005) Oligosaccharide analysis by capillary-scale high-pH anion-exchange chromatography with on-line ion-trap mass spectrometry. *J Chromatogr B Analyt Technol Biomed Life Sci* **829,** 136-143.
26. Bruggink C, Poorthuis BJ, Piraud M, Froissart R, Deelder AM, & Wuhrer M (2010) Glycan profiling of urine, amniotic fluid and ascitic fluid from galactosialidosis patients reveals novel oligosaccharides with reducing end hexose and aldohexonic acid residues. *FEBS J* **277,** 2970-2986.

27. Packer NH, Lawson MA, Jardine DR, & Redmond JW (1998) A general approach to desalting oligosaccharides released from glycoproteins. *Glycoconj J* **15,** 737-747.
28. Rocklin RD, Clarke AP, & Weitzhandler M (1998) Improved long-term reproducibility for pulsed amperometric detection of carbohydrates via a new quadruple-potential waveform. *Anal Chem* **70,** 1496-1501.
29. Yamashita K, Kochibe N, Ohkura T, Ueda I, & Kobata A (1985) Fractionation of L-fucose-containing oligosaccharides on immobilized Aleuria aurantia lectin. *J Biol Chem* **260,** 4688-4693.
30. Michalski JC & Klein A (1999) Glycoprotein lysosomal storage disorders: alpha- and beta-mannosidosis, fucosidosis and alpha-*N*-acetylgalactosaminidase deficiency. *Biochim Biophys Acta* **1455,** 69-84.
31. Strecker G, Fournet B, Bouquelet S, Montreuil J, Dhondt JL, & Farriaux JP (1976) Chemistry of urinary mannosides excreted in mannosidosis. *Biochimie* **58,** 579-586.
32. Yamashita K, Tachibana Y, Mihara K, Okada S, Yabuuchi H, & Kobata A (1980) Urinary oligosaccharides of mannosidosis. *J Biol Chem* **255,** 5126-5133.
33. Matsuura F, Nunez HA, Grabowski GA, & Sweeley CC (1981) Structural studies of urinary oligosaccharides from patients with mannosidosis. *Arch Biochem Biophys* **207,** 337-352.
34. Yamashita K, Ohkura T, Okada S, Yabuuchi H, & Kobata A (1981) Urinary oligosaccharides of GM1-gangliosidosis. Different excretion patterns of oligosaccharides in the urine of type 1 and type 2 subgroups. *J Biol Chem* **256,** 4789-4798.
35. Klein A, Lebreton A, Lemoine J, Perini JM, Roussel P, & Michalski JC (1998) Identification of urinary oligosaccharides by matrix-assisted laser desorption ionization time-of-flight mass spectrometry. *Clin Chem* **44,** 2422-2428.
36. Warner TG, Robertson AD, & O'Brien JS (1983) Diagnosis of GM1 gangliosidosis based on detection of urinary oligosaccharides with high performance liquid chromatography. *Clin Chim Acta* **127,** 313-326.
37. Lundblad A (1978) Oligosaccharides from human urine. In *Methods in Enzymology* (Ginsburg V, ed), pp. 226-235. Academic Press, New York.
38. Michalski JC (1996) Normal and pathological catabolism of glycoproteins: catabolic pathway. In *Glycoproteins and Disease* (Montreuil J, Vliegenthart JF & Schachter H, eds), pp. 55-88. Elsevier Science.
39. Lowden JA & O'Brien JS (1979) Sialidosis: a review of human neuraminidase deficiency. *Am J Hum Genet* **31,** 1-18.
40. van Pelt J, Kamerling JP, Vliegenthart JF, Hoogeveen AT, & Galjaard H (1988) A comparative study of the accumulated sialic acid-containing oligosaccharides from cultured human galactosialidosis and sialidosis fibroblasts. *Clin Chim Acta* **174,** 325-335.
41. Spina E, Sturiale L, Romeo D, Impallomeni G, Garozzo D, Waidelich D, & Glueckmann M (2004) New fragmentation mechanisms in matrix-assisted laser desorption/ionization time-of-flight/time-of-flight tandem mass spectrometry of carbohydrates. *Rapid Commun Mass Spectrom* **18,** 392-398.
42. Harvey DJ (2000) Electrospray mass spectrometry and fragmentation of *N*-linked carbohydrates derivatized at the reducing terminus. *J Am Soc Mass Spectrom* **11,** 900-915.
43. Weiskopf AS, Vouros P, & Harvey DJ (1998) Electrospray ionization-ion trap mass spectrometry for structural analysis of complex *N*-linked glycoprotein oligosaccharides. *Anal Chem* **70,** 4441-4447.
44. Ramsay SL, Meikle PJ, Hopwood JJ, & Clements PR (2005) Profiling oligosaccharidurias by electrospray tandem mass spectrometry: quantifying reducing oligosaccharides. *Anal Biochem* **345,** 30-46.
45. Jardine I, Matsuura F, & Sweeley CC (1984) Electron ionization mass spectra of reduced and permethylated urinary oligosaccharides from patients with mannosidosis. *Biomed Mass Spectrom* **11,** 562-568.
46. Kunz C, Rudloff S, Baier W, Klein N, & Strobel S (2000) Oligosaccharides in human milk: structural, functional, and metabolic aspects. *Annu Rev Nutr* **20,** 699-722.
47. Finke B, Stahl B, Pfenninger A, Karas M, Daniel H, & Sawatzki G (1999) Analysis of high-molecular-weight oligosaccharides from human milk by liquid chromatography and MALDI-MS. *Anal Chem* **71,** 3755-3762.
48. Pfenninger A, Karas M, Finke B, & Stahl B (2002) Structural analysis of underivatized neutral human milk oligosaccharides in the negative ion mode by nano-electrospray MS(n) (part 1: methodology). *J Am Soc Mass Spectrom* **13,** 1331-1340.
49. Naarding MA, Ludwig IS, Groot F, Berkhout B, Geijtenbeek TB, Pollakis G, & Paxton WA (2005) Lewis X component in human milk binds DC-SIGN and inhibits HIV-1 transfer to CD4+ T lymphocytes. *J Clin Invest* **115,** 3256-3264.
50. Parkkinen J & Finne J (1983) Isolation and structural characterization of five major sialyloligosaccharides and a sialylglycopeptide from normal human urine. *Eur J Biochem* **136,** 355-361.
51. Koseki M & Tsurumi K (1977) A convenient method for the isolation of 3'-sialyllactose from normal human urine. *J Biochem* **82,** 1785-1788.

52. Hardy MR & Townsend RR (1988) Separation of positional isomers of oligosaccharides and glycopeptides by high-performance anion-exchange chromatography with pulsed amperometric detection. *Proc Natl Acad Sci U S A* **85,** 3289-3293.
53. Townsend RR, Hardy MR, Hindsgaul O, & Lee YC (1988) High-performance anion-exchange chromatography of oligosaccharides using pellicular resins and pulsed amperometric detection. *Anal Biochem* **174,** 459-470.
54. Townsend RR, Hardy MR, & Lee YC (1989) Separation of oligosaccharides using high-performance anion-exchange chromatography with pulsed amperometric detection. *Methods Enzymol* **179,** 65-76.
55. Vellodi A (2005) Lysosomal storage disorders. *Br J Haematol* **128,** 413-431.
56. Strecker G, Fournet B, & Montreuil J (1978) Structure of the three major fucosyl-glycoasparagines accumulating in the urine of a patient with fucosidosis. *Biochimie* **60,** 725-734.
57. Tsay GC & Dawson G (1976) Oligosaccharide storage in brains from patients with fucosidosis, GM1-gangliosidosis and GM2-gangliosidosis (Sandhoff's disease). *J Neurochem* **27,** 733-740.
58. Tsay GC, Dawson G, & Sung SS (1976) Structure of the accumulating oligosaccharide in fucosidosis. *J Biol Chem* **251,** 5852-5859.
59. Nishigaki M, Yamashita K, Matsuda J, Arashima S, & Kobata A (1978) Urinary oligosaccharides of fucosidosis. Evidence of the occurrence of X-antigenic determinant in serum-type sugar chains of glycoproteins. *J Biochem* **84,** 823-834.
60. Warner TG, deKremer RD, Mock AK, & Sjoberg ER (1985) Characterization and analysis of branched-chain *N*-acetylglucosaminyl oligosaccharides accumulating in Sandhoff disease tissue. Evidence that biantennary bisected oligosaccharide side chains of glycoproteins are abundant substrates for lysosomes. *J Biol Chem* **260,** 6194-6199.
61. Dorland L, Haverkamp J, Vliegenthart JF, Strecker G, Michalski JC, Fournet B, Spik G, & Montreuil J (1978) 360-MHz 1H nuclear-magnetic-resonance spectroscopy of sialyl-oligosaccharides from patients with sialidosis (mucolipidosis I and II). *Eur J Biochem* **87,** 323-329.
62. Charlwood J, Tolson D, & Camilleri P (1999) A detailed analysis of neutral and acidic carbohydrates in human milk. *Anal Biochem* **273,** 261-277.
63. Fong BY, Ma K, & McJarrow P (2011) Quantification of Bovine Milk Oligosaccharides Using Liquid Chromatography Selected Reaction Monitoring-Mass Spectrometry. *J Agric Food Chem* **59,** 9788-9795.
64. Anumula KR (2006) Advances in fluorescence derivatization methods for high-performance liquid chromatographic analysis of glycoprotein carbohydrates. *Anal Biochem* **350,** 1-23.
65. Ruhaak LR, Zauner G, Huhn C, Bruggink C, Deelder AM, & Wuhrer M (2010) Glycan labeling strategies and their use in identification and quantification. *Anal Bioanal Chem* **397,** 3457-3481.
66. Bruggink C, Maurer R, Herrmann H, Cavalli S, & Hoefler F (2005) Analysis of carbohydrates by anion exchange chromatography and mass spectrometry. *J Chromatogr A* **1085,** 104-109.
67. Rabin S, Stillian JR, Barreto V, Friedman K, & Toofan M (1993) New membrane-based electrolytic suppressor device for suppressed conductivity detection in ion chromatography. *J Chromatogr* **640,** 97-109.
68. Liu Y, Srinivasan K, Pohl C, & Avdalovic N (2004) Recent developments in electrolytic devices for ion chromatography. *J Biochem Biophys Methods* **60,** 205-232.

6

GENERAL DISCUSSION

6.1 LIQUID CHROMATOGRAPHY HYPHENATED TO MASS SPECTROMETRIC DETECTION

Glycoconjugates have different biological functions which often depend on the structure of the glycan part. Hence, for fully determining structure-function relationships the elucidation of the glycan structure is essential. Isomeric carbohydrates often have different biological functions too, and it is therefore critical to be able to distinguish between these forms, for example by separating them chromatographically prior to performing mass spectrometric analysis. Liquid chromatography is the technique most commonly used for separating carbohydrates, the major separation principles being reversed-phase chromatography (RPLC), porous-graphitized-carbon chromatography (PGC), hydrophilic interaction liquid chromatography (HILIC), ion-exchange chromatography (IEC), and high-performance anion-exchange chromatography (HPAEC). Of these methods, RPLC, PGC and HILIC are well suitable for MS coupling, while MS coupling of IEC and HPAEC has so far not been straightforward. This thesis reports on major advances in HPAEC-PAD-MS with the successful development and application of the first capillary scale system (column 400 µm I.D.) with online desalting and online ESI-MS coupling suitable for high-sensitivity analysis of glycans. Together with the well-established high separation power and selectivity of HPAEC, this has resulted in an attractive glycoanalytical tool which may be broadly applied in the future.

Several components of the system had to be adapted to fulfill the requirements of capillary HPAEC-PAD. The original amperometric detection cell was modified to minimize its void volume. The band dispersion, caused by the modified amperometric cell, was investigated by separating an inulin solution with an acetate gradient, and comparing its chromatographic resolution with that obtained by a standard HPAEC-PAD equipped with a narrow-bore column (2 mm I.D.). The obtained chromatograms from these two systems showed very similar band dispersion, indicating that the minimization of the void volume made the electrochemical detection cell suitable for capillary-scale use (Chapters 2 and 3). While with the narrow-bore system (chapter 2) a minimum detection limit (MDL) of 120 fmol was obtained, the capillary-scale setup resulted in an MDL of 22 fmol (Chapter 3), indicating that the capillary-scale setup resulted in increased sensitivity when employing PAD detection. Finally, the modified amperometric cell proved to be appropriate for the sensitive detection of native carbohydrates in capillary-scale chromatography.

A bigger challenge than the PAD analysis was the development of a capillary desalter to make hyphenation of capillary HPAEC to MS possible. To enable an online setup, the desalter had to convert the eluting solution into an MS-compatible solvent. The challenge was to obtain enough desalting efficacy to remove from the solution the sodium ions – arising from sodium hydroxide and sodium acetate present in the applied eluents - without sacrificing too much of the obtained chromatographic resolution. The desalting capacity obtained was 225 mM Na^+ at 10 µl/min flow rate (Chapter 3). This capacity is high enough to desalt eluents used for the elution of glycans with a maximum of three negative charges, e.g. three sialic acid groups contained in oligosaccharide structures (Chapter 4). The change in resolution caused by the developed desalter was determined by comparing the results of a gradient separation of an inulin solution with the capillary amperometric detection cell directly following the capillary column, with that of the same separation with the desalter installed between the column and the amperometric cell. This comparison demonstrated that the capillary-scale online desalter

only resulted in a minor loss of chromatographic resolution and was, therefore, suitable for MS coupling of capillary-scale HPAEC in oligosaccharide analysis (Chapter 3).

By downscaling the column dimension to 400 µm I.D. an important sensitivity gain was obtained in electrospray ionization and MS detection. This improved sensitivity can be essential for biomedical research. The minimum detection limit (MDL) obtained for underivatized glycans with capillary-scale HPAEC-MS was found to be 160 fmol using a conventional electrospray ionization source (Chapter 3), while nano-scale HILIC-MS approximately with an online-nano electrospray ionization source gives an MDL of 5 fmol [1]. This difference in MDL largely reflects the difference in column diameters (400 µm I.D. for HPAEC, 75 µm I.D. for HILIC) indicating that the sensitivity of HPAEC-MS and HILIC-MS might be similar if both techniques are performed with identical column dimensions, and identical mass spectrometric detectors.

The high pH of the eluent used in HPAEC causes a fast conversion of anomers, which suppresses anomer separation completely, resulting in an excellent peak performance [2]. PGC often separates anomeric forms [3], which phenomenon can interfere with the necessary resolution between different carbohydrates. This effect can often be reduced by elevating the column temperature. Likewise, HILIC separations of reducing-end oligosaccharides performed at acidic pH show at least partial anomer separation, thereby complicating the analysis of complex samples [1].

The analysis of urinary oligosaccharides by HPAEC-MS as performed in this thesis required only a single sample pretreatment step, namely solid-phase extraction with porous graphitized carbon material. Eluates were dried and reconstituted in small volumes of water, allowing the injection of analytes in high concentrations, as a result of which we obtained an in-depth analysis of complex samples. In contrast, HILIC separations of oligosaccharides are performed with very high concentrations (80% and higher) of organic solvents as starting condition [4], which reduces the solubility of oligosaccharides and may cause problems in the event of high concentrations of glycans, especially at low temperatures (such as may occur in the cooled tray of an autosampler). During the phase of method development, our group has indeed experienced irreproducibility of results due to the initial high organic solvent concentration.

HPAEC is known for its ability to separate glycan isomers differing in linkage type and compositional order [2,5-7], and the capillary HPAEC-PAD-MS indeed gave a complete separation of the 6-arm and the 3-arm monoantennary complex oligosaccharides both with galactose and with *N*-acetylglucosamine at the non-reducing end (Chapters 3 and 5). Many other examples of the separation of structural isomers of complex *N*-glycans are reported in Chapter 4. This chapter reports mainly about the separation of sialylated glycans. The observed separation order of oligosaccharides with α2-3- or α2-6 linked sialic acid was in accordance with that described in literature [8]. In addition, we observed charge-based separation of oligosaccharides with a terminal, reducing-end hexose and of related species with a terminal aldohexonic acid instead (Chapter 4): the additional charge caused by the aldohexonic acid (generated by C_1-oxidation of hexose) consistently resulted in an increase of retention time, which is primarily based on ionic interactions. At least two features are responsible for the selectivity of glycans in HPAEC: (i) the difference in acidity of the various hydroxyl groups [9] and (ii) the accessibility of oxyanions of the oligosaccharides to the functional groups of the stationary phase [5]. PGC and HILIC also show separation of glycan isomers, but this isomer separation has been determined to be based on other interaction mechanisms than that of HPAEC. In general, PGC shows selectivity on the basis of glycan size, charge of acidic glycans,

and the 3D-structure of glycans resulting from linkage between the sugar monomers [10-12]. A glycan with a relatively planar structure tends to have a longer retention with PGC material than glycans with a more globular structure, which is due to differences in contact area between analyte and graphite surfaces [10,13]. The selectivity of HILIC for glycans is mainly based on hydrophilic interaction between the bulk eluent and a water-rich layer, partially immobilized on the stationary phase [14,15]. The observed selectivity rules for glycans in HILIC show separation on glycan size, and linkage between the sugar monomers [16,17]. So, the isomer separation of HPAEC is different from that of PGC and HILIC, and therefore these three kinds of chromatography selectivities are orthogonal to each other.

The research described in this thesis was done on a prototype capillary ion chromatograph. Our challenge in the coming years will be to make capillary-scale HPAEC-MS more generally available. In 2010 the first commercially available capillary ion chromatograph was introduced [18], but this system did not yet provide all the modules necessary for HPAEC-MS of oligosaccharides, such as a capillary-scale ternary gradient pump and the required capillary-scale HPAEC separation columns. The main field of application for the present instrument is the analysis of small anions and cations and this field can be of potential value for the analysis of smaller ionic compounds such as nucleotides, sugar phosphates, and organic acids in the fields of metabolomics and metabonomics [19]. The instrument includes a capillary desalter, a capillary amperometric detection cell, a capillary eluent generator, and an isocratic capillary pump, and this combination of modules is suitable for analyzing mono- and disaccharides with capillary HPAEC-PAD-MS [20,21], but not for larger, potentially charged oligosaccharides.

Instead of manually checking the desalting efficacy prior to the start of a sample analysis sequence only once, a more robust approach would be an online desalting monitor that protects the mass spectrometer from possible contamination caused by insufficient desalting. Such a monitor could contain the desalter, a connection for introducing make-up liquid, and an electronic output to stop the chromatograph to prevent salt from entering into the electrospray ionization source, thus contaminating the mass spectrometer.

To obtain a higher sample throughput while retaining selectivity and resolution, a faster separation would be desirable. One possible way to achieve this would be the development of ion exchange monolithic columns [22], which has already started for small ions [23]. Another possibility would be the use of smaller particles than the 4-µm materials which have just been introduced for IC. Particles of the envisaged size (≤ 2-µm) are already in use for HPLC [24] in RP and HILIC columns, resulting in vastly increased peak capacities [25,26]. However, the use of ion exchange columns packed with smaller particles requires an ion chromatography system capable of running at higher pressures than 34.5 MPa, which is the present pressure limit of ion chromatographs.

To develop optimal LC methods for monolithic columns and columns packed with smaller particles, the kinetic-plot method is a valuable tool [27]. A kinetic-plot is a graphical approach allowing the selection of column specifications (i.e. optimum particle size and column length) and LC conditions (operating pressure and temperature) to generate a specific number of plates or peak capacity in the shortest possible analysis time [27]. Kinetic plot measurements for small ions have been published by Causon *et al.* [28,29] for an analytical-scale column. Wouters *et al.* are now carrying out similar measurements for a capillary-scale ion-exchange column [30].

An important part of the instrumental setup for this work obviously was the MS. Again, enhanced sensitivity is vital in cases where only very small sample amounts are available. In

the last decades many developments in mass spectrometers have led to a strongly improved sensitivity of MS instruments by decreasing the noise level and increasing the signal. The expected gain in sensitivity which would be realized by using a state of the art MS instrument instead of the MS used for the research reported in this thesis is approximately two orders of magnitude and should make new high-sensitivity applications accessible. Further enhancement of the sensitivity could be realized by further miniaturization of the column. Biomedical research makes a more and more frequent use of nano-scale liquid chromatographs, and a similar development is expected for ion chromatography. The main challenge here is to minimize the void volume, caused in particular by the desalter. A possible approach would be to integrate the separator column and the desalter, thus avoiding fitting and tubing materials [31]. The improvements in instrumentation setup, as described above, could be of high value for limited sample amounts, such as in studies on posttranslational modification of proteins. An example of such a modification would be provided by glycans released from extracted electrophoretic bands. Another example of applications where sensitivity is of importance is in the analysis of ionic compounds and carbohydrates in smaller objects, such as biopsy samples.

6.2 LYSOSOMAL STORAGE DISORDERS

The capillary-scale HPAEC-PAD-MS system developed in this study was used for the characterization of free glycans in urine, amniotic fluid and ascitic fluid samples. The analyses have highlighted relevant glycan structures which are potential markers for each of the different lysosomal storage disorders examined. While we here applied our newly developed capillary-scale HPAEC-PAD-MS for the characterization of disease-associated urinary glycans, it should be stated that other modern glycoanalytical techniques would most likely be similarly suitable to reveal the characteristic urinary glycan profiles from urine as well as other body fluids. Such alternative techniques include the analysis of fluorescently labeled glycans by e.g. UPLC with fluorescence detection (HILIC, reverse-phase or graphitized carbon), capillary gel electrophoresis with laser-induced fluorescence (CGE-LIF) as well as various types of mass spectrometry including MALDI-TOF-MS of native or derivatized glycans, and various LC-MS approaches [11,32]. It should be stated, however, that the distinct properties of these detection methods are certainly expected to influence the (sub-)set of urinary glycans which is amenable to analysis by the various methods. For example, relying on reducing-end labeling via aldehyde groups will preclude the detection of the C_1-oxidized glycans described in this thesis. Moreover, the use of a powerful separation technique (such as in LC-MS, UPLC with fluorescence detection, or CGE-LIF) will favor isomer differentiation [16,25,33].

On another note, when aiming at the glycan analysis from a large set of urinary samples, a two-step analytical approach may be advantageous: analysis of the urinary glycan profiles may be achieved by a fast, high-throughput method such as HPLC with fluorescence detection or CGE-LIF, and only a selected set of samples where the structural assignment cannot be performed satisfactorily using the profiling methods would be subjected to (tandem) mass spectrometry as a more costly and time-consuming in-depth analytical method.

While many of glycan structures which were identified in this thesis had already been reported in the literature for the different disorders investigated, it is remarkable that in the various body

fluids from galactosialidosis patients new glycan structures with a reducing-end hexose were found, which structures are assumed to be derived from glycolipids. The levels of oligosaccharides with reducing-end hexose found in the body fluids were surprisingly high and they are comparable to the levels of glycans derived from glycoproteins. It is unclear why these oligosaccharides have not been observed in earlier studies. A possible explanation can be the strong focus in earlier research on *N*-glycans and *O*-glycans [34] and the use of a different analytical approach than in this thesis [35-37]. The analytical approach used in earlier studies required extensive sample cleanup and was targeted to sialyl-oligosaccharides [35,36,38]. In another study the urine sample to be analyzed was first fractionated by gel permeation chromatography (GPC). Structural eludication of one fraction by NMR analysis was reportedly not successful [37]. Obviously, in these studies some glycan may have been missed due to extensive sample cleanup procedures and the targeted nature of the approaches. In contrast, the approach used in this thesis, only requires desalting of the urine samples with PGC material and no further fractionation.

The observed glycan structures which would appear to be derived from glycolipids could be explained by the possible existence of an endoglycosylceramidase. This endoglycosylceramidase would be involved in an alternative glycosphingolipid catabolic pathway, although such an enzyme has not yet been described for vertebrates, as discussed in Chapter 4 of this thesis. In addition to the glycan structures mentioned, the same samples were also observed to contain the aldohexonic acid forms of these glycolipid-derived glycans. Furthermore, some aldohexonic acid glycans were also detected in the sialidosis urine when the MS was operated in the negative mode.

It should be emphasized that in the studies done for this thesis, only free glycans in body fluids were examined. It would be worthwhile to investigate the possible presence of urinary glycopeptides in various lysosomal storage disorders. Additionally, the analysis of intact glycolipids in the urines would help to obtain a comprehensive picture of storage products. Further investigation of the postulated endoglycosylceramidase would be helpful to gain better understanding of the catabolism of glycolipids in the human body. With the investigation into glycopeptides and the endoglycosylceramidase activity in combination with the enzyme defect, more could be learned about the catabolism in the lysosomes. Another potentially valuable approach would be to examine the oxidation reaction of glycans derived from glycolipids into their aldohexonic acid form to potentially reveal new insights in glycoconjugate degradation pathways.

In conclusion, using the newly developed capillary HPAEC-PAD-MS setup we were able to determine and characterize a number of oligosaccharides that had not previously been reported in various types of body fluids. The increased sensitivity achieved by using the capillary-scale HPAEC-MS also allowed detection of a number of sulfated *N*-glycans. The developed analytical method together with the semi-targeted approach to the MS data analysis were successfully applied to urine and ascitic fluid samples of patients suffering from lysosomal storage diseases and to amniotic fluid samples from the mothers carrying a fetus suffering from an LSD. Finally it can be stated that detection of urinary oligosaccharides may not only represent a suitable method for the diagnosis of lysosomal storage diseases, but that, in addition, monitoring of the profiles and amounts of these glycans during the therapy of LSDs may provide a powerful tool for assessing therapeutic efficacy.

REFERENCES

1. Wuhrer M, Koeleman CA, Deelder AM, & Hokke CH (2004) Normal-phase nanoscale liquid chromatography-mass spectrometry of underivatized oligosaccharides at low-femtomole sensitivity. *Anal Chem* **76,** 833-838.
2. Lee YC (1990) High-performance anion-exchange chromatography for carbohydrate analysis. *Anal Biochem* **189,** 151-162.
3. Koizumi K (1996) High-performance liquid chromatographic separation of carbohydrates on graphitized carbon columns. *J Chromatogr A* **720,** 119-126.
4. Thaysen-Andersen, M. (2010) Analysis of protein glycosylation using HILIC. *Merck Sequant Technical Summary* TS-001, 1-4.
5. Hardy MR & Townsend RR (1988) Separation of positional isomers of oligosaccharides and glycopeptides by high-performance anion-exchange chromatography with pulsed amperometric detection. *Proc Natl Acad Sci U S A* **85,** 3289-3293.
6. Cataldi TR, Campa C, & De Benedetto GE (2000) Carbohydrate analysis by high-performance anion-exchange chromatography with pulsed amperometric detection: the potential is still growing. *Fresenius J Anal Chem* **368,** 739-758.
7. Bruggink C. (2012) Oligosaccharide analysis by high-performance anion-exchange chromatography hyphenated to integrated pulsed amperometric detection and on-line ion-trap mass spectrometry. In *Applications of ion chromatography for pharmaceutical and biological products* (Bhattacharyya,L. & Rohrer,J.S., eds), pp. 379-391. John Wiley & Sons, Inc..
8. Townsend RR, Hardy MR, & Lee YC (1989) Separation of oligosaccharides using high-performance anion-exchange chromatography with pulsed amperometric detection. *Methods Enzymol* **179,** 65-76.
9. Koizumi K, Kubota Y, Ozaki H, Keiko S, Fukuda M, & Tanimoto T (1992) Analyses of isomeric mono-O-methyl-d-glucoses, d-glucobioses and d-glucose monophosphates by high-performance anion-exchange chromatography with pulsed amperometric detection. *J Chromatogr A* **595,** 340-345.
10. Pereira L (2008) Porous Graphitic Carbon as a Stationary Phase in HPLC: Theory and Applications. *J Liq Chrom Rel Technol* **31,** 1687-1731.
11. Wuhrer M, Deelder AM, & Hokke CH (2005) Protein glycosylation analysis by liquid chromatography-mass spectrometry. *J Chromatogr B Biomed Sci App* **825,** 124-133.
12. Ruhaak LR, Deelder AM, & Wuhrer M (2009) Oligosaccharide analysis by graphitized carbon liquid chromatography-mass spectrometry. *Anal Bioanal Chem* **394,** 163-174.
13. Westphal Y, Schols HA, Voragen AG, & Gruppen H (2010) Introducing porous graphitized carbon liquid chromatography with evaporative light scattering and mass spectrometry detection into cell wall oligosaccharide analysis. *J Chromatogr A* **1217,** 689-695.
14. Alpert AJ (1990) Hydrophilic-interaction chromatography for the separation of peptides, nucleic acids and other polar compounds. *J Chromatogr* **499,** 177-196.
15. Ikegami T, Tomomatsu K, Takubo H, Horie K, & Tanaka N (2008) Separation efficiencies in hydrophilic interaction chromatography. *J Chromatogr A* **1184,** 474-503.
16. Zauner G, Deelder AM, & Wuhrer M (2011) Recent advances in hydrophilic interaction liquid chromatography (HILIC) for structural glycomics. *Electrophoresis* **32,** 3456-3466.
17. Marino K, Bones J, Kattla JJ, & Rudd PM (2010) A systematic approach to protein glycosylation analysis: a path through the maze. *Nat Chem Biol* **6,** 713-723.
18. Swartz M (2010) HPLC systems and components introduced at Pittcon 2010: a brief review. *LCGC North America* **28,** 377-385.
19. Burgess K, Creek D, Dewsbury P, Cook K, & Barrett MP (2011) Semi-targeted analysis of metabolites using capillary-flow ion chromatography coupled to high-resolution mass spectrometry. *Rapid Commun Mass Spectrom* **25,** 3447-3452.
20. Dionex Corp (2011) Determination of carbohydrates in fruit juice using capillary high-performance anion-exchange chromatography. *Application Brief 127*, 1-2.
21. Dionex Corp (2010) Product manual for capillary CarboPac® PA20. *Rev. 02.*
22. Hutchinson JP, Hilder EF, Shellie RA, Smith JA, & Haddad PR (2006) Towards high capacity latex-coated porous polymer monoliths as ion-exchange stationary phases. *Analyst* **131,** 215-221.
23. Pohl C (2010) Recent developments in ion-exchange columns for inorganic ions and low molecular weight ionizable molecules. *LC GC*.

24. Mellors JS & Jorgenson JW (2004) Use of 1.5-microm porous ethyl-bridged hybrid particles as a stationary-phase support for reversed-phase ultrahigh-pressure liquid chromatography. *Anal Chem* **76,** 5441-5450.
25. Ahn J, Bones J, Yu Y, Rudd PM, & Gilar M (2010) Separation of 2-aminobenzamide labeled glycans using hydrophilic interaction chromatography columns packed with 1.7 μm sorbent. *J Chromatogr B Analyt Technol Biomed Life Sci* **878,** 403-408.
26. Bones J, Mittermayr S, O'Donoghue N, Guttman A, & Rudd PM (2010) Ultra performance liquid chromatographic profiling of serum N-glycans for fast and efficient identification of cancer associated alterations in glycosylation. *J Chromatogr B Analyt Technol Biomed Life Sci* **878,** 403-408.
27. Causon TJ, Broeckhoven K, Hilder EF, Shellie RA, Desmet G, & Eeltink S (2011) Kinetic performance optimisation for liquid chromatography: principles and practice. *J Sep Sci* **34,** 877-887.
28. Causon TJ, Hilder EF, Shellie RA, & Haddad PR (2010) Probing the kinetic performance limits for ion chromatography. I. Isocratic conditions for small ions. *J Chromatogr A* **1217,** 5057-5062.
29. Causon TJ, Hilder EF, Shellie RA, & Haddad PR (2010) Probing the kinetic performance limits for ion chromatography. II. Gradient conditions for small ions. *J Chromatogr A* **1217,** 5063-5068.
30. Wouters B, Bruggink C, Desmet G, Agroskin Y, Pohl C, & Eeltink S (2012) Capillary ion chromatography at high pressure and temperature. *Anal Chem* **84,** 7212-7217.
31. Gritti F & Guiochon G (2012) Kinetic performance of narrow-bore columns on a micro-system for high performance liquid chromatography. *J Chromatogr A* **1236,** 105-114.
32. Selman MH, Hoffmann M, Zauner G, McDonnell LA, Balog CI, Rapp E, Deelder AM, & Wuhrer M (2012) MALDI-TOF-MS analysis of sialylated glycans and glycopeptides using 4-chloro-α-cyanocinnamic acid matrix. *Proteomics* **12,** 1337-1348.
33. Ruhaak LR, Henning R, Huhn C, Borowiak M, Dolhain RJ, Deelder AM, Rapp E, & Wuhrer M (2010) Optimized workflow for preparation of APTS-labeled N-glycans allowing high-throughput analysis of human plasma glycomes using 48-channel multiplexed CGE-LIF. *J Proteome Res* **9,** 6655-6664.
34. van Pelt J, Damm JBL, Kamerling JP, & Vliegenthart JF (1987) Separation of sialyl-oligosaccharides by medium pressure anion-exchange chromatography on Mono Q. *Carbohydr Res* **169,** 43-51.
35. Koseki M & Tsurumi K (1978) Structure of a novel sialooligosaccharide from the urine of a patient with mucolipidosis. *Tohoku J Exp Med* **124,** 361-366.
36. Kuriyama M, Ariga T, Ando S, Suzuki M, Yamada T, Miyatake T, & Igata A (1985) Two positional isomers of sialylheptasaccharides isolated from the urine of a patient with sialidosis. *J Biochem* **98,** 1049-1054.
37. van Pelt J, Hard K, Kamerling JP, Vliegenthart JF, Reuser AJ, & Galjaard H (1989) Isolation and structural characterization of twenty-one sialyloligosaccharides from galactosialidosis urine. An intact N,N'-diacetylchitobiose unit at the reducing end of a diantennary structure. *Biol Chem Hoppe Seyler* **370,** 191-203.
38. Strecker G, Peers MC, Michalski JC, Hondi-Assah T, Fournet B, Spik G, Montreuil J, Farriaux JP, Maroteaux P, & Durand P (1977) Structure of nine sialyl-oligosaccharides accumulated in urine of eleven patients with three different types of sialidosis. Mucolipidosis II and two new types of mucolipidosis. *Eur J Biochem* **75,** 391-403.

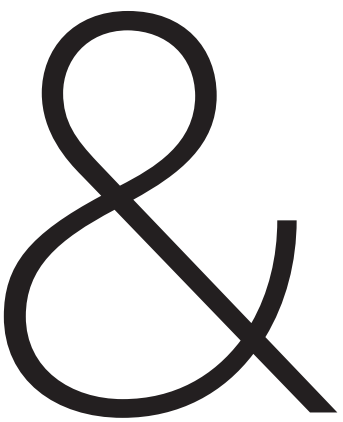

ADDENDUM

SUMMARY

The research described in this thesis is structured in two parts which are both introduced in Chapter 1. The first part of the research focuses on method development with regard to the hyphenation of mass spectrometry (MS) with high performance anion exchange chromatography and pulsed amperometric detection (HPAEC-PAD) for carbohydrate analysis. For many decades HPAEC-PAD has been successfully applied for the analysis of oligosaccharides, and its combination with mass spectrometric detection allows the resolved analysis of complex mixtures and provides a plethora of structural information. This thesis has addressed the challenge of improving the sensitivity of HPAEC-PAD-MS by miniaturization in order to make the method applicable for the analysis of biological samples which may be available in only limited amounts.

The second part of the thesis describes the application of the developed capillary HPAEC-PAD-MS system for a specific biomedical research question. The aim was to characterize the oligosaccharides excreted in urine and other body fluids from patients suffering from lysosomal storage diseases. In these patients the catabolism of glycoproteins and glycolipids is disturbed by specific enzymatic defects, and the structural analysis of the excreted urinary glycans provided insights into the catabolisms of glycoconjugates under these disease conditions.

The results section of this thesis starts with the description of the hyphenation of a standard ion chromatograph with a quadrupole mass spectrometer (Chapter 2). This system was successfully tested for the analysis of native carbohydrates with the aid of a membrane desalter. This desalter is necessary to overcome the incompatibility of the eluent needed for HPAEC-PAD with electrospray-MS (ESI-MS). The desalter removes cations from the column eluate thereby making the eluate compatible with MS detection. After the desalter, a make-up liquid is added to the eluate which enhances the sensitivity of the mass spectrometric detection of glycans, while the composition of the make-up liquid also influences glycan adduct formation. The performance of this system was tested by comparing the chromatograms obtained with both detectors. When applying isocratic elution, slightly broader peaks were observed with MS than with PAD detection; however, this peak broadening was found to be still acceptable. Tests with gradient elution also showed satisfactory resolution, when tested for the separation of native chicory inulin. The sensitivity of this system was investigated with glucose, fructose and sucrose and the result was a minimum detection limit of <0.2 pmol for PAD and of <1.5 pmol for MS in single ion monitoring (SIM). The formed glycan lithium adducts were readily fragmented by in-source decay which allowed the search for carbohydrates in the chromatogram based on specific fragment ions.

While the system described in Chapter 2 was found to be suitable for analyzing rather complex oligosaccharide mixtures such as inulin, its sensitivity was judged to be limiting for various biomedical applications. Therefore, in order to increase the sensitivity, a capillary format ion chromatographic system hyphenated to an MS was developed. The details of this system are described in Chapter 3. The necessary prototype capillary anion exchange column and prototype desalter were made available by the research and development department of Dionex. The capillary ion chromatograph was hyphenated to an ion trap mass spectrometer and instead of lithium adducts, sodium adducts of carbohydrates were formed and detected by positive ion mode MS. The performance test of this capillary system was mainly focused on the obtained resolution and desalting capacity. As described in Chapter 2, the peak broadening was studied by comparing the chromatograms obtained from the MS and the PAD and was

expressed as resolution. The chromatogram obtained with MS detection showed very limited peak broadening compared with that of the PAD. The desalting capacity was determined by pumping a sodium hydroxide solution at 10 µl/min flow rate and monitoring the conductivity and pH of the eluate. The desalting capacity was found to be 225 mmol/l Na^+-ions, which is equal to a capacity of 2.25 meq/min. In view of the biomedical character of the envisioned research the response of both detectors was examined with a complex type asialo diantennary glycan. The response of the detectors was investigated in the range of 0.16 – 100 pmol. The signal of the PAD was found to be linear up to 20 pmol and for the MS over the whole range. The minimum detection limit as compared to the earlier published ion chromatograph-mass spectrometer combination was found to be about two orders of magnitude better, namely 160 fmol for the MS and 50 fmol for PAD respectively.

The focus of the second part of this thesis was on the application of the developed ion chromatograph to biomedical research questions. To this end, oligosaccharides in urine samples from patients suffering from various lysosomal storage disorders were analyzed. The lysosome is a cellular organelle digesting all kinds of materials which are either produced by the cell itself or taken up by the cell. This digestion is enzymatically catalyzed in an acidic environment. When one or more enzymes are defect the degradation of a product will not be completed and storage of these undegraded fragments will be accumulated in the lysosome. The stored products will eventually be released in various body fluids. After excretion, increased concentrations of these partly degraded products can be detected in urine. In this study the excretion of free glycans derived from glycoproteins and glycolipids was analyzed for various lysosomal storage diseases.

First, the applicability of the developed capillary IC-PAD-MS was tested with a urine sample derived from a G_{M1} gangliosidosis patient and this is described in Chapter 3. The result illustrates the excellent selectivity of anion exchange chromatography in separating glycan isomers and the possibility to elucidate structures on the basis of tandem mass spectrometric data. While tandem mass spectrometric analysis routinely reveals structural features of the detected oligosaccharides, full structural elucidation is often not possible with mass spectrometry alone. Instead, by combining information obtained from mass spectrometry, from the known selectivity behavior of the chromatographic system with the knowledge from literature on glycan structures in specific biological sources it is often possible to assign structures to observed mass spectrometric signals.

Chapter 4 describes the research performed on urinary oligosaccharides of galactosialidosis patients with the mass spectrometer operated in negative ion mode. Urine from galactosialidosis patients contains sialylated glycans which could be detected with high selectivity by negative ion mode mass spectrometry. Unexpectedly, free glycan structures derived from glycolipids were detected in addition to glycoprotein-derived *N*-glycan degradation products that are known to be characteristic for galactosialidosis. These free, glycolipid-derived glycan structures were found in various urine samples as well as in ascitic fluid and amniotic fluid samples from galactosialidosis patients. The occurrence of glycolipid-derived free oligosaccharides in patients' body fluids cannot be explained by the known catabolic pathway for glycolipids. Therefore, to explain this observation, a possible endoglycosylceramidase activity is postulated in Chapter 4. Interestingly, oxidized versions of many of these glycans were likewise detected, exhibiting a carboxylic acid group at the C_1 position of the innermost hexose, thereby forming an aldohexonic acid. The

mechanism causing this oxidation is unknown, and one could speculate about an enzymatic as well as non-enzymatic process underlying the occurrence of these glycans.

A comparative study of urinary oligosaccharides from five different lysosomal storage disorders (fucosidosis, α-mannosidosis, G_{M1} gangliosidosis, G_{M2} gangliosidosis, and sialidosis) is reported in Chapter 5. For each disease a characteristic glycan pattern was observed that reflected the specific blockage of the glycan catabolic pathway, indicating that mass spectrometric detection of urinary oligosaccharide profiles may have diagnostic potential for lysosomal storage diseases.

The general discussion in Chapter 6 points out that the observation of glycolipid-derived oligosaccharides at high relative abundances is surprising, as one would expect that these glycans should have been noted and described in earlier reports on urinary oligosaccharides – which is not the case.

Likewise, the technological progress achieved in this thesis is evaluated in Chapter 6. It is concluded that, due to the successful miniaturization of HPAEC-PAD-MS, for glycan analysis the method presents a valuable addition to other LC-MS methods. The added value of HPAEC is based on its unique separation principle, making it orthogonal to other separation techniques such as hydrophilic interaction liquid chromatography (HILIC) and porous graphitized carbon chromatography (PGC). Also, HPAEC is particularly suitable for separating native oligosaccharides, as anomer separation is efficiently suppressed under the applied chromatographic conditions. In conclusion, capillary-scale HPAEC-PAD-MS as developed in this thesis was found to be suitable for analyzing the glycosylation of biological samples available in only limited amounts. In order to make the system available to a broader group of analytical scientists, it should be brought from a prototype to commercially available instrumentation which will hopefully take place in the near future.

SAMENVATTING

Het onderzoek beschreven in dit proefschrift omvat twee hoofdlijnen, zoals geïntroduceerd in Hoofdstuk 1. De eerste lijn betreft het koppelen van massaspectrometrie (MS) aan "high performance" anionenchromatografie en "pulsed amperometric" detectie (HPAEC-PAD). HPAEC-PAD wordt al vele decennia met succes gebruikt voor de analyse van oligosaccharides. Door het combineren van deze analysetechniek met massaspectrometrie wordt het mogelijk om monsters te analyseren die complexe oligosaccharides bevatten en levert naast selektiviteit structuurinformatie van de eluerende oligosaccharides op. Om de analyse van biologische monsters die slechts in kleine hoeveelheden voorhanden zijn mogelijk te maken, was het echter noodzakelijk de gevoeligheid te verbeteren van HPAEC-PAD-MS. Deze gevoeligheidsverbetering is bereikt door het miniaturiseren van de HPAEC-PAD, zoals in dit proefschrift beschreven.

De tweede hoofdlijn van het onderzoek betreft het inzetten van de ontwikkelde capillaire HPAEC-PAD-MS bij biomedisch onderzoek. Hierbij is gekozen voor de analyse van oligosaccharides in urine en andere lichaamsvloeistoffen van patiënten die lijden aan een lysosomale stapelingsziekte. Bij deze patiënten is de afbraak van glycoproteïnen en glycolipiden verstoord door een defect in specifieke enzymen. Structuuranalyse van de uitgescheiden glycanen in urine geeft inzicht in het katabolisme van glycoconjugaten bij deze patiënten.

Dit deel van het proefschrift begint met het beschrijven van de koppeling van een standaard ionenchromatograaf aan een quadrupole massa spectrometer in Hoofdstuk 2. Dit systeem is getest met ongederivatiseerde koolhydraten en de koppeling tussen de ionenchromatograaf en de MS gaat middels een membraanontzouter. De ontzouter is nodig omdat de voor HPAEC-PAD gebruikelijke eluent samenstellingen niet verenigbaar zijn met elektrospray-MS (ESI-MS). De ontzouter verwijdert kationen uit het kolom eluaat wat de matrix voor MS-detectie geschikt maakt. Na de ontzouter wordt aan het eluaat een make-up vloeistof toegevoegd, waardoor de gevoeligheid van de MS-detectie verbetert. Door de samenstelling van de make-up vloeistof kan tevens de adductvorming van de koolhydraten worden beïnvloed. Dit systeem is getest op zijn prestaties door de signalen van beide detectoren te evalueren. Uit de vergelijking van de MS en PAD signalen bleek de piekverbreding onder isocratische eluent condities minimaal te zijn. Ook de test met gradiënt-elutie waarbij polyfructanen werden gescheiden gaf een uitstekend resultaat, zoals aangetoond met een monster natieve chicorei inuline. Het signaalgedrag van glucose, fructose en sucrose is onderzocht in een range van 2.5 – 1000 pmol en de aantoonbaarheidsgrens bleek met PAD < 0.2 pmol en met MS in "single ion monitoring" (SIM) <1.5 pmol te zijn. De lithium glycaan adducten werden gefragmenteerd met behulp van in-source fragmentatie wat het zoeken naar koolhydraten in het chromatogram op basis van specifieke fragmentionen mogelijk maakte.

Hoewel het systeem dat is beschreven in Hoofdstuk 2 geschikt bleek voor het analyseren van complexe monsters, zoals inuline, is een betere gevoeligheid nodig voor biomedische toepassingen. Hiertoe is een ionenchromatograaf in capillair formaat ontwikkeld, die gekoppeld is aan een MS, hetgeen in Hoofdstuk 3 is beschreven. Prototypes van een capillaire scheidingskolom en een ontzouter werden beschikbaar gesteld door de afdeling onderzoek en ontwikkeling van de firma Dionex. De capillaire ionenchromatograaf was gekoppeld aan een "ion-trap" massaspectrometer en bij de experimenten met dit systeem worden in plaats van lithiumadducten, natriumadducten van de koolhydraten gevormd terwijl de

massaspectrometer in de positieve "ion mode" is gebruikt. Het testen van de prestaties van deze capillaire ionenchromatograaf was vooral gericht op het bepalen van de ontzoutingscapaciteit en de piekverbreding die de capillaire ontzouter veroorzaakt. Net als in Hoofdstuk 2 werd de piekverbreding bestudeerd door het MS-signaal te vergelijken met het signaal van de PAD en het effect van de piekverbreding op de scheiding werd uitgedrukt in resolutie. In het MS-signaal werd in vergelijking tot het PAD-signaal een zeer geringe piekverbreding waargenomen, waardoor de scheiding ruim voldoende bleef voor het met MS verkregen chromatogram. De ontzoutingscapaciteit werd bepaald door het verpompen van een natriumhydroxide oplossing met een debiet van 10 µl/min terwijl na de ontzouter de geleidbaarheid en de pH werden gemonitoord. Een oplossing van 225 mmol/l Na^+ ionen kon worden ontzout wat overeenkomt met een capaciteit van 2.25 µeq/min. Gelet op het biomedische kader van het vervolgonderzoek is de respons van beide detectoren onderzocht met een complex type asialo diantenne glycaan over een bereik van 0.16 – 100 pmol. Het signaal voor de PAD bleek lineair tot 20 pmol en voor de MS over het gehele onderzochte gebied. De aantoonbaarheidsgrens was ongeveer twee grootte orders beter dan dat van eerder beschreven ionenchromatograaf-massaspectrometer combinaties voor koolhydratenonderzoek, namelijk 160 fmol voor MS en 50 fmol voor PAD.

De tweede onderzoekslijn in dit proefschrift beschrijft het toepassen van de ontwikkelde ionenchromatograaf voor biomedisch onderzoek. Voor dit biomedisch onderzoek waren urinemonsters afkomstig van patiënten met diverse lysosomale stapelingsziektes beschikbaar. Het lysosoom is een organel in de cel waarin afbraak plaatsvindt van allerlei componenten afkomstig van of opgenomen door de cel. Deze degradatie vindt plaats met behulp van enzymen. Als een of meerdere enzymen defect zijn vindt geen volledige afbraak plaats en stapelen deze producten zich op in het lysosoom. De gestapelde producten komen uiteindelijk vrij in diverse lichaamsvloeistoffen. Na uitscheiding in urine worden verhoogde concentraties van deze producten teruggevonden. In dit onderzoek werden de gestapelde vrije glycanen die afkomstig zijn van glycoproteinen en glycolipiden bepaald bij diverse lysosomale stapelingsziekten.

In Hoofdstuk 3 is de praktische toepasbaarheid van de ontwikkelde capillaire IC-PAD-MS onderzocht met een urine monster van een G_{M1} gangliosidose patiënt. De resultaten tonen de speciale selectiviteit voor het scheiden van glycaan isomeren met behulp van anionenchromatografie en de mogelijkheden voor structuuropheldering met behulp van tandem massaspectrometrie aan. Massaspectrometrie alleen leidt vaak niet tot volledige structuuropheldering, maar door het combineren van gepubliceerde glycaanstructuren, de beschreven selectiviteit van het scheidingssysteem en de tandem massaspectrometrie resultaten is het vaak mogelijk om een structuur toe te wijzen aan een glycaan.

In Hoofdstuk 4 wordt onderzoek beschreven verricht aan urines van galactosialidose patiënten. In deze urines werden sialylglycanen gevonden waarbij de massaspectrometer in de negatieve "ion mode" gebruikt werd om deze sialylglycanen met hoge selectiviteit te detecteren. Naast de verwachte *N*-glycanen, die relevant zijn voor galactosialidose, werden onverwacht ook vrije glycaanstructuren gevonden van glycolipiden, die niet verklaard konden worden met hetgeen er bekend is over het mechanisme van de afbraak van glycolipiden. Na het beschikbaar komen van additionele monsters urine, buikvocht en vruchtwater, konden deze resultaten worden bevestigd. In dit hoofdstuk is naast de mogelijkheid voor het onderzoeken van glycaanstructuren, een mogelijke endoglycosylceramidase-activiteit gepostuleerd om de gevonden glycaanstructuren van glycolipiden te verklaren. Van deze gevonden

glycaanstructuren werden tevens de geoxideerde vormen gedetecteerd. Het opvallende aan deze glycanen is dat ze een carboxylgroep op de C_1 plaats hebben en daardoor tot de groep aldohexonzuren behoren. Het achterliggend oxidatie mechanisme is onbekend en kan zowel enzymatisch als niet-enzymatisch van aard zijn.

In Hoofdstuk 5 worden de resultaten beschreven van een vergelijkend onderzoek van glycanen in urine van vijf lysosomale stapelingsziekten, fucosidose, α-mannosidose, G_{M1} gangliosidose, G_{M2} gangliosidose en sialidose. Voor elke ziekte is een histogram gemaakt van de gevonden relatieve hoeveelheid van elk glycaan en het patroon dat zo ontstond toont een goed beeld van de blokkade die optreedt in het katabolisme van de glycanen. De uitbreiding met tandem MS-detectie voor de karakterisering van glycanen in urine is mogelijk een aanvullende methode voor de diagnostiek van lysosomale stapelingziekten.

Het is verrassend dat de relatief grote hoeveelheid oligosaccharides afkomstig van glycilipiden niet is gevonden in eerdere onderzoeken. Hierover wordt gediscussieerd in Hoofdstuk 6. In hetzelfde hoofdstuk wordt de in dit promotieonderzoek bereikte technologische vooruitgang besproken. De conclusie is dat door het miniaturiseren van HPAEC-PAD-MS met succes een waardevolle methode kon worden toegevoegd aan reeds bestaande LC-MS methoden voor het analyseren van glycanen. De toegevoegde waarde van HPAEC ligt vooral in het unieke scheidingsprincipe die orthogonaal is met andere scheidingstechnieken, zoals “hydrophilic interaction liquid chromatography” (HILIC) en “porous graphitized carbon chromatography” (PGC). HPAEC is in het bijzonder geschikt voor de scheiding van ongederivatiseerde oligosacchariden, omdat anomere scheiding niet plaats vindt onder de gebruikte chromatografische condities. Samenvattend kan gesteld worden dat capillaire HPAEC-PAD-MS zoals ontwikkeld tijdens dit promotieonderzoek, geschikt is gebleken voor het analyseren van glycanen in biologische monsters, waarbij de hoeveelheid monster beperkt mag zijn. Om dit capillaire systeem meer algemeen beschikbaar te hebben voor onderzoek, moet het wel van prototype tot een commercieel beschikbaar instrument worden ontwikkeld, wat hopelijk spoedig zal gebeuren.

ABBREVIATIONS

Asn	Asparagine
ASRS	Anion self regeneration suppressor
Cer	Ceramide
CMD	Carbohydrate membrane desalter
Da	Dalton (atomic mass unit)
DP	Degree of polymerization
DNA	Deoxyribonucleic acid
EIC	Extracted ion chromatogram
ESI	Electrospray ionization
F, Fuc	Fucose
FOS	Fructan oligosaccharide
FUCA1	Gene symbol for α-L-fucosidase
Gal	Galactose
GalNAc	*N*-acetylgalactosamine
GALNS	N-acetylgalactosamine-6-sulfate sulfatase
GD1b	Gal(β1-3)GalNAc(β1-4)(Neu5Ac(α2-8) Neu5Ac(α2-3))Gal(β1-4)Glc
GD3	Neu5Ac(α2-8)Neu5Ac(α2-3)Gal(β1-4)Glc
Glc	Glucose
GlcNAc	*N*-acetylglucosamine
GluconA	Gluconic acid
GM_1	Monosialotetrahexosylganglioside; Neu5Ac(α2-3)Gal(β1-3)GalNAc(β1-4) Gal(β1-4)Glc
GM_2	Monosialotrihexosylganglioside; GalNAc(β1-4)(Neu5Ac(α2-3))Gal(β1-4)Glc
GM_3	Monosialodihexosylganglioside
GPC	Gel permeation chromatography
GSL	Glycosphingolipid
H, Hex	Hexose
HexA	Hexonic Acid
HexNAc	*N*-acetylhexosamine
HexonA	Aldohexonic acid
$HexSO_3$	O-Sulfated hexose
HILIC	Hydrophilic interaction chromatography see NPLC
HPAEC	High performance anion exchange chromatography
HPLC	High performance liquid chromatography
I.D.	Internal diameter
IEC	Ion exchange chromatography
IPAD	Integrated amperometric detection, see also PAD
LC	Liquid chromatography
LSD	Lysosomal storage disorder
Man	Mannose
MDL	Minimum detection limit
MPS	Mucopolysaccharidosis

MS	Mass spectrometry
N	*N*-acetylhexosamine
Neu5Ac	*N*-acetylneuraminic acid
NMR	Nuclear magnetic resonance spectroscopy
NPLC	Normal phase liquid chromatography see HILIC
PAD	Pulsed amperometric detection see also IPAD
PGC	Porous graphitized carbon
pH	Potentia hydrogenii -log[H^+]
pK_a	-log of the dissociation constant
RNA	Ribonucleic acid
PPCA	Cathepsin A, protective protein/carboxypeptidase C
RPLC	Reversed phase liquid chromatography
R_s	Resolution
S	Sialic acid or *N*-acetylneuraminic acid
Sap	Saposin
SEM	Scanning electron microscope
Ser	Serine
SIM	Selected ion monitoring
SO_3	Sulfate
TFA	Trifluoroacetic acid
Thr	Threonine
TLC	Thin layer chromatography
UV	Ultra violet
X	Aldohexonic acid
Xyl	Xylose

CURRICULUM VITAE

Cornelis Bruggink was born on June 29th 1951 in Amsterdam, the Netherlands. After passing his exam of the MULO B in 1969, he started his education in analytical chemistry at the evening classes of the Analisten School Amsterdam and passed the HBO-A in 1974 and HBO-B in 1976. During the time of the HBO education he was employed as junior analytical chemist at Ketjen (AKU, AKZO) in Amsterdam (1969–1971) and from 1971 until 1978 employed at the pharmaceutical company "De Watermolen", later named Pharbita, where he got involved in analytical method development. In 1978 he started an application and demo facility for several brands of analytical equipment including Dionex represented by Pleuger in Amstelveen (later Lamers Pleuger in Den Bosch). Around that time he learned from Prof. Dr. J. Weiss the theoretical backgrounds of ion chromatography so that he could start with giving ion chromatography courses, which developed into an advanced course "method development for ion chromatography". Likewise he started giving a course entitled "HPAEC-PAD for carbohydrate analysis" based on information provided by Dr. J.D. Olechno and Dr. J.S. Rohrer, as well as a course entitled "Electrochemical detection", and he still teach on these subjects in his current function.

In 1988 Dionex started an own subsidiary for the sales of ion chromatography in the Netherlands and his main responsibility was to develop methods and applications in ion chromatography and for a few years also for capillary electrophoresis. He was responsible for setting up and managing the application laboratories in Breda and Mechelen, in which four application chemists were employed. He helped in setting up laboratory facilities for the agriculture company "Relab Den Haan BV" and did analytical method development for this laboratory. Dionex gave me several times the opportunity to do research together with the Leiden University and Wageningen University on the characterization of plant oligosaccharides using ion chromatography hyphenated to mass spectrometry resulting in several publications together with Prof. Dr. W.M.A. Niessen and Dr. H.A. Schols in the period from 1993 until 1998. He started his PhD study in 2004 under supervision of Prof. Dr. A.M. Deelder and Dr. M. Wuhrer at the Department of Parasitology (LUMC) resulting in this thesis with the title "Characterization of oligosaccharides with capillary high performance anion exchange chromatography hyphenated to pulsed amperometric detection and ion trap mass spectrometry: Application to the analysis of human lysosomal disorders". This PhD has been performed in part-time, while still employed for 4 days a week by Thermo Scientific for Dionex products. In his current function as "Support Specialist Dionex Products" he develops customer applications for ion chromatography, gives trainings to users, represent Dionex at scientific and commercial events, create marketing, training and support materials for the sales organization and customers, and keep close contact with the Dionex USA and Europe organizations.

LIST OF PUBLICATIONS

1. Eghbali H, Bruggink C, Agroskin Y, Pohl CA, & Eeltink S (2012) Performance evaluation of ion-exchange chromatography in capillary format. *J Sep Sci*. doi: 10.1002/jssc.201200680.
2. Wouters B, Bruggink C, Desmet G, Agroskin Y, Pohl C, & Eeltink S (2012) Capillary ion chromatography at high pressure and temperature. *Anal Chem* **84,** 7212-7217.
3. Bruggink C. (2012) Oligosaccharide analysis by high-performance anion-exchange chromatography hyphenated to integrated pulsed amperometric detection and on-line ion-trap mass spectrometry. In Applications of ion chromatography for pharmaceutical and biological products (Bhattacharyya,L. & Rohrer,J.S., eds), pp. 379-391. John Wiley & Sons, Inc.
4. Bruggink C, Poorthuis BJ, Deelder AM, & Manfred Wuhrer M (2012) Analysis of urinary oligosaccharides in lysosomal storage disorders by capillary high-performance anion-exchange chromatography-mass spectrometry. *Anal Bioanal Chem*.**403**, 1671-1683.
5. Bruggink C, Poorthuis BJ, Piraud M, Froissart R, Deelder AM, & Wuhrer M (2010) Glycan profiling of urine, amniotic fluid and ascitic fluid from galactosialidosis patients reveals novel oligosaccharides with reducing end hexose and aldohexonic acid residues. *FEBS J* **277,** 2970-2986.
6. Ruhaak LR, Zauner G, Huhn C, Bruggink C, Deelder AM, & Wuhrer M (2010) Glycan labeling strategies and their use in identification and quantification. *Anal Bioanal Chem* **397,** 3457-3481.
7. Bruggink C, Wuhrer M, Koeleman CA, Barreto V, Liu Y, Pohl C, Ingendoh A, Hokke CH, & Deelder AM (2005) Oligosaccharide analysis by capillary-scale high-pH anion-exchange chromatography with on-line ion-trap mass spectrometry. *J Chromatogr B Analyt Technol Biomed Life Sci* **829,** 136-143.
8. Bruggink C, Maurer R, Herrmann H, Cavalli S, & Hoefler F (2005) Analysis of carbohydrates by anion exchange chromatography and mass spectrometry. *J Chromatogr A* **1085,** 104-109.
9. Bruggink, C. (2000) Backgrounds and possibilities for electrochemical detection in conjunction with anion exchange chromatography. Conference proceeding AVH Association - 7th Symposium - Reims, March 2000**,** 3-9.
10. van der Hoeven RAM, Tjaden UR, van der Greef J, van Casteren WHM, Schols HA, Voragen AGJ, & Bruggink C (1998) Recent progress in high-performance anion-exchange chromatography/ionspray mass spectrometry for molecular mass determination and characterization of carbohydrates using static and scanning array detection. *J Mass Spectrom* **33,** 377-386.
11. Torto N, Hofte A, Tjaden UR, Gorton L, Marko-Varga G, Bruggink C, & van der Greef J (1998) Microdialysis-introduction high-performance anion-exchange chromatography/ionspray mass spectrometry for monitoring of online-desalted carbohydrate hydrolysates. *J Mass Spectrom* **33,** 334-341.
12. van der Hoeven RAM, Hofte AJP, Tjaden UR, van der Greef J, Torto N, Gorton L, Marko-Varga G, & Bruggink C (1998) Sensitivity improvement in the analysis of oligosaccharides

by online high-performance anion-exchange chromatography/ionspray mass spectrometry. *Rapid Commun Mass Spectrom* **12,** 69-74.

13. Schols HA, Mutter M, Voragen AG, Niessen WM, van der Hoeven RA, van der GJ, & Bruggink C (1994) The use of combined high-performance anion-exchange chromatography-thermospray mass spectrometry in the structural analysis of pectic oligosaccharides. *Carbohydr Res* **261,** 335-342.
14. Niessen WM, van der Hoeven RA, van der Greef J, Schols HA, Voragen AG, & Bruggink C (1993) Recent progress in high-performance anion-exchange chromatography thermospray mass-spectrometry of oligosaccharides. *J Chromatogr* **647,** 319-327.
15. Niessen WMA, van der Hoeven RAM, van der Greef J, Schols HA, lucaslokhorst G, Voragen AGJ, & Bruggink C (1992) High-performance anion-exchange chromatography thermospray mass-spectromtry in the analysis of oligosaccharides. *Rapid Commun Mass Spectrom* **6,** 474-478.
16. van der Hoeven RAM, Niessen WM, Schols HA, Bruggink C, Voragen AG, & van der Greef J (1992) Characterization of sugar oligomers by on-line highperformance anion-exchange chromatography thermospray mass spectrometry. *J Chromatogr* **627,** 63-73.
17. Schols HA, Voragen AG, & Bruggink C (1992) Analyse van koolhydraten met HPAEC/PAD: aanvulling of doorbraak? *Voedingsmiddelentechnologie* **7,** 30-33.
18. Cook K, Dewsbury P, Burgess K, & Bruggink C (2010) Ion Chromatography Coupled to MS for Metabolomic Analysis. *Chromatography Today* 16-19.
19. Bruggink C, van Rossum WJ, Spijkerman E, & van Beelen ES (2007) Iodide analysis by anion-exchange chromatography and pulsed amperometric detection in surface water and adsorbable organic iodide. *J Chromatogr A* **1144,** 170-174.
20. Bruggink C, van Rossum WJ, & Smeenk JGMM (1995) Ionchromatografische spooranalyse van bromaat in drink- en oppervlaktewater met behulp van een macro-injectiesysteem. *H_2O* **28,** 343-347.

DANKWOORD – ACKNOWLEDGEMENTS

De belangrijkste persoon waar mijn dank naar uitgaat, is mijn echtgenote Helen. Zij heeft mij altijd liefdevol de ruimte gegund om me te ontwikkelen en dat “schat”, zal niet altijd eenvoudig zijn geweest. Als je dit leest is de vraag: ‘is je promotieonderzoek nu af?’, beantwoord. Ongetwijfeld ben ik vergeten om personen te noemen die hebben geholpen bij het tot stand komen van dit proefschrift en ik bied u mijn welgemeende excuses aan. Ik hoop dat u toch kan genieten van wat bereikt is. Aan Franck van Veen en anderen heb ik te danken dat het mogelijk werd om dit promotieonderzoek te starten. Je zorgde voor de nodige toestemmingen en stimuleerde me om niet op te geven. Je verzuchtte een keer “you are a person that needs high maintenance” ... maar je hield het met mij vol. Chris Pohl I would like to thank you for providing all custom made materials required for my PhD research. The research described in Chapter 2 was performed in the laboratory of Dionex in Olten. Frank Höfler thank you for giving me this opportunity. Rob, mijn beste broer, je geduldig luisteren en het samen discussiëren over diverse zaken van technische aard heb ik enorm gewaardeerd. Ook hartelijk dank voor het bouwen en creëren van de onderdelen die nodig waren voor het promotieonderzoek. Manfred en André, jullie wil ik in het bijzonder bedanken voor het geduld en de discussies die mijn blik verbreedde. Zonder jullie zou dit proefschrift niet tot stand zijn gekomen. Collega’s van de afdeling Parasitologie en Biomoleculaire Massa Spectrometrie, jullie wil ik bedanken voor de gezelligheid, aanmoedigingen en discussies. Dat gaf en geeft me een thuis op het LUMC. Tanja, Henk, Ans, Rebecca, Yvonne en Angela bedankt voor jullie ondersteuning in het corrigeren van mijn teksten.